Final Report to the

New Jersey Department of Environmental Protection (NJDEP)

Michael Aucott, Program Manager

The New Jersey Atmospheric Deposition Network (NJADN)

John R. Reinfelder, Lisa A. Totten, and Steven J. Eisenreich, PIs

Department of Environmental Sciences, Rutgers University
14 College Farm Road, New Brunswick, NJ 08901

Science Team
Paul Brunciak*
Cari L. Gigliotti
Eric D. Nelson
Daryl A. Van Ry
Rosalinda Gioia
John H. Offenberg
Yan Zhuang

Project Contributors
Jordi Dachs
Songyan Du
Kristie M. Ellickson
Thomas R. Glenn IV
Sandra Goodrow
Yvonne Koelliker
Maya V. Panangadan
Shu Yan

January 2004

Acknowledgements

This project was made possible by the support of the New Jersey Department of Environmental Protection, Office of Science and Research and the guidance and support of its program managers Stuart Nagourney and Michael Aucott. We wish to thank Drs. Joel E. Baker and Robert P. Mason from the University of Maryland, and Dr. Bruce Hicks from NOAA/ARL for serving as an expert panel at the NJADN Review Workshop, May 5, 2003.

The New Jersey Atmospheric Deposition Network (NJADN)

Final Report

Executive Summary

The New Jersey Atmospheric Deposition Network (NJADN) was a collaborative environmental research and monitoring effort between Rutgers University and the New Jersey Department of Environmental Protection (NJDEP). The objectives of the project were to quantify current concentrations and deposition fluxes of atmospheric chemicals and assess their spatial and seasonal trends. The evaluation of the potential impact of atmospheric deposition to terrestrial and aquatic ecosystems and the identification of local and regional sources of atmospheric contaminants were also implicit goals of the project. Ultimately NJADN results will establish baseline levels of atmospheric chemicals that will be useful in the evaluation of long-term trends and the effectiveness of pollution control efforts.

Begun in 1997 with support from the Hudson River Foundation and the NJ Sea Grant Program, the NJADN was greatly expanded in 1998 with support from the NJDEP to include nine sampling sites around the state. In 2001, when monitoring activities were scheduled to end, additional support from NJDEP was provided for a year of sampling at the three original NJADN sites and an additional site near the lower Delaware River estuary and support was also provided by NJDEP through the Rutgers Center for Environmental Indicators for the analysis of total phosphorus in NJADN rain samples.

Over the course of this project, the concentrations and deposition fluxes of 116 organic compounds representing polycyclic aromatic hydrocarbons (PAHs), polychlorinated biphenyls (PCBs), and organo-chlorine pesticides (including chlordanes, DDTs, HCHs, Endosulfan I and II, Aldrin and Dieldrin), particulate organic and elemental carbon in fine aerosols (PM2.5), and 21 inorganic analytes including mercury, nitrate, and phosphate were determined on a 12 d sampling cycle throughout New Jersey. This report presents the results for organic compounds for the period of October 1997 to January 2003 and the results for inorganic analytes for the period of July 1999 to January 2003. Results for inorganic analytes for the period 1997 to 1998 are available in the Reports of Y. Gao to the Hudson River Foundation and New Jersey Sea Grant.

This report includes three sections: I. NJADN Objectives and Methods, II. NJADN Results, and III. Appendices with complete data sets and QA results.

Organic contaminants in air, aerosols, and precipitation

The organic compounds examined in the NJADN project derive from combustion processes (PAHs), the remobilization of chemicals from historical uses in urban-industrial centers (PCBs), and from past agricultural practices (DDT, DDE) and chemicals used today as pesticides but in areas mostly removed from New Jersey (chlordanes). In great portions of New Jersey encompassing forested, coastal, and suburban environments, gas-phase ΣPCB concentrations were essentially uniform (averaging 150-220 pg m^{-3}). The highest concentrations of ΣPCBs in the gas phase were observed at urban sites such as Camden and Jersey City (3250 pg m^{-3} and 1260 pg m^{-3}, respectively). The spatial distribution suggests that the influence of urban areas on atmospheric PCB concentrations extends less than 40 km. Atmospheric ΣPCB deposition fluxes (gas absorption by water plus dry particle deposition plus wet deposition) ranged from 7.3 to 340 ug m^{-2} y^{-1} and increased with proximity to urban areas. Because the Hudson River Estuary is adjacent to urban areas such as Jersey City, it is subject to depositional fluxes of PCBs that are at least 2-10 times those estimated for the Chesapeake Bay and Lake Michigan. Inputs of PCBs to the Hudson River Estuary from the upper Hudson River and from wastewater treatment plants are estimated to be 8-18 times greater than atmospheric inputs, and volatilization of PCBs from the estuary exceeds atmospheric deposition of low molecular weight PCB congeners.

Gas phase and particle phase the combined concentrations of 36 PAHs (Σ_{36}PAH) in New Jersey ranged from 0.45 to 118 ng m^{-3} and 0.046 to 172 ng m^{-3}, respectively, and precipitation concentrations ranged from 13 to 16,200 ng L^{-1}. PAH concentrations varied spatially across the state with the highest concentrations occurring at the most heavily urban and industrial locations. Although the absolute concentrations varied spatially, the PAH profiles are statistically similar at all NJADN sampling sites indicating that the mix of sources is relatively constant around New Jersey. Increased emissions of PAHs attributed to elevated fossil fuel use in winter resulted in elevated particle phase PAH concentrations at most NJADN sites. Annual average Σ_{36}PAH total atmospheric deposition fluxes in New Jersey range from 5.4×10^2 to 7.3×10^3 ug m^{-2} year. Gas absorption represents the single largest component of total atmospheric deposition of PAHs for

each of the sites (55 to 92%), followed by dry particle deposition (4 to 31%). Wet deposition constitutes the smallest fraction of the total atmospheric PAH flux (3 to 16%). Average gas absorption (by water) and dry particle deposition fluxes of individual PAHs ranged from 0.004 to 5040 ng m^{-2} d^{-1} and 0.11 to 300 ng m^{-2} d^{-1}, respectively. Average atmospheric wet deposition fluxes of individual PAHs ranged from 0.50 to 140 ng m^{-2} d^{-1}.

Gas-phase organo-chlorine pesticides (OCPs) comprise about 95% of the total atmospheric OCPs across New Jersey. Concentrations of all OCPs except aldrin were significantly correlated with temperature at every site. Sampling days with residuals greater than one standard deviation from the ln P of chlordanes versus 1/T were checked with three-day back trajectories. Lower than expected concentrations were observed when the air mass came from the northwest (Canada and Great Lakes), whereas higher than expected concentrations show no correlation with the air mass origin.

The concentrations of organic carbon (OC) and elemental carbon (EC) associated with $PM_{2.5}$ mass were quantified by a thermal-optical transmittance (TOT) method. No consistent seasonal patterns in either $OC_{2.5}$ or $EC_{2.5}$ concentrations or OC/EC ratios were observed. Periods of secondary organic aerosol formation and periods in which most $OC_{2.5}$ arises from primary emissions were identified using ozone and carbon monoxide data as well as meteorological data (temperature, wind direction etc.). Ozone was used as an indicator of periods of photochemical activity, while CO was used as an indicator of combustion sources. Nearly 40% of all sample dates show evidence of secondary organic aerosol formation with the exception of the Pinelands site where 77% of samples show evidence of aerosol not deriving from primary formation.

Atmospheric Concentrations and Deposition of Trace Elements

The trace metals included in the NJADN study are mostly associated with combustion processes (power plants, incinerators, automobiles, trucks), mechanical wear and tear on automobiles and trucks, and soils. For many trace elements, the highest concentrations in precipitation and fine aerosols (PM2.5) were observed in Jersey City, Camden, and New Brunswick with lower levels in the more rural and coastal Pinelands, Tuckerton, and Delaware Bay sites. However, important exceptions to this pattern were found including elevated levels of Ag, Mg, Mn, P, and Sb in the Pinelands and the highest precipitation concentrations of As, Mg, Sb, and Zn in Alloway Creek (Salem County). Thus local, intrastate spatial trends in

atmospheric trace element concentrations exist, but they vary by element and are not related to land use patterns in a simple way.

Seasonal variations in the concentrations of trace elements in precipitation were generally not uniform across New Jersey, indicating the importance of local sources and/or atmospheric transport processes. However, the seasonal variation in the concentrations of Pb in precipitation was similar at all sites and showed the highest levels in the spring and the lowest levels in the fall or winter indicating that the atmospheric Pb is at least partly controlled by regional emissions and transport phenomena.

The wet deposition fluxes of Cd, Cu, and Pb at New Brunswick, Jersey City, Camden are elevated with respect to the regional background while those at the Pinelands are similar to fluxes measured in the early 1990's at rural sites in Maryland and Florida. This trend is similar for the dry particle fluxes of Cd, Cu, and Pb, although the Pinelands appears to have elevated particulate Cu with respect to the regional background as recorded at the Chester and Delaware Bay sites. The annual wet deposition fluxes of As in Jersey City and Camden are greater than those recorded in Maryland and Florida, and, given the uncertainty, those in New Brunswick and the Pinelands are similar to those recorded in the other two states. Dry particle deposition fluxes of As in New Jersey (with the exception of the Pinelands) based on geometric mean concentrations in PM2.5 are about twice that estimated from the geometric mean PM2.5 As concentration measured in Vermont. On an arithmetic mean basis, however, dry particle As fluxes in New Jersey are similar to that estimated from arithmetic mean PM10 As concentrations for Maryland.

The relative contributions of wet and dry atmospheric deposition varied among the elements, but for each element showed similar patterns at all five sites where wet deposition was measured. It should be noted that the total atmospheric deposition fluxes estimated in this project exclude dry gaseous deposition which could be important components of the total fluxes of the volatile elements Hg and As. For Cu, Pb, Mn, and Hg, more than 70% of the total atmospheric deposition was due to wet deposition. However, less than 30% of the total deposition of Cr was due to wet deposition. Since the large particles (> 2.5 μm) that are excluded from the fine aerosol impactors are scavenged by rain, these observations may reflect differences in the particle size distributions of different metals. The relatively greater contribution of PM2.5-based dry particle deposition fluxes of Cd, Cu, and Pb in the Pinelands

than at Camden indicate that large metal-bearing particles are important to the total atmospheric metal flux in Camden, but are not transported to the Pinelands.

The range of Hg concentrations in New Jersey rain is similar to that measured at a number of sites around the U.S. including northern Wisconsin, Lake Michigan, southern Florida, Valley Forge PA, and the Chesapeake Bay. Much of the temporal variability in Hg concentrations in New Jersey followed statewide trends, and as a result, rain collected at all sites had similar Hg concentrations for a given sampling period. The significantly lower concentrations and deposition fluxes of Hg observed in New Jersey precipitation at all sites in the spring and summer of 2002 indicates a possible regional decline in the atmospheric deposition of Hg during that drought year. Possible mechanisms for this decline include decreased volatilization of Hg from soils or lower rates of Hg oxidation in the atmosphere during dry conditions. A seasonal pattern of the highest Hg concentrations in precipitation and wet deposition fluxes in the summer or fall was observed in New Jersey, consistent with studies in Florida and Maryland. The variability in rain water Hg concentrations among all sites except Alloway Creek was greatest in the summer and fall (maximum range of 35-40 pM) than in the winter and spring (20-28 pM) indicating that localized episodic phenomena are responsible for elevated average Hg concentrations in New Jersey rain during these seasons.

The Hg concentrations measured in New Jersey rain during the NJADN project (1999 – 2003) are lower by more than a factor of two than those measured by the NJ DEP during the spring, summer, and fall seasons of 1992-1994 at seven sites around New Jersey. This may indicate a downward trend in atmospheric Hg in the eastern U.S. during the 1990s as has been observed for particulate Hg in New York.

Annual precipitation fluxes of Hg in New Jersey ranged from 11 to 14 $\mu g\ m^{-2}\ y^{-1}$, similar to fluxes measured in Maryland, Delaware and eastern and south central Pennsylvania. However, the higher wet deposition fluxes of Hg in urban/industrial Jersey City and Camden than in suburban New Brunswick and rural Pinelands suggest that in addition to the regional Hg signal, local phenomena are also important to the wet deposition of Hg in New Jersey. NJADN wet deposition fluxes together with nearly synoptic National Atmospheric Deposition Network results for Pennsylvania, show a spatial gradient in Hg deposition with relatively low Hg deposition rates at the central Pennsylvania sites (Cambria and Tioga counties), higher deposition rates in eastern Pennsylvania (Valley Forge), and the highest deposition fluxes in New

Jersey. This west to east increase in Hg wet deposition could be the result of either increasing sources of Hg emissions or changes in atmospheric chemistry at this Mid-Atlantic latitude. The estimated dry particle deposition fluxes of Hg ranged from 0.8 to 2.5 μg m^{-2} y^{-1} which represents 7% to 29% of the total (wet plus dry) deposition. The deposition of reactive gaseous Hg, which could be an important component of the total Hg flux, was not quantified during the NJADN project.

Atmospheric Concentrations and Deposition of Nitrate and Phosphate

Nutrient nitrogen and phosphorus derived from anthropogenic combustion sources and intense agriculture are of interest with regard to their roles in the eutrophication of lakes, streams, estuaries and coastal waters. As such the inputs of these elements to surface waters from atmospheric deposition must be assessed in order to manage water bodies in which excessive or nuisance primary production has lead to the degradation of water quality and and the ecosystems they support and restricted the uses of water resources.

The lowest nitrate concentrations measured in New Jersey precipitation as part of the NJADN project were in winter samples at the Pinelands and New Brunswick sites and the highest were in Camden in the summer. All NJADN sites showed higher nitrate concentrations in the spring and summer than fall and winter. Average seasonal nitrate concentrations in rain collected at the NJADN sites are similar to those measured at the National Atmospheric Deposition Program's (NADP) Washington's Crossing site, but generally higher than those measured at the NADP's Forsythe Reserve site in southern coastal NJ. The annual wet deposition fluxes of nitrate in NJ ranged from 310 to 420 mg m^{-2} y^{-1} compared with 280 and 210 mg m^{-2} y^{-1} at Washington's Crossing and the Forsythe Reserve, respectively. Precipitation nitrate fluxes measured at NJADN sites are comparable to those (310 to 364 mg m^{-2} y^{-1}) measured at NADP sites in other Mid-Atlantic states including Pennsylvania, Maryland, and New York.

Annual wet deposition fluxes of phosphorus ranged from 5 to 8 mg m^{-2} y^{-1} with no statistically significant differences ($p > 0.9$) among NJADN sites. These fluxes are toward the low end of the range observed around the world (4 to 21 mg m^{-2} y^{-1}), but similar to those measured in Connecticut.

Atmospheric Inputs of Metals to the Lower Hudson River Estuary

Metal inputs to the Lower Hudson River Estuary (LHRE) are dominated by river inputs (Cd, Cu, Pb), sewage treatment plant effluent (Ag), or a combination of the two (Hg). Direct atmospheric deposition accounts for only 2% to 6% of the total inputs. Thus direct deposition of these metals to the surface of the LHRE is not a major source of *total* metal. For all of the metals examined except Cu, the atmospheric deposition flux to the Hudson River watershed was greater than the riverine flux from the watershed indicating significant retention (70% - 81%) of these metals in the aquatic or terrestrial ecosystems of the watershed. The watershed runoff efficiency estimated for Hg (18%) is similar to those estimated for other watersheds in North America. The very high "apparent" runoff of atmospheric Cu indicates significant additional sources of Cu in the Hudson River watershed.

Summary of Findings

- The results of the NJADN study provide an important overview of contaminant concentrations and deposition fluxes in New Jersey and provide benchmark levels for the assessment of spatial and temporal trends and the evaluation of emissions control strategies.
- Atmospheric ΣPCB deposition fluxes (gas absorption + dry particle deposition + wet deposition) increased with proximity to urban areas.
- PAH concentrations and deposition fluxes vary spatially across New Jersey with the highest occurring at the most heavily urban and industrial locations. PAH profiles are statistically similar at nine of the ten NJADN sites, indicating that the mix of sources around New Jersey is the same.
- Fluxes of PAHs and PCBs to the New York-New Jersey Harbor Estuary are estimated to be 2-20 times higher than those to the Great Lakes and Chesapeake Bay.
- Atmospheric deposition fluxes to the New York-New Jersey Harbor Estuary of the organo-chlorine pesticides dieldrin, aldrin, and the HCHs are similar to those received by the Great Lakes, but the inputs of DDTs, chlordanes, and heptachlor are higher in New Jersey than the Great Lakes.
- Inputs of PCBs to the Hudson River Estuary from the upper Hudson River and from wastewater treatment plants are 8-18 times atmospheric inputs, and volatilization of PCBs from the estuary exceeds atmospheric deposition of low molecular weight PCBs.

- Local spatial trends in atmospheric trace element concentrations were observed in New Jersey, but these trends vary by element and are not simply related to land use patterns.
- Wet deposition fluxes of some metals (Cd, Cu, and Pb) in urban areas (New Brunswick, Jersey City, Camden) are elevated with respect to the regional background.
- Higher wet deposition fluxes of Hg in urban/industrial Jersey City and Camden than in suburban New Brunswick and rural Pinelands suggest that local phenomena are important to the wet deposition of Hg in New Jersey.
- NJADN deposition fluxes together with nearly synoptic results from the National Atmospheric Deposition Network indicate a west to east increase in Hg wet deposition in the Mid-Atlantic region with the highest deposition fluxes in New Jersey.

Recommendations for further study

1. Basic research is needed to provide a more robust understanding of the physics of dry particle deposition which can account for significant deposition fluxes of organic and inorganic contaminants. Specific issues include the factors that control the deposition velocities of various sized aerosols and the importance and sampling of large particles in urban areas.
2. Local transport modeling and source apportionment studies should be supported and used to identify the major emissions sources of PCBs to the atmosphere.
3. The atmospheric chemistry associated with the oxidation of Hg in the atmosphere during clear sky conditions and precipitation events needs continued attention and should be linked to studies of heterogeneous reaction mechanisms and secondary organic aerosol formation as well as the production of reactive oxygen species associated with photochemical smog.
4. The assessment of reactive gaseous mercury (RGM) as an important component of the total atmospheric deposition of mercury is needed throughout the Northeastern U.S.
5. The quantification and identification of organic N and its sources in the atmosphere is needed to complement extensive research and monitoring of inorganic N.
6. Assessments of the concentrations and deposition fluxes of emerging atmospheric contaminants such as brominated compounds are needed in the Mid-Atlantic region.
7. Studies focused on the evaluation of the watershed retention and runoff and ecosystem impacts of atmospheric contaminants are needed to evaluate the real impacts of atmospheric deposition as a major non-point source of contaminants to surface waters.

CONTENTS

* **Paul Brunciak** was killed in a tragic swimming accident on November 20, 2000 in Australia within two months of the completion of his Ph.D. thesis. He assisted in the initial development of NJADN and its implementation.

List of Tables

List of Figures

I. Network Objectives and Methods

I.A. Description of the New Jersey Atmospheric Deposition Network

I.A1. Introduction

Wet deposition via rain and snow, dry deposition of fine and coarse particles, and gaseous air-water exchange are the major atmospheric pathways for persistent organic pollutant (POP) input to the Great Waters such as the Great Lakes and Chesapeake Bay *(1-3)* (**Figure 1**). Direct and indirect (runoff) atmospheric deposition is also of major importance to the accumulation of trace elements such as mercury and major nutrients in surface water ecosystems. The Integrated Atmospheric Deposition Network (IADN) operating in the Great Lakes *(4, 5)* and the Chesapeake Bay Atmospheric Deposition Study (CBADS) *(6)* were designed to capture the

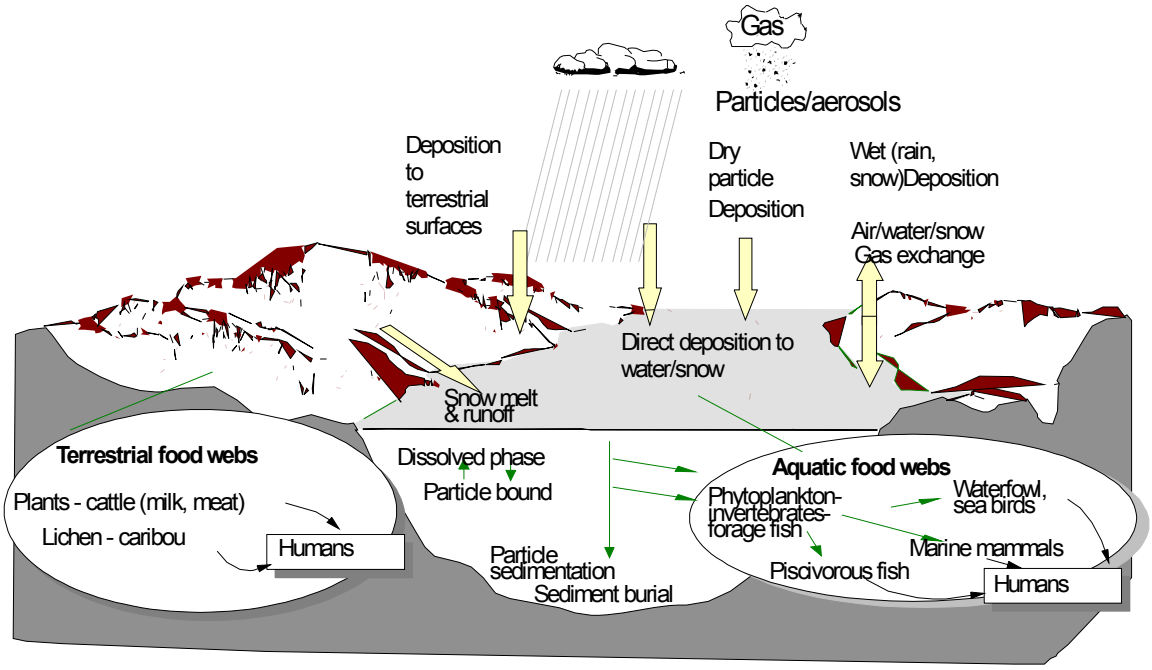

Figure 1. Aquatic and terrestrial ecosystem linkages to atmospheric contaminant cycles.

regional atmospheric signal, and thus sites were located in background areas away from local sources. However, many urban/industrial centers are located on or near coastal estuaries (e.g., Hudson River Estuary and NY Bight) and the Great Lakes. Emissions of pollutants into the

urban atmosphere are reflected in elevated local and regional pollutant concentrations and localized intense atmospheric deposition that is *not* observed in the regional signal *(4, 5)*. The southern basin of Lake Michigan, as one such location, is subject to contamination by air pollutants such as polycyclic aromatic hydrocarbons (PAHs), polychlorinated biphnyls (PCBs), Hg and trace metals *(1-3)* because of its proximity to industrialized and urbanized Chicago, IL and Gary, IN. Concentrations of PCBs and PAHs are significantly elevated in the Chicago and coastal lake area as compared to the regional signal *(7-10)*. Higher atmospheric concentrations are ultimately reflected in increased precipitation *(11)* and dry particle fluxes of PCBs and PAHs *(12)* and trace metals *(13, 14)* to the coastal waters as well as enhanced air-water exchange fluxes of PCBs *(15)*. The Chesapeake Bay also experiences enhanced concentrations of atmospheric contaminants when winds blow from the urbanized and industrialized regions surrounding Baltimore *(16, 17)*.

Processes of wet and dry deposition and air-water exchange of atmospheric pollutants reflect loading to the water surface directly. This is especially important for aquatic systems that have large surface areas relative to watershed areas (e.g., Great Lakes; coastal seas). Also, water bodies may be sources of contaminants to the local and regional atmosphere representing losses to the water column and inputs to the local atmosphere. This has been demonstrated in the NY/NJ Harbor Estuary for PCBs and nonylphenols. However, many aquatic systems have large watershed to lake/estuary areas emphasizing the importance of atmospheric deposition to the watershed (forest, grasslands, crops, paved areas, and wetlands) and the subsequent leakage of deposited contaminants to the downstream water body (**Figure 1**). Most lakes and estuaries in the Mid-Atlantic States have large watershed/water area ratios (e.g., Lower Hudson River Estuary; Chesapeake Bay) emphasizing the potential importance of atmospheric pollutant loading to the watershed and subsequent release to rivers, lakes and estuaries.

I.A2. Objectives

Atmospheric deposition of many organic and inorganic contaminants to aquatic and terrestrial systems in the Mid-Atlantic States is potentially important relative to other source pathways. Experience in the North American Great Lakes and in the Chesapeake Bay show that atmospheric deposition of toxic chemicals, metals and nutrient nitrogen represents an important, and frequently, the dominant source of contaminants to these systems. The New Jersey

Atmospheric Deposition Network (NJADN) was established in October 1997 (i) to support the atmospheric deposition component of the NY/NJ Harbor Estuary Program; (ii) to support the Statewide Watershed Management Framework and the National Environmental Performance Partnership System (NEPPS) for New Jersey; (iii) to assess the magnitude of toxic chemical deposition throughout the State; and (iv) to assess in-state versus out-of-state sources of air toxic deposition. The NJADN design was based on the well-developed experience in the Great Lakes and Chesapeake Bay, and was a collaborative effort of Rutgers University, the New Jersey Department of Environmental Protection (NJDEP), the Hudson River Foundation, and NJ Sea Grant College Program (NOAA). NJADN was a *research and monitoring* network designed to provide scientific input to the management of the various affected aquatic and terrestrial resources.

I.A3. Network History

The New Jersey Atmospheric Deposition Network (NJADN) was initiated in October 1997 with the establishment of a suburban master monitoring and research site at the New Brunswick meteorological station in Rutgers Gardens near Rutgers University. In February 1998, an identical site was established at Sandy Hook to reflect the marine influence on the atmospheric signals and deposition at a coastal site on the NY-NJ Harbor Estuary (HE) and Raritan Bay. In July 1998, a site was established at the Liberty Science Center in Jersey City to reflect the urban/industrial influence on atmospheric concentrations and deposition in the area of the HE. The Hudson River Foundation and the NJ Sea Grant Program funded these initial efforts.

In late 1998, the NJ Department of Environmental Protection (NJDEP) funded a major expansion of NJADN **(Figure 2).** NJADN (total of ten sites) included sites from Chester in the northwest sector of New Jersey to Cape May County on Delaware Bay, and from Tuckerton on the eastern shore north of Atlantic City to Camden in the heart of the urban-industrial complex of Camden-Philadelphia. An attempt was made to establish another site north of New York City with the assistance of US EPA Region II funding through the Hudson River Foundation, but suitable sites and/or collaborators were not found that satisfied established criteria. We suggest that the Chester site, located in a clean air vector for New Jersey, provided the data necessary to assess upwind effects. As part of another study on potential PCB emissions from stabilized

harbor sediment, additional air sampling was conducted from November 1999 to December 2000 at Bayonne, NJ. Sampling at this site was suspended in December 2000 until dredged sediment was applied on land in the summer of 2001.

In June 2001, NJADN operations were scaled back to include New Brunswick, Camden, and Pinelands sites. Under the continuation agreement with the NJDEP, a fourth site was established near Alloway Creek in Salem County to support flux estimates to the low salinity zones of the Delaware River estuary. Sampling at this site began in January 2002. This report is concerned with all of the atmospheric measurements of organic compounds made since the

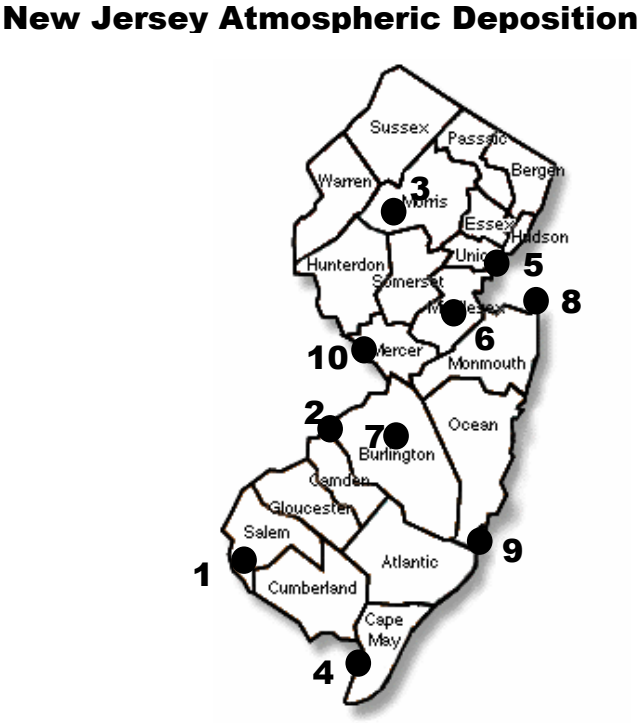

Figure 2. Collection sites of the New Jersey Atmospheric Deposition Network.

beginning of NJADN and the measurements of inorganic analytes made since the network expansion in 1999 until January 2003. Atmospheric measurements of inorganic analytes for some NJADN sites in 1997 and 1998 are available in the Reports of Y. Gao to the Hudson River Foundation and New Jersey Sea Grant.

I.A4. Site Locations and Land Use

The ten NJADN sites were Alloway Creek (Hancocks Bridge, NJ), Camden, Chester, Delaware Bay (Cape May County), Jersey City (Liberty Science Center), New Brunswick, Pinelands, Sandy Hook, Tuckerton, and Washington's Crossing. The locations and land use descriptors for each site are shown in Table 1.

Table 1. NJADN site locations, symbols, and land use.

Map #	Location	Symbol	Long/Lat	Land Use
1	Alloway Creek	AC	39.52N,75.51W	Wetlands
2	Camden	CC	39.93N,75.12W	Urban
3	Chester	XQ	40.79N,74.68W	Suburban
4	Delaware Bay	DB	39.05N,74.93W	Coastal
5	Jersey City	JC	40.71N,74.05W	Urban
6	New Brunswick	NB	40.48N,74.43W	Suburban
7	Pinelands	PL	39.96N,74.63W	Forested
8	Sandy Hook	SH	40.46N,74.00W	Coastal
9	Tuckerton	TK	39.50N,74.37W	Coastal
10	Washington's Crossing	WC	40.29N,74.87W	Suburban

I.A5. Analytes

Target analytes for this study include a range of semi-volatile organic compounds and trace elements that are known to adversely affect aquatic and terrestrial ecosystems and human health, either through direct exposure or food chain exposure **(Table 2).** The organic compounds derive from combustion processes (PAHs), remobilization of chemicals from historical uses in urban-industrial centers (PCBs), from past agricultural practices (DDT, DDE), and chemicals used today as pesticides but in areas mostly removed from New Jersey (chlordanes). The trace metals specified are mostly closely associated with combustion processes (power plants, incinerators, automobiles, trucks), mechanical wear and tear on automobiles and trucks, and soils. Nutrient nitrogen derived from anthropogenic combustion sources and intense agriculture is especially of interest in coastal areas and estuaries as nitrogen species are thought to dominate eutrophication in estuarine and coastal waters.

Table 2. Target analytes for atmospheric samples in the NJADN. Organic analytes include polycyclic aromatic hydrocarbons (PAHs), polychlorinated biphnyls (PCBs), and organo-chlorine pesticides (OCs).

PAHs	PCBs	OCs
Fluorene	18	HCB
Phenanthrene	16+32	Heptachlor
Anthracene	28	4,4 DDE
1Methylfluorene	52+43	2,4 DDT
Dibenzothiophene	41+71	4,4 DDT
4,5-Methylenephenanthrene	66+95	Mirex
Methylphenanthrenes	101	Oxychlordane
Methyldibenzothiophenes	87+81	trans Chlordane
Fluoranthene	110+77	MC5
Pyrene	149+123+107	cis Chlordane
3,6-Dimethylphenanthrene	153+132	trans Nonachlor
Benzo[a]fluorene	163+138	cis Nonachlor
Benzo[b]fluorene	187+182	
Retene	174	
Benzo[b]naphtho[2,1-d]thiophene	180	
Cyclopenta[cd]pyrene	Sum of PCBs	
Benz[a]anthracene	Homologue Group	
Chrysene/Triphenylene	3	
Naphthacene	4	
Benzo[b+k]fluoranthene	5	
Benzo[e]pyrene	6	
Benzo[a]pyrene	7	
Perylene	8	
Indeno[1,2,3-cd]pyrene	9	
Benzo[g,h,i]perylene	77 PCB	
Dibenzo[a,h+a,c]anthracene	congeners in	
Coronene	all	

Trace Metals: Ag, Al, As, Cd, Co, Cr, Cu, Fe, Mg, Mn, Ni, Pb, Pd, Sb, V, Zn
Mercury (Hg)
Nutrient Nitrogen (NO_3^- + NO_2^-)
Phosphate
Chloride, Sulfate

I.B. Sampling and Analytical Methodologies

I.B1. Sampling Instrumentation

The NJADN sampling methods are outlined in Table 3. For organic compounds, air samples (24 hours) were collected using a modified high volume air sampler (Tisch Environmental, Village of Cleves, OH, USA) with a calibrated airflow of ~0.5 m^3 min^{-1}. Quartz fiber filters (QFFs; Whatman) were used to capture the total particulate phase and polyurethane foam plugs (PUFs) were used to capture the gaseous phase. QFFs were weighed before and after sampling to determine total suspended particles (TSP). Wet-only integrating precipitation samplers were employed (Meteorological Instrument Center, MIC, Richmond Hill, Ontario, Canada) at all but the Delaware Bay and Washington's Crossing sites to collect integrated precipitation samples over 12-24 days in a 0.212 m^2 stainless steel funnel that drained through a glass column containing XAD-2 resin.

Table 3. NJADN Sampling Instrumentation

Precipitation Collectors:

MIC-B:	Organic contaminants: wet-only integrating samplers with stainless-steel surface (0.212 m^2), every 24 days; 30cm × 1.5 cm I.D. glass column filled with XAD-2 adsorbent. Inorganic contaminants: wet-only integrating samplers with polyethylene funnels (0.018 m^2) and bottles (trace elements, nitrate, phosphate) or glass funnels (0.019 m^2) and Teflon bottles (Hg) supported by an acrylic insert.

Air Samplers:

Organics:	Modified Hi-Vols (Graeseby); Quartz fiber filter; polyurethane foam plug (PUF) 24 hours every 12 day
Metals:	Caltech Low Vol sampler; 20 L/min (split); PM2.5 cutoff Teflon filters for particulate $PM_{2.5}$, Trace Element and Hg
Meteorology:	Wind speed and direction (Mean over 24 hour sampling period) Temperature (Mean over 24 hour sampling period) Rainfall (Amount over 24-day sampling period) Back Trajectories for Selected Sampling Days

For inorganic analytes, integrated rain samples were collected using automatic rain collectors (MIC), fitted with Keeler-type (Landis and Keeler, 1997) acrylic inserts to support polyethylene funnels and collection bottles for trace elements, nitrate, and phosphate samples, and glass funnels and Teflon collection bottles for Hg samples. Fine aerosols were collected on Teflon filters (Gelman) held in acid-cleaned polypropylene cartridges by pulling air through a Caltech low volume impacter at a flow rate to achieve an aerodynamic particle diameter cutoff of 2.5 μm (*24*, *25*).

The sampling intervals covered in this report for each analyte group are listed in Tables 4 and 5. At each site, organic chemicals (PCBs, PAHs, organo-chlorine pesticides) were measured in precipitation and gaseous and particulate phases and trace elements are being measured in fine aerosols (PM2.5). Trace elements, nitrate, and phosphate were measured in precipitation at four NJADN sites with some coverage at Sandy Hook and Tuckerton by Y. Gao. Total suspended particulate matter (TSP) masses were also determined for the majority of sites. Atmospheric samples of gas and particulate phases (organics) were collected at all sites one day (24 hours) every 12th day, and wet-only integrated precipitation was collected over 12-24 days. Meteorological data were obtained from established meteorological stations (New Brunswick (Rutgers Gardens/PAMS site, Tuckerton (Rutgers Marine Station), from area airports (JFK, Newark, Philadelphia), and from other regional NOAA sites. Three-day back trajectories were calculated for each day using NOAA's HYSPLIT Model at locations in northern, middle and southern New Jersey.

Table 4. Atmospheric sampling intervals for organic compounds (gases, particles, precipitation).

Site	Sampling interval
Alloway Creek	January, 2002 – January, 2003
Camden	July, 1999 – August, 2002
Chester	May, 2000 – May, 2001
Delaware Bay	March, 2000 – May, 2001
Jersey City	July 1998 – May, 2001
New Brunswick	October, 1997 – November, 2002
Pinelands	June, 1999 – August, 2002
Sandy Hook	February, 1998 – January, 2001
Tuckerton	November, 1998 – May, 2001
Wash. Crossing	November, 1999 – May, 2001

Table 5. Precipitation and fine aerosol (PM2.5) sampling intervals for inorganic analytes.

Elements	Phase	Site	Sampling interval
TMs, N	Precip.	Alloway Creek	January, 2002 – January, 2003
		Camden	January, 2000 – August, 2002
		Jersey City	September, 1999 – February, 2001
		New Brunswick	July, 1999 – October, 2002
		Pinelands	December, 1999 – August, 2002
P	Precip.	Camden	January, 2000 – June, 2001
		Jersey City	September, 1999 – February, 2001
		New Brunswick	July, 1999 – June, 2001
		Pinelands	December, 1999 – June, 2001
Hg	Precip.	Alloway Creek	January, 2002 – January, 2003
		Camden	March, 2000 – August, 2002
		Jersey City	November, 1999 – May, 2001
		New Brunswick	November, 1999 – October, 2002
		Pinelands	February, 2000 – August, 2002
TMs, Hg	PM2.5	Alloway Creek	January, 2002 – January, 2003
		Camden	September, 1999 – July, 2002
		Chester	August, 2000 – April, 2001
		Delaware Bay	March, 2000 – May, 2001
		Jersey City	February, 2000 – January, 2001
		New Brunswick	February, 2000 – August, 2002
		Pinelands	September, 1999 – August, 2002
		Sandy Hook	February, 2000 – January, 2001
		Tuckerton	August, 2000 – May, 2001
		Wash. Crossing	November, 1999 – May, 2001

I.B2. Analytical Methods

Organic compounds. Samples were injected with surrogate standards before extraction. For PCBs the surrogates were 3,5 dichlorobiphenyl (#14), 2,3,5,6 tetrachlorobiphenyl (#65), 2,3,4,4',5,6 hexachlorobiphenyl (#166), and for PAHs the surrogates were d_{10}-anthracene, d_{10}-fluoranthene, and d_{12}-benzo[e]pyrene. Due to interferences with PCB 14, PCB 23 (2,3,5-trichlorobiphenyl) was added as a surrogate to samples collected after December, 1999. Samples were extracted in Soxhlet apparati for 24 hours in petroleum ether (PUFs), dichloromethane (QFFs), and 1:1 acetone:hexane (XAD). For XAD samples, the extracts were then liquid-liquid

extracted in 60 mL Milli-Q® water. The aqueous fractions were back-extracted with 3 × 50 mL hexane in separatory funnels with 1 g sodium chloride. These extracts, as well as extracts from all other types of sampling media, were then reduced in volume by rotary evaporation and subsequently concentrated via N_2 evaporation. The samples were then fractionated on a column of 3% water-deactivated alumina. The PCB fraction was eluted with hexane, concentrated under a gentle stream of nitrogen gas, and injected with internal standard containing PCB #30 (2,4,6-trichlorobiphenyl) and #204 (2,2',3,4,4',5,6,6'-biphenyl) prior to analysis by gas chromatography (GC). PCBs were analyzed on an HP 5890 gas chromatograph equipped with a ^{63}Ni electron capture detector using a 60-m 0.25 mm i.d. DB-5 (5% diphenyl-dimethyl polysiloxane) capillary column with a film thickness of 0.25 μm *(19)*.

The PAH fraction was eluted with 2:1 dichloromethane:hexane, and injected with internal standard solution consisting of d_{10}-phenanthrene, d_{10}-pyrene, and d_{12}-benzo[a]pyrene. The PAHs were analyzed on a Hewlett Packard 6890 gas chromatograph (GC) coupled to a Hewlett Packard 5973 Mass Selective Detector (MSD) operated in selective ion monitoring (SIM) mode. The column used was a 30 m × 0.25mm i.d., J&W Scientific 122-5062 DB-5 (5% diphenyl-dimethylpolysiloxane) capillary column with a film thickness of 0.25 μm. The PAH analysis method used was not a standard EPA method and did not allow for the separate quantification of the two benzofluoranthene isomers nor of the two benzanthracene isomers. These compounds are therefore reported as two separate sums: benzo[b+k] fluoranthene, and benz[a,h + a,c] anthracene.

Organo-chlorine compounds, were analyzed in fractionated sample extracts by gas chromatograph-mass spectrometry using a 60 meter DB-5 column, operating in negative chemical ionization mode. The organochlorine pesticide chromatographic peaks were identified using selective ion monitoring and quantified by the use of authentic calibration standards.

Trace Elements-Precipitation. Trace metal concentrations in rain were measured by ICP-MS (Finnigan Element) after acidification of samples with 2% v/v concentrated nitric acid. The magnetic sector mass analyzer in the HR-ICP-MS is capable of rapidly scanning the full mass range of the periodic table. The Element ICP-MS has three resolution settings (R=mass/delta mass at 10% peak height): low resolution (LR: R=300), medium resolution (MR: R=4300), and high resolution (HR: R=9300). Samples are analyzed in the solution phase and introduced to the

plasma using a μFlow PFA nebulizer (Elemental Scientific, Omaha, NE) adapted to fit a glass spray chamber. The free aspirating μflow nebulizer operates at flow rates of 50 to 100mL/min providing low blanks and excellent detection limits for small volume samples (<1mL). This instrument provides the high sensitivity (1 million cps/ppb In) and resolving powers necessary to separate most common interferences.

In our method, low (Ag, Cd, Mg, Pb, Pd, Sb), medium (Al, first row transition metals), and high (As) resolution powers were used. External standardization using indium as an internal drift monitor gives concentrations for all analytes, which generally agree within ± 10% of values determined using standard additions. Accuracy was determined with a combined standard (16 elements) diluted with nitric acid. Standard curves had r^2 values that were ≥ 0.997 for all elements. Method blanks contributed <1% to 10% of volume weighted mean trace element concentrations in precipitation (see section III.B4). Replicate analyses had RSDs of < 15%.

Nitrate-precipitation. Precipitation samples collected from 7/13/99 to 6/30/00 (except at Jersey City, 9/3/99 to 7/24/00) were analyzed for NO_3^- by ion chromatography (IC) and samples collected since 6/30/00 (7/24/00 Jersey City) were analyzed for $NO_3^- + NO_2^-$ by colorimetric assay of NO_2^- after reduction of NO_3^- to NO_2^- by metallic Cd (Parsons et al., 1984). The detection limit for the IC method was 1.9 μM. Standard solutions of KNO_3 were used to establish the accuracy of the IC method ($r^2 > 0.995$). The detection limit for the colorimetric method was 0.2 μM. Analytical accuracy of the colorimetric assay was established with standard solutions of $NaNO_2$ and standard curves had r^2 values of > 0.999. The efficiency of NO_3^- reduction (80 -90%) was determined with KNO_3 standards. Replicate analyses by both methods gave coefficients of variation of < 5%.

Phosphate-precipitation. Precipitation samples were reacted with ammonium molybdate and antimony potassium in an acid medium to form an antimony-phospho-molybdate complex. This complex was then reduced with ascorbic acid. Concentrations of phosphorus were quantified using an AutoAnalyzer II system (EPA Standard Method 365.1) via the colorometric method developed by Menzel and Corwin (1965)- EPA Standard Method 365.3.

Mercury-precipitation. Total Hg was measured in 150 ml rain subsamples by $SnCl_2$ reduction and cold vapor atomic fluorescence spectrometry (CVAFS; Bloom and Fitzgerald, 1988) after oxidation with bromine monochloride (Bloom and Crecelius, 1983). Analytical accuracy was established with measurements of gaseous Hg° injected directly into the analytical gas stream and trapped on the analytical gold column. Measurements of standard gaseous Hg injections yielded standard curves with r^2 values of ≥ 0.999. The efficiency of aqueous Hg reduction and trapping (100%) was checked through the analysis of aqueous $HgCl_2$ solutions. The detection limit for total Hg in precipitation was 85 pg L^{-1} (0.42 pM). Replicate analyses of Hg samples varied by no more than 20%. Two rain samples collected in Belvidere, NJ as part of a separate project were split and analyzed for total Hg by Frontier Geosciences, Inc. in Seattle, WA. The results of these two analyses were 29% higher and 35% lower than those obtained at Rutgers indicating that the concentrations of Hg in rain samples collected as part of NJADN are comparable to those collected as part of the National Atmospheric Deposition Program's Mercury Deposition Network within an uncertainty of about 30%.

Trace Elements and Mercury in Fine Aerosols (PM2.5). PM2.5 samples collected from 7/13/99 to 3/13/00 were digested with 20 ml concentrated sulfuric and nitric acids (3:7, H_2SO_4:HNO_3) in Teflon vials for 12 h at 60°C. This method was found to have a high blank for some metals (Cu, Zn) and samples collected after 3/13/00 were digested with 2 ml concentrated nitric and hydrofluoric acids (95:5, HNO_3:HF) in Teflon vials for 6 h at 100°C. After digestion, some of the samples were split for trace metal (25%) and mercury (75%) analysis. For the trace metal splits, the filters were rinsed and removed and the concentrated acids were evaporated. Residues were re-dissolved with 1 ml 0.1 M HNO_3. Trace metal concentrations in the PM2.5 digestates were measured by ICP-MS as described above except that accuracy was determined using a combined standard that reflected the proportions and concentrations of metals in fine aerosols. Method blanks contributed 1% to 23% of average PM2.5 trace element concentrations (see section III.B4). Total Hg concentrations in the PM2.5 digestates were measured as described above for rain except that the digestate was diluted with 150 ml ultrapure water before reduction. The detection limit for Hg in the PM2.5 samples was 3.7 pg m^{-3}.

I.C. Framework for Estimating Atmospheric Deposition

Atmospheric deposition may occur generally by dry particle deposition, wet deposition via rain and snow, and gaseous chemical partitioning into the water and onto terrestrial surfaces from the atmosphere. In this study, deposition to the water surface of the NY-NJ Harbor Estuary is calculated as the sum of dry particle deposition, wet deposition, and gaseous chemical absorption into the water column. When applied to the State of New Jersey as a whole, only wet and dry particle deposition fluxes to the inland regions of New Jersey are estimated in this report. The framework for estimating the contribution of atmospheric deposition for target chemical species to the inland water management areas of New Jersey must await the development of a new quantitative framework based on atmosphere-vegetation/soil interactions and the development of a NJ-specific model under a separate project.

I.C1. Dry Particle Deposition

Dry particle deposition describes the process of aerodynamic transport of a particle to the near-surface viscous sub-layer where diffusion, turbulent diffusion and gravitational settling deliver the particle to the surface. Water surfaces generally act as perfect receptors and no "bounce-off" occurs, whereas terrestrial surfaces are less efficient. Some vegetation is 'sticky' and retains particles falling or turbulently mixed to its surface. Particle deposition depends on properties of the atmosphere (wind speed, humidity, stability, temperature), the water surface (waves, spray, salt content) or dry land surface, and the depositing particles (size, shape, density, reactivity, solubility, hygroscopicity). The last may be especially important as humidity nears 100% near water surfaces permitting particles to absorb water, increase in density and size, and achieve higher deposition velocities (V_d). The dry deposition flux is calculated as:

$$\mathbf{Flux}_{\mathbf{dry\ part}}\ \mathbf{(ng\ m^{-2}\ d^{-1})} = \mathbf{V_d} \times \mathbf{C_{part}}$$

where C_{part} is the particulate concentration of a chemical in the atmosphere (ng m^{-3}). Zufall et al. (*18*) provide convincing evidence (**Figure 3**) that particle deposition is dominated by large particles although atmospheric particle size distributions are dominated by particles less than 1 μm mass median diameter (mmd). Thus we selected a value for V_d of 0.5 cm s^{-1} to reflect the disproportionate influence of large particles in dry deposition, especially in urbanized and

industrialized regions (see Franz et al., ref. 11). The dry particle deposition fluxes we estimated therefore represent total dry particle deposition of both organic contaminants (collected from whole air) and metals (collected as PM2.5) since both types of samples miss large particles.

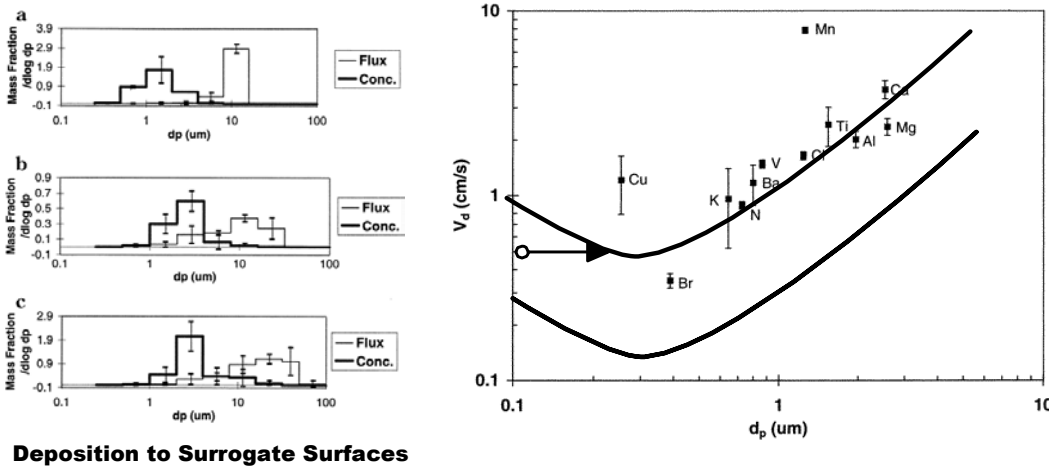

Figure 3. Relationship between particle size and deposition velocity for a range of elements in Lake Michigan aerosols (from Zufall et al., ref. 18).

I.C2. Wet Deposition

Wet deposition describes the process by which gases and particles are scavenged from the atmosphere (in cloud or below cloud) by raindrops and delivered by falling hydrometeors to the ground. The deposition fluxes of gases and particles by rain can be estimated from the fraction of the chemical in the particle and gas phase (f_{part}, f_{gas}), the total atmospheric concentration (C_T), the precipitation intensity (P), Henry's law constant as a function of temperature (H), and the particle scavenging coefficient (W_p) **(Figure 4)**. However, the best way available to estimate wet deposition is to collect all rainfall in suitable samplers, measure the contaminant concentrations, and calculate periodic wet deposition fluxes. Daily wet deposition fluxes are estimated for each sampling interval:

$$\mathbf{Flux_{wet,total}\ (ng\ m^{-2}\ d^{-1}) = C_{precip}\ (ng\ m^{-3})\ x\ Precipitation\ Intensity\ (m\ d^{-1})}$$

For seasonal and annual wet deposition fluxes, volume-weighted mean concentrations (VWM) are used as C_{precip} and VWM = total mass of chemical divided by total precipitation volume.

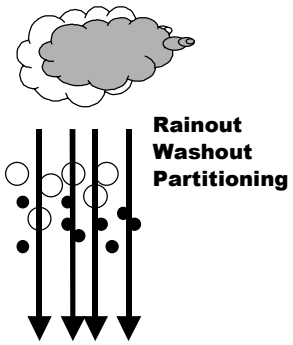

$$F_{w,gas} = W_{gas} \times f_{gas} \times C_T \times P \times SA$$

where $W_{gas} = RT/H$ (function of T)

$$F_{w,part} = W_{part} \times f_{part} \times C_T \times P \times SA$$

where $W_{part} = \sim 1\text{-}5 \times 10^5$

$$Flux_{wet,Total} = VWM\ Conc \times Precipitation\ Intensity$$

$(ng/m^2\ day)$ (ng/m^3) (seasonal, m)

Figure 4. Estimation of wet deposition fluxes.

I.C3. Diffusive Air-Water Exchange

The concepts of air-water exchange and mass transfer of organic chemicals across water surfaces have been described in detail elsewhere (see Eisenreich et al. (*19*)). Diffusive air-water exchange refers to the transfer of chemical across an air-water interface and may be visualized as diffusive transfer of a chemical across a near-stagnant layer of 0.1 to 1.0 mm thickness. At low wind speeds, insufficient wind energy exists to mix the air and water films or boundary layers, and a stagnant boundary layer is established (Stagnant Two-Film Model). Higher wind speeds generate more turbulence in the boundary layers, parcels of air and water are forced to the surface, and exchange is dependent on the renewal rate of air and water parcels. In highly turbulent seas, gas exchange is enhanced by breaking waves and bubble ejection. Under turbulence and wind conditions normally occurring in estuaries and lakes, the first two models are most applicable although wind extremes may be very important. The gas-phase concentration in the atmosphere (C_g) attempts to reach equilibrium with the concentration of dissolved gas in water (C_W). When equilibrium is achieved, the ratio of the gas activities in air and water are constant at a given temperature and are represented by Henry's Law constant (H): ($H = C_g\ C_W^{-1}$; Pa m^3 mol^{-1}). The direction of chemical transfer is from the water to the air when

the fugacity in the water exceeds the fugacity (gas phase concentration) in air and is referred to as volatilization. Chemical transfer from the air to the water occurs when the fugacity (i.e., activity) in the air (C_a $(RT)^{-1}$) exceeds the chemical fugacity in water ($C_W H^{-1}$) and is referred to as gas absorption. The processes of gas absorption and volatilization occur simultaneously, and their difference contributes to the net flux. The magnitude of mass transfer, $flux_{net}$ (mass m^{-2} d^{-1}), is determined by a mass transfer coefficient or piston velocity (K, m d^{-1}) and the concentration difference: $flux_{net} = K (\Delta C)$ where ΔC is the concentration or activity gradient across the interface. Thus, the direction and magnitude of gas transfer are a function of the free concentrations in air and water (activity gradient), wind speed (water side turbulence), interfacial temperature, characteristics of the water (water chemistry; surface films), and the physico-chemical properties of the chemical compound (Henry's Law constant; diffusivity).

The equations describing the flux of a chemical across the air-water interface are provided in **Figure 5**. For the NY-NJ Harbor Estuary, we estimated only the gaseous chemical absorption across the water surface. The relevant equation then becomes:

$$\textbf{Flux}_{A/W}\ (\textbf{ng m}^{-2}\ \textbf{d}^{-1}) = K_{ol}\ (C_w - C_g\ RT/H)$$

where the terms are described as in Figure 5. A negative sign on the flux indicates that the *net* direction of transfer is from the air to the water. The mass transfer coefficient is dependent on turbulent mixing in the boundary layers on either side of the air-water interface which is highly correlated with wind speed. In addition, the K_{ol} is dependent on Henry's law constant, which is a function of temperature, and the diffusivity of the compound in air and water. Of course, the direction and magnitude of air-water exchange fluxes is dependent on Henry's law constant, the concentration gradient and the value of the wind-driven mass transfer coefficient. Examples of the application of the calculation can be found in Zhang et al. (14), Nelson et al. (15), Bamford et al. (20), Totten et al. (21), and Gigliotti et al. (22).

$$Flux_{A/W} = K_{ol} (C_w - C_g RT/H)$$

$$1/K_{ol} = 1/k_w + (RT/k_{air}\ H$$

Kol = overalll gas mass transfer coefficient
k_w,k_{air} = water-side and air-side mass transfer coefficients
(Kol, k_w,k_{air} are a strong function of wind speed, sea state, H)
H = Henry's law constant = C_{gas}/C_w at equilibrium
(strong function of Temp)

$Temp_{water}$ = 0 - 30 °C
Wind Speeds = 0 - 10 m/s
H varies for compound,
and corrected for T, Salinity

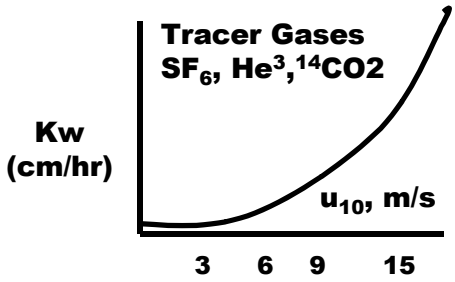

Figure 5. Diffusive air-water exchange of semi-volatile organic contaminant gases.

It is important that the corresponding volatilization term also be estimated for mass budget calculations but this requires dissolved water concentrations of the target chemical. Later in this report, we will provide results of intensive field measurements of air and water concentrations measured simultaneously in the HE in July 1998, and the resulting absorption, volatilization and *net* air-water exchange fluxes for PCBs and PAHs. Technically, only gas absorption contributes to atmospheric deposition. In the future, we will estimate the seasonal and annual cycle of air-water exchange fluxes (absorption, volatilization and *net* air-water exchange) for PCBs and PAHs utilizing water concentrations measured in all seasons by our group and as part of the New York/New Jersey Harbor Contaminant Assessment and Reduction Project (CARP; 23).

I.D. References

(1) Baker, J. E. In *Atmospheric Deposition of Contaminants in the Great Lakes and Coastal Waters*; Baker, J. E., Ed.; SETAC Press: Pensacola, FL., 1997, 451 p.
(2) Eisenreich, S. J.; Baker, J. E.; Zhang, H.; Simcik, M. F.; Offenberg, J. H.; Totten, L. *Environ. Sci. Tech.* 2000, In Review.

(3) Ondov, J. M.; Caffrey, P. F.; Suarez, A. E.; Borgoui, P. V.; Holsen, T.; Paode, R. D.; Sofuoglu, S. C.; Sivadechathep, J.; Lu, J.; Kelly, J.; Davidson, C. I.; Zufall, M. J.; Keeler, G. J.; Landis, M. S.; Church, T. M.; Scudlark, J. *Environ. Sci. Tech.* 2000, In Review.
(4) Hoff, R. M.; Strachan, W. M. J.; Sweet, C. W.; Chan, C. H.; Schakleton, M.; Bidleman, T. F.; Brice, K. A.; Burniston, D. A.; S., C.; Gatz, D. F.; Harlin, K.; Schroeder, W. H. *Atmos. Environ.* 1996, *30*, 3505-3527.
(5) Hillery, B. R.; Simcik, M. F.; Basu, I.; Hoff, R. M.; Strachan, W. M. J.; Burniston, D.; Chan, C. H.; Brice, K. A.; Sweet, C. W.; Hites, R. A. *Environ. Sci. Tech.* 1998, *32*, 2216-2221.
(6) Cotham, W. E.; Bidleman, T. F. *Environ. Sci. Tech.* 1995, *29*, 2782-2789.
(7) Simcik, M. F.; Zhang, H.; Franz, T.; Eisenreich, S. J. *Environ. Sci. Tech.* 1997, *31*, 2141-2147.
(8) Harner, T.; Bidleman, T. F. *Environ. Sci. Tech.* 1998, *32*, 1494-1502.
(9) Green, M. L.; Depinto, J. V.; Sweet, C. W.; Hornbuckle, K. C. *Environ. Sci. Tech.* 2000, In Review.
(10) Offenberg, J. H.; Baker, J. E. *Environ. Sci. Tech.* 1997, *31*, 1534-1538.
(11) Franz, T. P.; Eisenreich, S. J.; Holsen, T. M. *Environ. Sci. Tech.* 1998, *32*, 3681-3688.
(12) Paode, R. D.; Sofuoglu, S. C.; Sivadechathep, J.; Noll, K. E.; Holsen, T. M.; Keeler, G. J. *Environ. Sci. Tech.* 1998, *32*, 1629-1635.
(13) Caffrey, P. F.; Ondov, J. M.; Zufall, M. J.; Davidson, C. I. *Environ. Sci. Tech.* 1998, *32*, 1615-1622.
(14) Zhang, H.; Eisenreich, S. J.; Franz, T. P.; Baker, J. E.; Offenberg, J. H. *Environ. Sci. Tech.* 1999, *33*, 2129-2137.
(15) Nelson, E. D.; McConnell, L. L.; Baker, J. E. *Environ. Sci. Tech.* 1998, *32*, 912-919.
(16) Offenberg, J. H.; Beker, J. E. *J. Air & Waste Mngmt. Assoc.* 1999, *49*, 959-965.
(17) Iannuzzi, T. J.; Huntley, S. L.; Bonnevie, N. L.; Finley, B. L.; Wenning, R. J. *Arch. Env. Contam. Tox.* 1995, *28*, 108-117.
(18) Zufall, M.J.; Davidson, C.I.; Caffrey, P.F. Ondov, J.M. *Environ. Sci. Tech.* 1998, *32*, 1623-1628.
(19) Eisenreich, S.J.; Hornbuckle, K.C.; Achman, D.R. In *Atmospheric Deposition of Contaminants to the Great Lakes and Coastal Water*. Baker, J.E., Ed, SETAC Press: Boca Raton, FL, USA, 1997, p 109-136.
(20) Bamford, H.A.; Offenberg, J.H.; Larsen, R.K.; Ko, F.-C.; Baker, J.E. *Environ. Sci. Tech.* 1999, *33*, 2138-2144.
(21) Totten, L.A; Brunciak, P.A.; Gigliotti, C.L.; Dachs, J.; Glenn IV, T.R.; Nelson, E.D.; Eisenreich, S.J. *Environ. Sci. Tech.* 2001, *35*, 3834-3840.
(22) Gigliotti, C.L.; Brunciak, P.A.; Dachs, J.; Glenn IV, T.R.; Nelson, E.D.; Totten, L.A.; Eisenreich, S.J. *Environ. Toxicol. Chem.* 2002, *21*, 235-244.
(23) Contamination Assessment & Reduction Project (CARP), Sources and Loadings of Toxic Substances to New York Harbor, New York State Department of Environmental Conservation, Division of Water, Bureau of Watershed Assessment and Research, 1998.
(24) Camp, D.C., VanLehn, A.L. and Loo, B.W., 1978. EPA-600/2-78-118, U.S. Environmental Protection Agency, ESRL.
(25) Stevens, R.K. and Dzubay, T.G., 1978. EPA-600/2-78-112, U.S. Environmental Protection Agency, ESRL.

II.A. Semi-volatile Organic Compounds: Concentrations, Deposition Fluxes, and Importance to the NY-NJ Harbor Estuary

II.A1. Polychlorinated Biphenyls

Summary

The first estimates of atmospheric deposition fluxes of polychlorinated biphenyls (PCBs) to the Hudson River Estuary are presented. Concentrations of PCBs were measured in air, aerosol, and precipitation at ten sites representing a variety of land-use regimes at regular intervals from October 1997 through January 2003. Highest concentrations in the gas phase were observed at urban sites such as Camden and Jersey City (ΣPCBs averaged 3645, and 1260 pg m^{-3}, respectively). In great portions of the state encompassing forested, coastal, and suburban environments, gas-phase ΣPCB concentrations were essentially the same (averaging 150-220 pg m^{-3}). Atmospheric ΣPCB deposition fluxes (gas absorption + dry particle deposition + wet deposition) ranged from 7.3 to 340 ug m^{-2} y^{-1} and increased with proximity to urban areas. Because the Hudson Estuary is adjacent to urban areas such as Jersey City, it is subject to higher depositional fluxes of PCBs. These fluxes are at least 2-10 times those estimated for the Chesapeake Bay and Lake Michigan. Inputs of PCBs to the Hudson River Estuary from the upper Hudson River and from wastewater treatment plants are 8-18 times atmospheric inputs, and volatilization of PCBs from the estuary exceeds atmospheric deposition of low molecular weight PCBs.

Introduction

Wet deposition via rain and snow, dry deposition of fine/coarse particles, and gaseous air-water exchange are major pathways for persistent organic pollutant (POP) input to the Great Waters such as the Great Lakes and Chesapeake Bay *(1, 2)*. Many urban/industrial centers are located on or near coastal estuaries (e.g., NY-NJ Harbor Estuary, NY Bight, and Delaware River) and the Great Lakes (e.g., Chicago, IL and southern Lake Michigan). Emissions of pollutants into the urban atmosphere are reflected in elevated local and regional pollutant concentrations and localized intense atmospheric deposition that are *not* observed in the regional signal *(3, 4)*. The NY-NJ Harbor Estuary has been impacted by anthropogenic inputs of PCBs from many sources, including wastewater discharges *(5)* and historical contamination of the upper Hudson River *(6)*. Because of its long history of contamination and its economic and environmental importance, the fate and transport of POPs in the NY-NJ Harbor Estuary are areas

of major study *(7-9)*. The New Jersey Atmospheric Deposition Network (NJADN) was established in late 1997 as a research and air monitoring network with the following objectives: (i) to characterize the regional atmospheric levels of hazardous air pollutants, (ii) to estimate atmospheric loadings to aquatic and terrestrial ecosystems, (iii) to identify and quantify regional versus local sources and sinks, and (iii) to identify environmental variables controlling atmospheric concentrations of PCBs, polycyclic aromatic hydrocarbons (PAHs), chlorinated pesticides, trace metals, Hg, and nutrients. The first three sites were located within the Lower Hudson River Estuary: New Brunswick, Jersey City, and Sandy Hook. The NJADN was gradually expanded during 1997-2001 to a total of ten sites representing a variety of land-use regimes.

The NJADN design is based on the well-developed experience in the Great Lakes and Chesapeake Bay. The Integrated Atmospheric Deposition Network (IADN) operating in the Great Lakes *(3, 4)* and the Chesapeake Bay Atmospheric Deposition Study (CBADS) *(10)* were designed to capture the *regional* atmospheric signal, and thus sites were typically located in background areas away from local sources. However, many urban/industrial centers are located on or near water bodies. The southern basin of Lake Michigan and the Chesapeake Bay are two such locations subject to contamination by air pollutants such as PCBs and PAHs, Hg and trace metals *(1)* because of their proximity to industrialized and urbanized areas *(11-20)*. Based on this experience in the Great Lakes and Chesapeake Bay, NJADN was designed to capture both the urban and regional signals of air pollution by locating monitoring sites in urban, suburban, forested, and coastal environments.

In addition to receiving atmospheric inputs of POPs, water bodies may be sources of contaminants to the local and regional atmosphere representing losses to the water column. This has been demonstrated in the NY-NJ Harbor Estuary for PCBs *(21)* and nonylphenols *(22)* and chlorinated dioxins and furans *(23)*. For this reason, the NJADN project also encompassed simultaneous measurements of POPs in the air and water of Raritan Bay (RB) and New York Harbor (NYH) in July of 1998 to estimate the dynamic air-water exchange fluxes of PAHs *(21)* and PCBs *(24)*. The objective of this work is to summarize the NJADN PCB data from October 1997 through January 2003.

Results and Discussion

Gas phase. A summary of the spatial variations in gas-phase PCB concentrations is presented in Figure 6. Gas-phase ΣPCB concentrations vary over more than 2 orders of magnitude from site to site in the region, with highest concentrations typically occurring in the urbanized areas of Camden and Jersey City. At Camden, Jersey City, New Brunswick, and Sandy Hook, gas phase ΣPCB concentrations averaged 3645, 1260, 456, and 430 pg m^{-3}, respectively, over the entire sampling period. In large portions of the area, represented by 6 sites (Alloway Creek, Pinelands, Chester, Delaware Bay, Washington Crossing, Tuckerton) encompassing forested, coastal, and suburban environments, ΣPCB concentrations are essentially the same (averaging 150 to 220pg m^{-3}). These concentrations are similar to those observed from 1996-1998 at remote areas surrounding the Great Lakes, where concentration averages ranged from 63 to 260 pg m^{-3} *(41)*. The similar gas-phase ΣPCB concentrations observed at sites surrounding the Great Lakes and in New Jersey suggests this level of contamination represents a regional (Northeastern United States) background.

High concentrations of gas-phase PCBs at Camden have led to concerns that the sampler there might be influenced by emissions of PCBs from the roof of the Rutgers Camden Library, upon which the sampler is located. We do not believe the roof is a significant source of PCBs for the following reasons. First, levels of PCBs in Camden are similar to levels measured at Swarthmore, PA as part of the expanded air monitoring network run by our laboratory for the Delaware River Basin Commission. Gas-phase ΣPCBs averaged 3340 pg/m^3 over approximately one year of sampling at Swarthmore. Thus these high levels of PCBs in the Camden/Philadelphia area are not unusual. Second, samples collected simultaneously at ground level and on the roof of the library do not demonstrate the presence of a large PCB source on the roof. In two sets of simultaneous samples, ΣPCBs were 2500 pg/m^3 at ground level and 5500 pg/m^3 on the roof on August 12, 2003, and 5600 pg/m^3 at ground level and 7000 pg/m^3 on the roof on August 13th. If the reproducibility in the PCB measurements is taken to be ± 20%, then the August 13th samples are not truly different in concentration. The August 12th samples do show a higher concentration on the roof than at ground level. However, for both sets of samples, the congener patterns at ground level and on the roof were identical, suggesting that any PCB source on the roof was either too small to significantly affect the congener pattern on the roof relative to that on the ground, or was so large that it swamped the background PCB congener

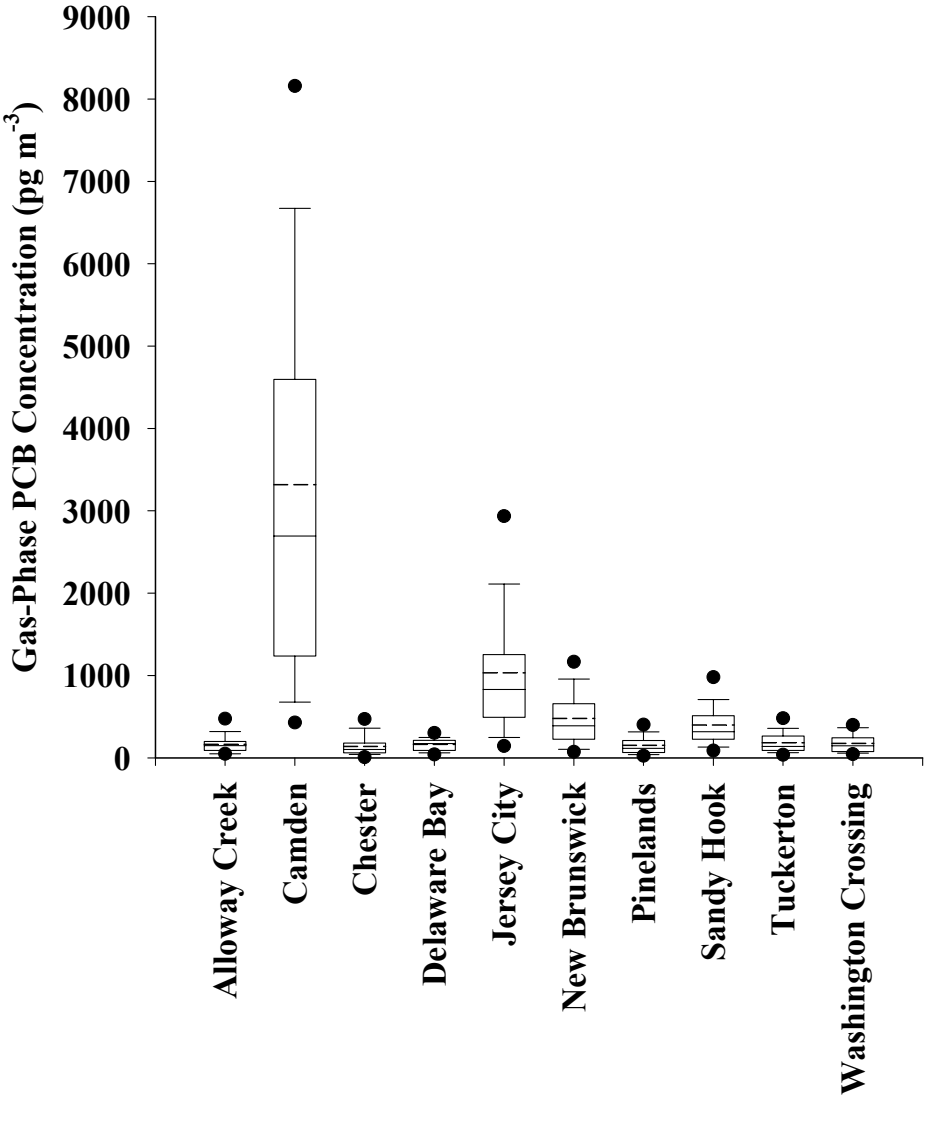

Figure 6. Box and whisker plot of gas-phase ΣPCB concentrations at all ten NJADN sites. Upper dot, upper error bar, upper edge of box, lower edge of box, lower error bar, and lower dot represent 95th, 90th, 75th, 25th, 10th and 5th percentile concentrations, respectively. Within each box, mean and median concentrations are shown as dashed and solid lines, respectively.

pattern at both locations. We suggest that the former is more likely and that the roof of the Rutgers Camden Library is not a significant source of PCBs.

The influence of high PCB concentrations appears to be localized within the urban zone. For example, the urban/industrial complex of New York City/Newark/Northern New Jersey emits PCBs resulting in the high concentrations observed at Jersey City. The influence of these emissions is felt but noticeably diluted at the nearby Sandy Hook and New Brunswick sites, which are 30 and 40 km away from Jersey City, respectively. It should also be noted that the Hudson River Estuary emits PCBs to the atmosphere year-round *(24)*, and therefore likely contributes to the elevated gas-phase concentrations observed at the three sites surrounding the estuary (Jersey City, New Brunswick, and Sandy Hook). The urban/industrial area of Camden also emits PCBs resulting in gas-phase ΣPCB concentrations which are comparable to measurements in urban Chicago, IL *(11)*. This local signal is, however, diminished by dilution and removal to continental background at Washington's Crossing and Pinelands, which are both about 45 km from Camden. The strong correlation between urbanization and gas-phase PCB concentrations suggests that atmospheric PCBs in NJ arise primarily from highly localized, urban sources and are not transported from remote source regions.

The spatial pattern of concentrations observed near urban areas in NJ is similar to that observed around Chicago, IL; and Baltimore, MD. In Baltimore *(19)*, ΣPCB concentrations ranged from 680-3,360 pg m^{-3} (similar to the range observed at Jersey City), while 18 km away, the range dropped to 210-740 pg m^{-3} (similar to Sandy Hook) and thence to 20-340 pg m^{-3} at a rural site 23 km downwind of Baltimore (similar to the 5 "lesser-impacted" sites in the present study). In Chicago, high concentrations of ΣPCBs in the urban area (14,200-270 pg m^{-3}) are diluted to 780-230 pg m^{-3} at a rural site 125 km to the northwest *(11)*. This site, South Haven, is thought to be impacted by sources of PCBs other than the Chicago urban/industrial complex *(11)*. Thus the range of PCB concentrations measured there is slightly higher than the range observed at the 5 "lesser-impacted" sites in this study.

Gas-phase PCBs are dominated by tri- and tetrachlorinated congeners, which comprise about 50-65% of the total measured PCBs at each site, with heavier homologue groups comprising decreasing percentages with MW. The dichloro congeners comprised from 8 to 18% of the total measured, despite the fact that the analytical methods quantified a single dichloro chromatographic peak (consisting of PCBs 8 and 5).

The profiles of individual PCB congener concentrations between sites were compared to assess whether sites are affected by similar source types. The Delaware Bay site consistently demonstrated the lowest correlation coefficients with the other 9 sites ($R^2 = 0.59 – 0.74$), suggesting that Delaware Bay may be affected by a different source of PCBs than the other sites, which is not surprising considering the geographical separation of this site from the rest of the state. The next most dissimilar site was Camden; its correlation coefficients were the lowest in comparison to 5 out of the 8 remaining sites. This may reflect a strong PCB source located near the Camden sampling site which might account for the extremely high gas-phase ΣPCB concentrations observed there. The other 8 sites displayed correlation coefficients ranging from 0.76-0.98, suggesting that PCBs in the rest of the state arise from a single dominant source type or process.

The temperature dependence of atmospheric PCB concentrations is well documented *(42-47)*. Such temperature dependence can provide information about the distance of the monitoring site from the source of PCBs, with steeper slopes in Clausius-Clapeyron-type relationships indicating proximate sources *(43, 46)*. The relationship between gas-phase concentrations and temperature can be expressed as:

$$\ln P = \frac{a}{T} + b \qquad (1)$$

where P is the partial pressure of the ΣPCBs (in Pa, assuming an average molecular weight of 285 g mol^{-1}), *a* and *b* are fitting parameters, and T is temperature (K).

The high R^2 values and low p-values (less than 0.003) resulting from the Clausius-Clapeyron regressions for the NJADN sites (Table 6) demonstrate that temperature is a highly significant predictor of gas-phase PCB concentrations throughout the region. Although small differences in the slopes of these plots are evident, they are not statistically significant (as suggested by the 95% confidence limits). Thus it is not possible to discern any information about the proximity of each sampling location to possible sources from the results of these regressions. The slopes presented in Table 6 are similar to those reported by Hillery et al. *(45)* at remote sites surrounding the Great Lakes.

Gas-phase concentrations of PCBs drive the gross gas absorption component of total atmospheric deposition. Thus gross gas absorption is greatest at Camden and Jersey City (Table 7). Wind speed is also a critical parameter in the calculation of gas absorption, and the influence

of wind speed is evident in that the gas absorption flux is higher at Sandy Hook than at New Brunswick, despite higher gas-phase PCB concentrations at New Brunswick. For the same reason, fluxes are higher at Tuckerton and Washington Crossing than at New Brunswick. It must be noted that the wind speeds were measured at a variety of land-based sites. Wind speeds over open waters such as Raritan Bay and Delaware Bay are likely to be higher than those measured over land, and the corresponding gas absorption fluxes are therefore likely to be higher. If the wind speed is assumed to be constant at 5 m s^{-1}, the gross gas absorption fluxes are a direct function of gas-phase PCB concentration, and are therefore highest at the urbanized and impacted sites and lowest at the 6 "lesser-impacted" sites (Table 7).

Table 6. Results of regressions of ln P (partial pressure in Pa) vs. 1/T (T in K) at NJADN sites.

Site	Slope (*a*)	95% CL	R^2	N
Alloway Creek	-3698	2319	0.384	20
Camden	-6922	1147	0.664	75
Chester	-4161	2154	0.410	25
Delaware Bay	-4572	1468	0.541	36
Jersey City	-5363	1187	0.552	68
New Brunswick	-4731	978	0.357	166
Pinelands	-5570	918	0.676	72
Sandy Hook	-4419	953	0.512	83
Tuckerton	-4276	1661	0.397	43
Washington's Crossing	-3572	1770	0.305	40

The homologue profile of the gas absorption fluxes is dominated by the low MW congeners to an even greater extent than the gas-phase concentrations, with congeners containing 2-4 chlorines contributing 60-95% of the overall gas absorption flux at all sites.

No clear seasonal trend in gas absorption fluxes was observed. This lack of seasonality arises in part because low temperatures during the winter have two effects which partially negate each other: Henry's law constants decrease *(35, 36)*, resulting in an increased tendency toward gas

absorption, and gas-phase PCB concentrations are also lower during the cold winter months, with lower concentrations available for gas absorption.

Table 7. ΣPCB deposition fluxes at the NJADN sites.

Site	Gas Absorption Actual [a] ng m^{-2} d^{-1}	Gas Absorption Modeled [b] ng m^{-2} d^{-1}	Dry Deposition ng m^{-2} d^{-1}	Wet Deposition VWM conc ng L^{-1}	Wet Deposition Flux ng m^{-2} d^{-1}
Alloway Creek	7.3 (4.0)	10	2.0	0.74	2.2
Camden	224 (4.4)	295	52	13[c]	44[c]
Chester	4.1 (1.4)	21	2.1	0.52[c]	1.1[c]
Delaware Bay	2.5 (1.1)	18	6.5	NM	NM
Jersey City	127 (4.9)	119	23	3.9[c]	11[c]
New Brunswick	5.1 (1.7)	19	8.5	1.3[c]	3.0[c]
Pinelands	5.8 (2.8)	13	2.0	0.38[c]	1.0[c]
Sandy Hook	53 (5.4)	43	5.1	0.80[c]	2.1[c]
Tuckerton	15 (5.0)	18	2.9	0.35[c]	0.85[c]
Washington Crossing	19 (4.0)	24	3.8	NM	NM

[a] Gas absorption flux calculated using actual wind speeds (average wind speed in m s^{-1} given in parentheses).

[b] Gas absorption flux calculated assuming a constant wind speed of 5 m s^{-1}.

[c] From VanRy et al., 2002.

NM = not measured

Zhang et al. *(17)* calculated a gross gas absorption flux for southern Lake Michigan of approximately 27 ng m^{-2} d^{-1}, which is about half the gas absorption flux observed at Sandy Hook. Bamford *(39)* calculated gas absorption fluxes ranging from 6 to 120 ng m^{-2} d^{-1} in Baltimore Harbor and from 1 to 93 ng m^{-2} d^{-1} in northern Chesapeake Bay during 1997-1998.

Particle phase. Typically, less than 10% of the total atmospheric ΣPCB burden is found in the particle phase. This percentage is higher during colder sampling periods due to the decrease in vapor pressure of PCB congeners at lower temperatures, increasing sorption onto airborne particles. The percentage is also higher, of course, for the higher MW PCBs. For the octa- and nonachloro congeners, for example, perhaps 50% of their total atmospheric concentrations is in the particle phase during the warmer months, while essentially 100% is sorbed to particles in the winter. The homolog profile of particle-phase PCBs measured by NJADN is therefore different than the gas-phase profile. Dichloro congeners typically comprise less than 1% of ΣPCBs in the particle phase, while homologues containing 3, 4, 5, or 6 chlorines each typically comprise about 20% of the total. PCBs containing 7, 8, and 9 chlorines typically make up about 10%, 5%, and 2% of the total particle PCB burden, respectively.

ΣPCBs in the particle phase generally followed the same spatial trends as the gas phase with Camden and Jersey City exhibiting the highest concentrations and several sites (Chester, Pinelands, Sandy Hook, Tuckerton, Washington Crossing, Alloway Creek) displaying concentrations that rarely exceed 40 pg m^{-3} (Figure 7). Particle-phase ΣPCB concentrations at New Brunswick exceed this level in about 10% of samples. Delaware Bay exhibits relatively high particle phase PCB concentrations despite low (regional background) gas-phase concentrations. The TSP concentrations were also high at Delaware Bay, averaging 40 μg m^{-3} versus about 30 μg m^{-3} at the other more remote sites. These results are similar to observations at sites surrounding the Great Lakes *(31)*, where particle-phase ΣPCB concentrations in remote regions are usually less the 40 pg m^{-3}, but concentrations in Chicago frequently exceed 100 pg m^{-3}. Particle-phase concentrations of ΣPCBs of less than 40 pg m^{-3} thus appear to represent regional background. The spatial distribution of particle-phase PCBs observed in New Jersey demonstrates that, like gas-phase PCBs, particle-phase PCBs in this region arise from sources that are highly localized in urban areas. Decay of the particle-phase PCB signal appears to occur more rapidly than dilution of the gas phase, with particle-phase concentrations approaching regional background even at New Brunswick and Sandy Hook.

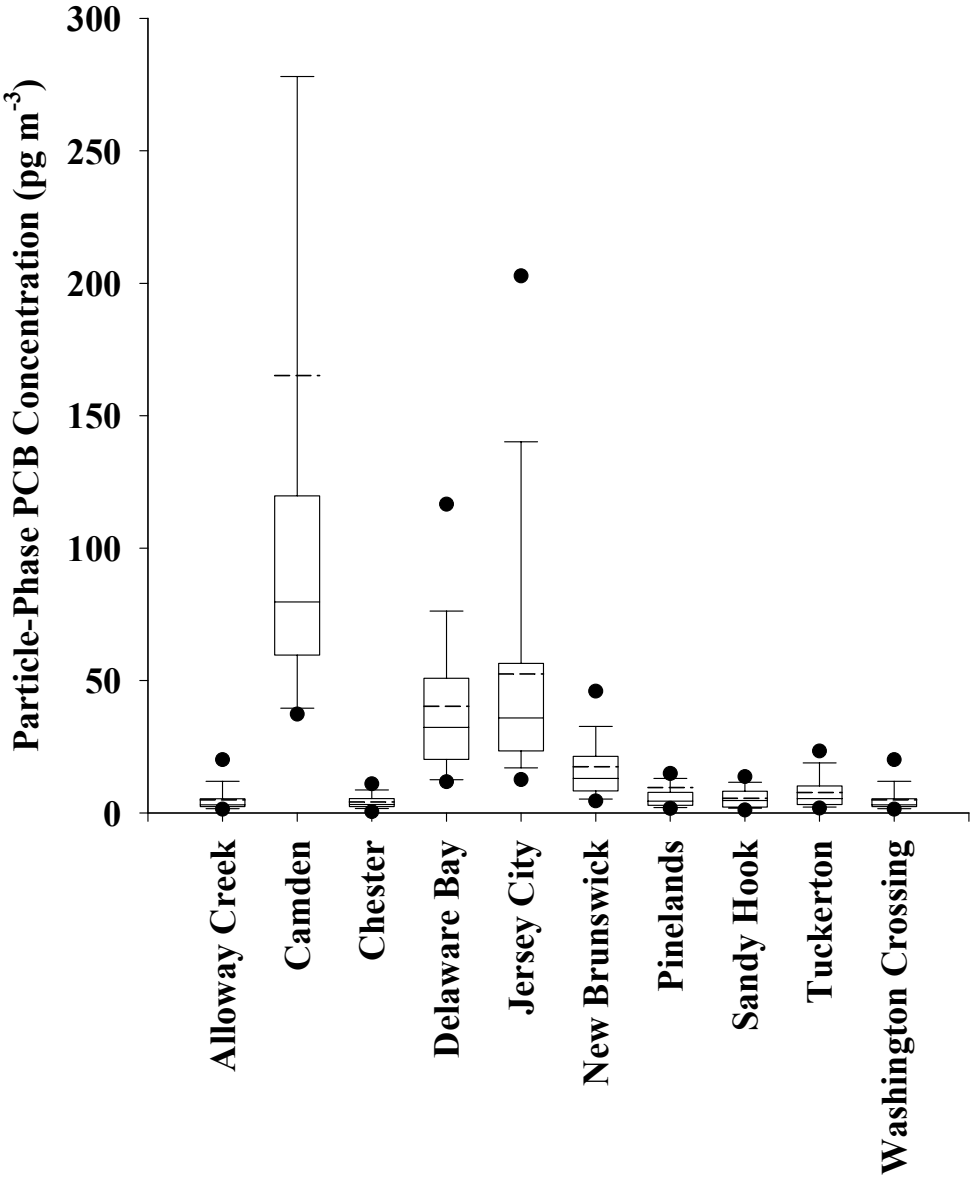

Figure 7. Summary of particle-phase ΣPCB concentrations at NJADN sites.

By the algorithm chosen to calculate dry deposition fluxes, higher particle-phase ΣPCB concentrations translate directly into higher dry deposition fluxes (Table 7). At most sites, the highest dry depositional flux occurs in winter, probably due to increased sorption of PCBs to particle surfaces at lower temperatures. Gross gas absorption exceeds dry deposition in most cases. At Delaware Bay and New Brunswick, dry deposition is equal to or greater than gas absorption, due to the low wind speeds experienced at these sites leading to low gas absorption fluxes. The calculated dry deposition fluxes are similar to those estimated for Lake Michigan *(31)*, which average 3.3 ng m^{-2} d^{-1} in remote regions and 15 ng m^{-2} d^{-1} in Chicago, assuming a deposition velocity of 0.2 cm s^{-1} (versus 0.5 cm s^{-1} in the present study). Hillery et al. *(4)* estimate ΣPCB dry deposition fluxes to Lakes Superior, Michigan, and Erie to be about 2 ng m^{-2} d^{-1} based on particle-phase measurements at remote locations and a deposition velocity of 0.2 cm s^{-1}.

Precipitation phase. A detailed analysis of VWM precipitation concentrations and wet deposition of PCBs has been conducted by VanRy et al. *(27)*, and will be summarized here (Table 7). VWM concentrations of ΣPCBs at the eight sites at which precipitation was collected varied over two orders of magnitude. The spatial variations in concentrations mirrored those of the gas-phase, with highest concentrations occurring at Camden and Jersey City, followed by New Brunswick and Sandy Hook. The "lesser-impacted" sites display the lowest VWM concentrations of all (rain samples were not collected at Delaware Bay and Washington Crossing, two of the "lesser-impacted" sites). These results are similar to those of Offenberg and Baker *(2)*, who observed that VWM concentrations of ΣPCBs in precipitation collected in Chicago, over Lake Michigan near Chicago, and at a remote site 125 km away (South Haven) were 29.3, 5.8, and 0.1 ng L^{-1}, respectively.

Wet depositional flux is a function of both the VWM concentration and the precipitation rate (m y^{-1}), but because precipitation rates are largely constant across the state, the wet depositional fluxes follow the same spatial trend as the VWM concentrations. This spatial trend once again suggests that highly localized, urban sources of PCBs exert an influence over atmospheric concentrations and deposition fluxes over a distance of a few tens of km. Hillery et al. *(4)* calculated wet deposition fluxes of ΣPCBs to the Great Lakes from observations at remote sites; the resulting averages ranged from 4 to 9 ng m^{-2} d^{-1}, slightly higher than the fluxes

calculated for the 4 "lesser-impacted" sites in New Jersey. Offenberg and Baker *(2)* calculated wet deposition fluxes on an event basis, but by applying a 30-year average precipitation flux for Chicago of 85 cm y^{-1}, their VWM concentrations may be converted to fluxes of 68, 14, 0.2 ng m^{-2} d^{-1} at Chicago, over Lake Michigan near Chicago, and at South Haven. Their results thus display a similar spatial pattern driven by urbanization, again suggesting that concentrations and fluxes of PCBs are diluted to background levels 30-50 km from the source.

At all sites except Camden, the homologue distribution of PCBs in precipitation was dominated by PCBs containing 3 to 6 chlorines (about 70-80% of the total), with dichloro congeners typically comprising less than 4% of ΣPCBs, and PCBs containing 7, 8, and 9 chlorines comprising about 8%, 8%, and 1% of the total PCB burden, respectively. At Camden, high MW congeners (octa- and nonachloros) make up a much larger proportion of the total (45%).

Summary of deposition by land use type and deposition mode. In order to make meaningful comparisons between sites, it is important to estimate the wet deposition flux at Delaware Bay and Washington Crossing. Both these sites could be considered "unimpacted" by PCBs, and might therefore be expected to experience wet deposition fluxes similar to those at Chester, Tuckerton, and Pinelands. The dry particle flux at Delaware Bay, however, is relatively high, suggesting that the wet deposition flux there may be significantly higher than the 0.8 to 1.2 ng m^{-2} d^{-1} measured at the other remote sites. The ratio of wet to dry deposition ranged from 0.3 to 0.5 at the other sites (except Camden, where the ratio was 0.8). Thus we estimate that the wet deposition flux was about 1 ng m^{-2} d^{-1} at Washington Crossing and between 2 and 5 ng m^{-2} d^{-1} at Delaware Bay. Using these numbers and assuming a constant wind speed of 5 m s^{-1}, gas absorption represents 75 to 85% of the total atmospheric deposition of ΣPCBs at all sites except Delaware Bay, where gas deposition contributes about 60% of the total. Dry deposition comprises 10-17% of the total, and wet deposition is typically 4-8%, except at Camden, where it contributes 12% of the total deposition. The relatively high wet deposition flux at Camden is partly a result of the predominance of octa- and nona- chlorinated congeners there, as seen in Figure 8 and discussed by VanRy et al. *(27)*. Examining the deposition fluxes by homolog group (Figure 8) demonstrates that congeners containing 2 to 5 chlorines are primarily deposited by gas absorption. Congeners with 6 or more chlorines are primarily deposited via wet + dry

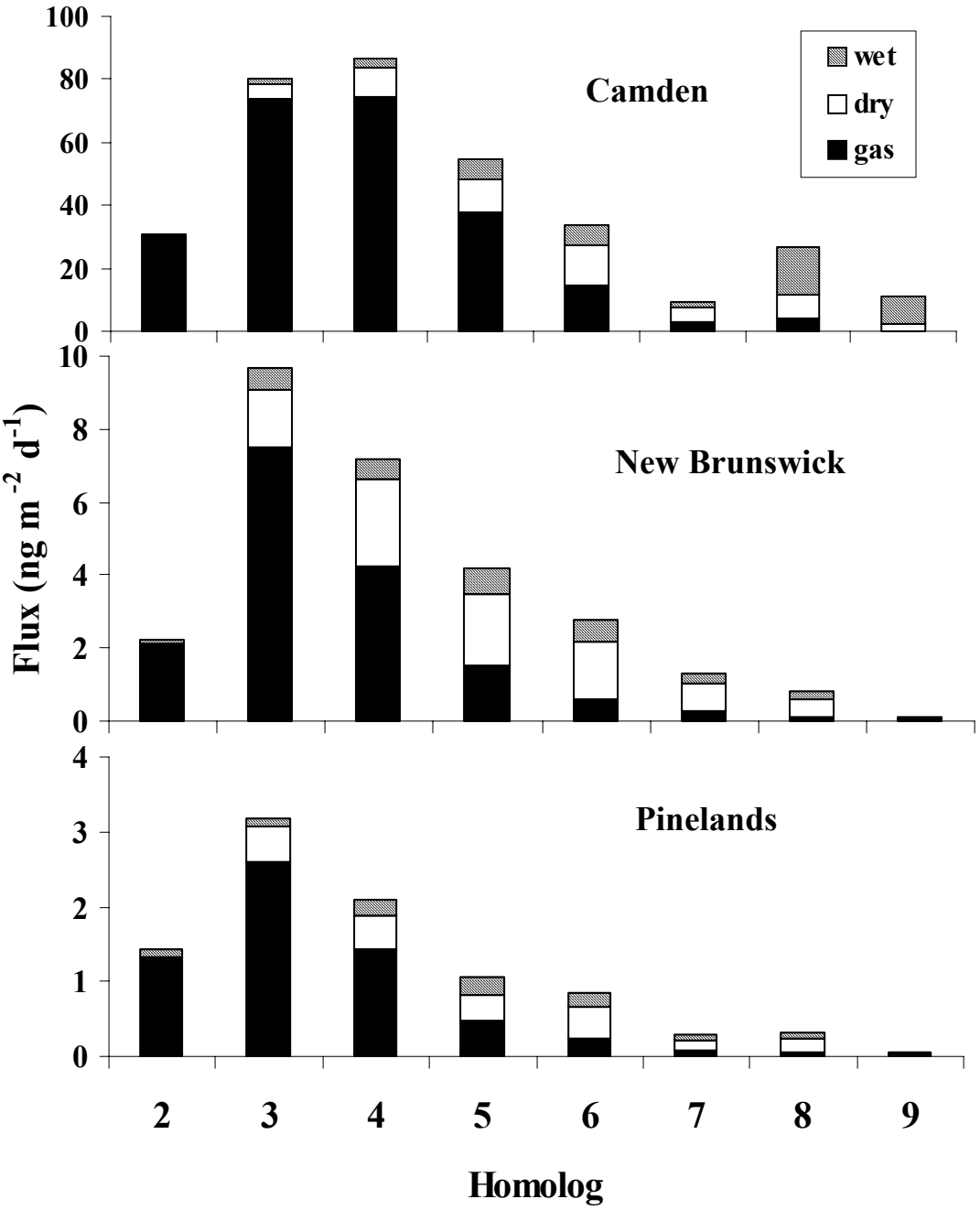

Figure 8. Gas absorption (black), dry particle deposition (white), and wet deposition (striped) fluxes of PCB homologs at three sites: Camden (top), New Brunswick (middle), and Pinelands (bottom). Note differences in the y-axis scales.

deposition. These deposition patterns apply generally to all the land-use types investigated in this study. While the magnitude of the fluxes may increase with urbanization, the relative proportions of wet, dry, and gaseous deposition remain largely constant, as demonstrated in Figure 8 for three sites: Camden (urban), New Brunswick (suburban) and Pinelands (forested). Delaware Bay represents an exception to this generalization. The gaseous, dry, and wet deposition fluxes at Delaware Bay are predicted to comprise about 60%, 25%, and 8-18% of the total, respectively. Thus gas absorption is less important at Delaware Bay, even assuming a wind speed of 5 m s^{-1}.

Importance of atmospheric deposition of PCBs to the Hudson River Estuary. The estimated fluxes of ΣPCBs to the NY-NJ Harbor Estuary may be compared with those estimated for other aquatic systems. The sum of wet and dry particle deposition of ΣPCBs to the Chesapeake Bay estimated from CBADS data *(1)* and for the Great Lakes from IADN data *(3, 4)* are 1.8-3.3 and 1.0-2.5 ug m^{-2} y^{-1}, respectively. Comparing only wet and dry particle deposition amongst the systems, the NY-NJ Harbor Estuary is loaded at a rate of approximately 2 to 10 times these aquatic systems. At Jersey City and Sandy Hook, gaseous deposition of ΣPCBs dominates the overall depositional flux. Lower air concentrations of ΣPCBs in the Great Lakes and Chesapeake Bay areas suggest that gas deposition fluxes to these waters are not likely to exceed those to the NY-NJ Harbor Estuary *(3, 11, 18, 42, 48, 49)*. Thus it is likely that the overall atmospheric deposition fluxes of PCBs to the NY-NJ Harbor Estuary are at least 2 to 10 times those experienced in the Great Lakes and Chesapeake Bay.

Compared with other inputs of PCBs to the NY-NJ Harbor Estuary, atmospheric deposition is small. Durell and Lizotte estimate that in 1998 the twenty-six water pollution control plants on the NY-NJ Harbor Estuary discharged about 88 kg of PCBs per year into the estuary *(5)*. In addition, Farley et al. *(7)* estimate that the annual input of PCBs from the upper Hudson River at the Federal Dam in Troy, NY is about 250 kg (1997 numbers). Assuming that the plume of atmospheric contamination extends throughout the Raritan Bay and the New York/New Jersey Harbor area (surface area ~ 4700 km^2), the current estimates of atmospheric deposition result in about 10 kg y^{-1} of ΣPCBs being deposited into the estuary.

Although the atmospheric load of PCBs is small relative to other inputs, it is large enough to be of concern. Pure water at 15°C in equilibrium with the average gas-phase PCB

concentrations measured at Sandy Hook would have about 60 pg/L ΣPCBs in the dissolved phase (using the Henry's Law Constants of Bamford et al. *(35, 36)*). This concentration is above both the New York state and federal water quality criteria of for the protection of aquatic life, and it does not include atmospherically-derived PCBs that become sorbed to the dissolved organic carbon and total suspended matter in the water column. Air-water exchange should be close to equilibrium in areas such as Raritan Bay, where the residence time of the water (about one month) is much longer than the time scale for air-water exchange (5-10 days). Thus the atmosphere is a large enough source of PCBs to the water column that current water quality criteria cannot be met without substantial decreases in atmospheric PCB concentrations. In consequence, the implementation of the PCB Total Maximum Daily Load for the NY-NJ Harbor Estuary must include efforts to identify and remediate sources of PCBs to the local atmosphere.

The high concentrations of PCBs in the water column of the Hudson River Estuary coming from upstream flow in the Hudson River, other tributary inputs, and discharges from wastewater treatment facilities contribute to a large volatilization flux *(24, 50)*. Yan *(50)* reports that air-water exchange in Raritan Bay results in a gas absorption flux of 160 ng m^{-2} d^{-1}, similar to the gas absorption flux estimated at Jersey City. The volatilization flux was 330 ng m^{-2} d^{-1}, however, resulting in a net loss of PCBs from the water column. Tri- and tetra-chlorinated PCBs constitute about 85% of the volatilization signal. In contrast, congeners containing 6-9 chlorines were near equilibrium with respect to air-water exchange. Thus the total interaction of Raritan Bay with the atmosphere, encompassing gas exchange, dry and wet deposition, probably results in a net *loss* of low MW PCBs (congeners containing 2-5 chlorines) from the water column, but a net *input* of PCBs containing 6-9 chlorines.

References

(1) Baker, J. E.; Poster, D. L.; Clark, C. A.; Church, T. M.; Scudlark, J. R.; Ondov, J. M.; Dickhut, R. M.; Cutter, G. Loadings of atmospheric trace elements and organic contaminants to the Chesapeake Bay. In *Atmospheric Deposition of Contaminants in the Great Lakes and Coastal Waters*; Baker, J. E., Ed.; SETAC Press: Pensacola, FL, 1997, 171-194.

(2) Offenberg, J.; Baker, J. Polychlorinated Biphenyls in Chicago Precipitation: Enhanced Wet Deposition to Near-Shore Lake Michigan. *Environ. Sci. Technol.* **1997**, *31*, 1534-1538.

(3) Hoff, R. M.; Strachan, W. M. J.; Sweet, C. W.; Chan, C. H.; Shackleton, M.; Bidleman, T. F.; Brice, K. A.; Burniston, D. A.; Cussion, S.; Gatz, D. F.; Harlin, K.; Schroeder, W. H. Atmospheric deposition of toxic chemicals to the Great Lakes: A review of data through 1994. *Atmos. Env.* **1996**, *30*, 3505-3527.

(4) Hillery, B. R.; Simcik, M. F.; Basu, I.; Hoff, R. M.; Strachan, W. M. J.; Burniston, D.; Chan, C. H.; Brice, K. A.; Sweet, C. W.; Hites, R. A. Atmospheric Deposition of Toxic Pollutants to the Great Lakes As Measured by the Integrated Atmospheric Deposition Network. *Environ. Sci. Technol.* **1998**, *32*, 2216-2221.

(5) Durell, G. S.; Lizotte, R. D. PCB levels at 26 New York City and New Jersey WPCPs that discharge to the New York/New Jersey Harbor Estuary. *Environ. Sci. Technol.* **1998**, *32*, 1022-1031.

(6) Bopp, R. F.; Simpson, H. J.; Olsen, C. R.; Kostyk, N. Polychlorinated biphenyls in sediments of the tidal Hudson River, New York. *Environ. Sci. Technol.* **1981**, *15*, 210-216.

(7) Farley, K. J.; Thomann, R. V.; Cooney, T. F. I.; Damiani, D. R.; Wands, J. R. "An Integrated Model of Organic Chemical Fate and Bioaccumulation in the Hudson River Estuary," The Hudson River Foundation, 1999. March 1999.

(8) Connolly, J. P.; Zahakos, H. A.; Benaman, J.; Ziegler, C. K.; Rhea, J. R.; Russell, K. A model of PCB fate in the upper Hudson River. *Environ. Sci. Technol.* **2000**, *34*, 4076-4087.

(9) Thomann, R. F.; Mueller, J. A.; Winfield, R. P.; Huang, C. R. *J. Environ. Eng.* **1991**, *117*, 161-178.

(10) Cotham, W. E.; Bidleman, T. F. *Environ. Sci. Technol.* **1995**, *29*, 2782-2789.

(11) Simcik, M. F.; Zhang, H.; Eisenreich, S. J.; Franz, T. P. Urban contamination of the Chicago/coastal Lake Michigan atmosphere by PCBs and PAHs during AEOLOS. *Environ. Sci. Technol.* **1997**, *31*, 2141-2147.

(12) Harner, T.; Bidleman, T. F. Octanol-Air Partition Coefficient for Describing Particle/Gas Partitioning of Aromatic Compounds in Urban Air. *Environ. Sci. Technol.* **1998**, *32*, 1494-1502.

(13) Green, M. L.; DePinto, J. V.; Sweet, C.; Hornbuckle, K. C. Regional Spatial and Temporal Interpolation of Atmospheric PCBs: Interpretation of Lake Michigan Mass Balance Data. *Environ. Sci. Technol.* **2000**, *34*, 1833-1841.

(14) Franz, T. P.; Eisenreich, S. J.; Holsen, T. M. Dry deposition of particulate polychlorinated biphenyls and polycyclic aromatic hydrocarbons to Lake Michigan. *Environ. Sci. Technol.* **1998**, *32*, 3681-3688.

(15) Paode, R. D.; Sofuoglu, S. C.; Sivadechathep, J.; Noll, K. E.; Holsen, T. M.; Keeler, G. J. Dry Deposition Fluxes and Mass Size Distributions of Pb, Cu, and Zn Measured in Southern Lake Michigan during AEOLOS. *Environ. Sci. Technol.* **1998**, *32*, 1629 -1635.
(16) Caffrey, P. F.; Ondov, J. M.; Zufall, M. J.; Davidson, C. I. Determination of Size-Dependent Dry Particle Deposition Velocities with Multiple Intrinsic Elemental Tracers. *Environ. Sci. Technol.* **1998**, *32*, 1615-1622.
(17) Zhang, H.; Eisenreich, S. J.; Franz, T. R.; Baker, J. E.; Offenberg, J. H. Evidence for increased gaseous PCB fluxes to Lake Michigan from Chicago. *Environ. Sci. Technol.* **1999**, *33*, 2129-2137.
(18) Nelson, E. D.; McConnell, L. L.; Baker, J. E. Diffusive Exchange of Gaseous Polycyclic Aromatic Hydrocarbons and Polychlorinated Biphenyls Across the Air-Water Interface of the Chesapeake Bay. *Environ. Sci. Technol.* **1998**, *32*, 912-919.
(19) Offenberg, J. H.; Baker, J. E. Influence of Baltimore's urban atmosphere on organic contaminants over the northern Chesapeake Bay. *J. Air Waste Manage. Assoc.* **1999**, *49*, 959-965.
(20) Iannuzzi, T. J.; Huntley, S. L.; Bonnevie, N. L.; Finley, B. L.; Wenning, R. J. Distribution And Possible Sources Of Polychlorinated-Biphenyls In Dated Sediments From The Newark Bay Estuary, New-Jersey. *Arch. Env. Contam. Tox.* **1995**, *28*, 108-117.
(21) Gigliotti, C. L.; Brunciak, P. A.; Dachs, J.; IV, G. T. R.; Nelson, E. D.; Totten, L. A.; Eisenreich, S. J. Air-Water Exchange of Polycyclic Aromatic Hydrocarbons in the NY-NJ Harbor Estuary. *Environ. Toxicol. Chem.* **2001**, *21*, 235-244.
(22) Dachs, J.; Van Ry, D. A.; Eisenreich, S. J. Occurrence of Estrogenic Nonylphenols in the Urban and Coastal Atmosphere of the Lower Hudson River Estuary. *Environ. Sci. Technol.* **1999**, *33*, 2676-2679.
(23) Lohmann, R.; Nelson, E.; Eisenreich, S. J.; Jones, K. C. Evidence for Dynamic Air-Water Exchange of PCDD/Fs: A Study in the Raritan Bay/Hudson River Estuary. *Environ. Sci. Technol.* **2000**, *34*, 3086-3093.
(24) Totten, L. A.; Brunciak, P. A.; Gigliotti, C. L.; Dachs, J.; IV, G. T. R.; Nelson, E. D.; Eisenreich, S. J. Dynamic Air-Water Exchange of Polychlorinated Biphenyls in the NY-NJ Harbor Estuary**.** *Environ. Sci. Technol.* **2001**, *35*, 3834-3840.
(25) Gigliotti, C. L.; Dachs, J.; Nelson, E. D.; Brunciak, P. A.; Eisenreich, S. J. Polycyclic Aromatic Hydrocarbons in the New Jersey Coastal Atmosphere. *Environ. Sci. Technol.* **2000**, *34*, 3547-3554.
(26) Brunciak, P. C.; Dachs, J.; Gigliotti, C. L.; Nelson, E. D.; Eisenreich, S. J. Atmospheric polychlorinated biphenyl concentrations and apparent degradation in coastal New Jersey. *Atm. Env.* **2001**, *35*, 3325-3339.
(27) VanRy, D. A.; Gigliotti, C. L.; T.R. Glenn, I.; Nelson, E. D.; Totten, L. A.; Eisenreich, S. J. Wet deposition of polychlorinated biphenyls in urban and background areas of the Mid-Atlantic states. *Environ. Sci. Technol.* **2002**, *36*, 3201-3209.
(28) Zufall, M. J.; Davidson, C. I.; Caffrey, P. F.; Ondov, J. M. Airborne Concentrations and Dry Deposition Fluxes of Particulate Species to Surrogate Surfaces Deployed in Southern Lake Michigan. *Environ. Sci. Technol.* **1998**, *32*, 1623-1628.
(29) Pirrone, N.; Keeler, G. J.; Holsen, T. M. Dry deposition of semivolatile organic compounds to Lake Michigan. *Environ. Sci. Technol.* **1995**, *29*, 2123-2132.

(30) Pirrone, N.; Keeler, G. J.; Holsen, T. M. Dry deposition of trace elements to Lake Michigan: a hybrid-receptor deposition modeling approach. *Environ. Sci. Technol.* **1995**, *29*, 2112-2122.
(31) Miller, S. M.; Green, M. L.; DePinto, J. V.; Hornbuckle, K. C. Results from the Lake Michigan Mass Balance Study: Concentrations and Fluxes of Atmospheric Polychlorinated Biphenyls and trans-Nonachlor. *Environ. Sci. Technol.* **2001**, *35*, 278-285.
(32) Achman, D. R.; Hornbuckle, K. C.; Eisenreich, S. J. Volatilization of polychlorinated biphenyls from Green Bay, Lake Michigan. *Environ. Sci. Technol.* **1993**, *27*, 75-87.
(33) Eisenreich, S. J.; Hornbuckle, K. C.; Achman, D. Atmospheric deposition of organic chemicals in the upper Great Lakes: The role of air-water exchange. In *Atmospheric Deposition of Contaminants in the Great Lakes and Coastal Waters*; Baker, J. E., Ed.; SETAC Press: Boca Raton, FL, 1997, 109-136.
(34) Bamford, H. A.; Offenberg, J. H.; Larsen, R. K.; Ko, F.-C.; Baker, J. E. Diffusive Exchange of Polycyclic Aromatic Hydrocarbons across the Air-Water Interface of the Patapsco River, an Urbanized Subestuary of the Chesapeake Bay. *Environ. Sci. Technol.* **1999**, *33*, 2138-2144.
(35) Bamford, H. A.; Poster, D. L.; Baker, J. E. Henry's Law constants of polychlorinated biphenyl congeners and their variation with temperature. *J. Chem. Eng. Data* **2000**, *45*, 1069-1074.
(36) Bamford, H. A.; Poster, D. L.; Huie, R.; Baker, J. E. Extrathermodynamic relationships and estimation of the temperature dependence Henry's Law constants for PCBs. *Environ. Sci. Technol.* **2002**, *36*, 4395-4402.
(37) Wanninkhoff, R. Relationship between gas exchange and wind speed over the ocean. *J. Geophys. Res* **1992**, *97*, 7373-7381.
(38) Schwarzenbach, R. P.; Gschwend, P. M.; Imboden, D. M. *Environmental Organic Chemistry;* 2nd ed.; Wiley and Sons: Hoboken, New Jersey, 2003.
(39) Bamford, H. A.; Ko, F. C.; Baker, J. E. Seasonal and annual air-water exchange of polychlorinated biphenyls across Baltimore Harbor and the northern Chesapeake Bay. *Environ. Sci. Technol.* **2002**, *36*, 4245-4252.
(40) Gigliotti, C. L.; Lee, J. H.; Offenberg, J. H.; Turping, B. J.; Eisenreich, S. J. Source Apportionment of Polycyclic Aromatic Hydrocarbons in New Jersey Air using Positive Matrix Factorization. *Environ. Sci. Technol.* **2003**, *In review*,
(41) Buehler, S. S.; Basu, I.; Hites, R. A. A Comparison of PAH, PCB, and Pesticide Concentrations in Air at Two Rural Sites on Lake Superior. *Environ. Sci. Technol.* **2001**, *35*, 2417 -2422.
(42) Hoff, R. M.; Muir, D. C. G.; Grift, N. P. Annual cycle of polychlorinated biphenyls and organohalogen pesticides in air in southern Ontario. Air concentration data. *Environ. Sci. Technol.* **1992**, *26*, 266-275.
(43) Wania, F.; Haugen, J.-E.; Lei, Y. D.; Mackay, D. Temperature dependence of atmospheric concentrations of semivolatile organic compounds. *Environ. Sci. Technol.* **1998**, *32*, 1013-1021.
(44) Hornbuckle, K. C.; Eisenreich, S. J. Dynamics of semivolatile organic compounds in a terrestrial ecosystem--Effects of diurnal and seasonal climate variations. *Atmos. Environ.* **1996**, *30*, 3935-3945.

(45) Hillery, B. R.; Basu, I.; Sweet, C. W.; Hites, R. A. Temporal and spatial trends in a long-term study of gas-phase PCB concentrations near the Great Lakes. *Environ. Sci. Technol.* **1997**, *31*, 1811-1816.
(46) Hoff, R. M.; Brice, K. A.; Halsall, C. J. Nonlinearity in the Slopes of Clausius-Clapeyron Plots for SVOCs. *Environ. Sci. Technol.* **1998**, *32*, 1793-1798.
(47) Simcik, M. F.; Basu, I.; Sweet, C. W.; Hites, R. A. Temperature dependence and temporal trends of Polychlorinated Biphenyl Congeners in the Great Lakes atmosphere. *Environ. Sci. Technol.* **1999**, *33*, 1991-1995.
(48) Leister, D. L. The distribution of organic contaminants in the atmosphere and in precipitation. PhD Thesis Thesis, University of Maryland, 1993.
(49) Stern, G. A.; Halsall, C. J.; Barrie, L. A.; Muir, D. C. G.; Fellin, P.; Rosenberg, B.; Rovinsky, F. Y.; Pastuhov, B. Polychlorinated biphenyls in the Arctic air. 1. Temporal and spatial trends: 1992-1994. *Environ. Sci. Technol.* **1997**, *31*, 3619-3628.
(50) Yan, S. Air-water exchange controls phytoplankton concentrations of polychlorinated biphenyls in the Hudson River Estuary. Master's Thesis Thesis, Rutgers University, 2003.

II.A2a. Polycyclic Aromatic Hydrocarbons Part I – Atmospheric concentrations

Abstract

Atmospheric concentrations of polycyclic aromatic hydrocarbons (PAHs) were measured at urban/industrial, suburban, coastal and rural areas in New Jersey, USA, as part of the New Jersey Atmospheric Deposition Network (NJADN). Concentrations of 36 PAH compounds were measured in the gas and particle phases in air and in precipitation at nine sites at regular intervals from October 1997 through May 2001. Gas phase and particle phase Σ_{36}PAH concentrations ranged from 0.45 to 118 ng/m^3 and 0.046 to 172 ng/m^3, respectively, and precipitation concentrations ranged from 11 to 16200 ng/L. PAH concentrations vary spatially across the State of New Jersey with the highest concentrations occurring at the most heavily urban and industrial locations. Although the absolute concentrations vary spatially, the PAH profiles are statistically similar at nine of the ten sampling sites indicating that the mix of sources around New Jersey is the same. On average, temperature accounts for 25% of the total variability in gas phase PAH concentrations indicating that air-surface exchange is not the primary mechanism for controlling concentrations in air. Gas phase PAH concentrations increase in the warmer seasons; whereas, the opposite trend is seen for predominantly particle phase PAHs with concentrations at a maximum in colder seasons. Increased emission of PAH attributed to elevated fossil fuel use in winter drives the particle phase PAH concentrations at most of the NJADN sites. Volume weighted mean (VWM) precipitation concentrations are highest at the more highly urban/industrial sites and do not display a consistent seasonal pattern across the state of New Jersey.

Introduction

Densely populated and heavily industrialized regions contain numerous, proximate PAH emission sources and as such, contribute to elevated atmospheric PAH concentrations *(1-4)*. Many of these urban/industrial regions are located on or near coastal estuaries (e.g., the New York – New Jersey Harbor estuary and the Delaware River estuary) and adjacent to large lake systems (e.g. southern Lake Michigan) making such water bodies susceptible to high levels of urban contaminant loading via the atmosphere. The New York/ New Jersey metropolitan area is

home to an estimated 20.2 million people (http://www.census.gov/population/estimates/metro-city/ma99-03a.txt -U.S. Census Bureau- 1999 statistics). This region is transected by major traffic arteries carrying large volumes of both gasoline and diesel-powered vehicular traffic. With such a densely urbanized population, natural gas and oil consumption for both commercial and home heating contributes to elevated PAH emissions. The NY-NJ Harbor estuary is the entry point for heavy ship traffic heading towards busy local ports such as Port Elizabeth, Port Newark, and New York City. Along the Hudson River separating New York City from New Jersey, there exist a multitude of other PAH sources to the air such as natural gas production facilities, petrochemical and oil refineries, petroleum storage facilities, a coal-fired power plant, and two major international airports (Energy Information Administration- 2001 statistics) (See Figure 9).

The Delaware River estuary is another heavily traveled waterway leading toward the Ports of Philadelphia (Pennsylvania) and Camden (New Jersey). The southwestern New Jersey area, particularly along the banks of the Delaware River, has a number of petrochemical and natural gas facilities, two coal-fired power plants, and is interlaced by numerous heavy traffic arteries that allow access to the southern New Jersey/Philadelphia metropolitan area, home to the Philadelphia International Airport.

NJADN was implemented in October 1997 as a research and monitoring network to assess the magnitude of atmospheric deposition of a suite of semi-volatile, toxic organic compounds (SOCs), including polychlorinated biphenyls (PCBs), polycyclic aromatic hydrocarbons (PAHs), and target organo-chlorine pesticides to New Jersey. NJADN was designed to quantify both the local and regional signals of air toxics concentrations by locating monitoring sites in areas with different geographical land-use regimes, including urban/industrial, suburban, rural, and coastal environments. The concentrations are then translated into deposition fluxes to both terrestrial and aquatic systems in New Jersey. This section focuses on the measured concentrations of PAHs from approximately 4 years of air and precipitation sampling at nine sites around the state of New Jersey.

Results and Discussion.

Gas and Particle Phase PAHs: spatial differences. Box and whisker plots of the gas- and particle-phase Σ_{36}PAH concentrations are shown in Figure 10, with the 10 NJADN sites listed in

order of decreasing urban/industrialization, with Jersey City and Camden as the most highly urbanized and industrialized areas and the rural Pinelands being the least. The air monitoring station located at Chester, New Jersey was selected to represent the regional PAH signal due to its location in a clean air vector in New Jersey. The Chester site displays lower average gas and

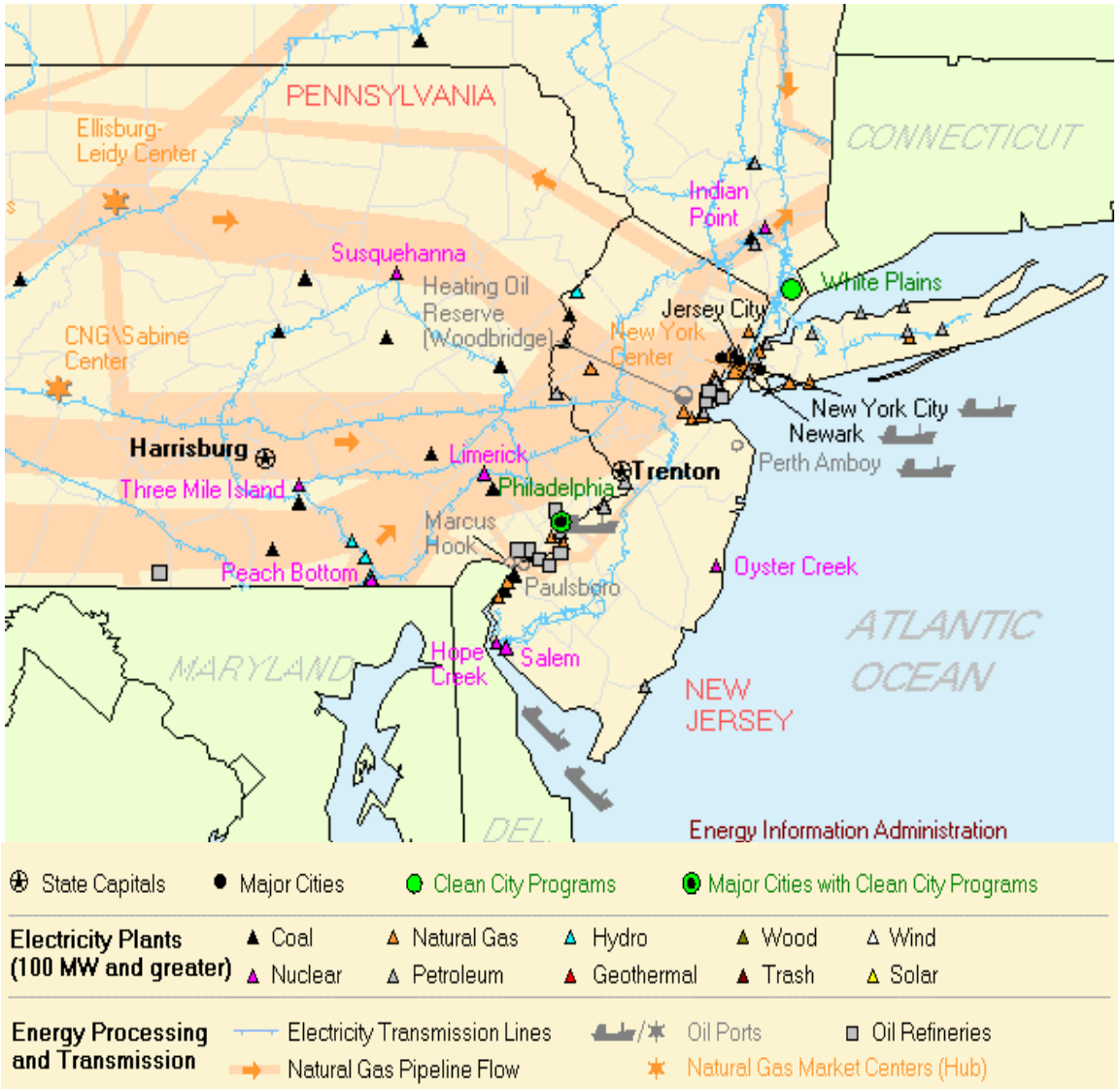

Figure 9. PAH sources to New Jersey's atmosphere. (Map found at http://www.eia.doe.gov- Energy Information Administration Statistics- 2001).

particle phase Σ_{36}PAH concentrations than those at the urban/industrial locations, Jersey City and Camden, and higher concentrations than those measured at the rural Pinelands and Delaware Bay sites. The average gas and particle phase Σ_{36}PAH concentrations at the regional Chester station

are 10 and 1.0 ng/m^3, respectively. The Jersey City and Camden display urban/industrial sites have Σ_{36}PAH concentrations that are 4 to 6 times higher than the regional signal of PAHs for both gas and particle phases.

The gas phase PAH distribution (Figure 11) is dominated by low to medium molecular weight PAHs (fluorene to chrysene) which contribute greater to the total gas phase PAH concentration than do the higher molecular weight PAHs (benz[a]anthracene to coronene) as dictated by their vapor-particle partitioning.

Gas phase PAH concentrations vary from below the limits of analytical detection for some compounds, such as naphthacene, to as much as 45 ng/m^3 for phenanthrene. The average gas phase phenanthrene concentration varies by as much as a factor of 6 and pyrene by an order of magnitude across the sites. Although the average concentrations vary spatially across New Jersey, the average PAH profiles at all sites except Alloway Creek are statistically similar (r^2= 0.92 to 0.99) with p-values less than 0.05, indicating that while the source strength is different at each site, the mix of sources is similar, yielding the same average profiles. Concentrations of gas phase methylphenanthrenes are significantly lower at Alloway Creek than the other 9 sites. If this compound is excluded, the PAH profile at Alloway Creek site is statistically similar with the other nine sites (r^2= 0.91 to 0.99).

Particle phase PAHs display a similar spatial pattern (Figure 12). Particle phase PAH concentrations are often more than an order of magnitude lower than gas phase PAH concentrations. The distribution of PAHs also changes in that the low to medium molecular weight PAHs are less important in the particle phase. There is a larger contribution of high molecular weight PAHs to the total particulate PAH mass.

Particle phase phenanthrene varies by less than a factor of 5 from between sites in New Jersey with the highest PAH concentrations occurring the more urban/industrial areas. Due primarily to gravitational settling and turbulent motion, the largest particles in the emissions deposit in close proximity to the source area leading to elevated dry particle deposition fluxes nearest to sources. As was seen for the gas phase PAHs, the average particle phase PAH concentrations differ spatially, but profiles are statistically similar (r^2 = 0.70 to 0.94) at all sites except Alloway Creek with all p-values < 0.05, such that all of these nine NJADN sites 'see' the same mix of PAH sources. Again, the methylphenanthrenes are lower at Alloway Creek than at

any of the others sites. When this compound is removed from the regression, the PAH profile at Alloway Creek is statistically similar to those of all the other sites (r^2 = 0.70 to 0.89).

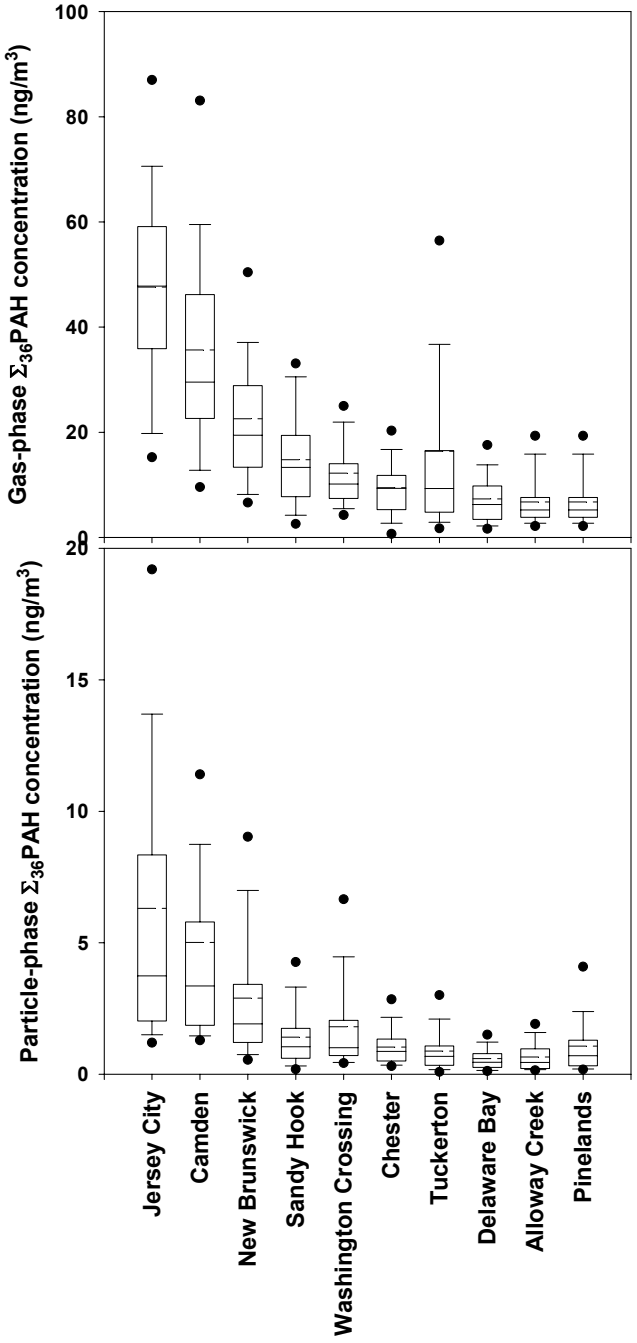

Figure 10. Box and whisker plot of gas (top) and particle (bottom) phase Σ_{36}PAH concentrations at NJADN sites.

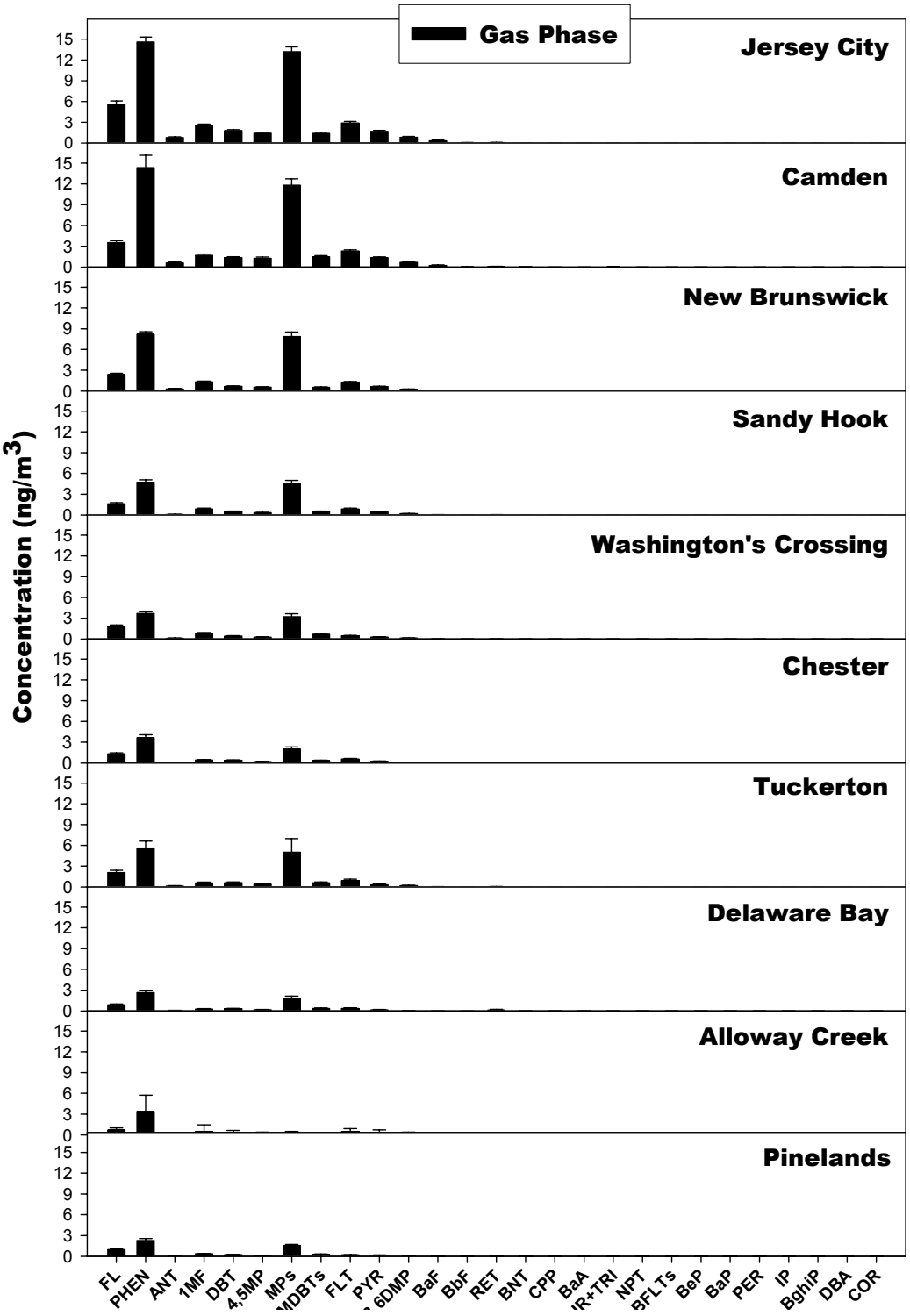

Figure 11. Annual average gas phase PAH concentrations (ng/m^3) at NJADN air monitoring stations. Error bars represent one standard deviation about the average concentrations.

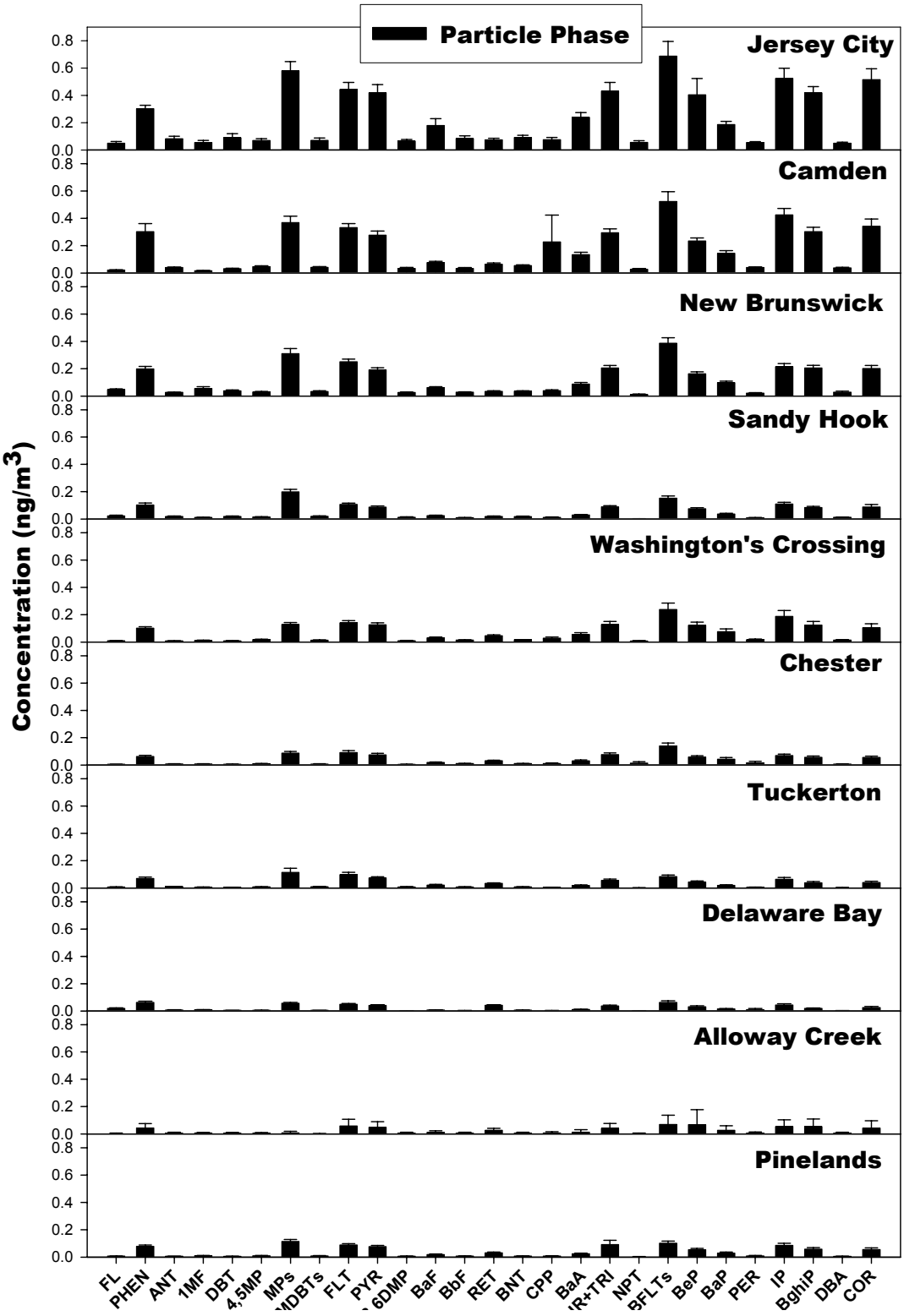

Figure 12. Annual average particle phase PAH concentrations (ng/m^3) at NJADN air monitoring stations. Error bars represent one standard deviation about the average concentrations.

As would be predicted based upon increased density of localized, proximate PAH sources in urban and industrial areas, the overall highest PAH concentrations are measured at the most highly urban and industrial sites, Camden and Jersey City. Mid-range concentrations are measured in the suburban areas, New Brunswick, Washington's Crossing, Chester, and Tuckerton. The lowest concentrations are found in coastal (Delaware Bay, Alloway Creek) and rural (Pinelands) areas, with one notable exception, the coastal Sandy Hook site.

The Sandy Hook site, although located in a coastal area away from the immediate impact of heavy traffic arteries, industry, or urbanization, can be classified as "urban/industrial"-impacted. This is because the site is located downwind (southeast) of New York City and the New Jersey urban industrial complex. This finding is consistent with what has been seen in PAH studies in other regions, such as in Lake Michigan *(1)* and the Chesapeake Bay *(2)* which are both considered impacted due to their proximity to large urban/industrial centers, Chicago and Baltimore, respectively.

In Table 8, a comparison is made of PAH concentrations measured in this study with those measured in other regions of the United States. PAH concentrations measured in urban/industrial New Jersey (Jersey City and Camden) are of a similar magnitude to those measured in urban/industrial Baltimore, Maryland *(2)* and over the southern basin of Lake Michigan adjacent to Chicago, Illinois and Gary, Indiana, two heavily urban and industrialized areas *(1)*. However, the concentrations measured in the city of Chicago, Illinois were as much as an order of magnitude larger than those measured at any of the NJADN sampling sites *(1)*. PAH concentrations measured at Washington's Crossing, Chester, Tuckerton, Delaware Bay, Alloway Creek, and the Pinelands are all similar in magnitude to concentrations measured over-water in the Chesapeake Bay and at the three rural Chesapeake Bay Atmospheric Deposition Study sites adjacent to Chesapeake Bay (Wye, Elms, and Haven Beach) *(5)*.

Gas Phase PAHs-seasonal differences. No clear seasonal trend is apparent in the concentrations of any of the PAHs. In order to look at seasonality in a more quantitative way, we can assess the seasonality as a function of temperature, looking at the variability of gas phase PAHs concentrations using a Clausius-Clapeyron type expression. One of the primary differences between PAHs and polychlorinated biphenyls (PCBs) is their emission or loading mechanisms. The manufacture of PCBs in the U.S. was banned in the 1970s when it was determined that PCBs have the potential to bioaccumulate in aquatic and terrestrial organisms.

Since that time, the only PCBs that are available to enter the atmosphere are those that are currently in use or have been disposed of in such a way that they are available to the air. Thus,

Table 8. Gas plus particle phase PAH concentrations at various locations[a]

Site Location	Reference	Phenanthrene (ng/m^3)	Pyrene (ng/m^3)	Benzo[a]pyrene (ng/m^3)
NJADN sites:				
Jersey City	this study	15 (0.19 - 32)	2.1 (0.018 - 10)	0.19 (0.012 - 1.4)
Camden	this study	15 (0.66 - 98)	1.6 (0.062 - 4.6)	0.14 (0.027 - 0.90)
New Brunswick	this study	8.4 (0.71 - 21)	0.85 (0.027 - 3.0)	0.10 (0 - 0.37)
Sandy Hook	this study	4.9 (0.078 - 16)	0.52 (0.008 - 2.7)	0.038 (0 - 0.23)
Washington Crossing	this study	3.8 (0.41 - 10)	0.43 (0.51 - 1.9)	0.077 (0.006 - 0.63)
Tuckerton	this study	5.7 (0.029 - 32)	0.41 (0.034 - 2.5)	0.021 (0.001 - 0.16)
Chester	this study	3.7 (0.029 - 10)	0.32 (0.032 - 0.94)	0.044 (0.008 - 0.34)
Delaware Bay	this study	2.7 (0.67 - 7.5)	0.22 (0.033 - 0.85)	0.015 (0.001 - 0.086)
Alloway Creek	this study	3.5 (0.043 - 10)	0.40 (.037 - 1.7)	0.032 (0.0017 – 0.12)
Pinelands	this study	2.3 (0.62 - 17)	0.21 (0.035 - 1.2)	0.031 (0.003 - 0.26)
Other locations:				
Chicago, IL	*(1)*	68 (8.6 - 250)	14 (1.8 - 100)	3.1 (1.9 - 32)
Baltimore, MD	*(2)*	21 (8.9 - 63)	2.1 (1.1 - 4.6)	0.18 (0.030 - 0.48)
Lake Michigan	*(1)*	10 (0.24 - 34)	1.8 (0.052 - 8.0)	0.18 (0.008 - 0.85)
Chesapeake Bay	*(2)*	2.4 (1.1 - 7.1)	0.38 (0.18 - 0.88)	0.040 (0 - 0.090)
Wye, MD	*(5)*	2.2 (0 - 6.2)	0.45 (0 - 2.5)	0.041 (0 - 0.30)
Elms, MD	*(5)*	1.8 (0 - 12)	0.4 (0 - 2.6)	0.045 (0 - 0.51)
Haven Beach, VA	*(5)*	2.6 (0.019 - 17)	0.76 (0.011 - 4.4)	0.030 (0 - 0.37)

[a] all concentration data reported as: Mean (Range)

PCBs enter the atmosphere primarily due to air-surface exchange processes, i.e. the re-mobilization of PCBs that were once sorbed to surfaces such as water, soil, and vegetation. In contrast, PAHs are being produced and emitted on a continuous basis every day from all combustion processes.

PCB concentrations are expected to vary to a large extent based upon temperature variations. That is, when temperatures are warm, PCBs volatilize from surfaces and re-enter the atmosphere. While this scenario occurs for PAHs as well, the constant new emission of PAHs to the air can overwhelm the temperature-driven exchange signal, thus making the temperature dependency of PAHs of lesser importance than for PCBs. This phenomenon can be seen by the

statistical results of the Clausius-Clapeyron type expression, or the R-squared values for the regression of the natural log of the partial pressure, *ln P* (in Pa), with inverse temperature, *1/T* (in K^{-1}). The sign associated with the slope of the regression line gives an indication of the differences in behavior of PAH compounds. Negative slopes (and thus positive correlations with temperature) indicate that as temperature decreases, concentrations decrease. Concentrations may decrease due to lower emissions during cold periods (less volatilization from surfaces) or due to condensation of gas-phase emissions onto particles or surfaces. The high number of statistically significant ($p < 0.05$) negative slopes for the low to medium molecular weight PAHs suggests that air-surface exchange contributes to the movement of PAHs in New Jersey (Table 9). Most of the statistically significant regressions result in negative slopes at relatively remote sites such as Alloway Creek, Pinelands, Chester, and Delaware Bay, suggesting (not surprisingly) that air-surface exchange processes are more important in determining gas-phase PAH concentrations at locations further removed from stationary sources.

For a few compounds at certain sites, temperature can be the dominant driver as is shown by the strong correlations at the Camden site for benzo[b]naphtha[2,1-d]thiophene (r^2=0.73) and chrysene/triphenylene (r^2=0.55), and at the Delaware Bay site for benzo[b]naphtha[2,1-d]thiophene (r^2=0.57) and benz[a]anthracene (r^2=0.50). If air-surface exchange as dictated by temperature is the 'dominant' mechanism for controlling atmospheric PAH concentrations, then the r-squared values should all be approaching 1.0. Overall, however, the low r^2 values (< 1.0) indicate that temperature does not control atmospheric gas phase PAH concentrations in New Jersey. It is likely that new emissions of PAHs into the air may also play a significant role in the observed concentrations. Because, on average, temperature accounts for less than 26% of the variability in atmospheric concentrations of most PAHs, seasonal variability cannot be attributed wholly to temperature-controlled air-surface exchange. This is in contrast to PCBs, where temperature explained as much as 78% of the variability in concentration *(6)*.

Particle Phase- seasonal differences. Figure 13 shows the seasonal variation in concentrations of benzo[a]pyrene and benz[a]anthracene, two predominantly particle phase high molecular weight PAHs, and in the sum of 36 particle phase PAHs, Σ_{36}PAHs. Each graphic shows that the highest particle phase concentrations occur in the colder winter season. The total winter particulate PAH signal is known to be dominated by higher molecular weight PAH

Table 9. Clausius-Clapeyron regression results. Values are number of statistically significant regressions ($p < 0.05$), and number of significant regressions yielding positive and negative slopes, organized by compound and by site.

PAHs	**Significant (out of 10)**	**Positive slope**	**Negative slope**
Fluorene	5	5	0
Phenanthrene	5	0	5
Anthracene	3	0	3
1Methylfluorene	1	1	0
Dibenzothiophene	7	0	7
4,5-Methylenephenanthrene	3	0	3
Methylphenanthrenes	3	0	3
Methyldibenzothiophenes	5	0	5
Fluoranthene	4	0	4
Pyrene	5	1	4
3,6-Dimethylphenanthrene	6	0	6
Benzo[a]fluorene	2	0	2
Benzo[b]fluorene	2	0	2
Retene	6	0	6
Benzo[b]naphtho[2,1-d]thiophene	5	0	5
Cyclopenta[cd]pyrene	2	1	1
Benz[a]anthracene	1	1	0
Chrysene/Triphenylene	2	0	2
Naphthacene	0	0	0
Benzo[b+k]fluoranthene	3	2	1
Benzo[e]pyrene	2	2	0
Benzo[a]pyrene	3	3	0
Perylene	4	4	0
Indeno[1,2,3-cd]pyrene	4	3	1
Benzo[g,h,i]perylene	5	4	1
Dibenzo[a,h+a,c]anthracene	3	0	3
Coronene	3	1	2

Sites	**Significant (out of 27)**	**Positive slope**	**Negative slope**
Jersey City	11	5	6
Camden	9	5	4
New Brunswick	8	3	5
Sandy Hook	8	7	1
Washington's Crossing	5	1	4
Chester	12	1	11

Tuckerton	3	1	2
Delaware Bay	14	1	13
Pinelands	9	1	8
Alloway Creek	15	3	12

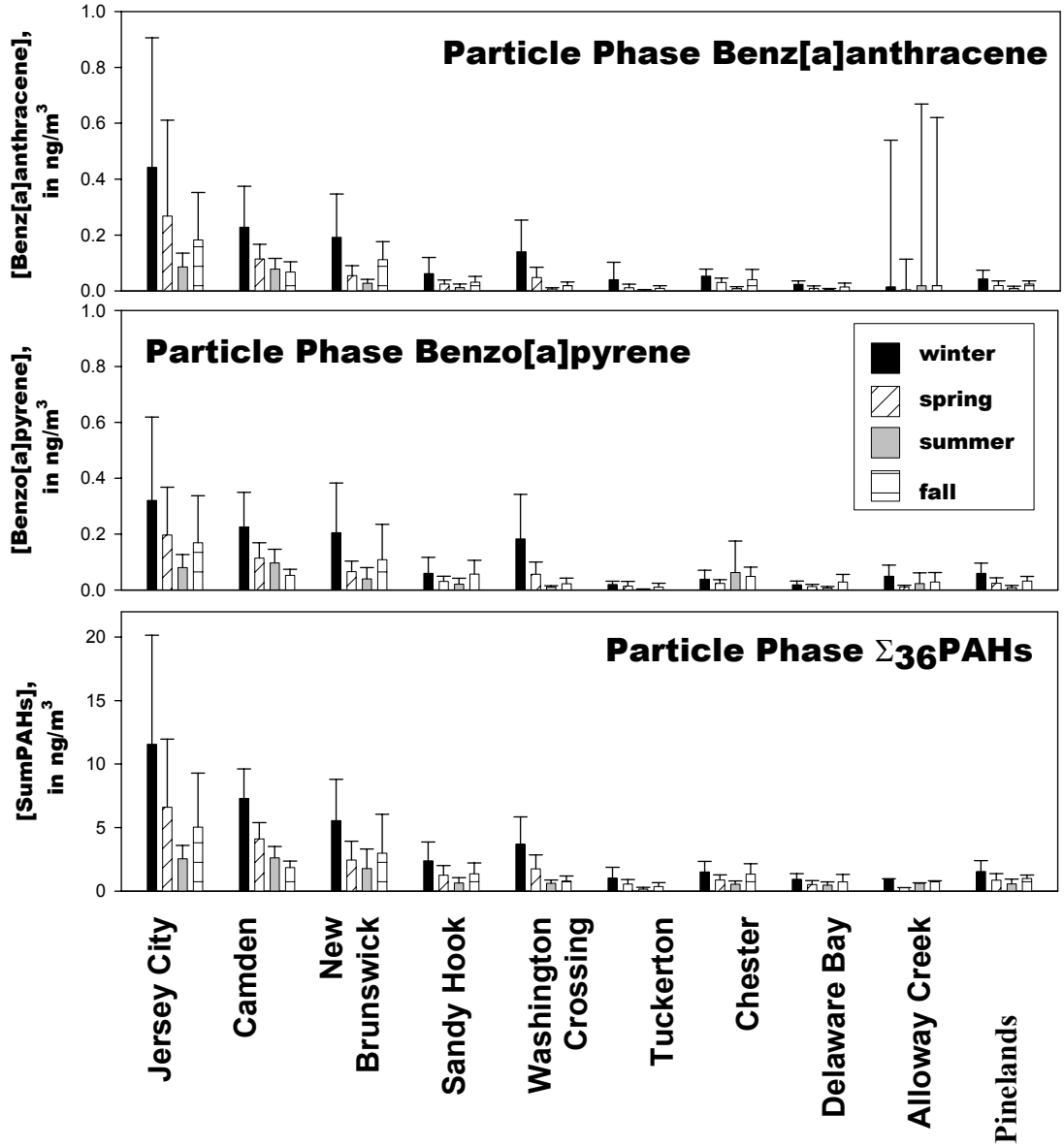

Figure 13. Seasonal particle phase concentrations of benz[a]anthracene, benzo[a]pyrene, and Σ_{36}PAHs.

compounds typically associated with atmospheric soot particles of combustion origin *(1, 7-9)*. There are a number of factors that can contribute to this increase in concentration in winter such as lower mixing heights and the decreased photolytic oxidative capacity of the atmosphere.

In contrast, although there is variability in the seasonal trends for individual PAHs, the overall particle phase Σ_{36}PAHs is lowest in the summer during warmer weather conditions. The question that arises is whether the seasonality associated with high molecular weight particle phase PAHs is primarily due to changes in temperature.

The direct influence of temperature is examined to determine if increased particulate PAH concentrations during the winter is a function of emissions rather than enhanced partitioning from the gas to the particle phase at lower temperatures. In Figure 14, a Clausius-Clapeyron type analysis examines the relationship between concentration and temperature at each of the ten sites. The graphic shows that the concentrations of particle phase PAHs are higher under lower temperature conditions as shown by the positive slopes.

However, perhaps there are fewer particles in colder weather and as such there are fewer surfaces available for PAHs to sorb, then the increase in PAH concentration could be attributed to a similar amount of PAHs sorbed to a smaller per unit particle-mass. To investigate this possibility, the particle phase PAH concentrations were normalized to total suspended particulate (TSP) concentrations, removing the influence of the amount of particle mass on the particle-phase PAH concentration. First an assessment of the behavior of TSP with temperature was performed. Regressing ln TSP versus 1/T shows statistically significant ($p < 0.05$) negative correlations at all ten sampling sites (See Figure 15). TSP mass is, therefore, higher in the warmer seasons. This is consistent with increased secondary aerosol formation under warmer temperature conditions *(7)*.

Figure 16 shows that taking into account the particle mass improves the relationship between particle-phase PAH concentrations and temperature. However, it does not change the relationship between particle phase concentrations and temperature, with lower temperatures leading to higher PAH concentrations at all ten NJADN sites. This suggests that increased emissions of PAHs in the winter drive increased concentrations of particle phase PAHs at many of the NJADN sites. However, strong positive correlations between particle phase Σ_{36}PAH concentrations and temperature are seen at Chester ($r^2 = 0.78$), Washington Crossing ($r^2 = 0.59$), and Pinelands ($r^2 = 0.59$), suggesting that gas-particle partitioning, rather than changes in emissions, dominate particle phase PAH concentrations at these sites.

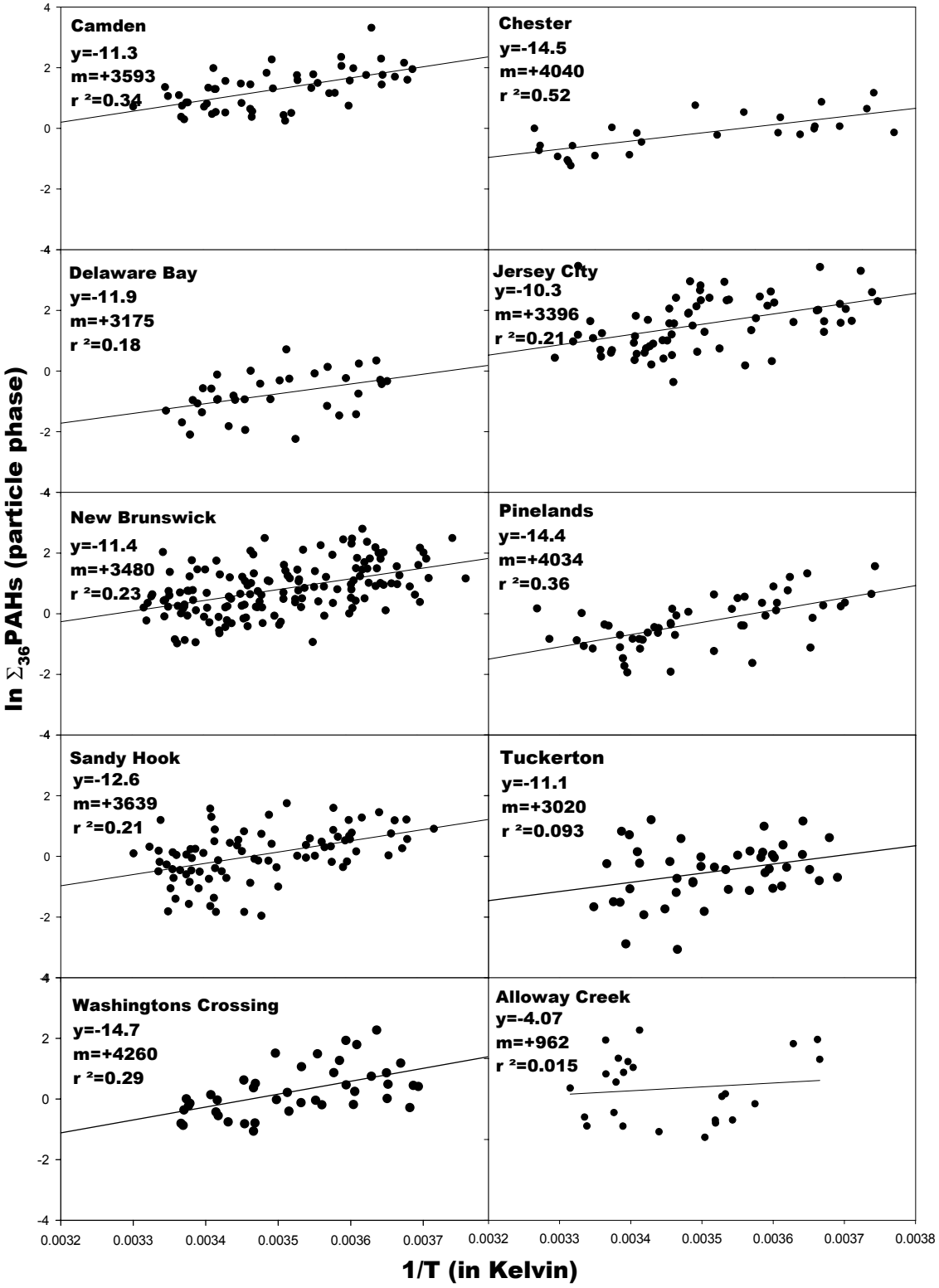

Figure 14. Clausius-Clapeyron type relationships for particulate Σ_{36}PAHs (ng/m^3).

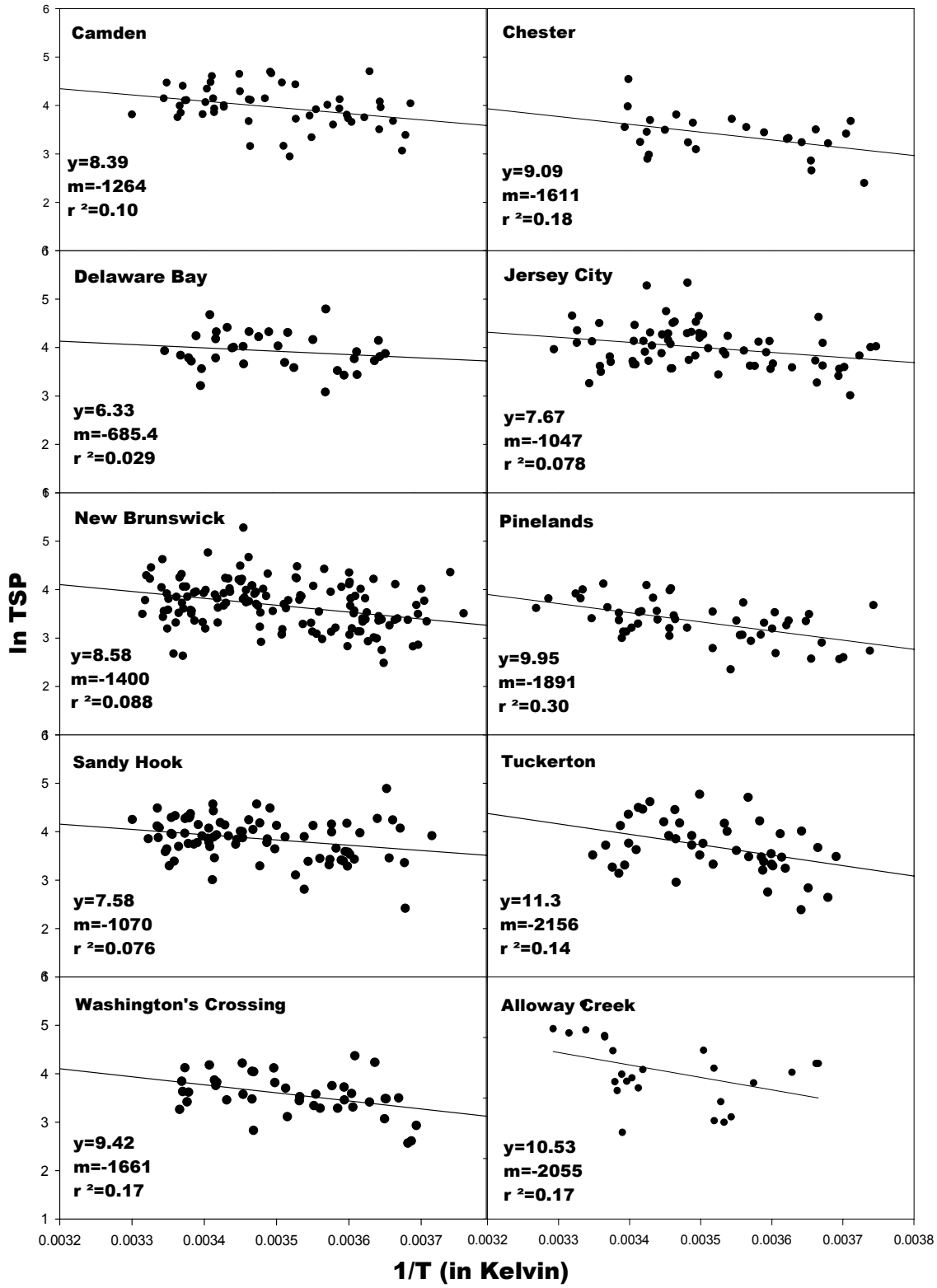

Figure 15. Clausius-Clapeyron type relationships for TSP (ug/m^3).

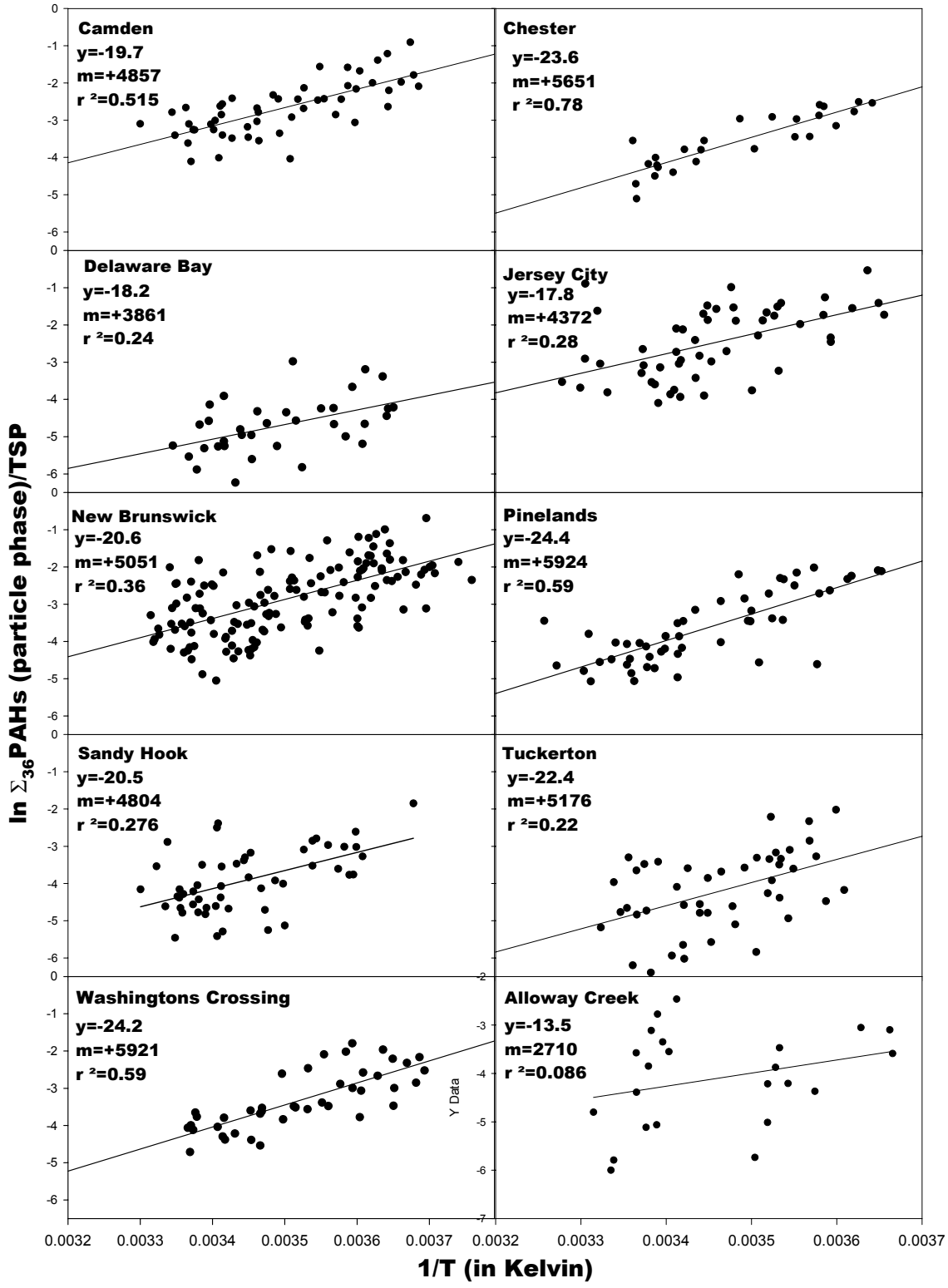

Figure 16. Clausius-Clapeyron type relationships for the ratio of particulate Σ_{36}PAHs/TSP (ng/ug).

PAH Concentrations in Precipitation-spatial differences.

Absolute PAH concentrations in precipitation vary from below detection limits (naphthacene) to as much as 3770 ng/L (fluorene). For the majority of the samples with the highest PAH concentrations, it is the small volume of water collected over that sampling period that causes the large absolute concentration values. To remove the influence of the volume collected, the data were transformed into volume weighted mean concentrations, *VWM*, (expressed as concentration *C*, in ng/L, multiplied by volume *V*, in L) in all samples, *i*, and dividing by the sum of the volumes (*V*) of the same samples, *i*.

$$VWM = \frac{\sum C_i V_i}{\sum V_i} \qquad (1)$$

The standard error of the VWM (SEM^2) can be calculated using the following equation as described in Endlich et al. *(10)* and Offenberg and Baker *(11)*.

$$(SEM)^2 = \frac{n}{(n-1)\left(\sum P_i\right)^2}\left[\sum\left(P_i X_i - \overline{PX_w}\right)^2 - 2X_w \sum\left(P_i - \overline{P}\right)\left(P_i X_i - \overline{PX_w}\right) + X_w{}^2 \sum\left(P_i - \overline{P}\right)^2\right]$$

(2)

where *n* is the number of samples, P_i is the amount of precipitation (L) in an individual sample, X_i is the concentration of the compound of interest in an individual sample (ng/L), and X_w is the VWM concentration (ng/L).

Phenanthrene, the methylated phenanthrenes, fluoranthene, and pyrene dominate the VWM precipitation PAH concentrations. Individually, the low to medium molecular weight PAHs, mostly in the gas phase, represent the highest concentrations (and together represent approximately half the total Σ_{36}PAH gas+particle precipitation concentration). The predominantly particle phase PAH compounds (BaA to COR) represent a more significant contribution to the total gas + particle precipitation signal (~33%) than for the (gas+particle) air samples (~6%).

Figure 17 shows the chemical profiles for gas, particle and precipitation concentrations for the New Brunswick site. For five of the eight sites (New Brunswick, Sandy Hook, Chester, Tuckerton, and Pinelands), the precipitation profiles are statistically similar to the particle phase

profiles in the air. This suggests, as is the case for PCBs in precipitation *(12)*, that atmospheric PAHs associated with atmospheric particles are efficiently scavenged by precipitation. Scavenging of particles by precipitation does not occur via equilibrium partitioning as is true for scavenging of gases. Rather, it is controlled by physical means, resulting in the collision of particles with rain droplets via interception, impaction, Brownian motion, coulombic and phoretic forces *(13, 14)* that are strongly influenced by the aerodynamic diameter of the particles.

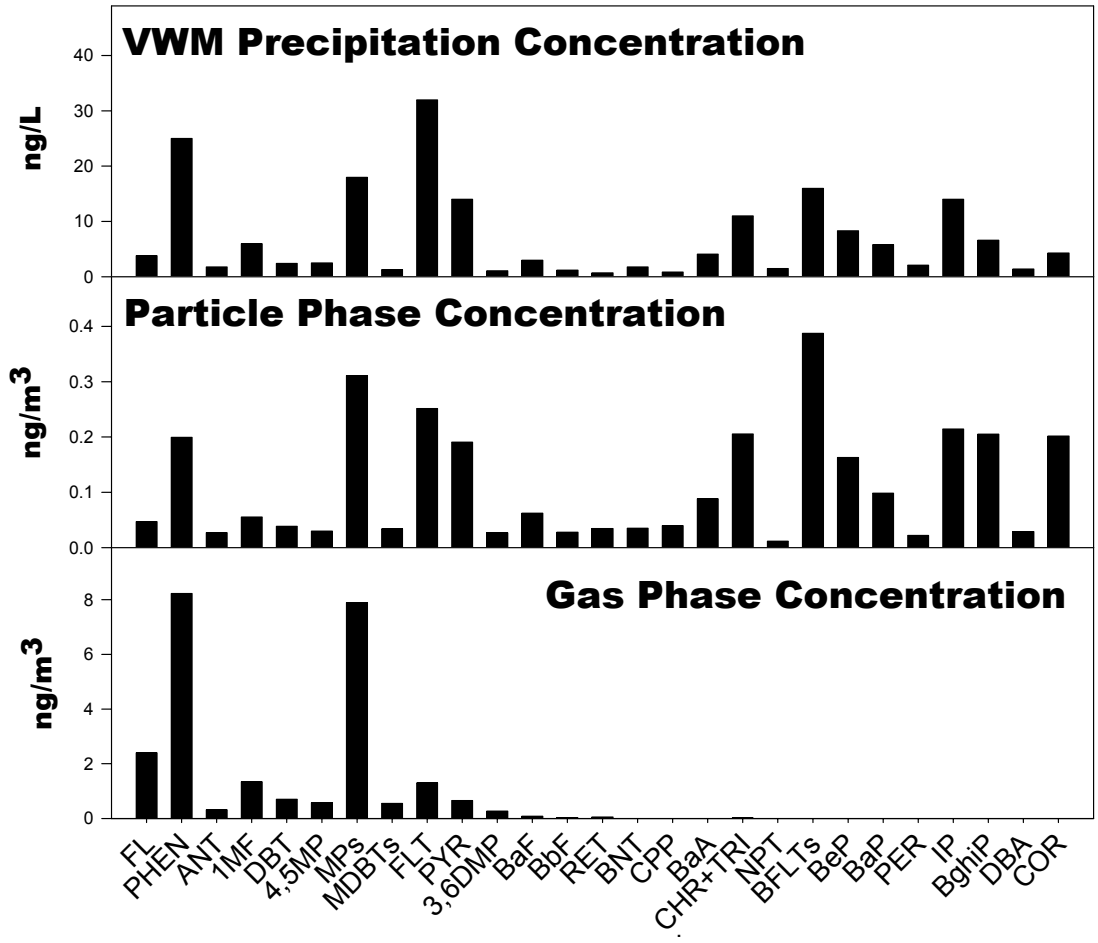

Figure 17. PAH profiles for precipitation and gas and particle phases in New Brunswick.

The similarity of profiles between the atmospheric particle phase and precipitation does not hold true for both the urban/industrial sites, Jersey City and Camden, where the precipitation profile is more similar to that of the gas phase. Other researchers have noted that particle washout ratios for inorganics increase with distance from emission sources due to an increase in vertical dispersion *(13, 15)*. This phenomenon could account for the differences in PAH profiles between atmospheric particles and precipitation at the urban NJADN sites.

Average VWM precipitation concentrations do not follow the same spatial pattern as the air concentrations. Although the highest concentrations occur at one of the highly urban/industrial sites (Jersey City), urban/industrial Camden and suburban New Brunswick demonstrate statistically similar concentrations ($p < 0.05$). In contrast to air PAH concentrations, precipitation PAH concentrations were lower at the "impacted" Sandy Hook site than at the lightly suburban Tuckerton, Chester, and Alloway Creek stations.

Table 10. VWM concentrations of PAHs in precipitation at NJADN and other sites.

Site Location	Land-use Classification	Ref.	Phenanthrene (ng/L)	Pyrene (ng/L)	Benzo[a]pyrene (ng/L)
Jersey City, NJ	urban/industrial	this study	43	23	8.2
Camden, NJ	urban/industrial	this study	29	15	5.2
New Brunswick, NJ	suburban	this study	25	14	5.8
Sandy Hook, NJ	coastal-impacted	this study	11	5.1	2.0
Chester, NJ	light suburban	this study	16	8.6	2.9
Tuckerton, NJ	coastal-light residential	this study	21	14	2.2
Alloway Creek, NJ	rural/coastal	this study	13	7.0	2.4
Pinelands, NJ	rural	this study	6.7	3.5	1.4
Chicago, IL	urban/industrial	*(16)*	7240	4901	2411
Lake Michigan	over-water	*(16)*	31	26	15
South Haven, MI	coastal-impacted	*(16)*	39	28	21
Wye, MD	rural	*(5)*	3.0	1.9	0.63
Elms, MD	rural	*(5)*	4.7	9.0	1.8
Haven Beach, VA	rural	*(5)*	4.3	2.1	0.70

In Table 10, a comparison is made of VWM precipitation PAH concentrations measured in this study with those measured in other regions of the United States by other researchers. PAH

concentrations in Chicago, IL *(16)* precipitation are often more than 2 orders of magnitude larger than those measured in urban/industrial New Jersey (Jersey City and Camden). Precipitation concentrations in Jersey City and Camden are of a similar magnitude to those measured over the southern basin of Lake Michigan and directly east of southern Lake Michigan, at the South Haven site *(16)*. Precipitation concentrations at the rural Pinelands were similar to those measured at the three rural Chesapeake Bay Atmospheric Deposition Study sites adjacent to Chesapeake Bay (Wye, Elms, and Haven Beach) *(5)*.

References

(1) Simcik, M. F.; Zhang, H.; Eisenreich, S. J.; Franz, T. P. Urban contamination of the Chicago/Coastal Lake Michigan atmosphere by PCBs and PAHs during AEOLOS. *Environ. Sci. Technol.* **1997**, *31*, 2141-2147.

(2) Offenberg, J. H.; and Baker, J. E. Influence of Baltimore's urban atmosphere on organic contaminants over the Northern Chesapeake Bay. *J. Air Waste Mngmt. Assoc.* **1999**, *49*, 959-965.

(3) Hoff, R. M.; Strachan, W. M. J.; Sweet, C. W.; Chan, C. H.; Shackleton, M.; Bidleman, T. F.; Brice, K. A.; Burniston, D. A.; Cussion, S.; Gatz, D. F.; Harlin, K.; Schroeder, W. H. Atmospheric deposition of toxic chemicals to the Great Lakes: A review of data through 1994. *Atmos. Environ.* **1996**, *30*, 3305-3527.

(4) Hillery, B. R.; Simcik, M. F.; Basu, I.; Hoff, R. M.; Strachan, W. M. J.; Burniston, D.; Chan, C. H.; Brice, K. A.; Sweet, C. W.; Hites, R. A. Atmospheric deposition of toxic pollutants to the Great Lakes as measured by the Integrated Atmospheric Deposition Network. *Environ. Sci. Technol.* **1998**, *32*, 2216-2221.

(5) Baker, J.E.; Poster, D.L.; Clark, C.A.; Church, T.M.; Scudlark, J.R.; Ondov, J.M.; Dickhut, R.M.; Cutter, G. Loadings of atmospheric trace elements and organic contaminants to the Chesapeake Bay. In *Atmospheric Deposition of Contaminants to the Great Lakes and Coastal Waters*; Baker, J. E., Ed.; **1997.**

(6) Totten, L. A. Gigliotti, C.L.; Van Ry, D.A.; Offenberg, J.H.; Nelson, E.D.; Dachs, J.; Reinfelder, J.R.; Eisenreich, S.J. The New Jersey Atmospheric Deposition Network: Atmospheric dynamics of PCBs and deposition to the Hudson River Estuary. *Environ. Sci. Technol.* **2003**, *in review*,

(7) Seinfeld, J. H.; Pandis, S. N. *Atmospheric Chemistry and Physics*; John Wiley & Sons, Inc.: New York, 1998.

(8) Allen, J. O.; Dookeran, N. M.; Smith, K. A.; Sarofim, A. F.; Taghizadeh, K.; Lafleur, A. L. Measurement of polycyclic aromatic hydrocarbons associated with size-segregated atmospheric aerosols in Massachusetts. *Environ. Sci. Technol.* **1996**, *30*, 1023-1031.

(9) Simó, R.; Grimalt, J. O.; Albaigés, J. Loss of unburned-fuel hydrocarbons from combustion aerosols during atmospheric transport. *Environ. Sci. Technol.* **1997**, *31*, 2697-2700.

(10) Endlich, R. M.; Eynon, B.P.; Ferek, R.J.; Valdes, A.D.; Maxwell, C.X. Statistical analysis of precipitation chemistry measurements over the Eastern United States: Part I. seasonal and regional patterns and correlations. *J. Appl. Metorol.* **1988**, *27*, 1326-1333.

(11) Offenberg, J. H.; Baker, J.E. Polychlorinated biphenyls in Chicago precipitation: enhanced wet deposition to near-shore Lake Michigan. *Environ. Sci. Technol.* **1997**, *31*, 1534-1538.
(12) Van Ry, D. A.; Gigliotti, C.L.; Glenn IV, T.R.; Nelson, E.D.; Totten, L.A.; Eisenreich, S.J. Wet deposition of polychlorinated biphenyls in urban and background areas of the Mid-Atlantic States. *Environ. Sci. Technol.* **2002**, 36, 3201-3209.
(13) Poster, D. L.; Baker, J. E. Influence of submicron particles on hydrophobic organic contaminants in precipitation: 1. Concentrations and distributions of Polycyclic Aromatic Hydrocarbons and Polychlorinated Biphenyls in rainwater. *Environ. Sci. Technol.* **1996**, *30*, 341-348.
(14) Offenberg, J. H.; Baker, J.E. Precipitation scavenging of polychlorinated biphenyls and polycyclic aromatic hydrocarbons along an urban to over-water transect. *Environ. Sci. Technol.* **2002**, *36*, 3763-3771.
(15) Hewitt, C. N.; Rashed, M.B. The deposition of selected pollutants adjacent to a major rural highway. *Atmos. Environ.* **1991**, *25A*, 979-983.
(16) Offenberg, J.H. Semi-volatile Organic Compounds in Urban and Over-water Atmospheres. Ph.D. Dissertation, University of Maryland, **1998**.

II.A2b. Polycyclic Aromatic Hydrocarbons Part II – Atmospheric deposition

Abstract

Atmospheric deposition fluxes of polycyclic aromatic hydrocarbons (PAHs) were estimated for multiple sites in the Mid-Atlantic region, representing urban/industrial, suburban, coastal and rural areas as part of the New Jersey Atmospheric Deposition Network (NJADN). Concentrations of 36 PAH compounds were measured in the gas and particle phases in air at nine sites and in precipitation at seven sites at regular intervals from October 1997 through May 2001 allowing for the estimation of total atmospheric deposition. Average gas absorption and dry particle deposition PAH fluxes ranged from 0.004 (naphthacene) to 5040 (methylphenanthrenese) ng/m^2 day and 0.11 (naphthacene) to 300 (benzo[b+k]fluoranthene) ng/m^2 day at the nine sites. Average atmospheric wet deposition PAH fluxes at the seven sites ranged from 0.40 (cyclopenta[cd]pyrene) to 140 (methylphenanthrenes) ng/m^2 day. The magnitude of the gas absorption fluxes is driven by gas phase concentrations and the influence of wind speed on the mass transfer. Wet deposition is controlled by gas and particle phase concentrations, as well as the precipitation amount at each of the sites. The magnitude of dry particle deposition is correlated with the degree of urbanization and industrialization with the largest fluxes measured at the two most highly urban/industrialized areas, Jersey City and Camden. The dominant process by which atmospheric deposition for each PAH compound occurs is affected by the gas-particle distribution in the air. The elevated atmospheric deposition of PAHs in this study is consistent with the proximity of higher local and regional emissions in the New York-New Jersey region and near NJADN monitoring stations.

Introduction

Continuous emissions of polycyclic aromatic hydrocarbons (PAHs) into the atmosphere from combustion-related emission sources such as motor vehicles and residential/commercial fossil fuel use, can lead to significant atmospheric deposition fluxes. Semi-volatile organic compounds, like PAHs, are removed from the atmosphere via dry particle deposition, gaseous air deposition, and wet deposition. The residence time for these compounds in the atmosphere (and therefore, the transport distance) is dependent on the distribution of the compounds between the

gas and particle phases in the air *(1, 2)*. These atmospheric pathways allow for the delivery of semi-volatile organic compounds to aquatic and terrestrial ecosystems located both near to and remote from emission sources. Thus, atmospheric deposition is likely an important input pathway that must be accounted for in the development of Total Maximum Daily Load (TMDL) standards for PAH compounds-of-concern in the mid-Atlantic region. One of the primary goals of the New Jersey Atmospheric Deposition Network (NJADN) is to provide estimates of the importance of atmosphere delivery processes to urban water bodies in New Jersey.

NJADN was implemented in October 1997 as a research and monitoring network to assess the magnitude of atmospheric deposition of a suite of semi-volatile, toxic organic compounds (SOCs), including polychlorinated biphenyls (PCBs), polycyclic aromatic hydrocarbons (PAHs), and target organo-chlorine pesticides to New Jersey. NJADN was designed to quantify both the local and regional signals of air toxics concentrations by locating monitoring sites in areas with different geographical land-use regimes, including urban, suburban, rural, and coastal environments. The concentrations are then translated into deposition fluxes to both terrestrial and aquatic systems in New Jersey. This paper focuses on the estimates of atmospheric deposition of PAHs from ~4 years of sampling (October 1997 – May 2001) at ten sites around the state of New Jersey.

Modeling Framework for Deposition Calculations.

Gas absorption. Models of SOC air-water transfer have been developed to calculate the magnitude and direction of the flux. Whitman *(5)* developed a two-film resistance model describing the rate of transfer as controlled by the compound's ability to diffuse across two thin stagnant films at the air-water interface, the water film and the air film. The concentration gradient drives the net direction of transfer. A modified Whitman two-film model is applied here, the specifics of which have been extensively described in numerous publications *(4, 6-10)*. The overall flux calculation is defined by

$$NetFlux_{air-water} = K_{OL}\left(C_{diss} - \frac{C_{gas}}{H'}\right) \quad (1)$$

where the net air-water flux is in units of ng/ m^2 day, K_{OL} (m/day) is the overall mass transfer coefficient and $(C_{diss}\text{-}C_{gas}/H')$ describes the concentration gradient (ng/m^3). C_{diss} (ng/m^3) is the dissolved phase concentration of the compound in water. C_{gas} (ng/m^3) is the gas phase

concentration of the compound in air which is divided by the dimensionless Henry's Law constant, *H'*, *H'= H/RT*, *R* is the universal gas constant (8.3145 Pa m^3/K mol), *H* is the temperature and salinity-corrected Henry's Law Constant (Pa m^3/mol), and *T* is the absolute temperature of the interface (K).

The net air-water flux can be divided into two components, one describing the volatilization flux, F_{vol}, the transfer from a surface (i.e. water or soil) to air, and one describing the gas absorption flux, F_{ga}, the transfer from air to a surface.

$$F_{vol} = K_{OL}\left(C_{diss}\right) \quad (2)$$

$$F_{ga} = K_{OL}\left(\frac{C_{gas}}{H'}\right) \quad (3)$$

The gross gaseous absorption flux was calculated in this study at all sites to represent the magnitude of PAHs depositing to water surfaces adjacent to the NJADN monitoring stations.

Dry particle deposition. Dry particle deposition is the process by which particles are transported from the air to surfaces via gravitational settling and turbulent diffusion. The dry particle deposition flux, F_{dry}, (ng/ m^2 day) was calculated by multiplying the concentration of PAHs on atmospheric particles, C_{part} (ng/m^3) by a deposition settling velocity, υ_d (cm/s or m/day).

$$F_{dry} = C_{part}\left(\upsilon_d\right) \quad (4)$$

Deposition settling velocities depend on a number of factors including wind speed, atmospheric stability, relative humidity, particle characteristics (diameter, shape, and density), and receptor surface characteristics *(11-15)*. Franz et al. *(11)* measured deposition settling velocities in the range of 0.6 to 0.9 cm/s for PAHs in urban areas where large particles overwhelmingly dominate the atmospheric particle distribution. In this study, a deposition settling velocity of 0.5 cm/s was selected to take into account the disproportionate influence that large particles have upon the overall settling velocity for areas adjacent to urban and industrial regions.

Wet deposition. ***Wet deposition is the process by which particles and gases are scavenged from the atmosphere by precipitation (rain, snow, hail, sleet) and deposited to terrestrial and aquatic surfaces. Wet deposition fluxes,*** $\mathbf{F_{wet}}$***, (ng/ m^2 day) are calculated by multiplying the dissolved + particle volume weighted concentration of the PAH compound in precipitation,*** $\mathbf{C_{precip}}$ ***(ng/L) by the total precipitation flux,*** **P** ***(L/m^2 day).***

$$F_{wet} = C_{precip}(P) \tag{5}$$

The volume weighted mean concentration (*VWM*) is calculated by summing the PAH masses (expressed as concentration *C*, in ng/L, multiplied by volume *V*, in L) in all samples, *i*, and dividing that by the sum of the volumes (*V*) of the same samples, *i*.

$$VWM = \frac{\sum C_i V_i}{\sum V_i} \tag{6}$$

Propagation of error estimates. It is critically important to assess the random errors associated with the flux calculations. This can be accomplished using a propagation of error estimation technique as described by *(9, 16-18)* and as shown in detail below.

Error estimate- gas absorption (F_{ga}):

$$\lambda^2(F_{ga}) = \left(\frac{\partial F_{ga}}{\partial K_{ga}}\right)^2 (K_{OL}\lambda_{K\,OL})^2 + \left(\frac{\partial F_{ga}}{\partial C_{gas}}\right)^2 (C_{gas}\lambda_{C\,gas})^2 + \left(\frac{\partial F_{ga}}{\partial H'}\right)^2 (H'\lambda_{H'})^2 \tag{7}$$

where F_{ga} is the gas absorption flux (ng/m^2 day), K_{OL} is the mass transfer coefficient (m/day), C_{gas} is the gas phase PAH concentration in air (ng/m^3), *H'* is the dimensionless Henry's Law constant, and λ is the coefficient of error. Total λC_{gas} uncertainties were in the range of 17 to 28% for all PAHs as determined based upon an error estimation in Chapter 3 *(19)*. The final term associated with the error in *H'* was not incorporated into the final calculation. Because the estimated value *H'* is a constant, it can be assumed that errors in *H* (deviations from the "true" values of H) are not random, but are systematic *(16)*.

The equation for K_{OL} is used to calculate the error associated with K_{OL} (λK_{OL}) as given by

$$\frac{1}{K_{OL}} = \frac{1}{k_w} + \frac{H'}{k_a} \tag{8}$$

where $1/k_w$ is the resistance to transfer encountered by the compound as it crosses the water side of the air-water interface and H'/k_a is the resistance encountered as it crosses the air side. The error is therefore calculated as

$$\left(K_{OL}\lambda_{K\,ga}\right)^2 = \left(\frac{(k_w H')^2}{(k_w H' + k_a)^2}\right)^2 (k_a \lambda_{k\,a})^2 + \left(\frac{k_a{}^2}{(k_w H' + k_a)^2}\right)^2 (k_w \lambda_{kw})^2 \quad (9)$$

Bamford *(20)* estimated errors associated with K_{OL} for PAHs to range from 10% - 80% with an average of 60%. The majority of the error associated with gas absorption fluxes could be attributed to the value of K_{OL}, specifically regarding the uncertainties due to the effect variations in wind speed has on the k_w. A large portion of the underlying uncertainty lies in the choice of which of the three common wind speed-k_w relationships is used for the flux calculation. Different relationships for k_w have been developed by various researchers including Wanninkhof *(21)*, Wanninkhof and McGillis *(22)*, and Liss and Merlivat *(23)*.

Wanninkhof *(21)*:

$$k_{w,CO2} = 0.45 u_{10}{}^{1.64} \quad (10)$$

Wanninkhof and McGillis *(22)*:

$$k_{w,CO2} = 0.0283 u_{10}{}^{3} \quad (11)$$

Liss and Merlivat *(23)*:

$$\begin{aligned} k_{w,CO2} &= 0.17 u_{10} \quad for \;\; u_{10} < 3.6 \; m/s \\ k_{w,CO2} &= 2.85 u_{10} - 9.65 \quad for \;\; 3.6 < u_{10} < 13 \; m/s \\ k_{w,CO2} &= 5.9 u_{10} - 49.3 \quad for \;\; u_{10} > 13 \; m/s \end{aligned} \quad (12)$$

The differences in $k_{w,\,CO2}$ values are shown in Figure 18, which displays all three wind speed relationships from 0 to 15 m/s. At a maximum, the value of $k_{w,\,CO2}$ differs by as much as a factor of 16 at a wind speed of ~1 m/s.

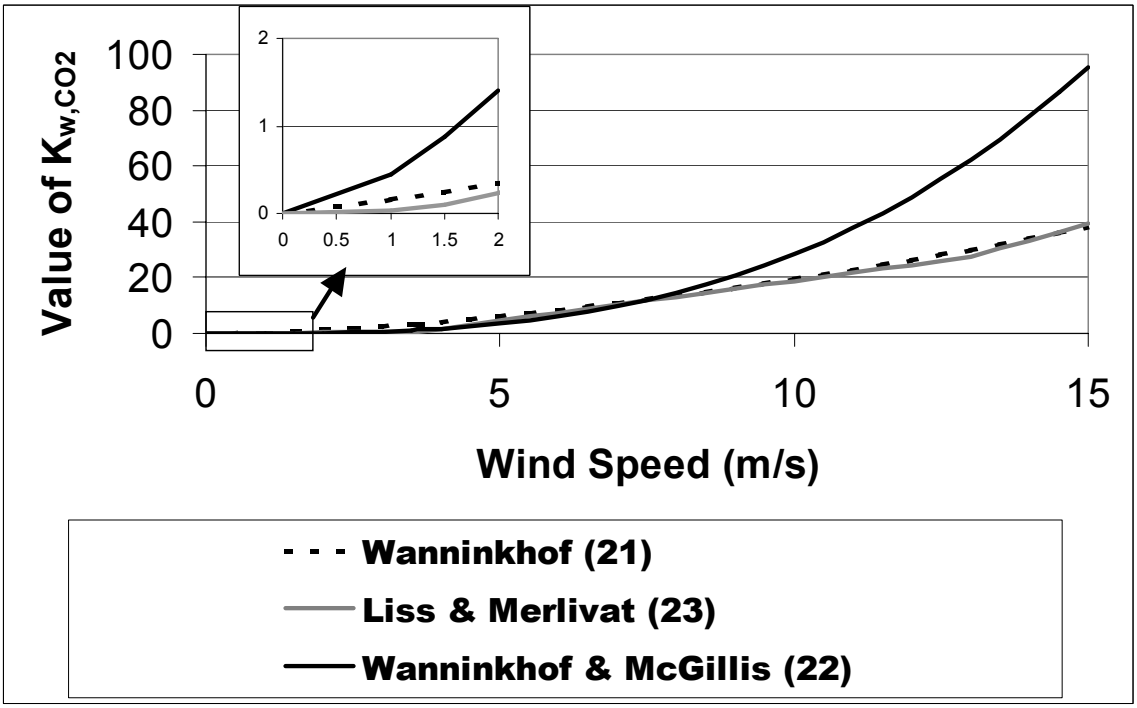

Figure 18. Comparison of wind speed-k_w relationships.

In this work, we have assumed the uncertainty associated with K_{OL} for PAHs is 60% based upon uncertainties surrounding the Wanninkhof *(21)* relationship (Eq. 10) alone as determined in *(20)*. Therefore, the propagation of error leads to an average uncertainty of from 62 to 66% for gas absorption fluxes.

Error estimate- wet deposition (F_{wet}):

$$\lambda^2\left(F_{wet}\right)=\left(\frac{\partial F_{wet}}{\partial ppt}\right)^2\left(ppt\lambda_{ppt}\right)^2+\left(\frac{\partial F_{wet}}{\partial VWM}\right)^2\left(VWM\lambda_{VWM}\right)^2 \qquad (13)$$

The error associated with the precipitation intensity (λ_{ppt}) is a factor of the uncertainty about the physical measurement of the volume of precipitation collected in the carboy after draining through the XAD-2 column. That uncertainty is assumed to be 5%.

The standard error of the VWM (λ_{VWM}) can be calculated using the following equation as described in Endlich et al. *(24)* and Offenberg and Baker *(25)*.

$$(\lambda_{VWM})^2 = \frac{n}{(n-1)(\sum P_i)^2}\left[\sum\left(P_i X_i - \overline{PX_w}\right)^2 - 2X_w\sum\left(P_i - \overline{P}\right)\left(P_i X_i - \overline{PX_w}\right) + X_w{}^2\sum\left(P_i - \overline{P}\right)^2\right] \quad (14)$$

where n is the number of samples, P_i is the amount of precipitation (L) in an individual sample, X_i is the concentration of the compound-of-interest in an individual sample (ng/L), and X_w is the VWM concentration (ng/L). The calculated error associated with the VWM ranges from 18 – 30% for the NJADN PAH precipitation data. Overall, the average uncertainty associated with wet deposition fluxes ranges from 19 to 31%.

Error estimate- dry particle deposition (F_{dry}):

$$\lambda^2(F_{dry}) = \left(\frac{\partial F_{dry}}{\partial C_{part}}\right)^2 (C_{part}\lambda_{C\,part})^2 + \left(\frac{\partial F_{dry}}{\partial \upsilon_d}\right)^2 (\upsilon_d \lambda_{\upsilon d})^2 \quad (15)$$

where F_{dry} is the dry particle flux (ng/m^2 day), C_{part} is the particle phase PAH concentration in air (ng/m^3), $\lambda_{C\,part}$ is the error associated with C_{part}, υ_d is the depositional settling velocity (m/day), and $\lambda_{\upsilon d}$ is the error associated with υ_d. Total λC_{part} uncertainties were in the range of 17 to 28% for all PAHs as determined based upon an error estimation in Gigliotti et al. *(19)*.

For all calculations of dry particle deposition, a deposition settling velocity, υ_d, of 0.5 c/m was applied as discussed in the Modeling Framework section. Other researchers *(26, 27)* have proposed the use of a smaller value of υ_d of 0.2 cm/s. The difference in the depositional settling velocity ($\lambda_{\upsilon d}$) between these two values yields an error of 250%. Propagation of error, therefore, gives an average uncertainty of 250 to 252% associated with the dry deposition fluxes. The uncertainty surrounding the choice of the υ_d applied could be reduced if particle size distribution data were available.

Results and Discussion

The distribution of target PAHs between the gas and particle phases in the atmosphere is important in determining the dominant deposition process and the magnitude of total atmospheric deposition. For example, phenanthrene occurs predominantly in the gas phase and thus can be loaded by gas absorption onto aquatic or terrestrial surfaces**.** In contrast, benzo[a]pyrene is primarily particle-bound in the atmosphere and thus is removed by wet and

dry particle deposition with only a minor contribution from gas phase absorption. This demonstrates the importance of accurate and precise measurements of each compound in the atmospheric gaseous and particle phases for the estimation atmospheric deposition. The data presented herein represents the first comprehensive estimates of PAH deposition to New Jersey.

Gas Absorption – spatial differences. Gas-phase PAH concentrations are an important driver of the magnitude of the gross gas absorption flux. As discussed previously in this report, gas phase PAH concentrations in New Jersey generally increase as the degree of urbanization/industrialization increases. Therefore, if gas phase concentrations were the dominant driver of the gross absorption flux, then the fluxes would follow the same spatial trend as the gas phase concentrations: urban/industrial Jersey City and Camden > suburban New Brunswick > coastal-"impacted" Sandy Hook > light suburban Chester, Tuckerton, Washington Crossing > coastal Delaware Bay and Alloway Creek > rural Pinelands. However, in addition to gas phase concentrations, other parameters involved in the calculation of the mass transfer coefficient value, K_{OL}, can dramatically affect the flux, such as wind speed. This is seen when we evaluate the gross gas absorption fluxes relative to the average wind speeds at each of the sites.

Table 11 shows that the average annual gas absorption fluxes range from 0.004 (naphthacene) to 5040 (methylphenanthrenes) ng/m^2 day in New Jersey. While the highest gross gas absorption fluxes do occur at the sites with the highest gas phase Σ_{36}PAH concentrations, Jersey City (16200 ± 10200 ng/m^2 day) and Camden (11400 ± 6960 ng/m^2 day), the next highest fluxes were measured at the Sandy Hook (6080 ± 4000 ng/m^2 day) and Tuckerton (5800 ± 3660 ng/m^2 day) sites; whereas the degree of urbanization argument would have predicted New Brunswick as the next highest after Jersey City and Camden. The Sandy Hook (5.4 m/s) and Tuckerton (5.0 m/s) sites have average wind speeds that are significantly higher than those at New Brunswick (1.8 m/s), which likely accounts for the lower-than-predicted flux at New Brunswick. To prove this theory, we re-calculated the Σ_{36}PAH gas absorption flux at New Brunswick using an average wind speed of 5.0 m/s and found that New Brunswick would indeed have the next highest flux after Jersey City and Camden. In fact, if the fluxes were all re-calculated using an average wind speed of 5.0 m/s, the order of highest to lowest flux follows the highest to lowest gas phase concentrations as predicted by the degree of

urbanization/industrialization. Therefore, it is a combination of concentration and wind speed that drives the spatial variability in gross gas absorptive fluxes in New Jersey.

Table 11. Average annual gas absorption fluxes of individual PAHs at NJADN sites (ng/m^2/d).

PAH	JC	CC	NB	SH	CH	WC	TK	DB	AC	PL
Fluorene	1587	812	214	582	99	372	580	46	96	128
Phenanthrene	4923	3860	1015	1764	310	1038	1977	136	579	351
Anthracene	241	149	31	47	4.3	26	63	3.0	12	5.2
1Methylfluorene	685	386	120	332	25	175	153	12	67	44
Dibenzothiophene	517	298	65	169	24	103	189	12	52	32
4,5-Methylenephen	477	320	66	134	16	76	168	8.2	33	21
Methylphenanthrenes	5039	3683	1214	2160	201	1070	1875	113	55	298
Methyldibenzothiophenes	429	350	58	185	23	174	169	17	12	39
Fluoranthene	1147	755	204	373	65	158	395	26	115	44
Pyrene	706	477	113	199	29	101	151	14	69	31
3,6-Dimethylphen	275	169	31	84	6.1	39	57	3.1	26	9.5
Benzo[a]fluorine	106	60	9.1	19	2.0	11	14	1.4	6.4	2.8
Benzo[b]fluorine	26	15	3.2	5.0	0.72	2.7	4.4	0.48	3.1	0.55
Retene	31	28	8.7	17	3.2	18	16	10	17	7.2
Benzo[b]naphtho[2,1-d]thiophene	7.6	11	0.57	4.6	0.32	2.6	3.3	0.47	2.3	1.4
Cyclopenta[cd]pyrene	3.5	1.3	1.4	0.23	0.12	0.33	0.43	0.10	0.12	0.34
Benz[a]anthracene	4.5	3.3	0.61	0.68	0.17	0.84	0.60	0.18	0.30	0.22
Chrysene/ Triphenylene	21	20	4.5	5.5	1.4	5.0	6.2	1.5	7.6	1.7
Naphthacene	1.5	0.41	0.46	0.087	0.037	0.017	0.15	0.0038	0.19	0.10
Benzo[b+k]fluoranthene	4.4	2.9	1.1	0.83	0.13	0.78	0.99	0.14	0.55	0.14
Benzo[e]pyrene	1.9	2.0	0.56	0.64	0.10	0.38	0.80	0.14	0.63	0.079
Benzo[a]pyrene	1.8	1.4	0.40	0.44	0.057	0.22	0.49	0.043	0.81	0.055
Perylene	0.40	0.28	0.091	0.097	0.0081	0.038	0.094	0.0041	0.46	0.0085
Indeno[1,2,3-cd]pyrene	1.3	1.3	0.34	0.37	0.077	0.12	0.31	0.040	0.17	0.042
Benzo[g,h,i]perylene	0.99	0.66	0.51	0.29	0.024	0.062	0.14	0.013	0.26	0.021
Dibenzo[a,h+a,c] anthracene	0.18	0.10	0.038	0.054	0.044	0.053	0.089	0.022	0.017	0.023
Coronene	0.77	0.63	0.29	0.38	0.23	0.30	0.51	0.13	0.12	0.16
Σ_{36}PAHs	16239	11407	3165	6084	810	3374	5824	405	1155.84	1017

Although the Pinelands site is classified as rural, gas absorption fluxes are often higher than in areas that are significantly more urbanized. This may be due to the proximity of the Pinelands site to the Camden/Philadelphia urban/industrial area located ~40 km the west and Interstate 295 and the New Jersey Turnpike (~25 km to the west). With the dominant winds in New Jersey coming from the west, the Pinelands site is likely influences by air masses derived

from the west. In addition, the Pinelands site is less than 5 km south of Fort Dix Military Reservation and less than 10 km south of McGuire Air Force Base.

In Table 12, gas absorption fluxes for select PAH compounds measured as part of the Integrated Atmospheric Deposition Network (IADN) for remote sites adjacent to the Laurentian Great Lakes *(26)* are presented. Fluxes measured at the sites adjacent to Lake Superior, Lake Michigan and Lake Ontario are on the same order as those measured at the Chester and Pinelands NJADN sites which represent two of the sites with the lowest measured fluxes in New Jersey. The annual average flux at Lake Erie resembles most closely the Washington Crossing and New Brunswick fluxes which are mid-range fluxes relative to the rest of New Jersey.

Gas Absorption –- seasonal differences. The NJADN gross gas absorption fluxes of Σ_{36}PAH as well as individual PAH compounds display no consistent seasonal trend in New Jersey.

Table 12. Atmospheric deposition fluxes (ng/m^2/d) of selected PAHs at IADN sites *(26)*, CBADS sites *(28)*, and selected NJADN sites.

	Phenanthrene	Pyrene	Benzo[b+k]fluoranthene	Benzo[a]pyrene
GROSS GAS ABSORPTION				
IADN sites				
Eagle Harbor	260	67		3.3
Sleeping Bear Dunes	308	41		4.4
Sturgeon Point	1173	192		5.4
Point Petre	246	52		1.1
NJADN sites				
JC	4923	706	4.4	1.8
NB	1015	113	1.1	0.40
SH	1764	199	0.83	0.44
PL	351	31	0.14	0.055
DRY PARTICLE DEPOSITION				
IADN sites				
Eagle Harbor	3.3	4.0		1.9
Sleeping Bear Dunes	5.2	6.6		3.6
Sturgeon Point	9.2	12		6.7
Point Petre	6.8	10		8.7
CBADS sites				
Wye	13	9.3	15	3.6
Elms	17	12	15	3.8
Haven Beach	11	6.6	12	4.7
NJADN sites				
JC	132	184	302	83
NB	90	86	179	45
SH	43	39	71	18
PL	31	33	52	13
WET DEPOSITION				
IADN sites				
Eagle Harbor	8.7	5.3		4.7
Sleeping Bear Dunes	17	10		8.1
Sturgeon Point	53	35		19
Point Petre	10	9.5		8.1
CBADS sites				
Wye	10	6.0	7.1	2.7
Elms	11	6.3	8.5	1.9
Haven Beach	8.2	3.3	5.2	1.1
NJADN sites				
JC	122	86	46	30
NB	106	69	77	26
SH	26	12	15	4.4
PL	20	11	12	4.2

Table 13. Annual average wet deposition fluxes (ng/m^2/d) of individual PAHs at NJADN sites.

PAH	JC	CC	NB	SH	CH	TK	AC	PL
Fluorene	24	16	15	5.9	4.8	7.6	4.3	4.0
Phenanthrene	122	93	106	26	33	44	41	20
Anthracene	14	7.0	7.6	2.8	2.3	3.3	4.1	1.1
1Methylfluorene	18	13	33	9.2	2.3	3.6	5.0	3.7
Dibenzothiophene	14	8.9	8.9	7.5	2.6	3.2	2.9	1.7
4,5-Methylenephenanthrene	19	9.6	10	2.9	2.5	3.9	2.8	1.6
Methylphenanthrenes	138	74	78	26	15	22	3.9	13
Methyldibenzothiophenes	10	4.5	5.5	2.6	1.3	1.4	0.72	0.80
Fluoranthene	116	75	107	18	30	51	41	17
Pyrene	86	48	69	12	17	29	21	11
3,6-Dimethylphenanthrene	9.5	4.4	5.2	2.6	0.83	0.70	3.2	0.78
Benzo[a]fluorene	17	9.9	14	4.2	3.2	5.0	3.4	2.3
Benzo[b]fluorene	7.5	8.9	5.3	1.3	1.3	1.9	3.6	0.93
Retene	4.2	5.7	3.8	1.1	1.2	0.55	3.4	1.7
Benzo[b]naphtho[2,1-d]thiophene	8.3	6.7	6.6	1.8	2.7	3.5	3.0	1.7
Cyclopenta[cd]pyrene	2.6	5.8	6.5	1.2	0.64	1.0	1.3	0.42
Benz[a]anthracene	30	15	18	3.5	3.8	6.9	3.3	2.7
Chrysene/Triphenylene	49	32	50	8.0	12	18	20	7.7
Naphthacene	72	6.9	6.2	1.1	1.6	2.6	1.3	0.50
Benzo[b+k]fluoranthene	46	43	77	15	17	12	22	12
Benzo[e]pyrene	37	23	42	7.1	11	11	16	7.5
Benzo[a]pyrene	30	16	26	4.4	5.9	4.8	7.2	4.2
Perylene	10	5.6	21	2.4	2.0	1.3	4.6	1.7
Indeno[1,2,3-cd]pyrene	59	32	70	9.6	13	7.2	9.7	9.5
Benzo[g,h,i]perylene	28	16	33	5.5	5.8	3.7	10	5.0
Dibenzo[a,h+a,c]anthracene	7.6	3.9	5.6	0.86	1.1	0.71	1.7	0.62
Coronene	18	8.2	22	3.9	3.4	1.1	6.5	2.5
Σ_{36}PAHs	997	592	853	185	198	250	246	135

Wet Deposition – spatial differences. Annual average wet deposition fluxes were calculated for the 8 sites where precipitation was collected and are presented in Table 13. Wet deposition fluxes ranged from 0.42 (cyclopenta[cd]pyrene) to 138 (methylphenanthrenes) ng/m^2 day across New Jersey. The highest annual Σ_{36}PAH flux was measured at the urban/industrial Jersey City site (1000 ± 250 ng/m^2 day). However, as with the gas absorption fluxes, the wet deposition fluxes are not well correlated with degree of urbanization/industrialization. The Sandy Hook, Chester, Tuckerton, Alloway Creek and Pinelands sites all have similar annual average wet deposition fluxes.

Table 12 also presents the wet deposition fluxes of four select PAH compounds calculated for the eight NJADN sites to four IADN remote sites adjacent to the Laurentian Great Lakes *(26)* and to three Chesapeake Bay Atmospheric Deposition Study (CBADS) sites on the

shores of the Chesapeake Bay *(28)*. Fluxes at all of the remote IADN and rural CBADS sites (with the exception of Sturgeon Point on Lake Erie) are, on average, lower than those measured at the NJADN sampling stations. Fluxes at the remote Sturgeon Point site are most similar in magnitude to those at the light residential-coastal Tuckerton site located on the coast in southeast New Jersey.

Dry Deposition – spatial differences. Table 14 shows that the annual average dry particle fluxes ranged from 0.11 (naphthacene) to 302 (benzo[b+k]fluoranthene) ng/m^2 day across New Jersey with the highest fluxes occurring at the most highly urbanized/ industrialized sites: Jersey City, Camden, and New Brunswick. Dry particle deposition fluxes are reasonably well-correlated with degree of urbanization such that: urban/industrial sites > suburban sites > light suburban sites > coastal. However, the rural Pinelands site does not follow this trend, having fluxes greater than the light residential-coastal Tuckerton and the coastal Delaware Bay sites. The same argument made for higher gas absorption fluxes at Pinelands applies here as well. The proximity to the Camden and Philadelphia, Interstates 295 and the New Jersey Turnpike, and McGuire Air Force Base may explain slightly higher PAH concentrations and fluxes at the Pinelands site.

In Table 12, dry particle deposition fluxes measured by IADN *(26)* and CBADS *(28)* are presented for the four selected PAH compounds. All flux data from the IADN and CBADs studies have been recalculated using a deposition settling velocity of 0.5 cm/s in order to perform a comparison with NJADN dry deposition fluxes. Dry particle deposition fluxes at the remote IADN sites and the CBADS coastal Chesapeake Bay sites are similar in magnitude to the non-urban/industrial NJADN stations. It is of interest to note that the ratio of phenanthrene: benzo[b+k]fluoranthene is nearly unity at all three coastal CBADS sites and the ratio at the majority of NJADN sites is significantly lower. However, a ratio of near unity does occur at the two most southerly coastal sites in New Jersey, Tuckerton and Delaware Bay. It is these same two sites that have concentrations most similar to those measured at the CBADS stations suggesting that the coastal meteorology may be similar.

Table 14. Annual average dry particle deposition fluxes (ng/m^2/d) of individual PAHs.

	JC	CC	NB	SH	CH	WC	TK	DB	AC	PL
Fluorene	21	7.9	18	9.6	2.8	4.6	3.2	9.4	1.9	3.2
Phenanthrene	132	141	90	43	28	44	16	30	19	31
Anthracene	38	16	12	7.2	3.8	3.9	2.4	3.6	2.5	2.6
1Methylfluorene	23	8.5	19	5.1	3.8	7.4	3.0	3.8	3.2	4.8
Dibenzothiophene	39	15	17	8.3	2.8	4.7	2.5	2.7	2.7	2.5
4,5-Methylenephen	30	18	13	6.5	4.5	6.5	2.4	2.9	2.5	4.2
Methylphenanthrenes	251	160	142	77	39	59	19	25	3.7	42
Methyldibenzothiophenes	32	17	15	8.8	3.6	6.3	2.3	2.6	0.89	3.7
Fluoranthene	196	130	113	49	41	57	21	23	26	38
Pyrene	184	106	86	39	33	55	20	19	21	33
3,6-Dimethyl phenanthrene	28	14	12	5.0	2.5	4.5	1.3	1.0	2.8	2.5
Benzo[a]fluorene	79	32	29	11	8.7	13	4.0	3.6	5.7	7.1
Benzo[b]fluorene	37	12	13	4.7	4.9	5.6	1.7	1.9	2.8	2.8
Retene	34	28	15	7.9	14	21	13	20	12	15
Benzo[b]naphtho[2,1-d]thiophene	41	19	16	6.3	4.9	6.0	2.5	3.0	3.0	3.3
Cyclopenta[cd]pyrene	33	18	17	4.5	5.8	11	2.2	1.9	3.3	3.9
Benz[a]anthracene	106	53	42	14	14	23	6.8	5.7	5.9	10
Chrysene/ Triphenylene	192	107	93	38	34	51	15	18	18	25
Naphthacene	24	10	4.9	1.4	7.3	2.5	0.11	0.79	1.2	0.82
Benzo[b+k]fluoranthene	302	203	179	71	62	94	22	31	30	52
Benzo[e]pyrene	179	90	74	33	26	46	13	16	30	23
Benzo[a]pyrene	83	53	45	18	19	29	4.8	7.2	12	13
Perylene	25	15	10	4.3	6.8	6.8	2.5	9.0	2.9	6.6
Indeno[1,2,3-cd]pyrene	236	152	100	50	31	74	13	20	23	37
Benzo[g,h,i]perylene	185	133	96	38	25	55	13	9.5	23	28
Dibenzo[a,h+a,c]anthracene	23	13	14	5.6	3.4	6.0	1.6	1.7	2.8	2.4
Coronene	229	143	93	40	25	44	15	13	19	27
Σ_{36}PAHs	2781	1713	1379	608	459	742	224	284	283	427

Dry Deposition – seasonal differences. For all ten NJADN sites, the dry particle deposition fluxes are highest in winter. For all sites except Camden and Alloway Creek, the lowest dry particle deposition fluxes occur in the summer. The temperature correlation analysis presented above indicates that increased emissions of PAHs in winter drive increased particle-phase PAH concentrations at many of the NJADN sites and thus drive the dry particle deposition fluxes as well. For three sites (Chester, Washington Crossing, and Pinelands), the strong correlations with

temperature suggest that gas-particle partitioning, rather than changes in emission levels, drive particle phase PAH concentrations.

Annual Deposition across the State of New Jersey.

Total atmospheric deposition of phenanthrene, a low molecular weight, predominantly gas phase PAH (typically 98% gas phase), is dominated by gas absorption. Wet and dry particle deposition fluxes are of approximately the same magnitude. For the eight NJADN sites where precipitation was measured, these two fluxes differed by 7 - 40%. For pyrene, a mid-molecular weight PAH which is typically found to be ~85% gas phase in nature, gas absorption dominates the total atmospheric flux for the majority of sites, however wet and dry particle deposition play a larger role than in the case of phenanthrene. The predominantly particle phase benzo[a]pyrene (typically 99% particle phase) displays different deposition behavior with dry particle deposition constituting the largest portion of the total atmospheric flux, followed by wet deposition. In contrast to phenanthrene and pyrene, gas absorption plays only a minor role in the total flux estimates for benzo[a]pyrene. This demonstrates that differences in gas-particle distribution affect the relative importance of the three atmospheric deposition processes discussed above.

For the Σ_{36}PAHs, gas absorption represents the single largest component of total atmospheric deposition for each of the sites (55 to 92%), followed by dry particle deposition (4 to 31%). Wet deposition constitutes the smallest fraction of the total atmospheric flux (3 to 16%).

Annual average Σ_{36}PAH total atmospheric deposition fluxes in New Jersey range from 5.4×10^2 to 7.3×10^3 ug/m^2 year. The order of highest to lowest fluxes follows the trend: Jersey City, Camden, Sandy Hook, Tuckerton, New Brunswick, Alloway Creek, Pinelands, and Chester. Delaware Bay and Washington Crossing are not included in the trend evaluation due to lack of precipitation data. Overall, the fluxes do not increase with degree of urbanization.

References

(1) Bidleman, T. F. Atmospheric Processes. *Environ. Sci. Technol.* **1988**, *22*, 361-367.
(2) Offenberg, J. H.; Baker, J.E. Precipitation scavenging of polychlorinated biphenyls and polycyclic aromatic hydrocarbons along an urban to over-water transect. *Environ. Sci. Technol.* **2002**, *36*, 3763-3771.
(3) Gigliotti, C.L.; Dachs, J.; Nelson, E.D.; Brunciak, P.A.; Eisenreich, S.J. Polycyclic aromatic hydrocarbons in the New Jersey coastal atmosphere. *Environ. Sci. Technol.* **2000**, *34*, 3547-3554.
(4) Gigliotti, C. L. B., P.A.; Dachs, J.; Glenn IV, T.R.; Nelson, E.D.; Totten, L.A.; Eisenreich, S.J. Air-water exchange of PAHs in the New York-New Jersey, USA, Harbor estuary. *Environ. Tox. Chem.* **2002**, *21*, 235-244.
(5) Whitman, W. G. The two-film theory of gas absorption. *Chem. Metal. Eng.* **1923**, *29*, 146-148.
(6) Zhang, H.; Eisenreich, S. J.; Franz, T. R.; Baker, J. E.; Offenberg, J. H. Evidence for increased gaseous PCB fluxes to Lake Michigan from Chicago. *Environ. Sci. Technol.* **1999**, *33*, 2129-2137.
(7) Achman, D. R.; Hornbuckle, K. C.; Eisenreich, S. J. Volatilization of polychlorinated biphenyls from Green Bay, Lake Michigan. *Environ. Sci. Technol.* **1993**, *27*, 75-86.
(8) Eisenreich, S. J.; Hornbuckle, K. C.; Achman, D. R. Air-Water Exchange of Semi-Volatile Organic Chemicals (SOCs) in the Great Lakes. In *Atmospheric Deposition of Contaminants to the Great Lakes and Coastal Waters*; Baker, J. E., Ed.; **1997**.
(9) Nelson, E. D.; McConnell, L. L.; Baker, J. E. Diffusive exchange of gaseous polycyclic aromatic hydrocarbons and polychlorinated biphenyls across the air-water interface of the Chesapeake Bay. *Environ. Sci. Technol.* **1998**, *32*, 912-919.
(10) Totten, L. A.; Brunciak, P.A.; Gigliotti, C.L.; Dachs, J.; Glenn IV, T.R.; Nelson, E.D.; Eisenreich, S.J. Dynamic air-water exchange of polychlorinated biphenyls in the New York - New Jersey Harbor estuary. *Environ. Sci. Technol.* **2002**, *35*, 3834-3840.
(11) Franz, T. P.; Eisenreich, S. J.; Holsen, T. M. Dry deposition of particulate polychlorinated biphenyls and polycyclic aromatic hydrocarbons to Lake Michigan. *Environ. Sci. Technol.* **1998**, *32*, 3681-3688.
(12) Seinfeld, J. H.; Pandis, S. N. *Atmospheric Chemistry and Physics*; John Wiley & Sons, Inc.: New York, **1998**.
(13) Pirrone, N.; Keeler, G. J.; Holsen, T. M. Dry deposition of semivolatile organic compounds to Lake Michigan. *Environ. Sci. Technol.* **1995**, *29*, 2123-2132.
(14) Pirrone, N.; Keeler, G. J.; Holsen, T. M. Dry deposition of trace elements to Lake Michigan: A hybrid-receptor deposition modeling approach. *Environ. Sci. Technol.* **1995**, *29*, 2112-2122.
(15) Zufall, M. J.; Davidson, C.I.; Caffrey, P.F.; Ondov, J.M. Airborne concentrations and dry deposition fluxes of particulate species to surrogate surfaces deployed in Southern Lake Michigan. *Environ. Sci. Technol.* **1998**, *32*, 1623-1628.
(16) Bamford, H. A.; Ko, F.C.; Baker, J.E. Seasonal and annual air-water exchange of polychlorinated biphenyls across Baltimore Harbor and the Northern Chesapeake Bay. *Environ. Sci. Technol.* **2002**, *36*, 4245-4252.

(17) Offenberg, J. H.; Baker, J.E. The influence of aerosol size and organic carbon content on gas/particle partitioning of polycyclic aromatic hydrocarbons (PAHs). *Atmos. Environ.* **2002**, *36*, 1205-1220.
(18) Shoemaker, D. P; Garland, G.W.; Steinfeld, J.I. *Propagation of Errors;* 3rd edition ed.; McGraw-Hill: New York, **1974**, pp 51-58.
(19) Gigliotti, C. L.; Lee, J.H.; Offenberg, J.H.; Turpin, B.J.; Eisenreich, S.J. Source apportionment of polycyclic aromatic hydrocarbons in New Jersey air using Positive Matrix Factorization. *Environ. Sci. Technol.* **2003**, in review.
(20) Bamford, H. A. Determination of the Henry's Law Constants and Air-Water Exchange Fluxes of PAHs Across the Patapsco River and the Northern Chesapeake Bay. M.S. Thesis, University of Maryland, 1998.
(21) Wanninkhof, R. Relationship between wind speed and gas exchange over the ocean. *J. Geophys. Res.* **1992**, *97*, 7373-7382.
(22) Wanninkhof, R. M.; McGillis, W.R. A cubic relationship between air-sea exchange and wind speed. *Geophys. Res. Letters* **1999**, *26*, 1889-1892.
(23) Liss, P. S.; Merlivat, L. Air-sea gas exchange rates: Introduction and synthesis. In *The Role of Air-Sea Exchange in Geochemical Cycling*; Buat-Menard, P., Ed.; Reidel: Boston, 1986, 113-129.
(24) Endlich, R. M.; Eynon, B.P.; Ferek, R.J.; Valdes, A.D.; Maxwell, C.X. Statistical analysis of precipitation chemistry measurements over the eastern United States: Part I. Seasonal and regional patterns and correlations. *J. Appl. Meteorol.* **1988**, *27*, 1326-1333.
(25) Offenberg, J. H.; Baker, J.E. Polychlorinated biphenyls in Chicago precipitation: enhanced wet deposition to near-shore Lake Michigan. *Environ. Sci. Technol.* **1997**, *31*, 1534-1538.
(26) Hoff, R. M.; Strachan, W. M. J.; Sweet, C. W.; Chan, C. H.; Shackleton, M.; Bidleman, T. F.; Brice, K. A.; Burniston, D. A.; Cussion, S.; Gatz, D. F.; Harlin, K.; Schroeder, W. H. Atmospheric deposition of toxic chemicals to the Great Lakes: A review of data through 1994. *Atmos. Environ.* **1996**, *30*, 3305-3527.
(27) Strachan, W. M. J.; Eisenreich, S. J. "Mass Balancing of Toxic Chemicals in the Great Lakes: The Role of Atmospheric Deposition," International Joint Commission, 1988.
(28) Baker, J.E.; Poster, D.L.; Clark, C.A.; Church, T.M.; Scudlark, J.R.; Ondov, J.M.; Dickhut, R.M.; Cutter, G. Loadings of atmospheric trace elements and organic contaminants to the Chesapeake Bay. In *Atmospheric Deposition of Contaminants to the Great Lakes and Coastal Waters*; Baker, J. E., Ed.; **1997**.

II.A3. Organochlorine Pesticides

Abstract

Organochlorine Pesticides were measured in 2000-2001 at six locations in New Jersey as part of New Jersey Atmospheric Deposition Network (NJADN). Concentrations were measured for 22 organochlorine pesticides using GC/MS in NCI SIM mode. Pesticides measured includes chlordanes, DDTs, HCHs, Endosulfan I and II, aldrin and dieldrin. The spatial and temporal variations in OC concentrations are reported and discussed for all five locations. Gas-phase concentrations comprise about the 95% of the OCs across all samples in New Jersey. The relationship with temperature to gas-phase partial pressure was examined using the Clausius-Clapeyron equation and the relative environmental phase transition energies were calculated for each pesticide across all five locations. Significant temperature dependencies were found for all OC pesticides at every site with the exception of aldrin whose concentrations show no significant correlation with temperature at any of the sites all sites. Sampling days with residuals greater than one standard deviation from the ln P of chlordanes versus 1/T were checked with three-day back trajectories. Lower than expected concentrations were observed when the air mass came from North West (Canada and Great Lakes), whereas higher than expected concentrations show no correlation with the air mass origin.

Introduction

Organochlorine Pesticides (OCPs) were widely used in the North America until the 70's when most were banned. The global distribution of these compounds has increased during the last twenty years, due to their persistence in the environment, which allows them to be transported over great distances. As a result, OCPs have also been found in the Artic *(1, 2)* and they have been shown to bioaccumulate and biomagnify in animals of higher trophic levels such as whales, seals, polar bears, and humans *(3-5)*. Although the use of these compounds has been virtually eliminated in Western industrialized countries, many of them are still used in some subtropical countries in Africa, and South and Central America *(6, 7)*. These boundary countries still use OCPs for agricultural purposes and in order to control vector-diseases. Several long-

term studies have shown that concentrations of OCPs in the atmosphere of the Northern hemisphere have diminished over the last ten years *(8, 9)*. However, twenty years after they were banned, OCPs are ubiquitous in the environment. Therefore, transport from countries south of the USA border and re-emission from soils due to past usage support measurable levels of these compounds in the atmosphere *(7, 10, 11)*.

An important characteristic of most OCPs, already mentioned, is that they persist in the environment (e.g., they do not readily break down). DDT and its metabolites (DDE and DDD), aldrin and its metabolite dieldrin, while persistent in the environment, will eventually break down after a number of decades *(8, 12)*.

The New Jersey Department of Environmental Protection has conducted an historical review of organochlorine pesticide use in New Jersey in order to provide insight into the type and the possible geographical extent of potential residual pesticide contamination of these pollutants *(13)*. DDT (and its two break-down products DDD and DDE), aldrin, and dieldrin were considered "pesticides of concern" because these groups are among of the most widely used pesticides over the last century. Heptachlor, chlordane and Endosulfan (I and II) were also included in this study. Soil samples from typical agricultural areas in New Jersey indicate that the pesticides of concern were rarely present at concentrations greater than the Department's residential soil cleanup criteria. *(13)*.

Many studies have been conducted in the several areas of the United States where the past usage of these compounds was predominant or where the atmosphere can serve as a pathway for the delivery of these pollutants to water and terrestrial surfaces *(1, 7, 8, 12, 14-16)*. However, little research has been conducted on chlorinated pesticides in the air of the Mid-Atlantic region of the United States, such as New Jersey. The New Jersey Atmospheric Deposition Network (NJADN) was established in 1997 as a research and monitoring network in order to assess the fate and transport of persistent organic pollutants, including PAHs (Polycyclic Aromatic Hydrocarbons), PCBs (Polychlorinated Biphenyls), and OCPs, in the coastal, urban, suburban and rural Mid Atlantic area (Brunciak et al., 2001; Gigliotti et al, 2000 and 2001; VanRy et al., 2002). Originally, the NJADN project measured six OCPs via gas chromatography (GC) using an electron capture detector (ECD) in the same analytical run as the PCBs. This method was found to be unreliable for the quantification of most of these compounds, and therefore a new method was adopted and old NJADN samples were re-analyzed for OCPs. In

this study, OCPs concentrations for at least 12 months at New Brunswick, Jersey City, Delaware Bay, Sandy Hook, Camden, and Pinelands are presented.

The objectives of this work are (i) to assess the occurrence and spatial variability of OC pesticide concentrations (ii) to investigate the seasonality associated with the OC pesticides concentrations and (iii) to study the influence of meteorological parameters such as temperature and air mass movements on OC pesticide concentrations in the New Jersey coastal atmosphere.

OCP Methods

Air samples were collected at six different locations in New Jersey representing four different land-uses regimes: Camden (CC), Delaware Bay (DB), Jersey City (JC), New Brunswick (NB), Pinelands (PL), and Sandy Hook (SH). Air samples considered in this study include samples taken from January 2000 to May 2001 for Camden and Pinelands and from January 2000 to January 2001 for New Brunswick, Sandy Hook, and Jersey City. At Delaware Bay, samples were analyzed from March 2000 to May 2001. Air sampling occurred for 24 hours every twelfth day. Details of sample collection and processing have been described elsewhere in this report.

Details relevant to the OC Pesticides analysis will be described here. Because the new analysis procedure for OC pesticides, involving GC/MS NCI, was not in place when most of the sampling occurred, surrogates specifically chosen to track the recovery of OC pesticides were not added to the samples. All samples were spiked with a surrogate standard containing d_{10}-anthracene, d_{10}-fluoranthene, and d_{12}-benzo[e]pyrene for PAHs and PCBs 14, 23, 65, and 166 for PCBs. After extraction and volume reduction, each sample was eluted on a 3% water deactivated alumina column to fractionate the sample based on polarity and to remove any interfering compounds. Fraction 1 was designed to contain the PCBs by eluting with 13 mL hexane, and was found to contain some chlorinated pesticides (2,4'-DDE, Heptachlor, aldrin , 4,4'-DDE, 50% 2,4'-DDT). Fraction 2 was designed to capture the PAHs by eluting with 15 mL 2:1 dichloromethane:hexane, and also contained some chlorinated pesticides (trans- and cis-chlordanes, trans- and cis- nonachlors, dieldrin, 4,4'-DDT). Fraction 1 and Fraction 2 were each reduced in volume to ~0.5 mL under N_2 gas and Fraction 1 was spiked with 250 µL internal standard consisting of PCB 30 and PCB 204, while Fraction 2 was spiked with 100µL internal standard consisting of d_{10}-phenanthrene, d_{10}-pyrene, and d_{12}-benzo[a]pyrene. For the gas phase,

both fractions were analyzed for OCPs and the masses summed to determine the total concentration of OCPs in the sample. For the particle phase, only Fraction 2 was analyzed because the lower molecular weight pesticides (which elute in Fraction 1) were not detected in the particle phase. PCBs 30 and 204 were intended for use as internal standards to quantify OC pesticides, and were therefore spiked into Fraction 2 just prior to OCP analysis. However, only PCB 204 was used as the internal standard because PCB 30 was not detectable via NCI (Negative Chemical Ionization), probably due to poor fragmentation. Similarly, PCBs 14, 23, and 65 were not detectable. Surrogate recoveries were therefore calculated for Fraction 1 by using PCB 166 (the only PCB present in the surrogate detected with NCI). The surrogate recoveries for F1 fractions were relatively high, 90-105% and correlated very well with the PCB 166 surrogate recovery originally measured during PCB analysis by GC/ECD. It was not possible to calculate surrogate recoveries for Fraction 2 due to the low response of PAHs in NCI mode. However, surrogate recoveries for PAHs were good (70-98%) when originally analyzed by GC/MS in electron impact mode. For these two reasons, OCP concentrations were not corrected for surrogate recoveries.

Twenty-two OCPs were analyzed by using gas chromatography/mass spectrometry in negative chemical ionization (GC/MS-NCI) operating in Selective Ion Monitoring (SIM) mode, using a method developed by Brown *(17)*. Data for β-and δ-HCH, methoxychlor, and 4,4'-DDD are not presented because these compounds were always or almost always below detection limit. Prior to the adoption of this method, a smaller number of OCPs (hexachlorobenzene, heptachlor, mirex, 4,4'-DDT, 4,4'-DDE, and 2,4'-DDT) were quantified during PCB analysis using GC/ECD, in which compounds were identified based solely on their retention time. The presence of co-eluting compounds made the quantification of OCPs by this method unreliable. The new GC/MS NCI method uses unique ions for each analyte, allowing positive identification of each by major ion/secondary ion abundance ratio, as well as by retention time.

Concentrations of pesticides were determined using a Hewlett Packard 6890 Gas Chromatograph (GC) coupled to a Hewlett Packard 5973 Mass Selective Detector (MSD). The column used was a 30 m × 0.25mm i.d., J&W Scientific 122-5062 DB-5 (5% diphenyl-dimethylpolysiloxane) capillary column with a film thickness of 0.25 μm. The GC was operated with an injection port temperature of 280 ˚C and an initial oven temperature of 100 ˚C. The temperature program began at 100 ˚C for 1.00 minutes, increased to 240 at 2.50 ˚C/min, and

finally increased again to 280 at 13.00. The total run time was of 70.08 minutes. Helium was used as the carrier gas at a constant flow rate of 1.2 mL/min. The quadrupole and the source temperature were held at 106 ˚C and at 150 ˚C respectively. Negative Chemical Ionization (NCI) is a soft technique, which uses a reagent gas whose molecules are preferentially ionized from the electrical beam because they are much more abundant than the analyte molecules in the source. Once the ionization by energetic electrons has occurred in the source, thermal electrons (less energetic) are formed and they ionize the analyte. The reagent gas (methane) was introduced at 1 torr. In order to assure the exact quantification and identification of each compound, the ratio of the primary ion to the secondary ion was calculated and the compound was quantified only when the ratio was ± 20% of the ratio for the calibration standard. The mass of each organochlorine pesticide was determined and quantified as follows:

$$Mass_{OCs} = \frac{\frac{Area_{OC}}{Area_{IS}} \cdot Mass_{IS}}{RRF} \quad (1)$$

where RRF is the relative response factor determined for each organochlorine pesticide by calibration of five standards mixtures of varying concentration. The standard concentrations were in the range of 1ng/ml –100 ng/ml . The ratio of the area of the qualifier peak to the area of the internal standard ($area_{qual}$/ $area_{IS}$) and the ratio of the mass of the qualifier peak to the mass of the internal ($mass_{qual}/mass_{IS}$) standard were plotted and a linear regression was performed. The slope is the relative response factor (RRF). Intercepts were always close to zero (range: -0.002 to 0.01). The correlation coefficients (R^2) ranged between 0.95-0.99 and only R^2 values of 0.96 or higher were used to quantify OCPs in the study.

Quality Assurance/ Quality Control. Quality assurance and quality control were determined using laboratory blanks, field blanks and matrix spikes. None of the OCPs were detected in the lab and field blanks. Therefore, an instrumental detection limit was calculated. A calibration curve for four sets of 10 dilutions of each standard was performed by plotting the analyte mass versus the response of the instrument. The concentration at which the calibration curve is no longer linear is taken as the Limit of Detection (LOD), which was calculated as six times the standard deviation of the four replicates at the concentration where non-linearity began (Table 15). At a typical sample volume of 600 m^3, the detection limits ranged from 0.002 to 0.13

pg/m^3. For precipitation, a typical sample volume was about 10 L, yielding detection limits of 0.12 to 7.8 pg/L. Three or four replicates of some samples were also analyzed at the end of each run. The mass measured in the replicates varied by 10 to 15%.

Split PUFs were used to quantify potential breakthrough of gas phase OC pesticides. The second half of the split PUF accounted for 15 ± 5% (n=4) of the total mass collected on the entire PUF with the greatest breakthrough occurring for the OC with the lowest molecular weight, α-HCH (40-50%). Breakthrough was lower for other OCPs: 3-25% for γ-HCH, and 1-2% for chlordanes. Since α-HCH breakthrough was found to be relatively high, α-HCH concentrations reported in this study are a lower limit because of breakthrough losses.

Table 15. Retention time, major and secondary ion, and LOD for each OCP measured.

COMPOUNDS	**RT**	**MAJOR ION**	**SECONDARY ION**	**LOD(pg)**
alpha-HCH	23.48	71	255	20
beta-HCH	25.66	71	255	20
gamma-HCH	25.99	255	71	4.5
delta-HCH	27.96	71	325	20
Heptachlor	31.41	266	300	9.7
Aldrin	33.87	237	330	9.7
Heptachlor epoxide	37.01	318	380	9.7
Oxychlordane	37.015	350	424	9.7
trans Chlordane	38.64	410	266	11
2,4'-DDE	39.37	246	283	2.4
Endosulfan I	39.4	406	372	20
cis-Chlordane	39.75	410	266	9.8
trans-Nonachlor	40.15	444	300	5.5
Dieldrin	41.29	346	380	4.5
4,4' DDE	41.72	318	283	20
2.4'-DDD	42.21	248	71	4.8
Endosulfan II	43.44	406	372	9.7
cis-Nonachlor	44.56	444	294	12
4,4' DDD	44.62	294	366	78
2,4' DDT	44.89	71	248	1.2
Endosulfan sulfate	46.51	386	422	9.7
4,4' DDT	47.21	71	283	39
Methoxychlor	51.7	422	388	39

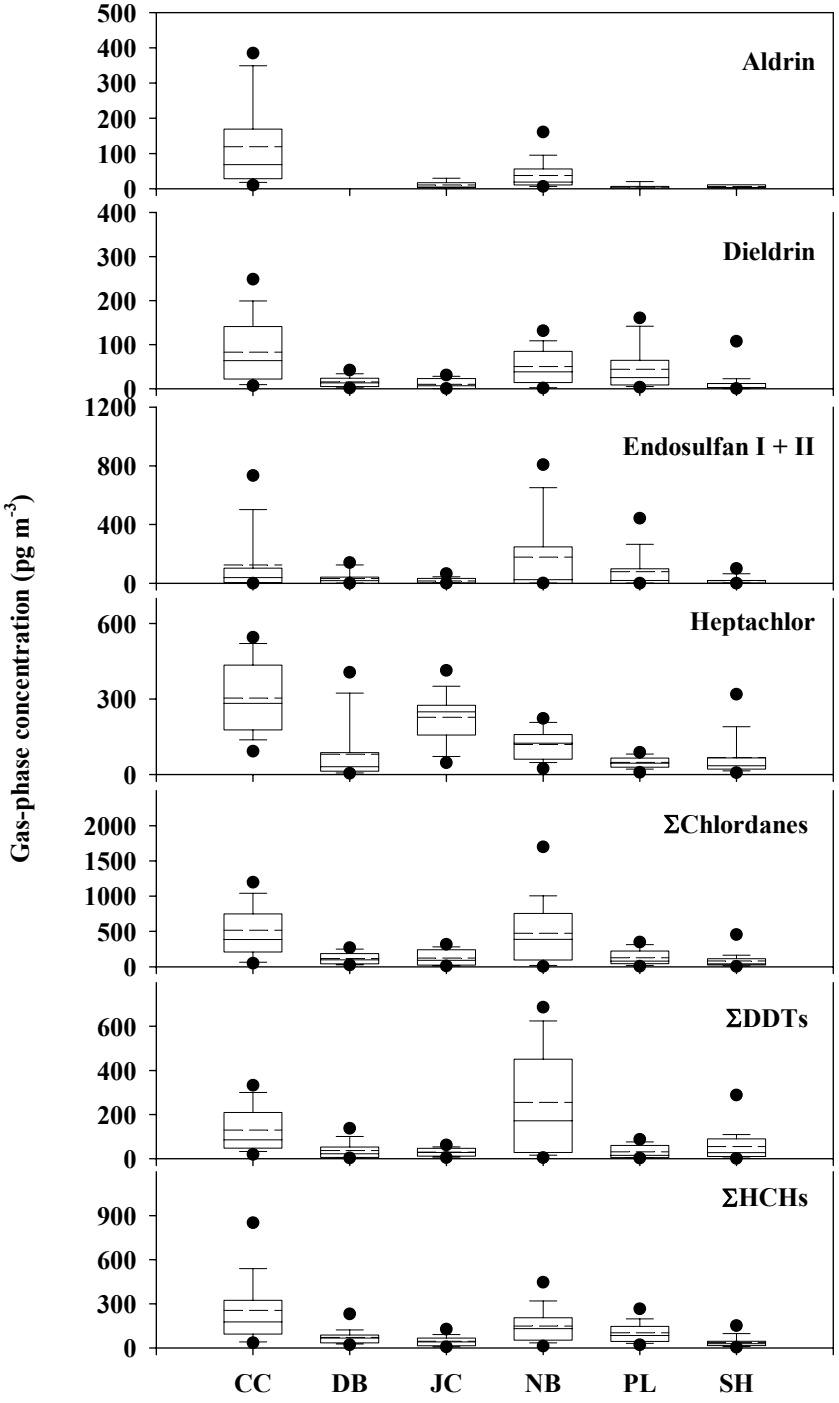

Figure 19: Box and whisker plot of gas-phase OCP concentrations. Upper dot, upper error bar, upper edge of box, lower edge of box, lower error bar, and lower dot represent 95th, 90th, 75th,

25th, 10th and 5th percentile concentrations, respectively. Within each box, mean and median concentrations are shown as dashed and solid lines, respectively.

Table 16. Average (avg) and geometric mean (GM) concentrations of gas-phase OCPs (pg/m^3) at six NJADN sites.

	Camden		Delaware Bay		Jersey City		New Brunswick		Pinelands		Sandy Hook	
	avg	GM	avg	GM	avg	GM	avg	GM	avg	GM	avg	GM
Heptachlor	304	269	32	21	228	200	115	101	48	41	65	41
Heptachlor Epoxide	45	26	11	9.3	8.1	3.5	19	12	14	16	1.8	1.5
Dieldrin	75	51	15	10	8.2	2.3	36	30	38	22	9.7	3.4
Aldrin	77	71	1.3	1.1	3.8	6.9	28	23	1.1	2.5	1.2	4.6
Endosulfan I	102	22	32	11	13	3.1	168	21	59	14	15	4.1
Endosulfan II	1.8	3.6	Not detected		1.9	0.7	10	2.6	10	8.4	2	0.76
α-HCH	96	73	37	34	23	16	84	62	55	49	19	16
γ-HCH	158	80	34	20	22	12	65	33	48	26	18	8.1
Σ-Chlordanes	518	354	119	87	114	72	474	223	127	83	83	45
Σ-DDTs	133	92	39	19	31	25	237	106	31	16	53	22

Results and Discussion

Figure 19 and Table 16 summarize the gas-phase OCP concentrations measured in this study. Gas-phase concentrations were always log-normally distributed. Therefore both the average and the geometric mean concentrations are presented in Table 16. Table 17 presents particle-phase concentrations of OCPs, and Table 18 presents the volume-weighted mean (VWM) concentrations of OCPs in precipitation. First, pesticide concentrations and deposition will be discussed for select classes of compounds separately. Then the temperature dependence of all the OCPs in the gas phase will be examined, followed by an examination of the importance of air mass origin on gas-phase chlordane concentrations.

Σ Chlordanes. Technical Chlordane was mostly used as an agricultural pesticide on corn and citrus, for home lawns and gardens and as termiticide in house foundations. The most abundant components in technical mixture are trans-chlordane (TC), cis-chlordane (CC), trans –nonachlor (TN), β-chlordane and heptachlor (HEPT) *(18)*.

Concentrations of particle-phase Σchlordanes averaged 1 to 10 pg/m^3, such that less than ~5% of all atmospheric Σchlordane was typically present in the particle phase (Table 17). For both particle- and gas-phase chlordanes, highest concentrations were typically observed at New Brunswick and Camden. Particle-phase Σchlordane concentrations were also high at Jersey City. In the precipitation phase (Table 18), VWM concentrations were lowest at Pinelands and significantly higher at Jersey City and Camden.

Gas-phase Σchlordanes at most of the New Jersey sites (Table 16) were similar to average concentrations measured in Alabama during 1996-1997 (98 pg/m^3) *(7)* and in South Carolina during 1994-1995 (180 pg/m^3) *(19)*. In contrast, concentrations of Σchlordanes were generally lower (averaging less than 40 pg/m^3) at remote sites around the Great Lakes during 1996-1998 *(20)*, in the Cornbelt region of the U.S. during 1996-1997 (56 pg/m^3) *(15)*, and around Lake Baikal in Russia during June 1991 (5 pg/m^3) *(21)*. Table 19 demonstrates that most NJADN sites displayed gas-phase Σchlordane concentrations similar to those detected in Chicago by IADN *(20)*.

Table 17. Average (avg) and geometric mean (GM) OC pesticide concentrations (pg m^{-3}) in the particle phase at five NJADN sites. Blank spaces indicate that the pesticide was never detected in the particle phase at that site.

	Camden		**Delaware Bay**		**Jersey City**		**New Brunswick**		**Pinelands**	
	Avg	**GM**	**Avg**	**GM**	**avg**	**GM**	**avg**	**GM**	**avg**	**GM**
Oxychlordane	0.12	0.12					0.22	0.17	0.063	0.080
Dieldrin					2.8	2.7				
Aldrin					0.23	6.6				
Endosulfan I	2.0	1.1	0.84	0.49	0.98	0.89	0.50	0.25	0.89	0.50
Endosulfan II	4.2	1.5	2.3	1.0	1.6	1.2	2.1	0.82	2.2	0.80
Endosulfan sulfate	1.7	0.76	1.0	0.68	0.81	0.52	1.0	0.50	1.4	0.59
Σ-Chlordanes	6.4	4.3	0.96	0.77	6.1	4.2	4.1	2.4	1.1	0.78
Σ-DDTs	3.4	3.6	1.7	1.5	4.9	10	2.8	2.0	0.58	0.47

Table 18. Volume weighted mean (VWM) and standard error of the mean (SEM) OCP concentrations in precipitation (pg/L) at NJADN sites.

	Camden		Jersey City		Pinelands	
	VWM	**SEM**	**VWM**	**SEM**	**VWM**	**SEM**
Endosulfan I	154	57	46	21	153	82
Endosulfan II	788	327	293	130	283	80
Endosulfan sulfate	444	140	219	70	378	68
Oxychlordane	3.2	1.2	3.3	1.6	8.3	5.9
Σ-DDTs*	190	75	367	184	58	19
Σ-Chlordanes	173	40	182	55	66	8.3

*4,4'-DDT was the only DDT compound detected in precipitation samples.

Table 19. Comparison of average gas-phase OCP concentrations (pg/m^3) at NJADN and IADN sites.

	ΣHCHs	**ΣChlordanes**	**Dieldrin**	**ΣDDTs**
NJADN 2000				
Camden	254	518	75	133
Delaware Bay	71	119	15	39
Jersey City	44	111	8.2	25
New Brunswick	149	474	36	237
Pinelands	103	127	38	31
Sandy Hook	36	79	9.3	42
IADN 1996-1998 ***(20)***				
Chicago	130	130	130	71
Sturgeon Point	82	38	19	31
Sleeping Bear Dunes	99	14	15	11
Brule River	89	7.8	8.4	2.9
Eagle Harbor	96	8.6	8.8	4.4

Table 20. Atmospheric deposition fluxes (ng m^{-2} d^{-1}) of select OCPs at NJADN sites. Blank spaces indicate that the pesticide was never detected in that phase at that site.

	Gas Absorption						Dry Particle Deposition					Wet Deposition		
	CC	**DB**	**JC**	**NB**	**PL**	**SH**	**CC**	**DB**	**JC**	**NB**	**PL**	**CC**	**JC**	**PL**
alpha-HCH	42	8.1	11	43	26	9.7								
gamma-HCH	68	10	11	34	22	9.1								
sum HCHs	110	18	22	77	48	19								
Heptachlor	10	0.12	11	5.1	1.7	1.6								
Dieldrin	25	2.4	3.2	15	15	4.2			1.2					
Aldrin	7.4	0.00048	0.43	2.6	0.19	0.20			0.10					
Endosulfan I	33	4.1	5.4	80	22	6.3	0.87	0.36	0.42	0.22	0.39	0.46	0.14	0.46
Endosulfan II	NC	NC	NC	NC	NC	NC	1.8	1.0	0.70	0.90	0.94	2.4	0.88	0.85
Endosulfan sulfate							0.72	0.44	0.35	0.43	0.60	1.3	0.66	1.1
Oxychlordane							0.052			0.097	0.027	0.0095	0.010	0.025
Σ-Chlordanes	144	16	34	147	39	27	2.8	0.42	2.7	1.8	0.46	0.52	0.55	0.20
Σ-DDTs	31	2.1	8.7	62	8.0	14	1.5	0.71	2.1	1.2	0.25	0.57	1.1	0.17

NC = Not calculated.

Jantunen et al. *(7)* calculated the predicted average proportions of TC : CC : TN in ambient air for technical chlordane at 25 ºC , which was estimated to be 1.00 : 0.61 : 0.23. Hinckley et al. *(22)* report that TC : CC : TN of Technical Chlordane at 20 ºC is 1.00 : 0.54 : 0.34. The average proportions of TC:CC:TN:CN in the New Jersey air samples (calculated from the geometric mean) were: 1.00 : 0.79 : 0.53 : 0.09 (Delaware Bay), 1.00 : 0.73 : 0.41 : 0.03 (Camden), 1.00 : 0.86 : 0.52 : 0.04 (Jersey City), 1.00 : 1.00 : 0.67 : 0.06 (New Brunswick), 1.00: 0.83: 0.52 : 0.02 (Sandy Hook) and 1.00 : 0.73 : 0.45 : 0.06 (Pinelands). These values can be compared for those measured in Columbia South Carolina during 1994-1995 (1.00 : 0.63 : 0.36 : 0.043) and Alabama during 1996-1997, where the ratios were 1.00 : 0.56 : 0.52 with CN not detected *(7)*. The values measured for New Jersey air show an increase in concentration for CC relative to TC as compared for those of Alabama and South Carolina, especially for the New Brunswick site where the concentrations of trans-chlordane and cis-chlordane are similar. This relative enrichment observed in these relative ratios suggests that transformation of trans-chlordane to cis-chlordane may occur in New Jersey air *(23)*.

Atmospheric deposition of chlordanes was calculated using Henry's Law Constants (HLCs) for cis and trans chlordane from Mackay et al. *(24)*, and from Iwata et al. *(25)* for trans-

nonachlor. For all chlordanes, the temperature dependence of the HLC was assumed to equal the enthalpy of vaporization, as taken from Hinckley et al. *(22)*. Both the HLC and the enthalpy of vaporization were assumed to be the same for cis-nonachlor as for trans-nonachlor. For all pesticides, the wind speed was assumed to be constant at 5 m s^{-1} (see the PCB and PAH sections for further discussion of the effect of wind speed on gas absorption). Atmospheric deposition of chlordanes is dominated by gas absorption, with dry and wet deposition comprising less than 10% of the total atmospheric deposition (Table 20).

Heptachlor and Heptachlor epoxides. Heptachlor is an organochlorine cyclodiene insecticide, first isolated from technical chlordane in 1946. During the 1960s and 1970s, it was used primarily by farmers to kill termites, ants, and soil insects in seed grains and on crops, as well as by exterminators and homeowners to kill termites. Before heptachlor was banned, formulations available included dusts, wettable powders, emulsifiable concentrates, and oil solutions. An important metabolite of heptachlor is heptachlor epoxide, which is an oxidation product formed from heptachlor by many plant and animal species (http://ace.ace.orst.edu/info/extoxnet/pips/heptachl.htm). Heptachlor is a moderately toxic compound in EPA toxicity class II. Phase out of heptachlor use began in 1978. In 1988, the EPA canceled all uses of heptachlor in the U.S. The only commercial use still permitted is for fire ant control in power transformers. Heptachlor is still available outside the U.S. *(7)*. Heptachlor is transformed in the environment by several pathways. Photolysis yields photoheptachlor and heptachlor epoxide, both of which are persistent, bioaccumulative and toxic *(26)*.

Neither heptachlor nor its epoxide were detected in the particle phase. As with the chlordanes, HEPT and HEPTX concentrations were generally higher at Camden and New Brunswick (Figure 19, Table 16), although in contrast to the chlordanes, HEPT and HEPTX levels were high at Jersey City as well. At these three sites, HEPT averaged 100-300 pg/m^3, while at the other three sites HEPT averaged 30-70 pg/m^3. These concentrations are well the above averages of 1.2 and 7.4 pg/m^3 of heptachlor and its epoxide (respectively) measured by the Integrated Atmospheric Deposition Network (IADN) near Lake Superior in 1996 and 1997 *(27)*. Leone et al. *(15)* measured an average of 9.3 pg/m^3 heptachlor in the cornbelt region of the U.S. during 1996 and 1997.

At all sites, the heptachlor epoxide/heptachlor ratio was highest in the summer (from May to September) and the lowest in the winter (from October to March). Higher heptachlor epoxide concentrations were most likely to occur at all sites during the summer. Higher HEPTX concentrations and a higher HEPTX/HEPT ratio are indicative of photolytic transformation of HEPT, which is likely to occur to a greater extent during the summer months when temperature and ozone levels are high.

The atmospheric deposition of heptachlor was calculated using the HLC from Mackay et al. *(24)* and the enthalpy of vaporization (which was assumed to equal the enthalpy of Henry's Law equilibrium) from Hickley et al. *(22)*. Gas absorption of heptachlor epoxide was not calculated because a reliable HLC for this compound could not be found. Because heptachlor was below detection limit in all particle and precipitation samples, dry and wet deposition fluxes cannot be calculated and are assumed to be negligible (Table 20).

DDTs. DDT was first used to control disease spreading insects and then as multipurpose insecticide. The peak of production of DDT in the U.S. was 82 million kg in 1962, and it was deregistered in 1972 except for public health emergencies *(28)*.

ΣDDTs are here defined to include 4,4'-DDT, 4,4'-DDE, 2,4'-DDT, and 2,4'-DDE. The DDDs were rarely above detection limit, and therefore they will not be discussed here. As with the chlordanes, gas-phase ΣDDT concentrations were generally highest at Camden and New Brunswick (Figure 19, Table 16), with geometric means of about 100 pg/m^3. At the other four sites, the geometric mean concentration of ΣDDTs was about 20 pg/m^3. The levels of DDT measured at the New Jersey sites is similar to those measured by IADN (Table 19) at Chicago and Sturgeon Point, but higher than levels at the other IADN sites *(20)*. Only 4,4'-DDT was detected in the particle and precipitation phases (Tables 17 and 18), except at Jersey City, where all of the DDT compounds were detected in the particle phase. The fraction of the total atmospheric concentration of 4,4'-DDT that was in the particle phase was typically about 10%, although at Jersey City the fraction averaged 58%.

The average percent abundance of 4,4'-DDE ranged from 85% at Delaware Bay to 64% in Sandy Hook, followed by 4,4'-DDT ranging from 26% in Pinelands to 7% at Delaware Bay. The less abundant components were 2,4'-DDT, 2,4'-DDE. 2,4'-DDE ranges from 16% in Sandy Hook to 3.64% in New Brunswick and 2,4' DDT ranges from 18% in Sandy Hook to 0% at Delaware Bay, where it was never detected. The average DDT/DDE ratio ranged from 0.06 to

0.5 and was lowest at Delaware Bay and highest at Pinelands. A ratio less than 1 indicates no new sources of DDT in the atmosphere. By comparison, ratios of 4,4'-DDT/4,4'-DDE were 0.2-0.8 around the Great Lakes *(8)* and 0.3-0.8 in the Canadian Artic *(29)*.

Atmospheric deposition of the DDTs was calculated using HLCs from Mackay et al. *(24)* and enthalpies of vaporization (which were assumed to equal enthalpies of Henry's Law equilibrium) from Hickley et al. *(22)*. The enthalpy of vaporization of 4,4'-DDE was used for 2,4'-DDE. Atmospheric deposition of DDTs is dominated by gas absorption at most sites, with wet+dry deposition constituting less than 10% of the total (gas+wet+dry) deposition (Table 20). At Delaware Bay and Jersey City, dry particle and wet deposition were significant, together comprising as much as 34% of the total.

Aldrin/Dieldrin. Aldrin and dieldrin were extensively used from the 1950s to the 1970s to fight insects on corn, cotton and citrus crops and also used as a termiticides. Aldrin is quickly metabolized to dieldrin in the environment *(30)*. The peak usage of aldrin and dieldrin was in 1956 and both OC pesticides were banned in 1987 by the EPA *(30)*.

Aldrin was frequently below detection limit in the gas phase and was detected in the particle phase only at Jersey City (Table 17). Similar to the chlordanes and DDTs, gas-phase aldrin concentrations were typically highest (frequently greater than 100 pg/m^3) at Camden and New Brunswick (Figure 19, Table 16), and lower (typically less than 20 pg/m^3) at the other four sites. In contrast, gas-phase dieldrin concentrations (Table 16) were more evenly distributed throughout the state and were generally higher than those of aldrin, consistent with the 1978 ban on aldrin use and the conversion of aldrin to dieldrin in the environment. Dieldrin levels measured by NJADN were very similar to those measured in the Cornbelt region of the US *(15)*, and by IADN at remote sites around the Great Lakes from 1996-1998 *(20)* (Table 19). The lowest average concentrations reported for both networks are about 8-9 pg/m^3, suggesting that this level may represent a regional (northeastern US) background. Interestingly, this background concentration was observed at Jersey City, a heavily urban and industrial area. Aldrin and dieldrin were not detected in precipitation, and were detected the particle phase only at Jersey City (Table 17), where the particle phase comprised 6% and 25% of the total atmospheric concentrations of aldrin and dieldrin, respectively.

The atmospheric deposition of aldrin and dieldrin was calculated using HLCs from Mackay et al. *(24)* and enthalpies of vaporization (which were assumed to equal enthalpies of

Henry's Law equilibrium) from Hickley et al. *(22)*. Atmospheric deposition of both aldrin and dieldrin is dominated by gas absorption (Table 20) at all sites except Jersey City, where dry deposition comprised about 20-30% of the total.

α and γ-Hexachlorocyclohexanes. Technical HCH is a mixture of α-HCH (60-70%), β-HCH (2-12%)and γ-HCH (10-15%) and several other minor isomers *(31)*. This technical mixture was used in the U.S. until 1978. After that, it was substituted by the purified γ-HCH isomer (lindane). Lindane has not been made in the United States since 1977 but it is still imported into the country. Its usage has been restricted by the U.S. EPA to certified individuals. Lindane is still used for seed treatments *(32)*.

Due to breakthrough of the HCHs during sampling, the gas-phase concentrations presented here are minimum estimates. Again, gas-phase concentrations of HCHs are generally highest at New Brunswick and Camden (Figure 19, Table 16), although differences between the sites are not statistically significant. The HCHs were not detected in the particle or precipitation phases at any of the sites. Average concentrations of ΣHCHs measured by IADN *(20)* (Table 19) were similar to levels reported here. HCH concentrations were lower at Jersey City and Sandy Hook than at the more remote IADN sites, but this may be an artifact of the breakthrough of α-HCH which lowered measured gas-phase concentrations in the present study.

Technical HCH mixture has typically a ratio of with α-HCH/γ-HCH ranging from 4 to 7 *(33)*. The average α-HCH/γ-HCH ratio ranges from 1.3±1 in Camden to 2.7±1.8 in Sandy Hook indicating current usage of lindane and a significant historical background of technical HCH in New Jersey. These values are similar to those reported for the NE Atlantic (0.3-4.6)*(34)* and also for the Artic (0.9-4.7) *(35)*. The ratio displays a distinct seasonal pattern, being typically less than 1 during the summer and greater than 1 during the winter. The higher concentration of γ-HCH relative to that of α-HCH during the summer may be due to differences in enthalpy of air-surface exchange between the two compounds or to current usage of lindane. γ-HCH has a higher vapor pressure than α-HCH, possibly leading to greater increases in γ-HCH volatilization (relative to the increased volatilization of α-HCH) from surfaces in the summer.

Because HCHs were not detected in the particle and precipitation phases, their wet and dry particle deposition fluxes cannot be calculated and are assumed to be negligible. In order to calculate gaseous deposition of the HCHs (Table 20), their HLCs and enthalpies of Henry's Law equilibrium were taken from Sahsuvar et al. *(36)*.

Endosulfan I and II. Endosulfan is a chlorinated hydrocarbon insecticide and acaricide of the cyclodiene subgroup which acts as a poison to a wide variety of insects and mites on contact. Technical Endosulfan is made up of a mixture of two molecular forms (isomers) of endosulfan, the alpha- and beta-isomers (referred as Endosulfan I and II respectively in this study). Endosulfan is a highly toxic pesticide in EPA toxicity class I. It is a Restricted Use Pesticide (RUP) *(37)*. The highest mean concentrations of Endosulfan I and II occurred at Camden. Endosulfan I is the most abundant component in the mixture and its concentration is always higher that Endosulfan II over all sites in New Jersey (Table 16). As with many of the other pesticides, gas-phase concentrations of Endosulfan I were generally highest at Camden and New Brunswick (Figure 19, Table 16). Both Endosulfans were detected in the particle phase at some sites (Table 17), with the particle phase typically comprising 2-8% and 17-70% of the total atmospheric burdens of Endosulfan I and II, respectively. Both Endosulfans were detected in precipitation (Table 18).

Atmospheric deposition of the Endosulfans (Table 20) was calculated using the HLC for Endosulfan I from Hargrave et al. *(38)*. Again, the enthalpy of Henry's Law equilibrium was assumed to be equal to the compound's enthalpy of vaporization. The enthalpy of vaporization of Endosulfan I was assumed to be 98 kJ/mol, based on the following reasoning. Endosulfan I elutes just after 2,4'-DDE in our GC analysis. In this analysis, compounds should elute roughly in order of vapor pressure, such that these compounds have similar vapor pressures. Because a linear correlation between the natural log of a compound's vapor pressure and its enthalpy of vaporization has been observed for a large number of organic chemicals *(39)*, it seems reasonable to assume that the enthalpy of vaporization for Endosulfan I is similar to that of 2,4'-DDE, or about 98 kJ/mol *(22)*. By our calculations, gas absorption constitutes >90% of the total atmospheric deposition of Endosulfan I. Gas absorption fluxes for Endosulfan II were not calculated due to the lack of a reliable HLC for this compound. From 17 to 70% of all atmospheric Endosulfan II measured was in the particle phase, vs. less than 8% for Endosulfan I. This distribution suggests that dry and wet deposition are likely to constitute a large fraction of the total deposition of Endosulfan II.

Seasonal Trend and Relationship with Temperature.

Gas phase concentrations of OCPs in New Jersey were generally higher in summer than winter. Exceptions include heptachlor, which shows a relatively constant concentration throughout the year, and aldrin, which is more abundant in winter. The Clausius-Clapeyron equation describes the relationship between ambient temperature and the gas-phase partial pressure of semi-volatile organic compounds (Hoff et al., 1992b; Wania et al., 1998):

$$\ln P = \frac{\Delta H}{R} \cdot \frac{1}{T} + \text{constant} \qquad (2)$$

where P is the partial pressure of the compound (Pa), ΔH is a characteristic environmental phase-transition energy of the compound (kJ mol^{-1}), R is the gas constant (8.314 Pa m^3 mol^{-1} = kJ mol^{-1}) and T is the temperature (Kelvin). In the Clausius-Clapeyron plots, all of the statistically significant regressions ($p < 0.05$) displayed a negative slope for all pesticides. Aldrin displays no significant correlation between the gas-phase concentration and the temperature at any of the sites, possibly due to the small number of samples in which aldrin was detected. In most other instances when the regression of lnP vs. 1/T were not significant, the compound was detected in less than half of all the samples gathered at that site. The exceptions (compounds for which lnP vs. 1/T regressions were not significant despite the compound being above detection limit in most samples) were: Heptachlor (not significant at Jersey City, New Brunswick, and Sandy Hook), 2,4'-DDT (not significant at Jersey City and Sandy Hook), and 2,4'-DDE and 4,4'-DDT at Sandy Hook. Negative slopes found for all other pesticides indicate that gas-phase concentration increase with increasing temperature. The slope for each OCPs of each Clausius-Clapeyron regression plot were then multiplied by the negative universal gas constant (-R) and the chemical's phase-transition energy (ΔH) was calculated (Table 21).

COMPOUND	Delaware Bay	Camden	Jersey City	New Brunswick	Pinelands	Sandy Hook	ΔH_{vap}	
	ΔH_{env}	ΔH_{env}	ΔH_{env}	ΔH_{env}	ΔH_{env}	ΔH_{env}	ΔH_{vap} [(a)]	ΔH_{oa} [(b)]
α-HCH	23±12	29±7	38±9	19±4	26±5	20±9	68.5	61.8
γ-HCH	60±22	86±9	57±12	47±9	73±6	49±14	70.5	65.3
Heptachlor	58±20	16±6	13±7	8±6	16±5	24±13	76.5	66.1
Heptachlor epoxide	38±15	83±9	112±23	55±9	37±9	38±20		
Oxychlordane	44±17	68±8	58±21	82±7	53±9	41±21		
Trans Chlordane	49±17	60±8	48±11	47±10	59±9	41±13	80.7	96.3
Cis Chlordane	54±16	65±7	61±11	60±8	64±8	44±14	82.0	98.0
Trans Nonachlor	56±16	68±8	61±11	66±8	68±10	47±14	85.5	105.2
Cis Nonachlor	108±48	86±10	58±19	65±6	57±12	43±17		
Endosulfan I	132±34	175±12	127±21	136±12	112±22	89±25		
Endosulfan II		158±16	66±22	94±10	51±34	86±30		
4,4'-DDE	92±19	62±7	35±6	72±9	66±9	58±17	87.2	97.8
2,4'-DDE	51±30	71±6	33±8	53±8	8.6±21	26±16		
4,4' DDT	142±58	73±14	49±25	73±9	40±23	36±23	93.2	88.0
2,4' DDT		62±7	76±27	35±15	27±21	-21±13	88.6	87.8
Dieldrin	68±22	68±12	116±32	68±16	64±15	49±22	82.5	72.5
Aldrin		-2.8±17	-2.6±20	-25±13	-11±26	0	75.1	70.9

Table 21. Phase transition energies (ΔH_{env} ± 95% confidence limits) in kJ/mol determined by linear regression of ln P (Pa) versus 1/T. $\Delta H = m/R$, where R= 8.314 J mol^{-1} K^{-1} and m is the slope from the linear least squares fit to the Clausius-Clapeyron equation. [(a)] ΔH_{vap} in kJ/mol from Hickley et al (1990). [(b)] ΔH_{oa} in kJ/mol from Shoeib and Harner (2002).

An increase in temperature can also affect a variety of environmental processes which may result in an increase in atmospheric gas-phase concentrations of pesticides, such as air/water exchange and gas/particle partitioning. As a result, the value of ΔH_{env} can aid an understanding of the environmental behavior of these compounds. In Table 21, ΔH_{env} calculated for each OCP is compared to ΔH_{vap} and ΔH_{oa}. All ΔH_{env} are lower than ΔH_{vap} and ΔH_{oa} which means that these compounds volatilize more easily from whatever environmental compartment they are in, than from pure octanol or the pure liquid phase.

The cyclodienes including trans-chlordane, cis-chlordane, trans-nonachlor, cis-conachlor, dieldrin and the metabolites hepthachlor epoxide and oxychlordane show the same temporal

pattern with a lower concentration in the winter and a higher concentration between late spring and early fall. Heptachlor was the only chlordane that did not display a seasonal pattern. Other investigators have similarly noted no correlation between gas-phase heptachlor concentrations and temperature, including Hoff et al. *(10, 11)* in southern Ontario and Janunten et al. *(7)* in Alabama. The natural log of the partial pressures of trans-chlordane, cis-chlordane, tarns-nonachlor, cis-nonachlor, oxychlordane and heptachlor epoxide were significantly correlated with 1/T ($P<0.001$) among all sites in New Jersey with the exception of Sandy Hook, with the r^2 range from 0.68 to 0.7 in Camden, from 0.3 to 0.6 in Jersey City, from 0.5 to 0.86 in New Brunswick and from 0.42 to 0.6 in Pinelands. Slopes are the highest in Camden (range: -7191 to - 10357) and the lowest at Sandy Hook (range: -797 to -5538). The average ΔH determined for trans-chlordane, cis-chlordane, trans-nonachlor and cis-nonachlor is significantly lower ($P<0.001$) at the Sandy Hook site as compared with the land-locked urban and sub-urban locations. (Correlation between gas-phase oxychlordane and temperature was not statistically significant at Sandy Hook ($P=0.10$), probably due to a low number of detects.) Thus temperature is a relatively weak driver of gas-phase concentrations of chlordanes at Sandy Hook, suggesting that other processes contribute to gas-phase chlordane concentrations there. Sandy Hook is coastal marine site and the presence of the large water mass may decrease the influence of temperature on the chlordane concentrations, similar to the effect noted by Cortes et al. *(8)*. The waters surrounding Sandy Hook may act as a sink or a source for these compounds. In general, temperature has a smaller effect on volatilization and deposition from water bodies than from terrestrial surfaces, an effect noted by Cortes et al. *(8, 9)* at IADN sites on the Great Lakes. Indeed, at Sandy Hook the average ΔH_{env} for chlordanes are similar to those measured by these researchers in 1994 (48 to 44 kJ/mol) *(8, 9)*.

Results indicate that concentrations of γ-HCH display a stronger temperature dependence ($P<0.001$) than those of α-HCH. Slopes for γ-HCH range from –5667 at The New Brunswick location to –10308 at the urban Camden site, while slopes for α-HCH range from –2288 at New Brunswick to –4516 at the urban/industrial Jersey City site. The differences in slopes suggest that α-HCH levels may be governed primarily by transport, whereas the γ-HCH levels are driven by temperature, perhaps due to air-surface exchange with nearby terrestrial surfaces. Many studies have shown that a steep slope indicates that the air concentrations are controlled by re-volatilization from surfaces, while a flatter slope indicates that advection of air is governing

atmospheric concentration levels *(9, 29, 40, 41)*. Thus the steeper slopes associated with γ-HCH concentrations may be a reflection of the current use of γ-HCH (lindane), while the shallower slopes associated with α-HCH concentrations reflect the fact that this chemical has been banned for 20 years.

Correlations between lnP vs 1/T for DDTs were statistically significant at Camden and New Brunswick ($P<0.001$). The r^2 values range from 0.46 (4,4'-DDT) to 0.78 (2,4'-DDE) at Camden and from 0.24 (2,4'-DDT) to 0.75 (4,4'-DDE and 4,4'-DDT) at New Brunswick. ΔH_{env} estimated for all of the DDTs at Camden and were statistically similar (range from 62±7 to 73±14 kJ/mol). Results of regressions at New Brunswick show flatter slopes than at Camden, with ΔH_{env} ranging from 35±15 to 73±9 kJ/mol. Values found for ΔH_{env} in Camden are higher than those estimated in the Great lakes for 4,4'-DDE and 4,4'-DDT (between 30 and 57 kJ/mol) *(9)*, whereas ΔH_{env} values estimated at the New Brunswick location are in that range. Correlation with temperature for 4,4'-DDE was statistically significant over all sites in New Jersey ($P<0.001$) with ΔH_{env} ranging from 35±6 kJ/mol at Jersey City to 72 ± 9 kJ/mol at New Brunswick. These differences among the sites may suggest that different processes control the concentration of these compounds at the different locations. The strongest temperature dependence in Camden and New Brunswick suggest a partitioning between the surfaces and the atmosphere and it can also be indicative of seasonal pesticide use; whereas a weak correlation with temperature for DDTs among the other sites may be indicative of long range transport.

Endosulfan I and II show the strongest correlation with temperature among all the other pesticides over all sites (Table 21). They also show the highest values for ΔH_{env}, ranging from 175±12 kJ/mol in Camden to 89±25 kJ/mol in Sandy Hook for Endosulfan I (the most abundant compound).

Dieldrin displays statistically significant correlations with temperature at all sites. ΔH_{env} values range from 49±22 kJ/mol at Sandy Hook to 116±32 kJ/mol at Jersey City. The strong temperature dependence at Jersey City may be indicative of partitioning between surfaces and the atmosphere and/or of seasonal pesticide use.

Influence of air mass transport for Chlordanes

As part of NJADN, Offenberg et al. *(23)* used back trajectory analyses to explain chlordane concentrations that deviate from values predicted by temperature from October 1997 to March 1999. No significant correlation was found between air mass origin and gas-phase chlordane concentrations. The same back trajectory analyses were performed for the present samples (taken during 2000 and 2001) at Camden, Delaware Bay, Jersey City, Pinelands, and Sandy Hook in order to validate the hypothesis of no correlation between gas-phase concentration and air mass movements.

Regressions of lnP versus 1/T are significant for all chlordanes. The correlation is also significant for the pooled data set (n=158) of all five sites (Figure 20) with r^2=0.27 and a slope of –6180. The r^2 value estimated for New Jersey is less than that reported for the Great Lakes (0.46) *(8, 9)* and from Columbia, SC (0.59) *(19)*. Points with residuals greater than one standard deviation from the predicted ln P vs 1/T relationship were checked against three-day back trajectories at the middle of the sampling period. Seventy-two hour back trajectories were obtained by using the NOAA HYSPLIT model *(42)*. Lower than expected concentrations were associated with air masses originating in the northwest (Canada and Great Lakes), whereas large positive residuals are not associated with air masses from any particular area. On those days, air masses may originate from the south or north. This means that in addition to the influence of temperature, air mass origin plays a role in the driving gas-phase concentrations of chlordanes in New Jersey, but the role of air mass origin is limited to dilution of chlordane concentrations with "clean" air from the north and west.

Summary

This data represents the first measurements of organochlorine pesticides in New Jersey air, and has allowed the first estimates of atmospheric deposition of such pesticides to the New York-New Jersey Harbor Estuary. Because of the uncertainties inherent in the calculation of deposition fluxes from atmospheric concentrations, it is difficult to detect significant differences in deposition fluxes between any of the NJADN sites. However, it may be reasonably assumed that higher concentrations will lead to higher deposition fluxes (although differences in particle size distributions, wind speeds, and salinity of receiving waters can shift spatial deposition patterns). Atmospheric concentrations of dieldrin, aldrin, and the HCHs are similar to those

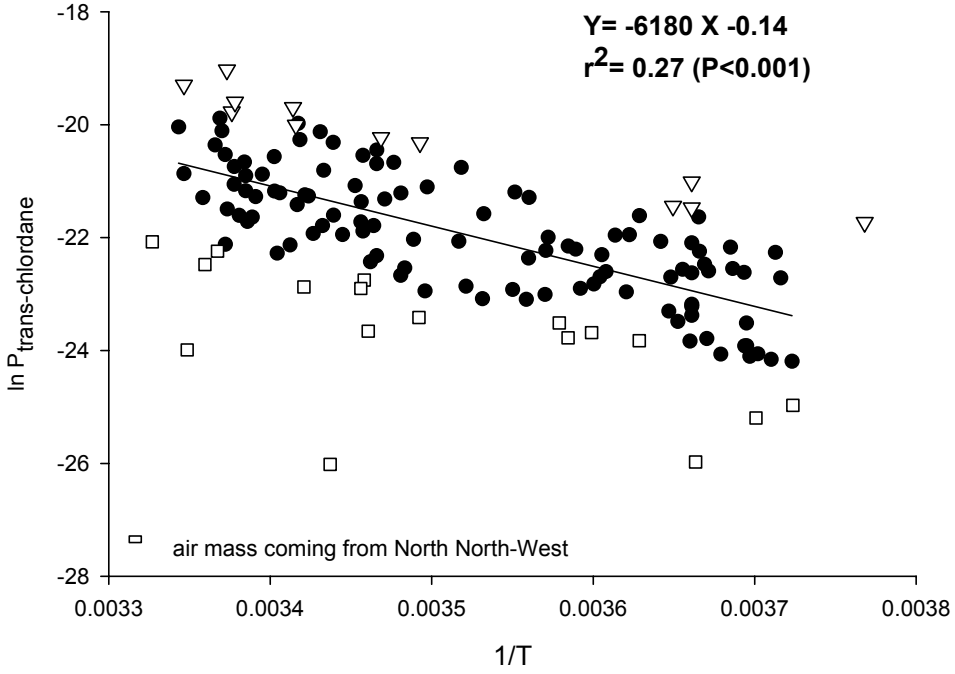

Figure 20. Clausius-Clapeyron type plot of gas phase trans-chlordane for the pooled data set (n=156). White squares indicate residuals (negative residuals) greater than 1 standard deviation associated with air mass coming from N or NW. White triangles indicate positive residuals greater than one standard deviation that are not associated with the air mass coming always from the same direction.

measured by IADN, suggesting that the New York-New Jersey Harbor Estuary receives atmospheric deposition fluxes of these compounds that are similar to those received by the Great Lakes. In contrast, concentrations of DDTs, chlordanes, and heptachlor are higher in NJADN than IADN, suggesting that the New York-New Jersey Harbor Estuary receives higher inputs of these chemicals per unit area than the Great Lakes. For comparison, fluxes of PAHs and PCBs to the New York-New Jersey Harbor Estuary are estimated to be 2-20 times higher than those to the Great Lakes and Chesapeake Bay (see sections II.A1. on PCBs and II.A2. on PAHs).

Most of the pesticides measured in this work display their highest concentrations at Camden and New Brunswick, although in many cases the differences in geometric mean concentrations are not statistically significant. High gas-phase concentrations of PCBs and, to a lesser extent, PAHs are strongly associated with urbanization. In contrast, OCP concentrations are not correlated with urbanization. If they were, OCP concentrations would be significantly higher at Jersey City. Thus it follows that the sources of atmospheric OCPs are different than the sources of atmospheric PCBs and PAHs. Atmospheric sources of PAHs include mobile emissions from automobiles, and

stationary emissions from home heating, power generation, incineration, etc. Clearly none of these are likely to be important sources of atmospheric OCPs. Atmospheric sources of PCBs are more difficult to identify, but they probably include landfills and brownfields (i.e. relatively urban locations were PCBs were used or disposed). The absence of a correlation between urbanization and high atmospheric OCP levels suggests that urban sources such as landfills and brownfields are not important sources of atmospheric OCPs. Were landfills significant sources of OCPs to the atmosphere, the presence of more than 10 current or former landfills in the New Jersey Meadowlands would almost certainly lead to high OCP concentrations at Jersey City.

High atmospheric OCP levels are likely to be associated with past or present pesticide use (i.e. agricultural areas). High OCP levels at New Brunswick are therefore not surprising, as this site is located within Rutgers Gardens and less than a mile from the fields used by Rutgers and Cook College for decades of agricultural research. This leads us to speculate that the high OCP levels observed in Camden may be due to its location downwind of rich agricultural areas in eastern Pennsylvania, not to its urban character. It should, however, be noted that DDT was manufactured at a plant on the Delaware River just south of Philadelphia, which might explain the high DDT levels measured in Camden.

References

(1) Bidleman, T. F.; Jantunen, L. M. M.; Helm, P. A.; Brorstrom-Lunden, E.; Juntto, S. Chlordane enantiomers and temporal trends of chlordane isomers in arctic air. *Environmental Science & Technology* **2002**, *36*, 539-544.

(2) Hung, H.; Halsall, C. J.; Blanchard, P.; Li, H. H.; Fellin, P.; Stern, G.; Rosenberg, B. Temporal trends of organochlorine pesticides in the Canadian Arctic atmosphere. *Environmental Science & Technology* **2002**, *36*, 862-868.

(3) Halsall, C. J.; Bailey, R.; Stern, G. A.; Barrie, L. A.; Fellin, P.; Muir, D. C. G.; Rosenberg, B.; Rovinsky, F. Y.; Kononov, E. Y.; Pastukhov, B. Multi-year observations of organohalogen pesticides in the Arctic atmosphere. *Environmental Pollution* **1998**, *102*, 51-62.

(4) Kucklick, J. R.; Baker, J. E. Organochlorines in Lake Superior's food web. *Environmental Science & Technology* **1998**, *32*, 1192-1198.

(5) Muir, D. C. G.; Ford, C. A.; Rosenberg, B.; Norstrom, R. J.; Simon, M.; Beland, P. Persistent organochlorines in beluga whales (Delphinapterus leucas) from the St. Lawrence River estuary. I. Concentrations and patterns of specific PCBs, chlorinated pesticides and polychlorinated dibenzo-p-dioxins and dibenzofurans. *Envionmnetal Pollution* **1996**, *93*, 219-234.

(6) Alegria, H. A.; Bidleman, T. F.; Shaw, T. J. Organochlorine pesticides in ambient air of Belize, Central America. *Environmental Science & Technology* **2000**, *34*, 1953-1958.

(7) Jantunen, L. M. M.; Bidleman, T. F.; Harner, T.; Parkhurst, W. J. Toxaphene, chlordane, and other organochlorine pesticides in Alabama air. *Environmental Science & Technology* **2000**, *34*, 5097-5105.

(8) Cortes, D. R.; Basu, I.; Sweet, C. W.; Brice, K. A.; Hoff, R. M.; Hites, R. A. Temporal trends in gas-phase concentrations of chlorinated pesticides measured at the shores of the Great Lakes. *Environmental Science & Technology* **1998**, *32*, 1920-1927.

(9) Cortes, D. R.; Hoff, R. M.; Brice, K. A.; Hites, R. A. Evidence of current pesticide use from temporal and Clausius-Clapeyron plots: A case study from the Integrated Atmospheric Deposition Network. *Environmental Science & Technology* **1999**, *33*, 2145-2150.

(10) Hoff, R. M.; Muir, D. C. G.; Grift, N. P. Annual cycle of polychlorinated biphenyls and organohalogen pesticides in air in southern Ontario. 1. Air concentration data. *Environ. Sci. Technol.* **1992**, *26*, 266-275.

(11) Hoff, R. M.; Muir, D. C. G.; Grift, N. P. Annual cycle of polychlorinated biphenyls and organohalogen pesticides in air in southern Ontario. 2. Atmospheric transport and sources. *Environ. Sci. Technol.* **1992**, *26*, 276-283.

(12) Hillery, B. R.; Simcik, M. F.; Basu, I.; Hoff, R. M.; Strachan, W. M. J.; Burniston, D.; Chan, C. H.; Brice, K. A.; Sweet, C. W.; Hites, R. A. Atmospheric Deposition of Toxic Pollutants to the Great Lakes As Measured by the Integrated Atmospheric Deposition Network. *Environ. Sci. Technol.* **1998**, *32*, 2216-2221.

(13) NJDEP "Findings and Recommendations for the Remediation of Historic Pesticide Contamination - Final Report.," 1999.

(14) Harner, T.; Wideman, J. L.; Jantunen, L. M. M.; Bidleman, T. F.; Parkhurst, M. J. Residues of organochlorine pesticides in Alabama soils. *Environmental Pollution* **1999**, *106*, 323-332.

(15) Leone, A. D.; Amato, S.; Falconer, R. L. Emission of chiral organochlorine pesticides from agricultural soils in the cornbelt region of the US. *Environmental Science & Technology* **2001**, *35*, 4592-4596.

(16) McConnell, L. L.; Kucklick, J. R.; Bidleman, T. F.; Ivanov, G. P.; Chernyak, S. M. Air-Water Gas Exchange of Organochlorine Compounds in Lake Baikal, Russia. *Environ. Sci. Technol.* **1996**, *30*, 2975-2983.

(17) Brown, S. N. Polychlorinated biphenyls and chlorinated pesticides in Lake Ontario air and water. Masters Thesis Thesis, University of Iowa, 2000.

(18) Abadin, H. G.; Baynes, R. "Toxicological Profile for Chlordane," US Department of Health and Human Services, Public Health Service, Agency for Toxic Substances and Disease Registry, 1994.

(19) Bidleman, T. F.; Alegrai, H.; Ngabe, B.; Green, C. Trends of Chlordane and Toxaphene in ambient air of Columbia, South Carolina. *Atm. Env.* **1998**, *32*, 1849-1856.

(20) Buehler, S. S.; Basu, I.; Hites, R. A. A Comparison of PAH, PCB, and Pesticide Concentrations in Air at Two Rural Sites on Lake Superior. *Environ. Sci. Technol.* **2001**, *35*, 2417 -2422.

(21) McConnell, L. L.; Bidleman, T. F.; Cotham, W. E.; Walla, M. D. Air concentrations of organochlorine insecticides and polychlorinated biphenyls over Green Bay, WI, and the four lower Great Lakes. *Environmental Pollution* **1998**, *101*, 391-399.

(22) Hinckley, D. A.; Bidleman, T. F.; Foreman, W. T.; Tuschall, J. R. *J. Chem. Eng. Data* **1990**, *35*, 232-237.

(23) Offenberg, J. H.; Nleson, E. D.; Gigliotti, C. L.; Eisenreich, S. J. Chlordanes in New Jersey Air: 1997-1999. *Environ. Sci. Technol.* **2004**, In review.

(24) Mackay, B.; Shiu, W.-Y.; Ma, K.-C. *Physical-Chemical Properties and Environmental Fate Handbook*; Chapman & Hall: 1999.

(25) Iwata, H.; Tanabe, S.; Ueda, K.; Tatsukawa, R. Persistent Organochlorine Residues in Air, Water, Sediments, and Soils from the Lake Baikal Region, Russia. *Environ. Sci. Technol.* **1995**, *29*, 792-801.

(26) Bidleman, T. F.; Jantunen, L. M. M.; Wiberg, K.; Harner, T.; Brice, K. A.; Su, K.; Falconer, R. L.; Leone, A. D.; Aigner, E. J.; Parkhurst, W. J. Soil as a source of atmospheric heptachlor epoxide. *Environmental Science & Technology* **1998**, *32*, 1546-1548.

(27) Glassmeyer, S. T.; Brice, K. A.; Hites, R. A. Atmospheric concentrations of toxaphene on the coast of Lake Superior. *Journal of Great Lakes Research* **1999**, *25*, 492-499.

(28) Faroon, O.; Harris, M. O.; Llados, F.; Swarts, S.; Sage, G.; Citra, M.; Gefell, D. "Toxicological Profile for DDT, DDE, and DDD," US Department of Health and Human Services, Public Health Service, Agency for Toxic Substances and Disease Registry, 2002.

(29) Bidleman, T. F.; Patton, G. W.; Hinckley, D. A.; Walla, M. D.; Cotham, W. E.; Gargrave, B. T. Chorinated pesticides and polychlorinated biphenyls in the atmosphere of the Canadian Arctic. In *Long-range Transport of Pesticides*; Kurtz, D., Ed.; Lewis: Chelsea, MI, 1999.

(30) Hanley, G. D.; Beblo, D. A.; Wohlers, D.; Avallone, A.; Bosch, S.; Plewak, D. "Toxicological profile for Alrin/Dieldrin," US Department of Health and Human Services, Public Health Service, Agency for Toxic Substances and Disease Registry, 2002.

(31) Iwata, H.; Tanabe, S.; Sakai, N.; Tatsukawa, R. Distribution fo persistent organochlorines in the oceanic air and surface seawater and the role of ocean on their global transport and fate. *Environ. Sci. Technol.* **1993**, *27*, 1080-1098.

(32) Walker, K.; Vallero, D. A.; Lewis, R. G. Factors influencing the distribution of lindane and other hexachlorocyclohexanes in the environment. *Environmental Science & Technology* **1999**, *33*, 4373-4378.

(33) Karlsson, H.; Muir, D. C. G.; Teixiera, C. F.; Burniston, D. A.; Strachan, W. M. J.; Hecky, R. E.; Mwita, J.; Bootsma, H. A.; Grift, N. P.; Kidd, K. A.; Rosenberg, B. Persistent chlorinated pesticides in air, water, and precipitation from the Lake Malawi area, southern Africa. *Environmental Science & Technology* **2000**, *34*, 4490-4495.

(34) Schreitmuller, J.; Ballschmiter, K. Air-Water Equilibrium of Hexachlorocyclohexanes and Chloromethoxybenzenes in the North and South-Atlantic. *Environmental Science & Technology* **1995**, *29*, 207-215.

(35) Kelly, T. J.; Mukund, R.; Spicer, C. W.; Pollack, A. J. *Environ. Sci. Technol.* **1994**, *28*,

(36) Sahsuvar, L.; Helm, P. A.; Jantunen, L. M.; Bidleman, T. F. Henry's law constants for alpha-, beta-, and gamma-hexachlorocyclohexanes (HCHs) as a function of temperature and revised estimates of gas exchange in Arctic regions. *Atmospheric Environment* **2003**, *37*, 983-992.

(37) Miller, L. L.; Gefell, D.; Avallone, A.; Llados, F. "Toxicological profile for Endosulfan," US Department of Health and Human Services, Public Health Service, Agency for Toxic Substances and Disease Registry, 2000.

(38) Hargrave, B. T.; Barrie, L. A.; Bidleman, T. F.; Welch, H. E. Seasonality in exchange of organochlorines between Arctic air and seawater. *Environmental Science & Technology* **1997**, *31*, 3258-3266.

(39) Goss, K. U.; Schwarzenbach, R. P. Empirical prediction of heats of vaporization and heats of adsorption of organic compounds. *Environmental Science & Technology* **1999**, *33*, 3390-3393.

(40) Coupe, R. H.; Manning, M. A.; Foreman, W. T.; Goolsby, D. A.; Majewski, M. S. Occurrence of pesticides in rain and air in urban and agricultural areas of Mississippi, April-September 1995. *Science of the Total Environment* **2000**, *248*, 227-240.

(41) Yeo, H. G.; Choi, M.; Chun, M. Y.; Sunwoo, Y. Concentration distribution of polychlorinated biphenyls and organochlorine pesticides and their relationship with temperature in rural air of Korea. *Atmospheric Environment* **2003**, *37*, 3831-3839.

(42) Draxler, R. R.; Hess, G. D. "Description of the Hysplit_4 modeling system," 1997.

II.A4. Organic and Elemental Carbon on PM2.5

Introduction

An understanding of the relative contributions of primary and secondary OC to ambient particulate OC is needed in order to develop control strategies for particulate matter. The concentrations of organic carbon (OC) and elemental carbon (EC) associated with $PM_{2.5}$ mass, measured as part of the New Jersey Atmospheric Deposition Network (NJADN), have been quantified by a Thermal-Optical Transmittance (TOT) method. Twenty-four hour average $PM_{2.5}$ samples were collected at five locations in New Jersey representing different geographical land-uses: suburban New Brunswick, coastal/marine Sandy Hook, urban/industrial Jersey City and Camden, and rural/forested Pinelands. Throughout the observational period, there were no distinct seasonal patterns in $OC_{2.5}$ or $EC_{2.5}$ concentrations or the OC/EC ratio. Periods of secondary organic aerosol formation and periods during which $OC_{2.5}$ arose mainly from primary emissions were identified using ozone, carbon monoxide and meteorological data. Ozone was used as an indicator of periods of photochemical activity, while CO was used as an indicator of combustion sources. Around 40% of the data at all sites display evidence of secondary organic aerosol formation.

Background

Carbonaceous aerosols are major components of urban and rural aerosols and an important constituent of the $PM_{2.5}$ (particulate matter with aerodynamic diameters less than 2.5 microns) mass in most of the U.S. Between 10 to 65% of the fine particulate mass has been identified as carbonaceous material for various regions of the country *(1-5)*. The formation of the carbonaceous fraction is associated with incomplete combustion, industrial processes and biological emissions, such as pollens and plants.

The carbonaceous fraction consists of elemental carbon (EC) and a variety organic compounds to which we collectively refer as organic carbon. (OC). Elemental carbon is a product of combustion processes and is commonly assumed to have minimal sources other than primary emissions *(2, 5, 6)*. Organic carbon can originate from both primary and secondary processes. Thus, EC is often used as a tracer of primary OC since primary OC is assumed to be

emitted from the same sources. Secondary organic carbon can be formed in the atmosphere by condensation of the products of photochemical reactions, due to species such as hydroxyl radical ($OH^{\cdot}$), ozone (O_3) and nitrate radical ($NO_3^{\cdot}$) *(7, 8)*. These reactions tend to create relatively lower vapor pressure semi-volatile organic compounds which partition onto aerosols in the atmosphere. These secondary organic aerosol constituents are indicative of strong atmospheric oxidation products.

The complexity of carbonaceous aerosols suggests that separation into organic (OC) and elemental carbon (EC) is useful to better understand the origins of the particulate organic carbon. When ambient measurements of [OC] and [EC] are made, they can be representative of both primary and secondary formation. Using the assumption that elemental carbon is a good tracer for organic carbon derived from primary emissions, many investigators have used the poor correlation between OC and EC and the OC/EC ratio exceeding the expected ratio for the primary aerosol to indicate the presence of secondary organic aerosols *(5)*. However, calculating the OC/EC ratio in primary aerosol is complex because emissions vary from source to source and because this ratio is also influenced by meteorology, local sources and diurnal and seasonal variation in emissions *(5, 6)*. In previous studies the primary OC/EC ratio has been estimated using different approaches, such as primary OC and EC emissions inventories (Intergovernmental Panel on Climate Change), monitoring locations dominated by primary source emissions *(5)*, estimating the OC/EC primary ratio when low photochemical activity occurs *(6)* or using the minimum OC/EC ratio during a study period. *(9)*.

These OC and EC portions of the total atmosphere particulate matter concentrations are of interest due to their roles in the dynamics of the particulate mass (PM). These species are also of utility in determining the relative importance of primary emissions versus atmospheric chemical reactions on the observed concentrations of atmospheric particulate matter. Additionally, these species play significant role in the gas / particle partitioning, which effects the environmental cycling of numerous organic contaminants found on the atmospheric PM, such as PAHs, PCBs, PCDDs, PCDFs and organo-chlorine pesticides *(10-12)*. Further interest in these species relates to the human health impacts on PM, as various epidemiological studies link atmospheric PM with excess respiratory and cardiovascular morbidity and mortality. *(13-16)*. Further indications suggest stronger impacts on human health for fine particles, those having aerodynamic diameter of less than <2.5 um, than of PM_{10} *(17, 18)*. $PM_{2.5}$ is a US EPA regulated

pollutant due to adverse human health effects and roles in visibility reduction *(19)*.

Several researchers have attempted to differentiate between primary and secondary aerosols in studies in the Los Angeles area; Atlanta, GA; Baltimore and the Chesapeake Bay *(2, 5, 6, 10)*. The SCAQS (Southern California Air Quality Study) investigated the concentrations of OC and EC in Los Angeles area, and calculated primary and secondary organic concentrations for several summer days *(5, 6)*. Unlike these highly studied regions, little work has been done to characterize OC and EC concentrations associated with the $PM_{2.5}$ mass in New Jersey air to determine how local emission effect the PM concentration in the atmosphere. One study, conducted in Brigantine National Wildlife Refuge (near Tuckerton), examined the elemental speciation and EC/OC content of $PM_{2.5}$ and identified some periods of secondary organic aerosol formation *(20)*. However, the New York/New Jersey metropolitan area, which hosts a dense population and large industrial sectors, lacks a comprehensive database for the atmospheric concentrations of Organic Carbon and Elemental Carbon associated with the $PM_{2.5}$ mass.

In this study, observations $EC_{2.5}$, and $OC_{2.5}$ are presented, which have been collected as part of New Jersey Atmospheric Deposition Network (NJADN). The objectives of this work are: (i) to measure the concentration of organic carbon (OC) and elemental carbon (EC) for each $PM_{2.5}$ sample collected; (ii) to assess the spatial and temporal OC and EC concentrations during NJADN for five sites representing different land-uses; and (iii) to identify periods of secondary organic aerosol formation and periods in which $OC_{2.5}$ is dominated by primary emissions by using ozone and carbon monoxide data as well as meteorological data (temperature, wind direction etc.).

Methodology

Air samples were collected at New Brunswick, NJ (40.48^{o}N/74.43^{o}W) beginning October 1997, at Sandy Hook, NJ (40.46^{o}N/74.00^{o}W) beginning February 1998, at Jersey City (40.71N/74.05W) beginning October 1998, at Camden (39.93N/75.12W) beginning in July 1999 and Pinelands (39.96N/74.63W) beginning in June 1999. New Brunswick, NJ is an urban/suburban community in close proximity to major traffic arteries including the New Jersey Turnpike and the Garden State Parkway. Sandy Hook, NJ is located on a peninsula extending

out into the Lower Hudson River Estuary/Atlantic Ocean approximately 10 km south of New York City and 30 km southwest of the Newark/Elizabeth/Jersey City urban/industrial complex. Jersey City and Camden are urban/industrial sites situated close the urban area of New York city and the industrial complex of Camden/Philadelphia respectively. Pinelands is a rural site located in forested area 35 km from Camden.

Sampling occurred for 24 hours every sixth day from October 1997 to August 1998, every ninth day until September 1999 to and every twelfth day thereafter. A total of 77 sampling events occurred prior to the changeover to the nine-day sampling regime and 41 from August 1998 to September 1999 and 49 sampling events thereafter. Twenty-four hours integrated samples were collected onto 47 mm Quartz Fiber Filter (QFF) using a low volume sampler operating at a flow of 20 L/min *(21)*(*29*). The sampler uses an oilless vacuum pump, and the exhaust is vented through a HEPA air filter to prevent contamination.

Prior the sampling, quartz fiber filters were pre-baked to remove contaminants. After sampling, filters were frozen at 4ºC until EC/OC analysis was performed. A section (1 cm^2) of each filter was removed using a steel puncher and it was analyzed for Organic Carbon ($OC_{2.5}$) and Elemental Carbon ($EC_{2.5}$). Organic Carbon and Elemental Carbon were analyzed by a thermal-optical transmittance method which operates under pressure and temperature control *(23)*. In the first step of the analysis carbon is evolved in a helium atmosphere while the temperature is raised to about 820˚C. At this temperature organic carbon is oxidized to CO_2, then reduced to CH_4 and then quantified by a flame ionization detector (FID) at 450˚C. In the second step of the analysis an optical feature corrects for the $EC_{2.5}$ generated pyrolytically and $EC_{2.5}$ measurement is made. The oven temperature decreases, a certain amount of oxygen is introduced into the helium atmosphere (10% oxygen in helium) and the temperature is raised to about 820˚C. The oxygen causes the $EC_{2.5}$ generated pyrolytically to oxidize, causing an increase in the transmittance. The point at which the filter transmittance reaches its initial value is considered to be the "split" between organic carbon and elemental carbon. In the same way as organic carbon, elemental carbon is quantified by the Flame Ionization Detector (FID). The total concentration of $OC_{2.5}$ and $EC_{2.5}$ on the filter is given in $\mu g/cm^2$. Calibration of the instrument was performed using an *internal calibration* and an *external calibration.* For the external calibration, a known mass of methane was injected into the apparatus and analyzed. For internal calibration, laboratory blank quartz fiber filters were spiked with different concentrations of sucrose to

develop an OC calibration curve.

Two instrument blanks and three peaks of internal calibration (methane) were run every day. The instrument blanks are used to detect any contamination in the analytical system. During the three-peaks calibration ($OC_{2.5}$, $EC_{2.5}$ and calibration peaks), a certain amount of methane is injected during each of the three different segments of the analysis. Since the instrument responds differently during these three periods, appropriate Relative Response Factors for $EC_{2.5}$ and $OC_{2.5}$ were calculated. Therefore, the concentration given in the data output is corrected by multiplying this concentration by the average of the two instrument blanks and dividing that by the relative response factors. The correction resulted in a change of about 0.01 $\mu g/cm^2$ for organic and elemental carbon compared to the calibration peak. The Relative Response Factors (RRF) for $OC_{2.5}$ was calculated by dividing the area of the calibration peak by the area of the Organic Carbon peak. The RRF for $EC_{2.5}$ was calculated by dividing the area of the calibration peak by the area of the Elemental Carbon peak. After the RRFs were determined, the average between the two instrument blanks for $OC_{2.5}$ and $EC_{2.5}$ was calculated and the concentration of Organic and Elemental Carbon were calculated as follows:

$$[OC] = (OC_{conc} - AVG_{oc\ blanks}) * RRF_{oc} \quad (1)$$

$$[EC] = (EC_{conc} - AVG_{ec\ blanks}) * RRF_{ec}$$

The [OC] and [EC] obtained from these calculations were then multiplied by the exposed area of the filter and then divided by the sampling volume. The final concentrations were expressed in $\mu g/m^3$.

QA/QC analysis. EC/OC analysis was occasionally performed multiple times on a given sample to assess instrumental precision and spatial variability in particulate matter loading on the filter surface. Replicates were performed every day and the analytical precision for the measurement of organic and elemental carbon was calculated as the mean of organic carbon and elemental carbon concentration divided by the square of the sum of variances of all replicates (for $OC_{2.5}$ and $EC_{2.5}$). The analytical precision is expressed as coefficient of covariance and it ranged about 5%-10% for both species. Field Blanks were collected in order to determine the limits of detection (average multiplied by three times the standard deviation) for both Organic and Elemental Carbon, which averaged approximately 1.07 and 0.15 $\mu g/m^3$, $OC_{2.5}$ and $EC_{2.5}$ respectively. $OC_{2.5}$ was above limit of detection in all but 2 samples out of 83 collected at Sandy

Hook. $EC_{2.5}$ was above the limit of detection for all samples except 7 samples out of 52 at Pinelands, in 8 samples out of 76 at Sandy Hook and in 3 samples out of 116 samples at New Brunswick.

Results and Discussion

$OC_{2.5}$ and $EC_{2.5}$ concentrations. Concentrations of $EC_{2.5}$ and $OC_{2.5}$ ranged from 23 to 5.8 μg/m^3, and from 7.1 to 0.93 μg/m^3, respectively over all sites. The average and range of concentrations are presented in Table 22. OC and EC concentrations at Jersey City and Camden are similar to those reported for other urban areas such as Baltimore (OC = 5.9 μg/m^3, EC = 1.3 μg/m^3), Chicago (OC = 5.4 μg/m^3, EC = 1.3 μg/m^3) and Chesapeake Bay (OC = 4.1 μg/m^3, EC = 1.5 μg/m^3), but lower than those measured in Los Angeles atmosphere (OC = 8.1 μg/m^3, EC = 3.8 μg/m^3) *(10, 22)*. The lowest average concentrations for OC and EC were observed at rural Pinelands where EC never exceeded 1 μg/m^3. The lowest $EC_{2.5}$ concentration at this site can be explained by its rural character. Similarly, Lee et al. *(20)* measured low EC (averaging 0.6 μg/m^3) and OC (averaging 1.8 μg/m^3) at Brigantine, NJ.

Site	Average $OC_{2.5}$ ± SD μg/m^3	Min. $OC_{2.5}$ μg/m^3	Max. $OC_{2.5}$ μg/m^3	n $OC_{2.5}$	Average $EC_{2.5}$ ± SD μg/m^3	Min. $EC_{2.5}$ μg/m^3	Max. $EC_{2.5}$ μg/m^3	n $EC_{2.5}$	Average OC/EC	Min. OC/EC	Max. OC/EC	n OC/EC
Camden	3.7±1.7	1.1	8.9	51	0.83±0.52	0.3	3.7	51	4.9±1.8	1.2	9.1	51
Jersey City	5.4±2.3	1.2	12	71	1.7±1.7	0.20	7.1	71	4.5±3.8	0.68	28	70
New Brunswick	3.4±1.5	1.2	9.0	116	0.74± 0.5	0.13	3.1	116	5.8±3.7	1.6	29	113
Pinelands	2.7±1.3	1.1	5.8	56	0.34±0.17	0.16	0.92	52	9.9±5.8	3.3	28	58
Sandy Hook	3.5±2.9	1.2	23	83	0.45±0.28	0.18	1.6	76	8.0±3.5	2.9	41	76

Table 22. Summary statistics describing concentrations of fine particle-bound elemental and organic carbon ($EC_{2.5}$ & $OC_{2.5}$) at various location in New Jersey (Expressed as: Mean ± 1 standard deviation).

The standard deviations on the average OC and EC concentrations indicate that there are no differences in concentrations among all sites. However, both an unpaired and a paired t-test were performed in order to determine whether average $OC_{2.5}$ and $EC_{2.5}$ concentrations were in fact statistically different at the various sites. Because of the different sampling periods at different sites, it was decided to run an unpaired t-test, in addition to the paired t-test for dates on

which sampling occurred simultaneously at all the five sites. The unpaired t-tests results indicated that there is no statistically significant difference between $OC_{2.5}$ concentrations at New Brunswick and Sandy Hook ($p=0.88$) as well as at New Brunswick and Camden ($p=0.76$) and Camden and the Sandy Hook ($p=0.47$). However, statistically significant differences in $OC_{2.5}$ concentrations did occur at Jersey City, which had higher $OC_{2.5}$ concentrations than at the other four sites ($P<0.001$). Also $OC_{2.5}$ concentrations at Pinelands were lower than those at Sandy Hook ($p=0.05$) and Camden ($p=0.002$). The unpaired t-test for $EC_{2.5}$ shows that statistical differences in $EC_{2.5}$ concentrations for three sites: at Jersey City, where $EC_{2.5}$ was higher than at the other four sites ($p<0.001$); at New Brunswick, where $EC_{2.5}$ was higher than at Sandy Hook and Pinelands ($p<0.001$); and at Camden, where $EC_{2.5}$ were higher than at Pinelands and Sandy Hook ($p<0.001$). However, the t-test indicates that there is no statistical difference between $EC_{2.5}$ concentrations at the suburban New Brunswick site and the urban Camden site ($p=0.20$). The paired t-test is more appropriate for this data set and confirms the unpaired t-test results.

No obvious seasonal trend in $OC_{2.5}$ and $EC_{2.5}$ concentrations on seasonal basis were observed (Figure 21), despite changes in seasonal energy consumption patterns, meteorological conditions (i.e. temperature, mixing height and others) and atmospheric chemistry.

Peaks of highest $OC_{2.5}$ and $EC_{2.5}$ concentrations occur most frequently between September and November at Jersey City. However, there are also peaks of high $OC_{2.5}$ concentration occurring in the summer at this site. The highest $EC_{2.5}$ concentrations occur between October-January at all sites, probably due to an increase in energy consumption (home heating) and changes in meteorology such as lower temperatures and mixing heights. $OC_{2.5}$ concentrations are high during the summer at all sites, but there are also peaks of higher $OC_{2.5}$ concentrations during the winter, which are usually associated with elevated $EC_{2.5}$ concentrations.

OC/EC ratio. The OC/EC ratio ranged from a maximum of 29 occurring at New Brunswick on June 28, 1998 to a minimum of 0.68 at Jersey City on December 30, 1998 (Table 22). The highest average OC/EC ratio occurs at Pinelands, while the lowest occurs at Jersey City. Low OC/EC ratios are characteristic of urban/industrialized sites such as Jersey City and Camden (average OC/EC ratios are 4.5±3 and 4.9±2 respectively) followed by the suburban sites such as New Brunswick (OC/EC = 5.8±3.7). Highest OC/EC ratios are typical of relatively remote sites such as Pinelands and Sandy Hook (9.9 and 8 respectively). Unpaired t-test results indicate that

there is no statistically significant difference between Jersey City and Sandy Hook ($p=0.44$) or Camden and New Brunswick ($p=0.10$). There is a statistical difference, however, between rural/forested Pinelands and coastal/marine Sandy Hook ($p=0.03$) as well as between New

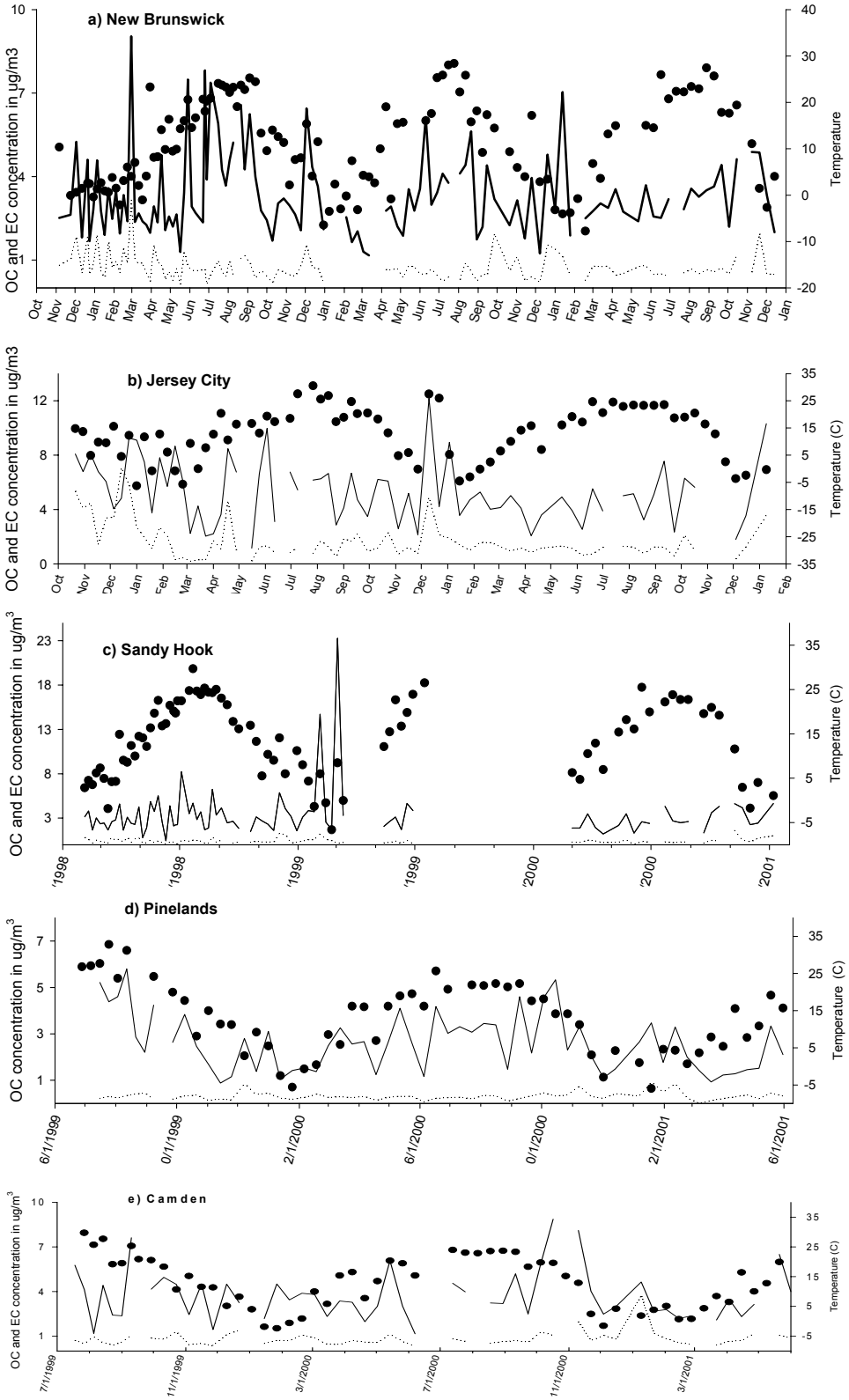

Figure 21. Temporal and seasonal variation in OC and EC concentrations at a) New Brunswick, b) Jersey City, c) Sandy Hook, d) Pinelands, and e) Camden.

Brunswick and Jersey City (p=0.02). A paired t-test was also performed between sites for the same sampling dates. In this case the number of samples per site is limited because sites were sampled over different time periods, which can lead to slightly different average OC/EC ratios. As a result, the paired t-test yields different results than the unpaired test for Camden and Jersey City. The paired test shows a difference between Jersey City and Camden (p=<0.001) when data collected after July 16, 1999 are used. In this case the OC/EC average at Jersey City (3.8±1.2) is slightly less than the average OC/EC ratio at Camden (5±1.9) For the other sites the paired and unpaired t-tests yield the same results, and the average OC/EC ratios are similar to those estimated using the unpaired t-test. Figure 22 shows the temporal trend of the OC/EC ratio at all sites.

At Jersey City, the highest OC/EC ratios (14 and 24) occur on February 13, 1999, and on March 3 and 12, 1999. Elevated OC/EC ratios can indicate the formation of secondary organic aerosols. However, this phenomenon is unlikely to occur in February and March when temperatures are low and elemental carbon concentrations are also relatively low (range: 0.2 to 0.4 $\mu g/m^3$). Thus it appears that other mechanisms may be driving the OC concentration in the atmosphere at Jersey City. Back trajectories for those days indicate that the air masses originated from the N (Canada) or the NW (Upper Midwest). Transport of $PM_{2.5}$ appears to be more important than local sources on those days in Jersey City. The OC/EC ratio at Camden is typically highest in summer, although high ratios are sometimes observed during the winter. Specifically, on October 9, 1999, November 14, 1999, January 25, 2000, and March 25, 2000 the OC/EC ratio was 1-3 units above the average. Back trajectories indicate that the air mass originated from the NW on those days. Thus relatively high OC/EC ratios at Jersey City and Camden during periods when secondary organic aerosol formation is not likely to occur are probably due to transport of $PM_{2.5}$ from the N or NW.

Figure 22 shows the OC/EC ratio plotted over time for all five sites. The urban sites (Camden and Jersey City) have the lowest variability in the OC/EC ratio (rarely above 10)

because they are close to local sources of OC and EC. OC/EC ratios generally increase with distance downwind from major source regions *(5)*. Higher ratios at other sites can be biogenic or can arise from secondary organic aerosol formation during travel time from urban areas. At New Brunswick, there is no distinct seasonal pattern in the OC/EC ratio. The OC/EC ratio at the rural/forested Pinelands site follows a seasonal pattern (Figure 22) with OC/EC ratios higher in summer and lower in winter. The relatively low EC concentrations (all below 1 $\mu g/m^3$) and the remote, forested nature of the site suggest that the elevated OC/EC ratios at Pinelands are due to primary or secondary biogenic, not anthropogenic, aerosols. There is no consistent seasonal pattern for the OC/EC ratio at the coastal/marine location of Sandy Hook. EC concentrations are relatively low there, similar to Pinelands, but the OC/EC ratio is often high at this site. The relatively high OC/EC ratios at Sandy Hook indicate that aerosols at this site may be different in character from those observed at Pinelands, perhaps due to the marine influence.

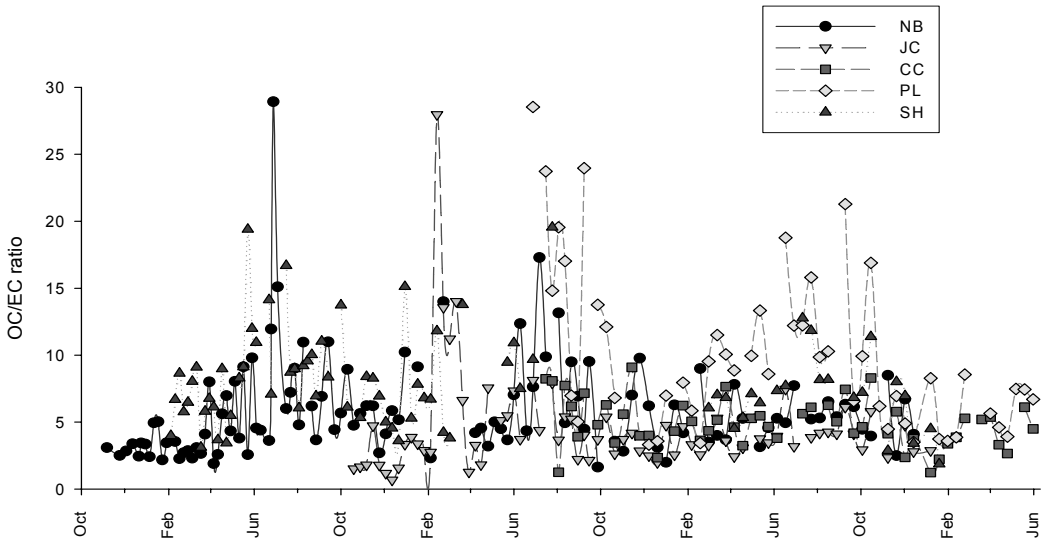

Figure 22. OC/EC ratio plotted over time at all five sampling locations across New Jersey.

OC/EC primary ratio and secondary organic aerosol. Based on the assumption that EC is a good tracer of primary combustion OC, regressions of OC *vs.* EC may be used to identify the occurrence of periods of secondary organic aerosol formation. The OC and EC emissions in the atmosphere vary consistently from source to source *(1)* and the OC/EC primary ratio will depend upon diurnal and seasonal variation in emissions, meteorology, and local sources. Many

investigators have shown that samples collected on a shorter time scale (less than the 24-hour sampling used in this study) are more appropriate for examining the dynamics of aerosol formation in the atmosphere *(2, 5, 6, 23)*. If secondary aerosol formation is only important during midday, its impact on the OC/EC ratio will be greatly diluted in a 24-hr average sample *(5)* such as those collected in this study. Nevertheless, the present data set can be used to identify periods of primary vs. secondary aerosol formation. The first step in the analysis is to derive the OC/EC ratio associated with primary aerosols. The following model was used *(6)*:

$$OC_{pri} = A + (OC/EC)_{pri} \times EC \qquad (2)$$

where the intercept, A, is the non-combustion generated primary OC (e.g. biogenic OC) and the slope, $(OC/EC)_{pri}$, is an estimate of the OC/EC ratio in primary aerosols. OC_{pri} is the sum of OC concentrations from non-combustion and combustion sources. In order to obtain a good estimate of $(OC/EC)_{pri}$, measured OC and EC were regressed via equation 2 for days when organic aerosol were likely to arise from primary sources, as suggested by high carbon monoxide levels. The secondary OC concentration (OC_{sec}) is calculated as the difference between the total OC (OC_{tot}) and the primary OC (OC_{pri}) derived from equation 2 ($OC_{sec} = OC_{tot} - OC_{pri}$).

Calculation of the OC/EC primary ratio. Strong variations in the OC/EC ratio are observed over all sites in New Jersey. Many factors contribute to this variation such as meteorology, photochemistry and primary emissions. Ozone data and carbon monoxide data (provided by the New Jersey Department of Environmental Protection) were used in order to understand when OC is likely to arise from primary or secondary sources. Elevated ozone concentration and relatively high temperature (> 25°C) indicate that secondary organic aerosol formation is likely to occur on a given day. For 24-hr average samples the maximum ozone concentration for each day was used as a reference instead of the 24-hr average concentration because the effect of the peak ozone concentration on a 24-hr average is diluted. Many studies have shown that carbon monoxide is a good tracer of motor vehicle emissions *(2, 25)*. As a result, EC concentrations are assumed to co-vary with carbon monoxide concentrations, such that carbon monoxide is a good indicator of periods when OC is likely to arise largely from primary emissions. Again, the maximum carbon monoxide concentration on a specific day was considered instead of the 24-

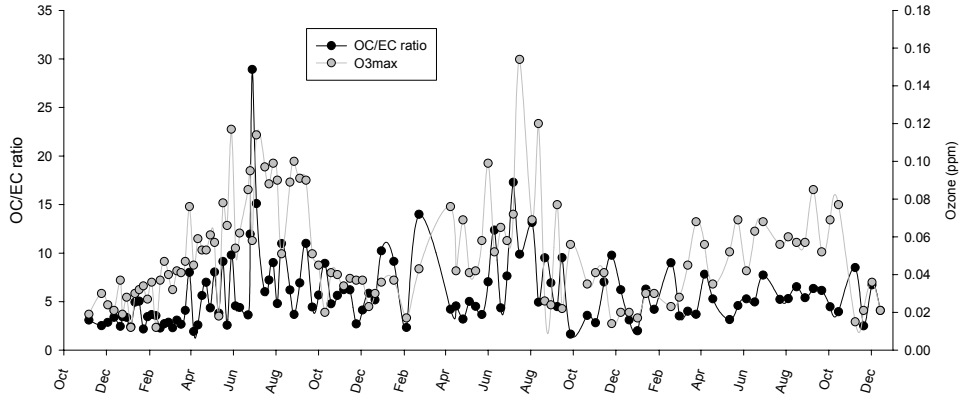

Figure 23. 24-hour OC/EC ratios and maximum ozone concentrations plotted over time at New Brunswick.

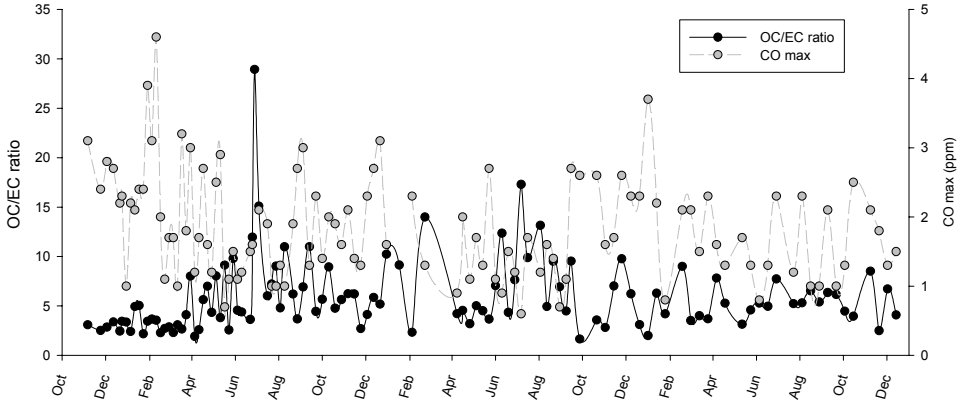

Figure 24: 24-hour OC/EC ratios and maximum carbon monoxide concentrations plotted over time at New Brunswick.

hour average concentrations.

The first step in determining the OC/EC primary ratio was to remove days from the data set on which secondary organic aerosol formation was likely to occur. Those are points of the data set that show a strong positive correlation between ozone and the OC/EC ratio (Figure 23).

Once those points are removed from the data set, days on which primary aerosol sources were important were identified. On these days, carbon monoxide peaked while the OC/EC ratio decreased (Figure 24). A Deming least-squares regression instead of a conventional linear least-squares regression was used to regress the OC and EC data that were determined to be due to

primary emissions. The Deming regression associates uncertainties with both variables (OC and EC), while the conventional least-squares regression associates uncertainties with the y dependent variable assuming the x dependent variable has no uncertainty. As a result, two different regression lines are estimated via the standard linear regression when OC is regressed against EC and vice versa *(6, 26)*. By using the Deming least-squares regression, the best estimates of the slope and the intercept are obtained. The slope of the Deming least square regression is the estimated OC/EC primary ratio and the intercept represents the contribution due to non-combustion processes (Equation 2, Table 23). For these days, OC and EC co-vary, due to common sources or transport from the same region. Estimates of $(OC/EC)_{pri}$ vary from 0.8 to 3.7. The intercept, A, varies from 0.07 to 1.9 μg C/m^3. Strong correlation between OC primary and EC have been found over all sites. The correlation coefficients range from 0.73±0.5 (P<0.0001) at Sandy Hook and 0.98±0.4 (P<0.0001) at Jersey City (Table 23).

Table 23. Estimated parameters for the linear fit of the "primary" OC and EC concentrations. The slope and the intercept represent the OC/EC primary ratio and the contribution from non-combustion sources, respectively.

Sites	slope	intercept	r^2	p value	n
Camden	0.78±0.08	1.91 ±0.1	0.85±0.23	p<0.0001	18
Jersey City	1.37±0.05	1.46 ±0.13	0.98±0.38	p<0.0001	21
New Brunswick	1.53±0.11	1.18±0.1	0.85±0.22	p<0.0001	33
Sandy Hook	3.4±0.3	0.93±0.17	0.73±0.50	p<0.0001	45
Pinelands	3.7±0.26	0.07±0.14	0.95±0.22	p<0.0001	13

$(OC/EC)_{pri}$ is highest at Pinelands and lowest at Camden; the intercept displays the opposite trend, being highest at Camden and lowest at Pinelands. The slope and the intercept values found for Camden, Jersey City and New Brunswick are compared with those reported from Turpin et al. *(5)* for the Los Angeles Basin, in which the primary $(OC/EC)_{pri}$ varied from 1.7 to 2.5 and A (the intercept) varied from 0.8 to 2.3 in 24-hr samples taken during the fall.

Other studies conducting in Los Angeles and using 24-hr average samples reported $(OC/EC)_{pri}$ was 1.4 *(1)*. Lim et al. *(2)* found an upper limit for $(OC/EC)_{pri}$ of 2.1 in Atlanta, GA.

$(OC/EC)_{pri}$ estimated for Sandy Hook and Pinelands is thus higher than reported in the literature, and may reflect the influence of marine aerosols at Sandy Hook and biogenic aerosols at Pinelands. However, $(OC/EC)_{pri}$ derived from 24-hr samples can also yield a higher slope than from 1-hr, 6-hr or 12-hr samples due to decreased variability among the points characteristic of primary emissions. In fact, several studies have shown than the primary ratio can vary from 1.5 to 2.9 over a 24-hour period *(5, 6)*. As a result, $(OC/EC)_{pri}$ observed in this study may not directly comparable with values in the literature. Furthermore, sampling artifacts can influence $(OC/EC)_{pri}$. Quartz fiber filters may adsorb significant quantities of gas-phase organic compounds, artificially increasing OC concentrations and $(OC/EC)_{pri}$ *(27, 28)*.

In Figure 25, the data points are sorted into three categories: days when primary emissions dominate aerosol characteristics (solid black diamonds), days when secondary aerosol formation is likely to occur (white squares), and days when the dominant source of aerosol mass is thought to be transport (grey triangles). Transport is thought to dominate on days when the OC/EC ratio is high, but secondary organic aerosols are not likely to form due to relatively low concentrations of ozone and low temperatures. These days are characterized by relatively high concentrations of $PM_{2.5}$. Thus we hypothesize that aerosols on these days arise primarily from long-range transport.

Typically, periods when primary emissions are more important than secondary organic aerosol formation occur between November and March, while secondary organic aerosol formation is usually most pronounced between May and September at Camden, Jersey City, New Brunswick and Pinelands. We estimate that secondary organic aerosol formation was important for 45% of the samples at Jersey City and New Brunswick, 32% at Camden, 40% at Sandy Hook, and 77% at Pinelands. At Pinelands and Sandy Hook, this percentage (i.e. the proportion of days when secondary organic aerosol formation was thought to occur) probably includes days when local biogenic or marine aerosols were dominant *(29-31)*. However, relatively high $(OC/EC)_{pri}$ at these two sites may also arise from ageing of aerosols during transport, since both of these sites are relatively remote and receive aerosols from urban centers located 20-40 km away. Additional research would be needed to determine whether high $(OC/EC)_{pri}$ at these two sites is due to biogenic/marine aerosols or intermediate-range transport.

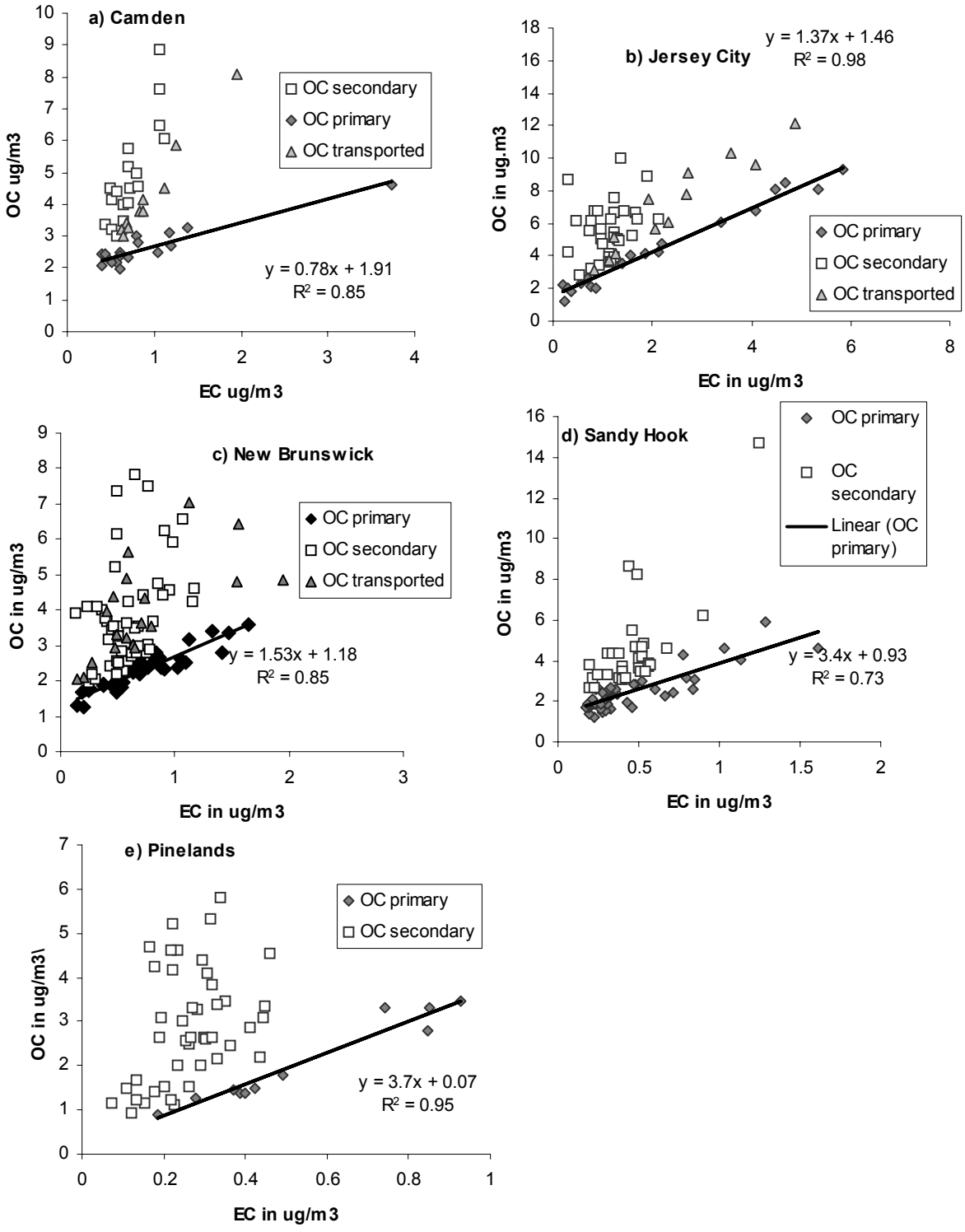

Figure 25. Deming regression plots at a) Camden, b) Jersey City, c) New Brunswick, d) Sandy Hook, and e) Pinelands. Grey diamonds indicate days when aerosols arise largely from primary emissions, white squares represent days when secondary organic aerosol formation is likely to dominate. In a, b, and c, the grey triangles are days when the aerosols are thought to arise primarily from long-range transport.

REFERENCES

(1) Gray, H. A., Cass, G.R.; Huntzicker, J.J., Heyerdahi, E.K., Rau, J.A. Characteristics of Atmospheric Organic and Elemental Carbon Particle Concentrations in Los Angeles. *Environmental Science and Technology* **1986**, *20*, 580-589.

(2) Lim, H. J. a. T., B.J. Origins of Primary and Secondary Organic Aerosol in Atlanta: Results of Time-Resolved Measurements during the Atlanta Supersite Experiment. *Environ. Science and Technology* **2002**, *36*, 4489-4496.

(3) Seinfeld, J. H. P., S.N. *In Atmospheric Chemistry and Physics: from Air Pollution to Global Change*; John Wiley and Sons, Inc: New York, 1998.

(4) Tolocka, M. P. S., P.A.; Mitchel, W.; Norris, G.A.; Gemmill, D.B.; Weiner, R.W.; Vaderpool, R.W.; Homolya, J.B.; Rice, J. East Versus in the US: Chemical Characteristics of Pm2.5 during the Winter of 1999. *Aerosol Science and Technology* **2001**, *34*, 88-96.

(5) Turpin, B. J. H., J.J. Secondary Formation of Organic Aerosol in the Los Angeles Basin: A Descriptive Analysis of Organic and Elemental Carbon Concentrations. *Atmos. Environ.* **1991**, *Part A 25*, 207-215.

(6) Turpin, B. J. H., J.J.;. Identification of Secondary Organic Aerosol Episodes and Quantitation of primary and Secondary Organic Aerosol Concentrations During SCAQS. *Atmos. Environ.* **1995**, *29*, 3527-3544.

(7) Jacobson, M. C., Hansson, H. C., Noone K. J., and Carlson R. J. Organic Atmospheric Aerosols: Reviews and State of the Science. *Review of Geophysics* **2000**, *38*, 267-294.

(8) Pandis, S. N. H., R. A.; Cass, G. R.; Seinfeld, J. H. Secondary Organic Aerosol Formation and Transport. *Atmos. Environ. Part A* **1992**, *26*, 2269-2282.

(9) Strader, R. L., F.; Pandis, S. Evalution of Secondary Organic Aerosol Formation in Winter. *Atmospheric Environment* **1999**, *33*, 4849-4863.

(10) Dachs, J., Eisenreich S. J. Absorption onto Aerosol Soot Carbon Dominates Gas-Particle Partitioning of Polycylic Aromatic Hydrocarbons. *Environ. Sci. Technol.* **2000**, *34*, 3690-3697.

(11) Finizio A., M. D., Bidleman T., Harner T. Octanol-Air Partition Coefficient as a Predator of Partitioning of Semivolatile Organic Chemicals to Aerosol. *Atmospheric Environment* **1997**, *31*, 2289-2296.

(12) Pankow, J. Further Discussion of Octanol Air Partion Coefficient K_{OA} as a Correlating

Parameters for Gas/Particle Partition Coefficient. *Atmospheric Environment* **1998**, *32*, 1493-1497.

(13) Dockery, D. W. P., C. A., III; Xu, X.; Spengler, J. D.; Ware, J. H.; Fay, M. E.; Ferris, B. G., Jr.; Speizer, F. E. An Association of Air Pollution and Mortality in Six U.S. Cities. *N. Engl. J. Med.* **1993**, *42*, 1753-1759.

(14) Pope, C. A., III; Thun, M. J.; Namboodiri, M. M.; Dockery, D. W.; Evans, J. S.; Speizer, F. E.; Heath, C. W., Jr. Particulate Air Pollution as a Predator of Mortality in a Prospective Study of U.S. Adults. *Am. J. 29 Respir. Crit. Care Med.* **1995**, *151*, 669-674.

(15) Pope, C. A., III; Hill, R. W.; Villegas, G. M. Particulate Air Pollution and Daily Mortality on Utah's Wasatch 31 Front. *Environ. Health Perspect.* **1999**, *107*, 567-573.

(16) Schwartz, J. D., D. W.; Neas, L. M.; Wypij, D.; Ware, J. H.; Spengler, J. D.; Koutrakis, P.; Speizer, F. E.; Ferris, B. G., Jr. Acute Effects of Summer Air Pollution on Respiratory Symptom Reporting in Children. *Am. J. Respir. Crit. Care Med.* **1994**, *150*, 1234-1242.

(17) Schwartz, J. D., D. W.; Neas, L. M. Is Daily Mortality Associated Specifically with Fine Particles? *J. Air Waste Manage. Assoc.* **1996**, *46*, 927-939.

(18) Schwartz, J. S., C.; Touloumi, G.; Bacharova, L.; Barumamdzadeh, T.; le Tertre, A.; Piekarksi, T.; Ponce de Leon, A.; Ponka, A.; Rossi, G.; Saez, M.; Schouten, J. P. Methodological Issues in Studies of Air Pollution and Daily Counts of Deaths or Hospitals Admissions. in: St Leger, S., ed. The APHEA project. Short Term Effects of Air Pollution on Health: A European Approach Using Epidemiological Time Series Data. *J. Epidemiol. Community Health* **1996**, *50*, S3-S11.

(19) National Ambient Air Quality Standards for Particulate Matter-Final Rule. *Fed. Regist.* **1997**, *62*, 38651-38760.

(20) Lee, J. H., Yoshida, Y., Turpin, B. J., Hopke, P. K., Poirot, R. L., Lioy, P. J., Oxley, J. C. Identification of sources contributing to Mid-Atlantic regional aerosol. *Journal of the Air and Waste Management Association* **2002**, *52*, 1186-1205.

(21) Georg, W. J. a. R. A Ciclone for Size-Selective Sampling of Ambient Air. *Journal of the Air Pollution Control Association* **1980**, *30*,

(22) Agency, U. S. E. P. Particulate matter (PM2.5) speciation guidance. Final Draft. **1999**, *Edition 1*,

(23) Turpin, B. J. C., R. A.; Huntzicker, J.J. An In Situ, Time-Resolved Analyzer for Aerosol

Organic abd Elemental Carbon. *Aerosol Sci. Technol.* **1990**, *12*, 161-171.

(24) Turpin, B. J. a. C. N. Evaluation of Time-Resolved $PM_{2.5}$ Data in Urban/Suburban Areas of New Jersey. *Journal of the Air & Waste Management Association* **2000**, *50*, 1780-1789.

(25) Polidori, A., Turpin, B. J., Lim, H. J., Cabala, J. C., Subramanian, R., Robinson, A. L., Pandis, S. N. Semi-Continuous Organic Particulate matter measurement during the Pittsburgh Air Qualitia Study (PAQS). *Aerosol Science and Technology. In Preparation* **2002**,

(26) Deming, W. E. *Statistical Adjustment of Data*; Wiley: New York, 1943.

(27) Turpin, B. J. H., J.J.;Hering, S. V. Investigation of organic aerosol sampling artifacts in the Los Angeles basin. *Atmos. Environ.* **1994**, *28*, 3061-3071.

(28) Turpin, B. J., Saxena P., Andrews, E. Measuring and Simulating Particle Organics in the Atmosphere: Problems and Prospects. *Atmospheric Environment* **2000**, *34*, 2983-3013.

(29) Yu, J. C., D. R. III; Griffin, R. J.; Flanagan, R. C.; Seinfeld, J. H. Gas-phase ozone oxidation of monoterpenes: gaseous and particulate products. *J. Atmos. Chem.* **1998**, *34*, 207-258.

(30) Yu, J. G. R. J. C., D. R., III; Flanagan, R. C.; Seinfeld, J. H. Observation of gaseous and particulate products of monoterpene oxidation in forest atmospheres. *Geophys. Res. Lett.* **1999**, *26*, 1145-1148.

(31) Zhang, S.-H. S., M.; Seinfeld, J. H.; Flanagan, R. C. Photochemical aerosol formation from "alpha"-pinene and "beta"-pinene. *J. Geophys, Res. [Atmos.]* **1992**, *97*, 717-729.

II.B. Trace Elements, Nutrients, Chloride, and Sulfate: Concentrations and Deposition

II.B1. Summary of Inorganic Concentrations and Fluxes

The following sections summarize the main features of the atmospheric concentrations and deposition fluxes of inorganic analytes in New Jersey precipitation and fine aerosols and highlight some important features of these results. More detailed evaluations of trace elements, mercury, and nutrients are found in separate sections below and the complete results are tabulated in the appendices.

The primary focus of the inorganic section of NJADN was the quantification of atmospheric concentrations and fluxes of mercury and other trace elements. However, the precipitation concentrations and wet deposition of nitrate and phosphorus were also important components of the Network and these plus a partial data set of chloride and sulfate results are discussed below.

Precipitation Concentrations and Wet Deposition of Inorganic Analytes

Volume-weighted mean (VWM) concentrations of the inorganic chemicals measured in rain collected in New Brunswick, Jersey City, the Pinelands, Camden and Alloway Creek are shown in Table 24. The concentrations of most elements were greatest in Jersey City and Camden, lowest in the Pinelands, and intermediate in New Brunswick (see As, Cl, Co, Cr, Pb, S, and V). Notable exceptions are Cd, Cu, and Zn for which New Brunswick concentrations were among the highest and Ag, Mn, P, and Sb for which the elevated concentrations were measured in the Pinelands. The Alloway Creek site near the upper Delaware Bay in Salem County, NJ recorded the highest VWM concentrations of As, Mg, Sb, and Zn, among the highest levels of Al, Fe, and Mn, and the lowest VWM concentration of Hg (Table 24). Since the Alloway Creek site was only operated during 2002, a year of drought and high temperatures in NJ, these results may reflect increased levels of atmospheric dust and soil particles. Since rain depths were similar at all four sites (82-106 cm y^{-1}), spatial differences may indicate the presence of local sources. By contrast, the fairly uniform VWM concentrations of Hg, nitrate, and phosphate at all sites except Alloway Creek indicate that regional processes are of equal or greater importance to the atmospheric concentrations and deposition of these chemicals.

Table 24. Volume-weighted mean concentrations (μg L^{-1} except Hg, ng L^{-1}) of inorganic chemicals in New Jersey precipitation. NA, not analyzed.

Element	New Brunswick	Jersey City	Pinelands	Camden	Alloway Creek
Ag	0.026	0.020	0.060	0.042	0.001
Al	36	26	24	59	43
As	0.069	0.15	0.066	0.16	0.16
Cd	0.064	0.072	0.024	0.076	0.049
Cl	380	730	360	540	NA
Co	0.048	0.12	0.021	0.17	0.038
Cr	0.15	0.17	0.057	0.33	0.081
Cu	1.6	2.1	0.48	2.1	0.99
Fe	48	45	23	93	47
Hg (ng/L)	13	15	11	15	6.3
Mg	66	90	54	90	110
Mn	2.6	1.8	2.9	3.7	3.4
Ni	0.67	1.1	0.29	1.0	0.34
NO_3-N	390	390	410	500	400
PO_4-P	7.1	5.8	7.6	7.3	NA
Pb	1.7	2.4	0.66	3.8	1.0
Pd	0.012	0.019	0.008	0.019	0.005
Sb	0.088	0.16	0.14	0.15	0.39
SO_4-S	720	840	700	910	NA
V	0.60	0.83	0.41	1.2	0.54
Zn	7.9	8.2	5.4	12	13

The annual wet deposition fluxes of inorganic contaminants are shown in Table 25. Because the annual rainfall in New Jersey is about 100 cm and the conversion factor between cm, μg L^{-1}, and μg m^{-2} is 10, wet deposition is approximately equal to 10^3 x VWM rainwater concentrations. These fluxes reflect the spatial patterns and uncertainty associated with the VWM concentrations. The uncertainty of VWM concentrations and wet deposition fluxes can be evaluated using the standard error of the VWM (*1*). Coefficients of variation (C.V., calculated as the standard error divided by the VWM) for trace element concentrations ranged from 6% to 69% and had a median of 14%. Excluding Ag at New Brunswick and Pinelands and Hg at Alloway Creek, all C.V.'s were less than 40%. Seventy-eight percent of all CV's were less than

20%. Thus the uncertainty in the estimated wet deposition fluxes due to the uncertainty associated with VWM concentrations is considered to be generally less than 50%.

Table 25. Annual deposition fluxes (μg m^{-2} y^{-1}) of inorganic chemicals in New Jersey precipitation. BD, flux not calculated since all VWM concentrations were below the detection limit. NA, not analyzed.

Element	New Brunswick	Jersey City	Pinelands	Camden	Alloway Creek
Ag	25	21	59	38	BD
Al	35,000	28,000	24,000	56,000	34,000
As	67	160	65	150	130
Cd	62	76	23	71	39
Cl	340,000	750,000	220,000	560,000	NA
Co	46	130	22	160	30
Cr	150	180	56	310	65
Cu	1,500	2,200	490	2,000	790
Fe	47,000	47,000	23,000	87,000	38,000
Hg	11	14	11	14	5
Mg	65,000	81,000	54,000	84,000	89,000
Mn	2,500	1,900	2,900	3,400	2,700
Ni	650	1,200	290	980	270
NO_3-N	360,000	360,000	390,000	420,000	310,000
PO_4-P	7,100	5,200	8,300	8,100	NA
Pb	1,700	2,500	650	3,500	770
Pd	10	20	8.1	18	3.6
Sb	85	170	140	140	310
SO_4-S	570,000	770,000	670,000	900,000	NA
V	580	880	410	1,100	430
Zn	7,800	8,800	5,500	12,000	10,000

Fine Aerosol (PM2.5) Concentrations and Dry Particle Deposition of Trace Elements

The arithmetic mean concentrations and annual dry particle deposition fluxes of trace elements in fine aerosols are presented in Tables 26 and 27. Element concentrations in atmospheric particles often show lognormal distributions in which the geometric mean may more accurately represent the frequency of a given concentration (*2*). Thus it is important to recognize

that in NJADN and other atmospheric monitoring networks, trace elements were measured in *samples* of fine aerosols collected periodically (every 12 d), not continuously and that high average concentrations and annual fluxes of PM-bound metals may result from a few high concentrations. For example, the very high average PM2.5 concentrations and annual dry deposition fluxes of Ag and Pb in Jersey City are partly due to very high values measured on a single day (August 4, 2000; see Appendix III.A5). However, the arithmetic mean does provide a conservative estimate of metal concentrations in atmospheric PM and dry deposition fluxes and is useful for comparing fluxes from NJADN sites with those from other atmospheric monitoring experiments.

Table 26. Arithmetic mean trace element concentrations (ng m^{-3}, except Hg, pg m^{-3}) in New Jersey fine aerosols (PM2.5).

Element	NB	JC	PL	CC	WC	TK	XQ	SH	DB	AC
Ag	0.21	0.84	0.08	0.20	0.036	0.029	0.044	0.037	0.032	0.089
Al	46	82	61	76	61	44	34	95	52	45
As	0.65	0.97	0.47	0.68	0.66	0.99	0.88	0.62	0.62	0.49
Cd	0.20	0.65	0.10	0.28	0.19	0.10	0.19	0.15	0.13	0.13
Co	0.99	0.53	0.35	0.42	0.18	0.13	0.18	0.22	0.18	1.6
Cr	73	6.1	26	25	4.7	1.9	10	2.7	3.1	125
Cu	14	17	7.7	8.1	29	7.2	1.5	4.0	2.0	6.4
Fe	420	243	176	255	107	74	77	135	52	617
Hg	7.5	12	4.9	16	6.3	5.5	14	7.4	7.6	13
Mg	26	41	80	56	36	32	10	75	35	18
Mn	11	4.5	3.6	5.1	2.4	1.5	2.0	3.5	1.4	16
Ni	63	12	22	19	11	3.6	6.9	5.6	2.3	98
Pb	7.0	27	2.9	5.7	7.2	3.3	2.7	5.2	2.2	3.1
Pd	0.055	0.025	0.062	0.090	0.018	0.026	0.022	0.021	0.023	0.088
Sb	0.81	5.3	0.40	1.3	0.61	0.40	0.34	0.73	0.29	0.33
V	2.8	10	2.0	5.2	2.5	3.6	1.5	6.4	2.6	3.2
Zn	23	35	16	34	22	22	27	33	23	16

The uncertainty associated with the estimates of fine aerosol concentrations and dry particle deposition fluxes of trace elements can be evaluated using the coefficients of variation (C.V., standard deviation divided by arithmetic mean) of the PM2.5 trace element

concentrations. The C.V.'s of PM2.5 concentrations ranged from 32% to 354% and had a median of 104%. Thus the uncertainty associated with dry particle deposition fluxes and the PM2.5 metal concentrations on which they are based is about 100% for half of the values in Tables 26 and 27 and up to 350% for the entire data set.

Table 27. Dry particle deposition fluxes (μg m^{-2} y^{-1}) of trace elements in New Jersey. Fluxes were estimated from the concentrations of metals in fine aerosols (PM2.5) and a deposition velocity of 0.5 cm s^{-1}. The chosen deposition velocity was selected to capture the deposition of all size classes of atmospheric particles, but may underestimate the flux of elements primarily associated with large particles and over estimate the deposition of elements primarily associated with small particles (see section I.C1, pp 13-14).

Element	NB	JC	PL	CC	WC	TK	XQ	SH	DB	AC
Ag	33	130	13	32	5.7	4.6	7.0	5.9	5.0	14
Al	7,200	13,000	9,700	12,000	9,700	6,900	5,400	15,000	8,300	7,000
As	100	150	75	110	100	160	140	99	100	77
Cd	32	100	16	44	30	16	30	23	21	21
Co	160	84	55	66	28	21	28	35	29	250
Cr	12,000	960	4,100	3,900	750	300	1,600	430	480	20,000
Cu	2,200	2,700	1,200	1,300	4,600	1,100	240	640	310	1,000
Fe	66,000	38,000	28,000	40,000	17,000	12,000	12,000	21,000	8,300	97,000
Hg	1.2	1.8	0.8	2.5	1.0	0.9	2.2	1.2	1.2	2.0
Mg	4,100	6,400	13,000	8,800	5,700	5,100	1,600	12,000	5,600	2,900
Mn	1,700	700	580	800	380	240	310	560	210	2,500
Ni	10,000	2,000	3,400	2,900	1,700	570	1,100	880	370	16,000
Pb	1,100	4,200	460	900	1,100	520	430	830	350	480
Pd	8.8	4.0	10	14	2.8	4.1	3.4	3.3	3.7	14
Sb	130	840	64	210	96	64	53	110	45	52
V	440	1,600	310	820	400	560	230	1,000	420	498
Zn	3,600	5,500	2,600	5,300	3,400	3,500	4,300	5,200	3,600	2,600

For a many of the contaminant metals (Cd, Hg, Pb, Sb, V, and Zn), the lowest fine aerosol concentrations were recorded at the rural and coastal sites of Pinelands, Tuckerton, and the Delaware Bay, but low levels of some of these metals were also observed at Washington Crossing and Chester. The urban-impacted, coastal site, Sandy Hook had intermediate concentrations of these metals. As was found for the precipitation concentrations and deposition

fluxes, the PM2.5 results generally show higher fine aerosol metal concentrations in the highly developed urban areas of Jersey City, Camden, and New Brunswick than in other more suburban or rural areas of the state. However, differences in the relative concentrations of metals in fine aerosols and precipitation are likely due to the fact that the precipitation samples are time integrated and include the washout of a wider range of particle sizes than is represented by PM2.5.

II.B2. Trace Elements

The following section presents a detailed examination of the atmospheric concentrations and fluxes of trace elements in New Jersey including seasonal variations, comparisons with other states, and an evaluation of the relative importance of wet and dry deposition fluxes. The

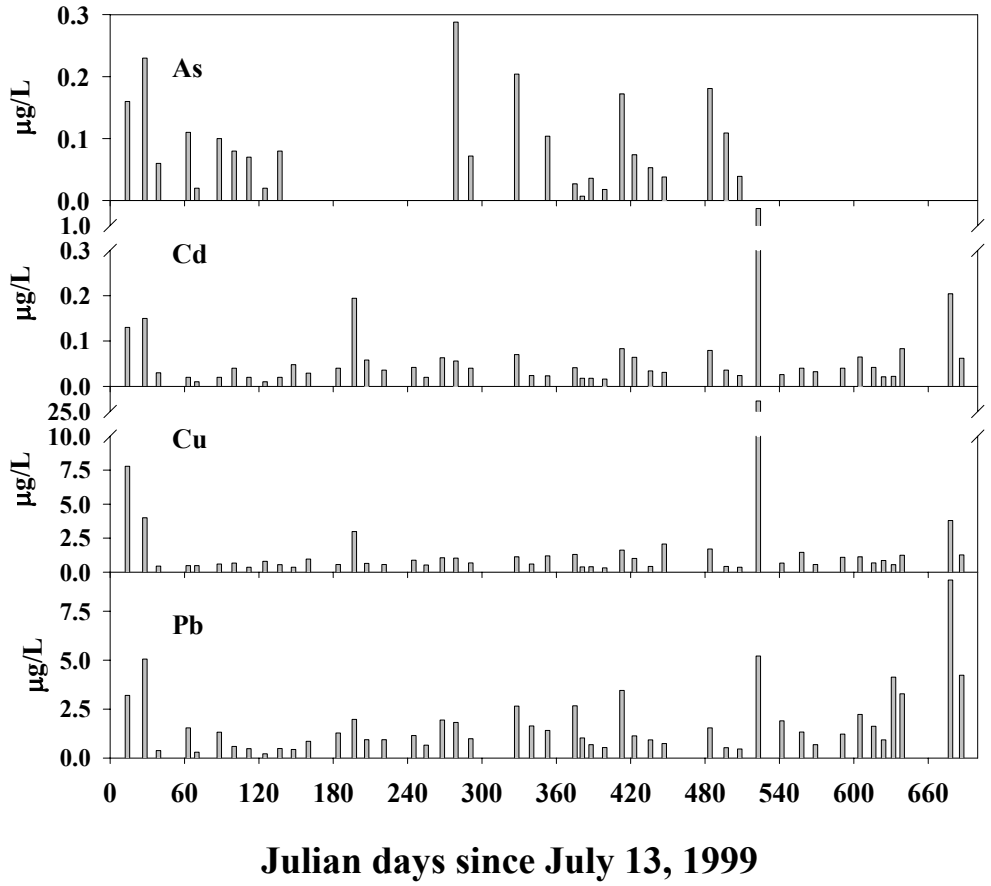

Figure 26. Precipitation concentrations of As, Cd, Cu, and Pb in New Brunswick versus time.

elements As, Cd, Cu, and Pb will be used to illustrate specific points and represent the behavior of the 16 elements analyzed. These elements are emitted from a variety of industrial and municipal sources and, with the exception of As, are strongly associated with particulate matter. As seen in Tables 24-27 above, the atmospheric concentrations and deposition of As, Cd, Cu, and Pb are generally lowest in the Pinelands and highest in Jersey City and Camden. However, the high intra- and inter-seasonal variability at each site (Figures 26, 27) complicates spatial comparisons.

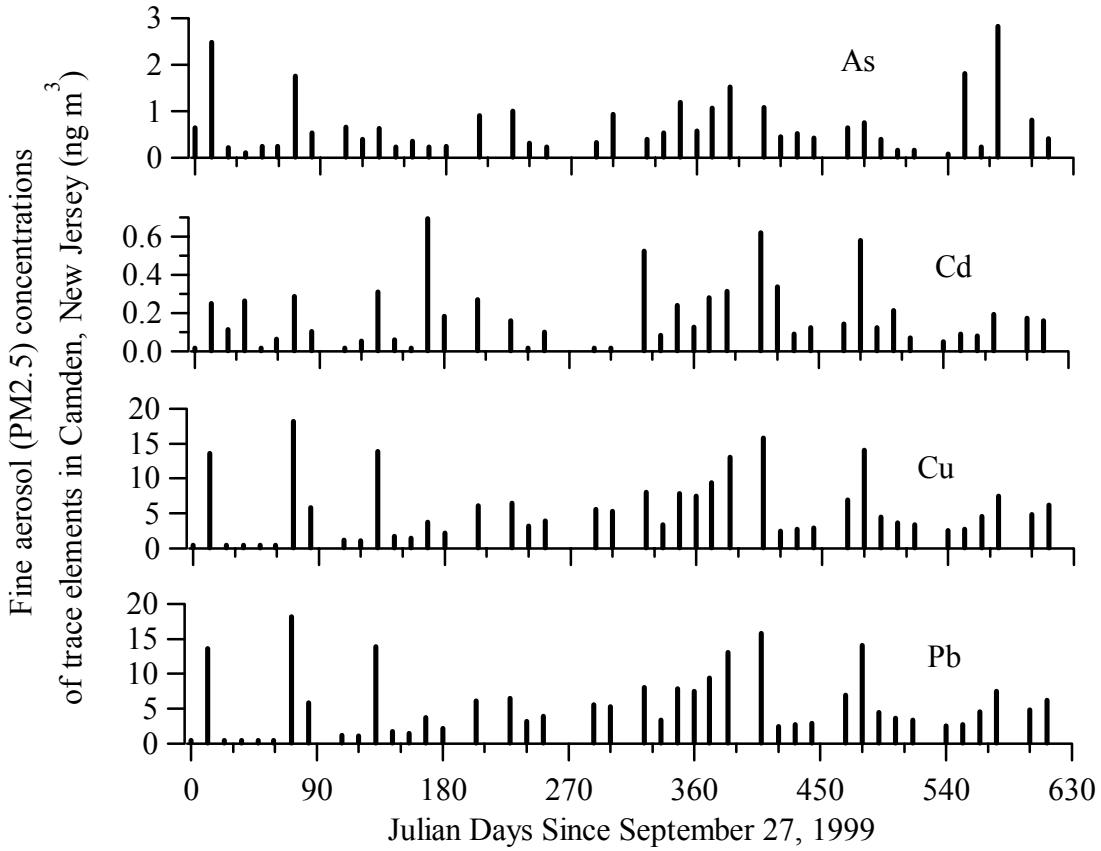

Figure 27. Fine aerosol concentrations of As, Cd, Cu, and Pb in Camden versus time.

Seasonal variations in the VWM concentrations of As, Cd, and Cu were not uniform across New Jersey (Figures 28-31), indicating the importance of local sources and/or atmospheric transport processes to the deposition of these trace elements in the state. In contrast, the seasonal variation in the concentrations of Pb was similar at all sites and showed the highest levels in the spring and the lowest levels in the fall or winter (Figure 31). Precipitation

concentrations of all four of these trace elements generally showed similar seasonal patterns at the two most urbanized sites, Jersey City and Camden, but these patterns differed among the elements.

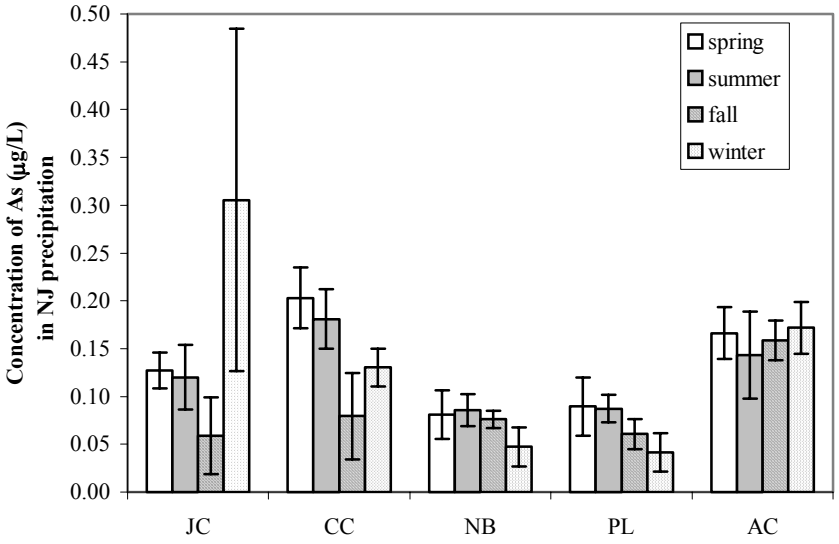

Figure 28. Seasonal VWM concentrations of As in New Jersey precipitation. Error bars are ± SE of VWM.

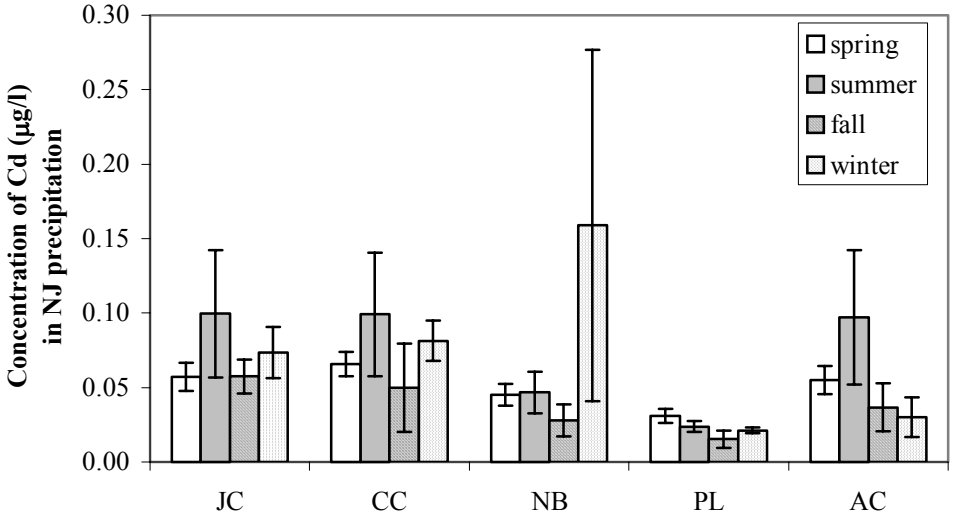

Figure 29. Seasonal VWM concentrations of Cd in New Jersey precipitation. Error bars are ± SE of VWM.

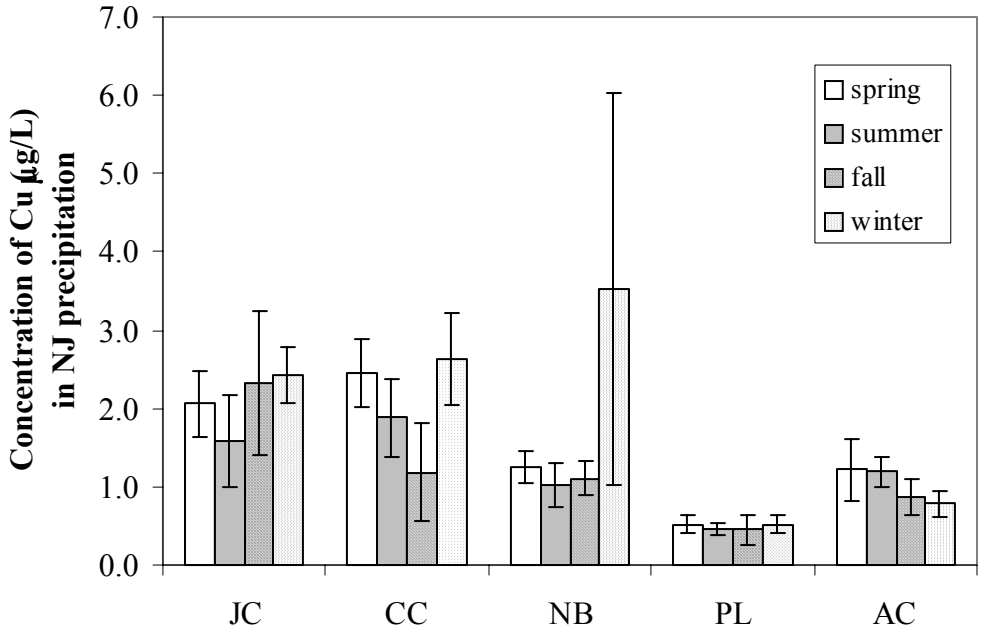

Figure 30. Seasonal VWM concentrations of Cu in New Jersey precipitation. Error bars are ± SE of VWM.

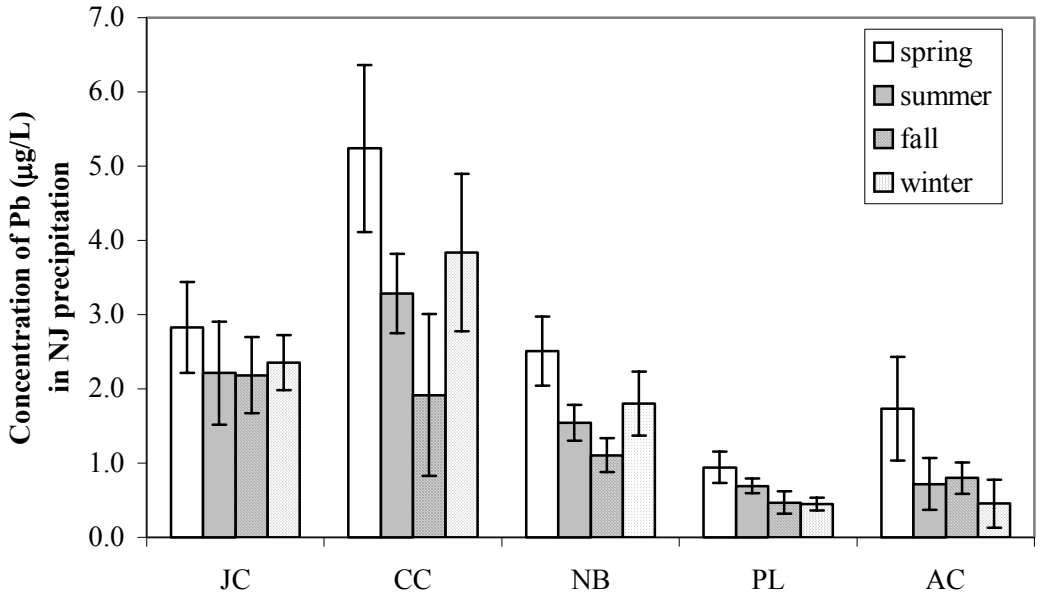

Figure 31. Seasonal VWM concentrations of Pb in New Jersey precipitation. Error bars are ± SE of VWM.

The atmospheric deposition fluxes of Cd, Cu, and Pb illustrate the presence of an urban signal above the regional background that may indicate local sources. The wet deposition fluxes of Cd, Cu, and Pb at the urban/suburban NJADN sites (New Brunswick, Jersey City, Camden; Table 25) are two to nine times higher than those measured in the early 1990's at rural sites (Table 28) in Maryland (Scudlark et al., 1994) and Florida (Landing et al., 1995). These differences do not appear to be the result of methodological difference since precipitation fluxes of Cd, Cu, and Pb in the New Jersey Pinelands (Table 25) are similar to those in rural Maryland and Florida. This trend is similar for the dry particle fluxes of Cd, Cu, and Pb, although the Pinelands appears to have elevated particulate Cu with respect to the regional background as recorded at the Chester and Delaware Bay sites.

Table 28. Annual precipitation and dry particle deposition fluxes ($\mu g\ m^{-2}\ y^{-1}$) of trace elements from other atmospheric deposition studies. Dry particle deposition fluxes were calculated from reported average PM concentrations (VT: geometric mean PM2.5; MD: arithmetic mean PM10) and a deposition velocity of 0.5 cm s^{-1}. The chosen deposition velocity was selected to capture the deposition of all size classes of atmospheric particles, but may underestimate the flux of elements primarily associated with large particles and over estimate the deposition of elements primarily associated with small particles (see section I.C1, pp 13-14).

	Wet deposition		Dry particle deposition	
Element	Maryland[1]	Florida[2]	Vermont[3]	Maryland[4]
As	45	86	36	99
Cd	36	20	-	21
Cr	48	-	55	104
Cu	244	430	156	369
Fe	6800	32,000	2696	22706
Mn	860	2130	118	445
Ni	240	1880	61	626
Pb	560	496	424	711
Zn	1100	5320	965	1892

[1]Scudlark et al., 1994 (Ref *3*)
[2]Landing et al., 1995 (Ref *4*)
[3]Polissar et al., 2001 (Ref *2*)
[4]Wu et al., 1994 (Ref *5*)

Arsenic wet deposition in NJ is highest at the urban sites (Jersey City and Camden), but also fairly high in the Pinelands perhaps indicating a shadow effect of Camden (Table 25; Figure 28). The annual wet deposition of As in Jersey City and Camden are greater than those recorded

in Maryland and Florida, and, given the uncertainty, those in New Brunswick and the Pinelands are similar to those recorded in the other two states (Table 28). Dry particle deposition fluxes of As in New Jersey (with the exception of the Pinelands) based on geometric mean concentrations in PM2.5 are about twice that estimated from the geometric mean PM2.5 As concentration

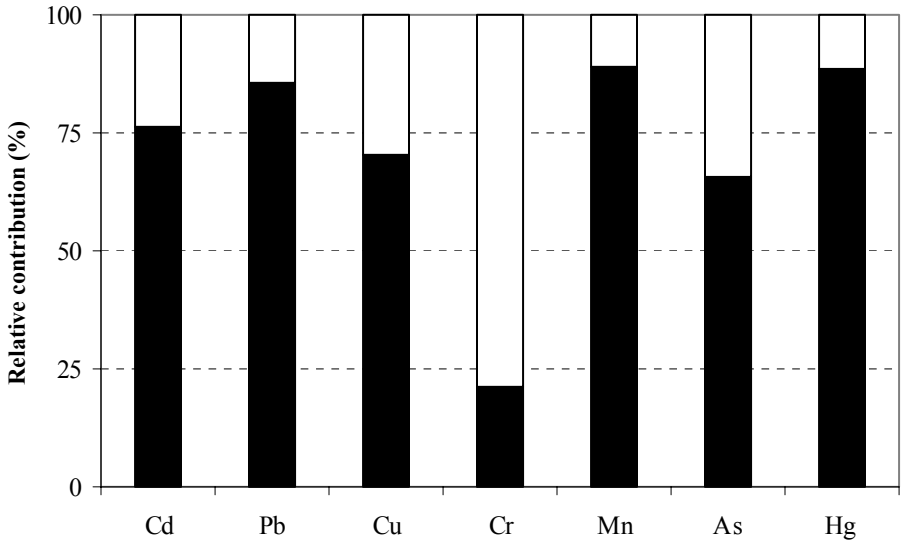

Figure 32. Relative contributions of precipitation (solid portions of bars) and dry particle (open portions of bars) deposition to the total atmospheric fluxes of metals and As in Camden.

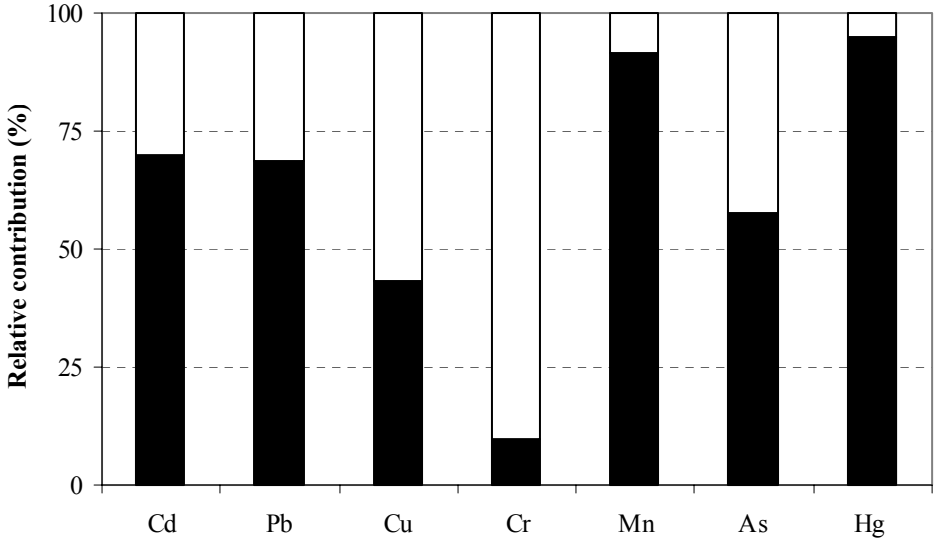

Figure 33. Relative contributions of precipitation (solid portions of bars) and dry particle (open portions of bars) deposition to the total atmospheric fluxes of metals and As in the Pinelands.

measured in Vermont. On an arithmetic mean basis, however, dry particle As fluxes in New Jersey are similar to that estimated from arithmetic mean PM10 As concentrations for Maryland.

The relative contributions of wet deposition and dry particle deposition to the total atmospheric flux of six metals and As in Camden and the Pinelands are shown in Figures 32 and 33. The patterns of relative wet and dry atmospheric deposition were similar at all five sites where wet deposition was measured. For Cu, Pb, Mn, and Hg, more than 70% of the total atmospheric deposition was due to wet deposition. However, less than 30% of the total deposition of Cr was due to wet deposition. Since the large particles (> 2.5 μm) that are excluded from the fine aerosol impactors are scavenged by rain, these observations may reflect differences in the particle size distributions of different metals. The relatively greater contribution of PM2.5-based dry particle deposition fluxes of Cd, Cu, and Pb in the Pinelands than at Camden indicates that large metal-bearing particles contribute to the elevated wet deposition fluxes, but not the PM2.5-based dry particle fluxes in Camden and that these large particles are not are not transported to the Pinelands.

II.B3. Mercury

Introduction. Mercury is of environmental concern because of the enrichment and toxicity of monomethylmercury in aquatic biota (*6, 7, 8*), birds (*9*), mammals (*10*), and humans (*11*). The methylation and bioaccumulation of Hg in aquatic and terrestrial ecosystems, however, is linked to the atmosphere (*12, 13*), which is often the main source of Hg to these environments (*14, 15*). In order to understand and manage the environmental impact of Hg, we therefore need to understand the mechanisms, variability, and trends of atmospheric Hg deposition.

The atmospheric concentration of Hg has tripled over the past 150 years (*14*) as a result of the huge increase in Hg emissions associated with human activities (*16*) and Hg accumulation rates in remote water bodies over the past two decades show that global atmospheric Hg contamination is still on the rise (*17 - 21*). Atmospheric Hg is present mainly as gas phase elemental Hg°, but deposits in association with rain, snow, or aerosols as Hg(II). Most Hg deposition studies show that precipitation dominates the atmospheric flux (*22 - 24*) although dry deposition of particle-bound Hg can be important in some urban areas (*25*). Results from Hg deposition studies in the eastern U.S. show annual and intra-annual variability in the concentrations of Hg in precipitation and aerosols and Hg deposition fluxes. This variability could be linked to variability in emission sources, regional transport processes, local meteorology, and atmospheric chemistry. In order to discern spatial and temporal trends of Hg deposition and to link these to Hg sources and environmental processes, long-term research and monitoring efforts are needed from geographically diverse sites (*26*).

In the northeastern U.S. Hg deposition is currently being monitored in upstate New York, Pennsylvania, and Maine as part of the National Atmospheric Deposition Program's Mercury Deposition Network (http://nadp.sws.uiuc.edu/mdn), but no such monitoring effort has been undertaken New Jersey. Thus prior to this project, there have been few data on the atmospheric concentrations and deposition of Hg in New Jersey for use in risk assessments and the evaluation of deposition trends.

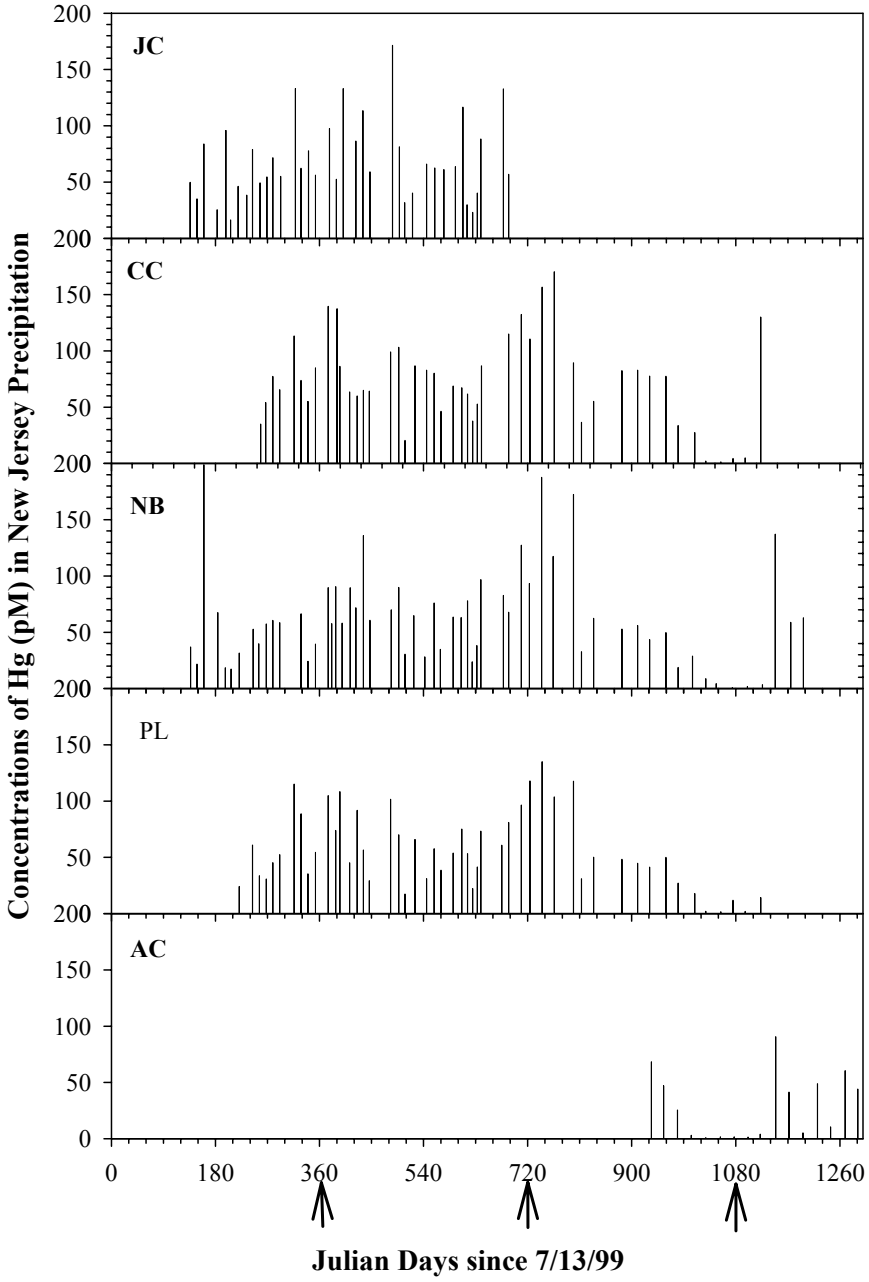

Figure 34. Concentrations of Hg in New Jersey rain for the period November, 1999 – January, 2003. Arrows indicate the summers (mid-July) of 2000, 2001, and 2002.

Mercury in precipitation. For the period of November 1999 to January 2003, the concentrations of Hg in New Jersey precipitation varied from 1 to 200 pM, but were generally in the range (10^{th} and 90^{th} percentiles) of 15 to 115 pM (Figure 34). The range of Hg concentrations in New Jersey rain is similar to that measured at a number of sites around the U.S. including northern Wisconsin (5-165 pM; *27*), Lake Michigan (6-300 pM; *28*), southern Florida (15-224 pM; *24*),

Valley Forge PA (14-173 pM; MDN), and the Chesapeake Bay (10 – 300 pM; *29*). Much of the observed variability in Hg concentrations in New Jersey rain resulted from intra-seasonal fluctuations. For example, from January 12 to February 4, 2000 in Jersey City, the concentration of Hg in rain increased from 26 pM to 96 pM and then decreased to 16 pM. These temporal fluctuations were statewide trends, and as a result, rain collected at all five sites had similar Hg concentrations for a given sampling period (Figure 35).

Daily wet depositional fluxes of Hg reflected the variability of Hg concentrations in New Jersey rain and thus varied from 0.3 to 178 ng m^{-2} d^{-1} (80% within the range of 4 to 84 ng m^{-2} d^{-1}) over the sampling period (Figure 35). Significantly lower concentrations and deposition fluxes of Hg in New Jersey precipitation were observed at all sites in the spring and summer of 2002 (Figures 34 and 35). This statewide trend indicates a possible regional decline in the atmospheric deposition of Hg during the drought year of 2002. Possible mechanisms for this decline include decreased volatilization of Hg from soils or lower rates of Hg oxidation in the atmosphere during dry conditions. Since Alloway Creek was only monitored in 2002, it will not be included in the general discussion of seasonal trends.

Volume-weighted average Hg concentrations in rain collected in Jersey City, New Brunswick, and Pinelands followed the seasonal pattern of increasing levels from spring to summer to fall with the highest levels observed in the fall and the lowest in the winter or spring (Figure 36). Volume-weighted average Hg concentrations in rain were highest at Camden in summer and lowest in the spring (Figure 36). The wintertime Hg concentration measured in Jersey City (54 pM) was lower than the wintertime suburban New Brunswick level (62 pM), and not much higher than the wintertime low observed at the Pinelands (43 pM), suggesting that under certain conditions, rain in urban Jersey City is no more contaminated with Hg than rain in the less developed New Brunswick, and even the more pristine Pinelands.

A seasonal pattern of the highest Hg concentrations in summer and fall precipitation was observed in Florida (*24*) and the Chesapeake Bay (*29*). The maximum differences in rain water Hg concentrations among four of the New Jersey sites (excluding Alloway Creek) were also greater in the summer and fall (35-40 pM) than in the winter and spring (20-28 pM). This would suggest that localized phenomena are responsible for much of the increase in Hg concentrations

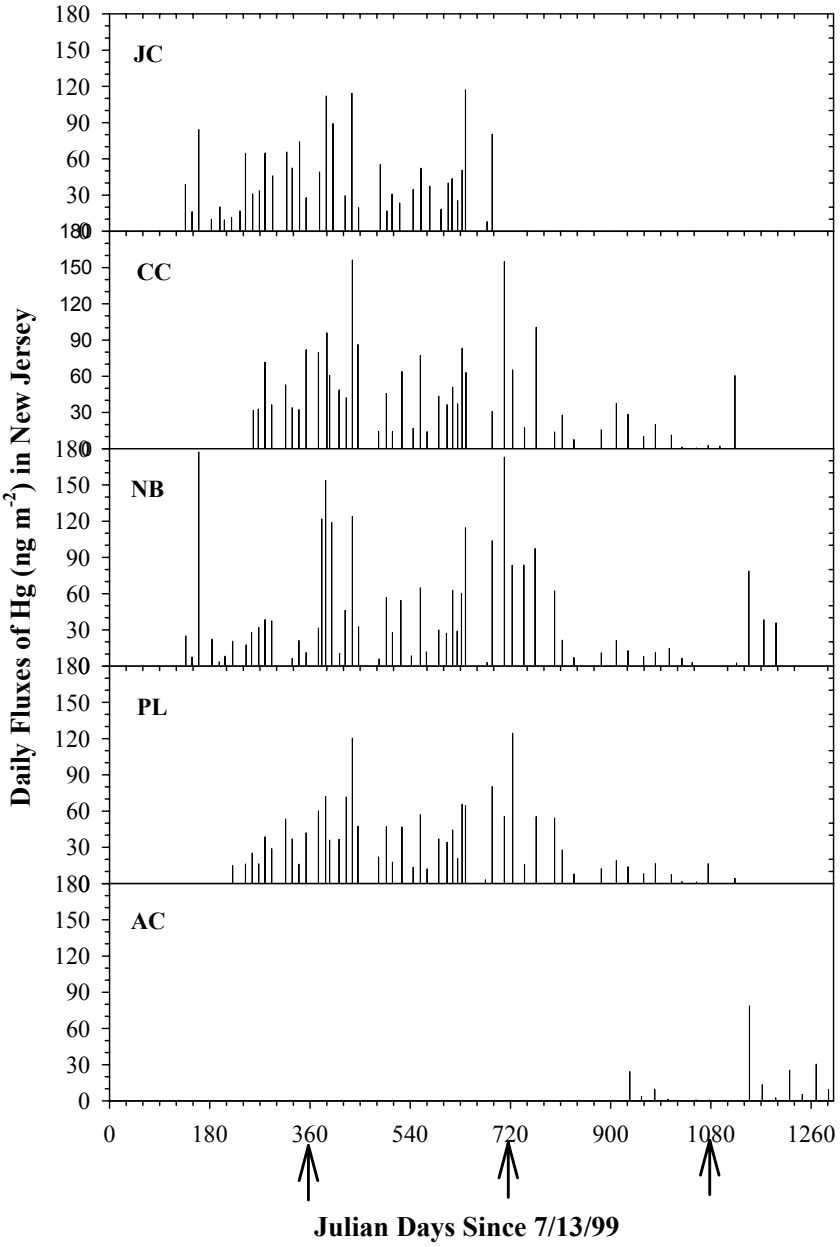

Figure 35. Daily wet deposition fluxes of Hg in New Jersey for the period of November, 1999 – January, 2003. Arrows indicate the summers (mid-July) of 2000, 2001, and 2002.

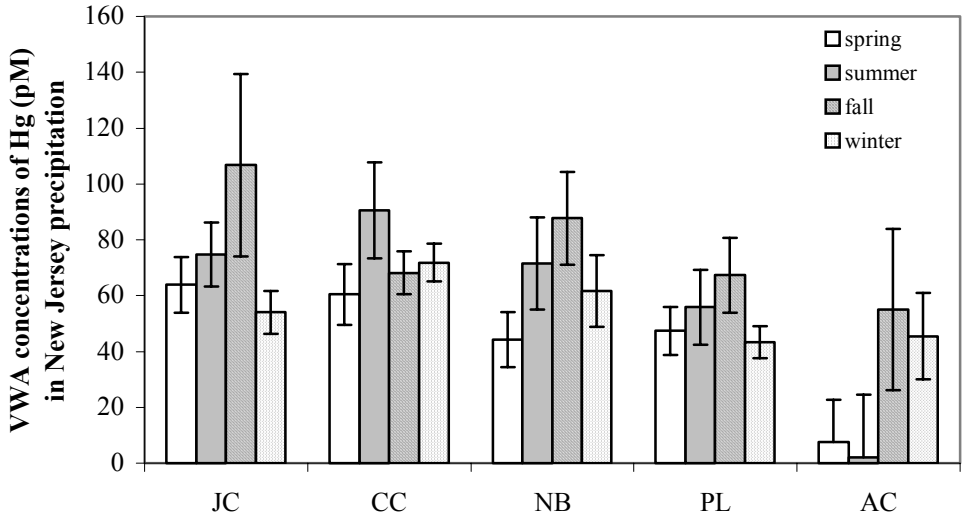

Figure 36. Seasonal variation in volume-weighted average concentrations of Hg in New Jersey rain.

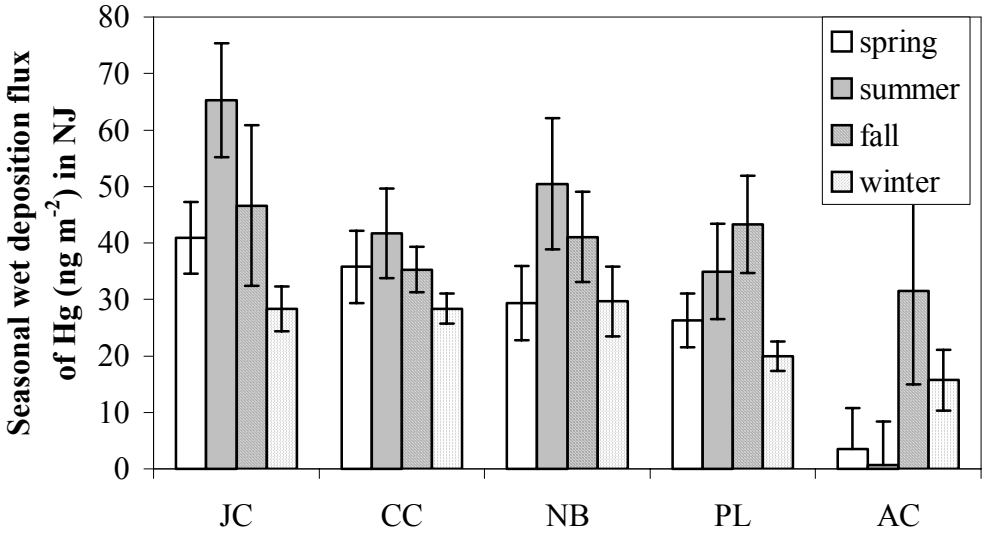

Figure 37. Seasonal variation in the wet deposition flux of Hg in New Jersey.

in New Jersey rain in the summer and fall. These phenomena may include greater emissions from local sources and/or higher Hg oxidation rates as a result of increased levels of atmospheric oxidants such as O_3 (see below).

The highest wet deposition fluxes of Hg in New Jersey occurred in the summer at all sites except the Pinelands and Alloway Creek where the highest deposition was recorded in the fall (Figure 37). These seasonal deposition trends are generally consistent with the trends of total Hg concentrations in rain, except that peak deposition rates were not recorded during the same season as peak concentrations (Figures 36 and 37). Differences in rainfall depths between the summer and fall likely account for this observation (see below).

Annual volume-weighted Hg concentrations in New Jersey rain range from 54 pM at the Pinelands site to 74 pM in Camden (Table 29). These data show that, on average, Pinelands rain is least contaminated with Hg, Camden and Jersey City rain is most contaminated with Hg, and New Brunswick rain is subject to intermediate contamination. New Jersey rain would appear to be similarly enriched in Hg as that collected throughout Florida (*24*) and around the Chesapeake Bay (*29*), but more enriched than rain in Delaware, Pennsylvania (MDN), and upper mid-western states (*28, 30*). Our recent Hg concentrations in New Jersey rain are lower than those measured during the spring, summer, and fall seasons of 1992-1994 at seven sites around New Jersey (*31*) (range 85 - 194 pM). This may indicate a downward trend in atmospheric Hg in the eastern U.S. during the 1990s as has been observed for particulate Hg in New York (*32*; see below).

Excluding Alloway Creek, annual precipitation fluxes of Hg ranged from 11 to 14 μg m^{-2} y^{-1}, similar to fluxes measured in Maryland, Delaware and eastern and south central Pennsylvania (Table 29). The wet deposition fluxes of Hg in suburban New Brunswick and the rural Pinelands were lower than those recorded at the more urban/industrial Jersey City and Camden locations suggesting that in addition to the regional Hg signal, local phenomena are also important to the wet deposition of Hg in New Jersey. Lower Hg concentrations in rain measured at rural sites (DE, NY/VT, and PA) than at more developed locations in New Jersey, Maryland, and Florida suggest that differences in local sources, meteorology, and atmospheric chemistry affect the variability of Hg concentrations in east coast rain. The New Jersey wet deposition fluxes of Hg, together with the nearly synoptic NADP results for Pennsylvania, show something of a spatial gradient in Hg deposition with relatively low Hg deposition rates at the central Pennsylvania sites (Cambria and Tioga counties), higher deposition rates in eastern Pennsylvania

(Valley Forge), and the highest deposition fluxes in New Jersey (Table 29). This west to east increase in Hg wet deposition could be the result of increasing Hg emissions, changes in atmospheric chemistry at this mid-Atlantic latitude, or both. A careful inventory of Hg emissions coupled with an assessment of the variation in atmospheric oxidant concentrations in this region could address this issue.

Table 29. Mercury in precipitation in New Jersey and other states. Values are volume-weighted mean concentrations and annual fluxes with 1 standard error.

New Jersey Sites	**n**	**Concentration (pM)**	**Flux (μg m^{-2} y^{-1})**
Jersey City	38	69 ± 6	14 ± 1.3
Camden	47	74 ± 7	14 ± 1.2
New Brunswick	59	65 ± 7	11 ± 1.2
Pinelands	50	53 ± 5	11 ± 1.1
Alloway Creek	16	32 ± 10	5.0 ± 1.6
Other sites			
Chesapeake Bay, MD (1995-1999)[a]		73	14
Baltimore, MD (1995-1996)[a]		135	30
Lake Champlain, NY/VT (1994)[b]		32	7.9
Upstate NY DE (1999-2001)[c] (Essex County)		33	7.2
Lewes, DE (1996)[c]		41	9.6
Valley Forge, PA (1999-2000)[c]		51	12
South Central PA (Cambria County; 1997-1999)[c]		48	10
North Central PA (Tioga County; 1997-1999)[c]		42	7.4
Lake Michigan (1995)[d]		48	8.3
Northern WI (1989-1990)[e]		51	8.7
Southern Florida [f]		70-80	20-23

a Ref. *29* b Ref. *33* c NADP, 2001
d Ref. *28* e Ref. *30* f Ref. *24*

The fine aerosol concentrations of Hg at the four central New Jersey sites (excluding Alloway Creek) ranged from a low of 1.9 pg m^{-3} (half of the methodological detection limit) to a maximum of 85 pg m^{-3} (Table 30). Average particulate Hg concentrations were lower in the Pinelands and at New Brunswick than at the urban Jersey City and Camden sites, but with

≥ 100% uncertainty at all four sites, the averages are not significantly different ($p > 0.999$). Fine aerosol Hg concentrations measured in New Jersey were significantly lower than PM2.5 Hg levels measured in 1992 in upstate New York (30-170 pg m^{-3}; *32*) and total aerosol Hg concentrations observed in 1994 (March) in Detroit, MI (average = 94 pg m^{-3}; *25*). This may reflect geographical or sampling differences, but could also be due to a decrease in particulate Hg levels in the northern U.S. regional atmosphere during the 1990's. Significant drops in particulate Hg concentrations were observed between 1992 and 1993 in northern Wisconsin (63 pg m^{-3} in the summer of 1992 to 14 pg m^{-3} in the summer of 1993; *27*) and upstate New York (30-170 pg m^{-3} in 1992 to 5-20 pg m^{-3} in 1993; *32*). In addition, there is some evidence that reduced emissions from regional sources have resulted in lower Hg accumulation rates in the sediments of mid-western lakes (*18*). Olmez et al. suggested that emissions controls at metal smelting facilities in Canada, which could impact Wisconsin and Michigan as well as the northeastern U.S., may have been responsible for the decline in fine particulate Hg they observed in upstate NY in 1993.

Table 30. Fine aerosol (PM2.5) mercury concentrations (pg m^{-3}) and annual dry particle deposition fluxes of mercury (μg m^{-2} y^{-1}) in New Jersey. Dry deposition fluxes were estimated using the average fine aerosol concentrations and a dry deposition velocity of 0.5 cm s^{-1}. The chosen deposition velocity was selected to capture the deposition of all size classes of atmospheric particles, but may underestimate the flux of elements primarily associated with large particles and over estimate the deposition of elements primarily associated with small particles (see section I.C1, pp 13-14).

		particulate mercury (pg m^{-3})				**dry deposition**
Site	n	min	max	mean	median	(μg m^{-2} y^{-1})
JC	17	1.9[a]	44	12 ± 12	7.1	1.8
CC	52	1.9	85	16 ± 16	10	2.5
NB	40	1.9	71	7.5 ± 12	4.8	1.2
PL	53	1.9	32	4.9 ± 5.5	1.9	0.78
AC	28	1.9	96	13 ± 23	5.8	2.0

Lower PM2.5 Hg concentrations in urban NJ sites than were found in Detroit MI may reflect differences in local sources to these cities. Our PM2.5 Hg concentrations are similar to background concentrations for New York state (7 - 12 pg m^{-3}; *32*) and Florida (4.9 – 9.3 pg m^{-3}; *24*) and they overlap the range of total particulate Hg concentrations measured in the early 1990's in rural Michigan (11-22 pg m^{-3}; *25*), rural Vermont (11 pg m^{-3}; *34*), those measured in 1989-1990 in northern Wisconsin (25 ± 23 pg m^{-3}; *30*) and in 1995-1996 adjacent to the Chesapeake Bay (Winter 16±15 pg m^{-3}, summer, 21 ± 20 pg m^{-3}; *35*). This may be explained by the decreasing trend in particulate Hg over the northern US during the past decade as discussed above, or the dilution of pollutant aerosols by marine air masses in New Jersey, Florida, and the Chesapeake Bay.

The estimated total dry particle deposition (for all aerosol sizes) of Hg ranged from 0.8 to 2.5 μg m^{-2} y^{-1} which represents 7% to 29% of the total (wet plus dry) deposition. These results are in accord with the findings of Mason et al. (*23*) who estimated that dry deposition accounted for 10 to 15 % of the total. Guentzel et al. (*24*) found no significant difference between bulk and wet deposition in Florida suggesting a minor role for dry deposition in that state. Although wet deposition typically accounts for 80-90% of total Hg deposition, dry deposition, including the deposition of particulate and gaseous species, can be important in some urban areas (*25*).

Recent studies (*36 -38*) have identified gas phase forms of Hg(II), including HgO, $HgCl_2$, $HgBr_2$, and $Hg(NO_3)_2 \cdot H_2O$, which are collectively referred to as reactive gaseous mercury (RGM). RGM typically accounts for 2% to 5% of the total gaseous Hg, but can reach as high as 30% under certain circumstances (*36, 38*). Unlike levels of total gaseous Hg, concentrations of RGM appear to follow daily and seasonal cycles and are correlated with temperature (*36*). As reactive gases, RGM species are expected to have relatively high deposition velocities similar to gases such as HNO_3. Thus very low concentrations of RGM could account for significant Hg deposition. For example, given an RGM concentration of 40 pg m^{-3} (average concentration measured for Solomons, MD, *38*) and a deposition velocity of 1 cm s^{-1}, the estimated annual deposition of RGM (13 μg m^{-2} y^{-1}) is comparable to wet deposition fluxes measured across New Jersey (14-18 μg m^{-2} y^{-1}). Although such estimates must be evaluated in light of the analytical difficulties associated with RGM measurements (*38*) and the limited number of measurements in the northeastern U.S., the formation and seasonal cycle of RGM in New Jersey need to be

studied in order to assess the full impact of the atmospheric deposition of Hg on the state's terrestrial and aquatic ecosystems.

The sources of Hg to wet deposition include particle scavenging and the scavenging of reactive gaseous Hg(II). In cloud water droplets, the aqueous phase oxidation of Hg° to Hg(II) and particle scavenging of Hg(II) will drive the gas-liquid Hg flux. The weak, but positive correlations between Hg fluxes and rain depths (Figure 38) suggest that aerosol washout is not the only mechanism controlling the concentration of Hg in New Jersey rain. A similar positive correlation was also observed in Maryland (*29*). The importance of particle scavenging to the concentration of Hg in precipitation can be evaluated further by comparing scavenging ratios of Hg and "conservative" metals for which there is no gas phase source such as Pb. This sort of analysis was done in northern Wisconsin in 1989-1990 where the Hg scavenging ratio was found to be 477 ± 547. It was concluded that aerosol washout controlled the concentration of Hg in northern Wisconsin rain (*22*). Based on these and other results from the equatorial Pacific and Sweden (*39*), it was proposed that gas phase-particle phase transfer and oxidation of Hg was an important mechanism leading to the deposition of Hg in rain (*30*). In contrast to the above results, the summertime scavenging ratios of Hg at the four New Jersey sites ranged from 1525 to 2600, while those for Pb ranged from 260 to 600. These scavenging ratios suggest a 2.5 to 10-fold enrichment of Hg in rain over that which could be contributed by the washout of aerosols. This additional Hg in precipitation likely arises from the scavenging of reactive gaseous Hg and the in cloud oxidation of Hg°.

In order to construct a balanced budget of Hg inputs to aquatic and terrestrial ecosystems, inputs from atmospheric deposition as well as other point and non-point sources need to be quantified. Studies of atmospheric Hg deposition, coupled with meteorological information, and deposition trends of other inorganic and organic contaminants will help scientists and regulators to identify important local and regional sources of atmospheric Hg and to assess efforts to control them. Once deposited, the biogeochemical cycling of Hg is expected to vary widely among different aquatic and terrestrial ecosystems in New Jersey which include kettle lakes, reservoirs, acid lakes in the Pinelands, and highly productive freshwater wetlands and marine estuaries. The importance of biogeochemical factors on Hg bioaccumulation is illustrated by the high Hg concentrations in fish from low pH (4-5) Pinelands lakes which are far from

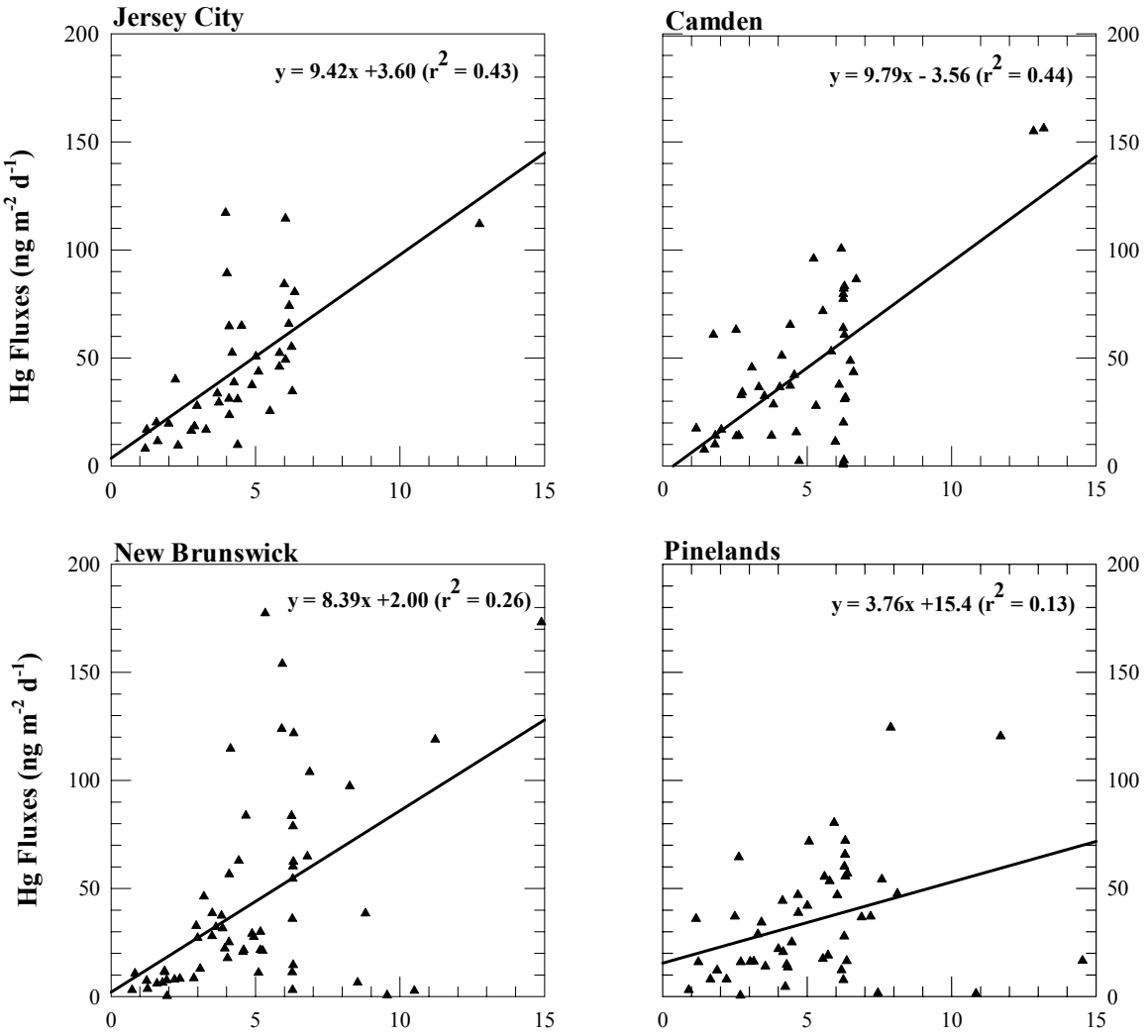

Figure 38. Relationships between Hg fluxes and rain depths in New Jersey.

urban/industrial sources of Hg, but are among the highest in the state and often (70%) exceed 1 μg g^{-1} (1 ppm), the US FDA action threshold (*40*). In order to predict and manage the impact of Hg in the environment, it is therefore necessary to link estimates of the atmospheric contribution of Hg to ecosystems with Hg methylation and food web bioaccumulation.

II.B4. Nitrate and Phosphate

Non-point source inputs, such as atmospheric deposition, are increasingly recognized as important factors with regard to surface water quality. This is especially true for macronutrients like nitrogen and phosphorus, which are linked to excess primary production in New Jersey's fresh and coastal waters. Atmospheric deposition of nitrogen and phosphorus has been shown to be a significant contributor to the total loading of nutrients to aquatic ecosystems (*41* - *44*). Due to its nature as a limiting nutrient in biological systems, excess phosphorus can lead to enhanced biological activity resulting in premature eutrophication that can damage aquatic systems for in-stream uses such as power generation, navigation, and recreation. Prior to the 1960s, most detergents contained phosphates that, when discharged to surface waters, acted as fertilizers perpetuating the growth of undesirable species, such as algae and excess amounts of aquatic plant life. Some detergents underwent tertiary wastewater treatment processing prior to discharge into streams and other water bodies that allowed for some degree of control of phosphate content. However, the same was not true for primary and secondary-treated wastewater streams, agricultural run-off of phosphates, phosphorus from bird droppings and insects (*45*), and the contribution from atmospheric deposition.

Introduction of nitrogen and phosphorus into water bodies can lead to the enhanced growth of primary producer species, like algae, which play an important role in the aquatic food chain. Algae convert carbon dioxide into biomass that is used by small aquatic organisms (i.e. zooplankton) as a food source. Hydrophobic organic compounds (HOCs), like PCBs, can enter the aquatic food chain by sorption to the algae, which can then be taken up by organisms progressively higher up the food chain. HOCs can also enter the food chain by direct passive sorption to phytoplankton, due to the organic-carbon rich nature of phytoplankton cells. The bioconcentrated HOCs can become incorporated into higher-level fish that can be consumed by humans. Therefore, the bioconcentration of HOCs in aquatic ecosystems is enhanced when phosphorus additions drive excessive algae production and subsequently, excessive growth in higher-level organisms (*46*).

Macronutrient wet deposition into the ocean and other major bodies of water can cause excessive growth of phytoplankton leading to dangerous blooms that affect the hierarchy of organisms in the ocean (*47*). These blooms can also pose a danger to humans, as the algae can poison filter-feeding organisms, and, when consumed by humans, lead to illness and death.

Considerable effort has gone into the abatement of point sources of nitrogen and phosphorus; however controlling non-point source additions (i.e. via agricultural runoff, weathering/soil erosion, atmospheric deposition, incineration and biomass burning (*47*) of these nutrients is significantly more difficult. Here we present results regarding the atmospheric deposition of nitrate and phosphorus in NJADN, which together with a comprehensive analysis of streamflow, surface water concentrations, and other nutrient sources, will be useful in modeling nutrient cycling in New Jersey's surface waters and estimating nutrient loads to impacted waterbodies.

Nitrate in New Jersey Precipitation

Nitrate concentrations in precipitation collected in New Brunswick, Jersey City, the Pinelands, and Camden ranged from 18 to 1800 μg L^{-1}, but volume-weighted mean (VWM) concentrations at all four sites ranged from 390 to 500 μg L^{-1} (Table 24). The lowest VWM nitrate concentrations (280 μg L^{-1}) were measured in the winter samples at the Pinelands and New Brunswick and the highest (530 μg L^{-1}) in Camden in the summer. All sites showed higher nitrate concentrations in the spring and summer than fall and winter. The average seasonal nitrate concentrations in rain collected at the NJADN sites are similar to those measured at Washington's Crossing (170 to 480 μg L^{-1}), but generally higher than those measured at the Forsythe Reserve in southern coastal NJ (140 to 240 μg L^{-1}) in 1999 as part of the NADP measurements (NADP, 2001). This spatial trend in nitrate concentrations in precipitation likely reflects greater NO_x emissions in the areas surrounding the primarily urban/suburban NJADN sites than at the relatively pristine, coastal Forsythe Reserve location.

The annual wet deposition flux of nitrate in New Jersey as measured in this study ranged from 310 to 420 mg m^{-2} y^{-1} (Table 25) compared with 280 and 210 mg m^{-2} y^{-1} at Washington's Crossing and the Forsythe Reserve, respectively. Since nitrate represents roughly half of the total dissolved nitrogen in New Jersey rain (S.P. Seitzinger, pers. comm.), the remainder being ammonium and dissolved organic nitrogen, total N fluxes are approximately twice these values. Precipitation nitrate fluxes measured at NJADN sites are comparable to those (310 to 364 mg m^{-2} y^{-1}) measured in other Mid-Atlantic states (Pennsylvania, Maryland, New York; *48*).

Phosphate in New Jersey Precipitation

Concentrations of total phosphorus in New Jersey precipitation generally ranged from 2 to 30 μg L^{-1} with the exception of two samples collected in New Brunswick which had concentrations of 56 and 92 μg L^{-1} (Figure 39). The lowest volume-weighted mean concentration for the entire sampling period occurred in Jersey City (5.9 μg L^{-1}). The volume-weighted mean concentrations of the other three sites were similar (Table 24).

The Jersey City site displayed the least amount of variability in total phosphorus concentration with a relative standard deviation of 38%. The New Brunswick, Camden and Pinelands sites showed larger degrees of variability with higher relative standard deviations: New Brunswick (168%), Camden (78%), and Pinelands (68%). The New Brunswick and Pinelands sites are both expected to be influenced by the localized application of phosphorus-containing fertilizers and the re-suspension of biogenic material (soil, plant debris) subject to previous fertilizer application. The Pinelands site may also be subject to phosphorus input from incineration of biomass due to controlled burns initiated in the area. The Camden site is situated in the middle of an urban center and is, therefore, not expected to be influenced by the localized use of fertilizers. This site is influenced more by industrially associated phosphorus loadings (i.e. incineration). Three of the samples taken at this site (May 2000, January 2000, and May 2001) had high total phosphorus concentration, but if their influence is removed, the relative standard deviation for Camden is 41%, and on the same order of magnitude as the Jersey City site. This may be an indication that urbanized areas such as Jersey City and Camden are experiencing 'background' signals of phosphorus relative to those measured in agricultural areas.

Seasonal VWM concentrations of phosphorus varied between 4.1 and 15 μg L^{-1} and no consistent seasonal or spatial trends in concentration or wet deposition of phosphorus were observed (Figures 40 and 41). The lowest wet-deposition flux occurred in Jersey City in the fall (3.9 mg m^{-2} y^{-1}) and the highest occurred in the Pinelands in the fall (14 mg m^{-2} y^{-1}). Annual wet deposition fluxes of phosphorus ranged from 5.2 to 8.3 mg m^{-2} y^{-1} (Table 25). There is no statistically significant difference ($p > 0.1$) between the annual wet phosphorus deposition fluxes at the four NJADN sites.

> Dozens of studies over the last twenty years have examined phosphorus rain concentrations and wet deposition. Pollman et al. (*49*) provide a tabular review of data from 1984-1999. The VWM concentrations of phosphorus measured in New Jersey are toward the

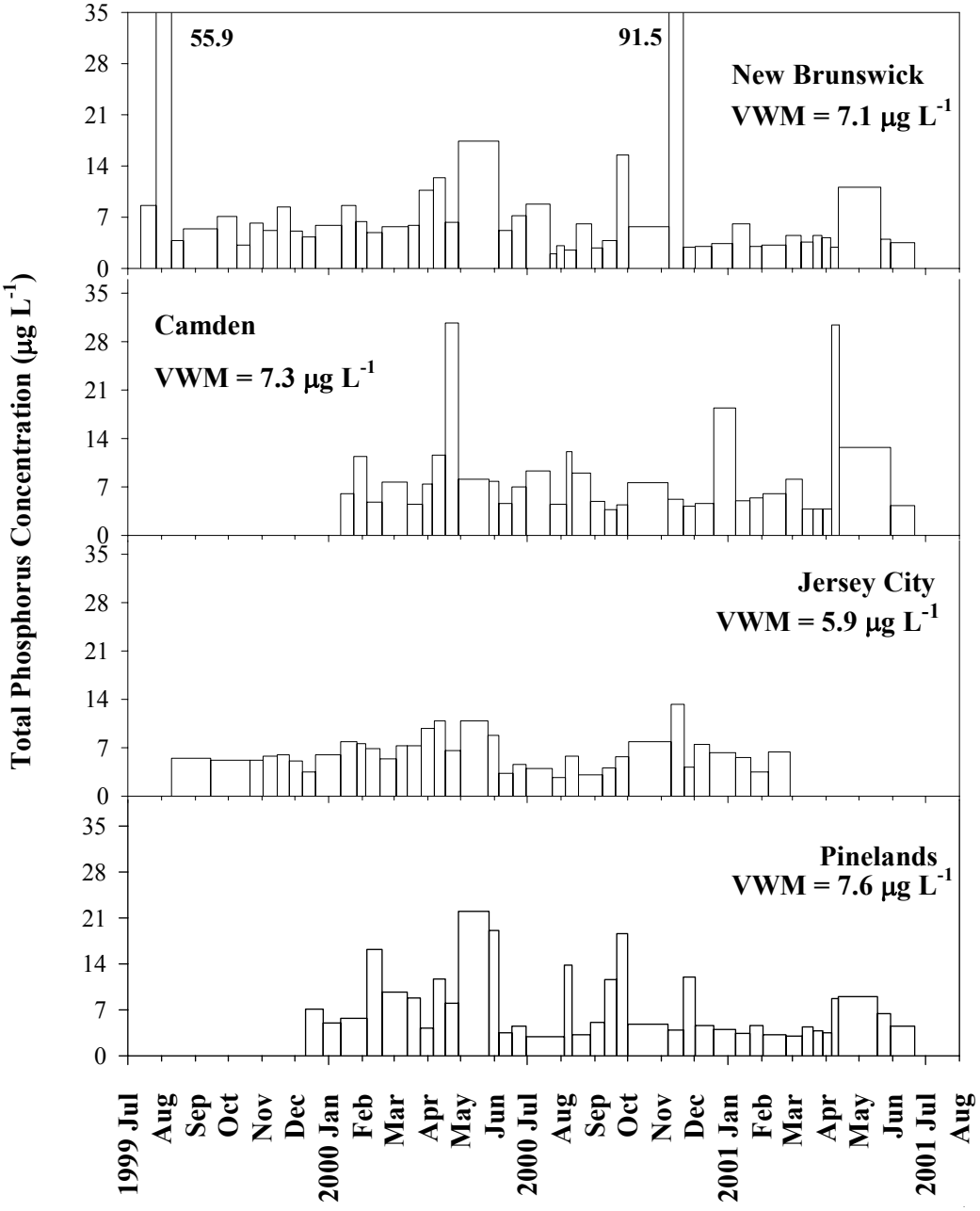

Figure 39. Concentrations of total phosphorus in New Jersey precipitation (μg L^{-1}). The width of the bars corresponds to the dates over which each sample was integrated.

low end of the range observed from 1984-1999. Total phosphorus concentrations as high as 200 μg L^{-1} have been observed elsewhere (*50*), but in most studies phosphorus concentrations were between 1 and 50 μg L^{-1}, similar to this study. A few newer studies not included in the Pollman et al. (*49*) review have also observed P concentrations in this range (*51 - 53*). Estimates of P wet deposition tabulated by Pollman et al. (*49*) range from 4 mg m^{-2} y^{-1} in Connecticut (*54*) to 21 mg m^{-2} y^{-1} in Ireland (*55*). Thus our measurements are within this range and similar to those observed in Connecticut, which is geographically close to New Jersey. A more recent study by Morales et al. (*42*) observed TP wet deposition fluxes of 20-80 mg m^{-2} y^{-1} in Venezuela.

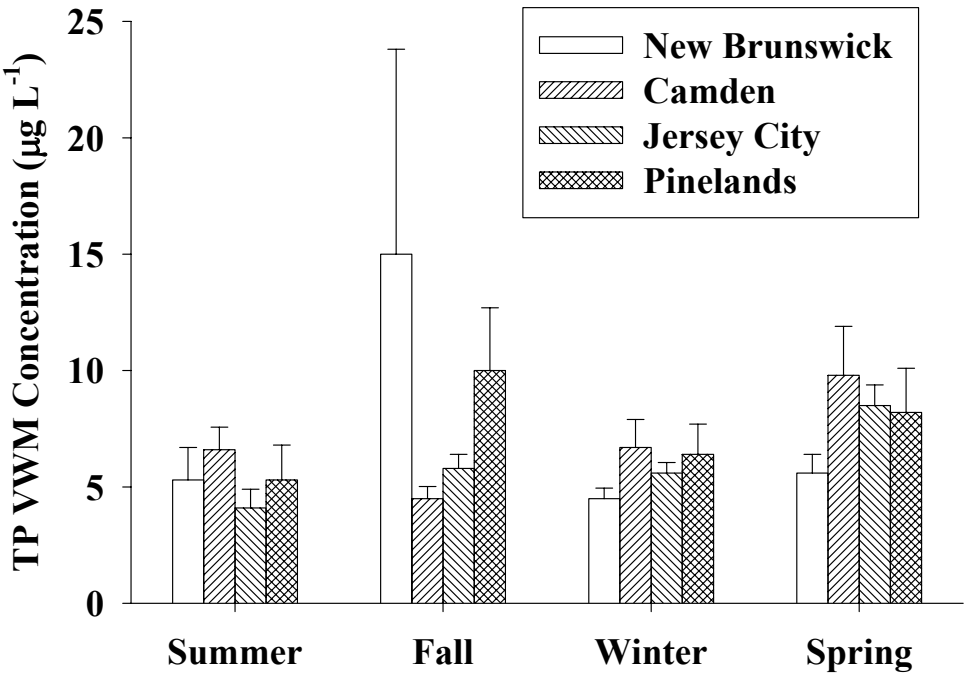

Figure 40. Seasonal volume-weighted mean concentrations of total phosphorus in New Jersey precipitation (μg L^{-1}).

Focusing on the east coast of the United States, the VWM concentrations measured in this study are similar to those measured in the Florida Everglades (*45*) and Chesapeake Bay (*56*). The wet deposition fluxes observed in this study are similar to those measured in Apalachicola, Florida (*57*) and Connecticut (*54*).

Because phosphorus in rain has been measured at different times and at various geographic locations, it is difficult to evaluate the spatial and/or temporal trends in phosphorus

wet deposition. In Lake Michigan during the mid-1970's, Eisenreich et al. (*41*) measured phosphorus VWM concentrations of 50-64 μg L^{-1}, resulting in wet deposition fluxes of 17-36 mg m^{-2} y^{-1}. Eisenreich et al. (*41*) proposed that the dominant sources affecting phosphorus deposition to Lake Michigan were derived from both urban/industrial activities and agricultural sources, such as wind-blown soil and re-entrained dusts. Miller et al. (*53*) measured phosphorus VWM concentrations in precipitation in the Great Lakes during 1994-1995 ranging from 4 to 11 μg L^{-1}, suggesting that phosphorus levels in precipitation have declined substantially in the Great Lakes over the last 30 years.

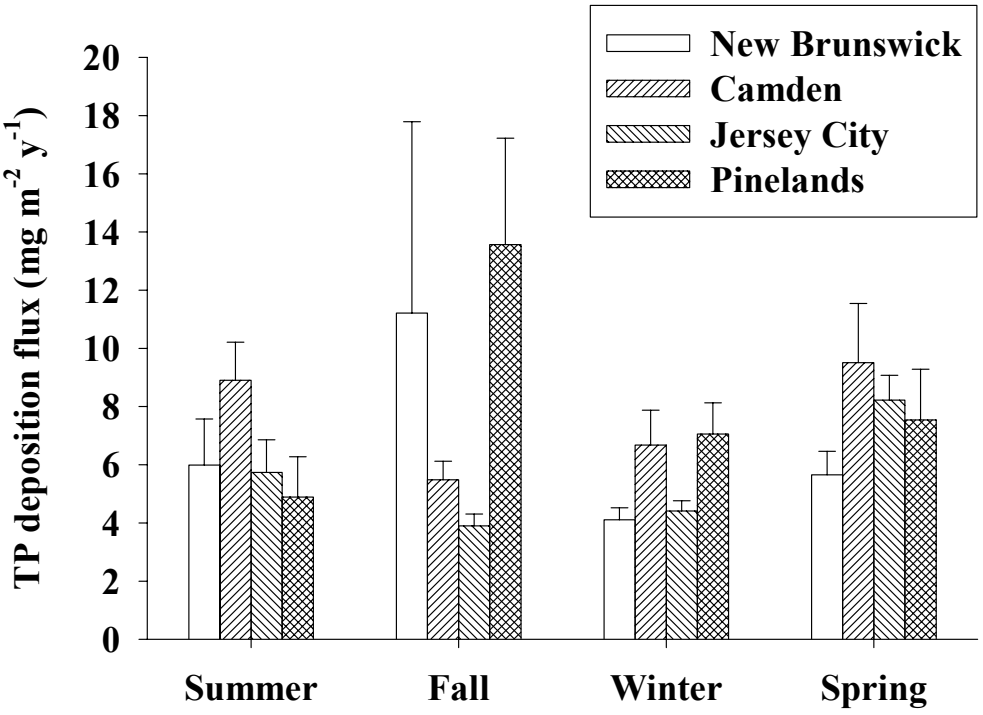

Figure 41. Seasonal total phosphorus deposition flux by site (mg m^{-2} $year^{-1}$).

The phosphorus concentrations in rain samples collected in South Florida (*52*) are similar to those measured in New Brunswick, Camden, and the Pinelands. The range of average phosphorus concentrations measured at the individual sites in the South Florida study (5.5 – 16 μg L^{-1}) is remarkably similar to the seasonal range observed in NJ. This may suggest that phosphorus concentrations in rain display relatively little spatial variability, at least in the Eastern United States. Despite similar VWM concentrations, the wet depositional flux of

phosphorus reported in South Florida is greater than that in NJ (*52*), reflecting the greater annual precipitation flux in South Florida.

Herut et al. (*51*) report VWM concentrations of phosphorus of 26 μg L^{-1} in samples from the Mediterranean coast of Israel collected during the mid-1990's. Although the concentrations of phosphorus in rain were higher than those measured in this study, the annual wet deposition fluxes of phosphorus calculated from these data are similar (9 mg m^{-2} y^{-1}) to those reported here, due mostly to lower precipitation flux in Israel's relatively arid climate.

Ahn and James (*52*) found no long-term trend in the magnitude of phosphorus deposition (wet and dry) in South Florida during 1992-1997. The higher VWM concentrations in Israel may reflect a larger reservoir of phosphorus in this area. This phosphorus may be less efficiently deposited to terrestrial and aquatic ecosystems due to the small precipitation flux. In contrast, the similar VWM concentrations of phosphorus in precipitation from New Jersey and south Florida may indicate that the reservoir of available phosphorus in the atmosphere is similar in both locations, but this phosphorus is more efficiently scavenged in south Florida (due to its higher precipitation intensity) than in New Jersey. Herut et al. (*51*) hypothesize that much of the phosphorus measured in the Israeli rain derives from desert dust from the Saudi Peninsula and North Africa. Dust sources of this magnitude are not present upwind of the eastern United States, possibly explaining the lower VWM concentrations of phosphorus measured there.

II.B5. Evaluation of Atmospheric Deposition as a Source of Trace Metals to the Hudson River Watershed and Estuary

One of the major concerns regarding metals in the environment is the potential accumulation of high concentrations of toxic metals in aquatic organisms with possible adverse effects on the health of natural ecosystems or that of consumers of fish and shellfish including humans (*58*). Understanding the relative magnitudes of metal sources to aquatic ecosystems and how the various inputs are processed by the biota is crucial to predicting deleterious effects of metals and managing their release in the environment. Metal inputs to surface waters from atmospheric deposition are not easily quantified since they include direct deposition and runoff from the watershed, but they may be a significant source to systems with large surface areas or watersheds. Moreover, atmospheric inputs represent a supply of new metals with potentially greater bioavailability than metals already present in a system that are often bound to suspended particles or dissolved organic ligands. This may be particularly important with respect to Hg in aquatic ecosystems since the methylation and bioaccumulation of Hg has been linked to atmospheric deposition (see II.B3. **Mercury** above).

In this section we use NJADN deposition results in a preliminary evaluation of the importance of atmospheric deposition as a source of Ag, Cd, Cu, Hg, and Pb to the Lower Hudson River Estuary (LHRE) and the Hudson River Watershed. These metals were selected for this exercise because of their potential toxicity in marine biota and the availability of concentration and source data for the LHRE. In addition, the direct atmospheric deposition of some of these metals (Cu, Hg, Pb) is expected to have significant impacts on surface water concentrations of bioavailable, inorganic pools.

The relative importance of atmospheric deposition as a source of metals to the LHRE was evaluated in a comparison of annual metal fluxes from river flow, sewage treatment plant discharge, and direct atmospheric deposition. This evaluation owes much to the framework and supporting data of Fitzgerald and O'Connor's assessment of the mercury cycle in the Hudson/Raritan River Basin (*59*). The indirect atmospheric inputs of metals to the LHRE via runoff were assessed through the comparison of atmospheric deposition and river fluxes per unit area of watershed and the estimation of potential runoff efficiencies. Sediments have been shown to be effective traps for metals in urban harbor estuaries (*60*) and thus sediment resuspension is not considered a net source to the water column of the LHRE. It should be pointed out, however, that as the largest reservoir of metals in the LHRE, sediments may be

sources of some metals (particularly Cd and Zn) through resuspension (Rosenthal and Field, pers. comm.).

Estimation of Metal Inputs to the LHRE from River Flow and Sewage Treatment Plant Effluents

River inputs of metals to the LHRE were estimated using average annual stream flow data for the main tributaries and the East River and the concentrations of total (dissolved plus particulate) for the low salinity zone of the tidal Hudson River. The stream flow of the Hudson River (664 $m^3 s^{-1}$) was estimated as the average annual flow measured at the USGS Green Island station over the period 1986 - 1996 multiplied by a watershed factor of 1.65. The combined stream flow of the Raritan, Passaic, and Hackensack Rivers (74 $m^3 s^{-1}$) was estimated as 10% of the total tributary flow (Hudson plus RPH). Inflow from the East River to the LHRE (310 $m^3 s^{-1}$) is that determined by Blumberg and Pritchard (*61*). Thus the total inflow to the LHRE is 1050 $m^3 s^{-1}$. Dissolved and particulate trace metal concentrations for the Hudson River (Table 31) were based on the measurements of Sañudo-Wilhelmy and Gill (*62*), Roditi et al. (*63*), and Windom (*64*) in the low salinity ($S < 1$) zone of the tidal Hudson River and were used as representative of all tributaries and the East River. The particulate Hg concentrations were calculated from the suspended particle concentrations for the Hudson River measured by Findley et al. (*65*) and the water-particle partition coefficients for Maryland rivers and Lake Michigan determined by Mason and Sullivan (*66*, *67*).

Trace metal inputs to the LHRE from sewage treatment plant effluent were estimated using the effluent discharge rate for the LHRE (95 $m^3 s^{-1}$; *68*) and the concentrations of metals in Connecticut treatment plant effluent (Table 31) measured by Rozan and Benoit (*60*; Ag, Cd, Cu, Pb) and Fitzgerald et al. (*69*; Hg).

Table 31. Dissolved and particulate metal concentrations in the low salinity zone of the tidal Hudson River and Connecticut sewage treatment plant (STP) effluent.

	Hudson River		
Metal	Dissolved	Particulate	STP
Ag (nM)	19 ± 17[1]	24 ± 14[2]	3.2 ± 0.93[3]
Cd (nM)	190 ± 92[1]	72 ± 30[2]	0.67 ± 0.45[3]
Cu (nM)	24 ± 4[1]	20 ± 2[4]	55 ± 24[3]
Hg (pM)	4.3 ± 1.7[1]	13.5 ± 5.6[5]	76 ± 27[6]
Pb (nM)	1.4 ± 1.3[1]	4.0 ± 3.8[4]	4.8 ± 2.4[3]

1 Sañudo-Wilhelmy and Gill (*62*)
2 Roditi et al. (*63*)
3 Rozan and Benoit (*60*)
4 Windom (*64*)
5 Calculated from the TSS concentrations of Findley et al. (*65*) and the Hg Kd's of Mason and Sullivan (*66, 67*)
6 Fitzgerald et al. (69)

Estimation of Metal Inputs to the LHRE and Hudson River Watershed from Atmospheric Deposition

Direct atmospheric inputs of metals to the LHRE (Table 32) were estimated using the total (wet plus dry particle) annual deposition fluxes (μg m^{-2} y^{-1}) measured in Jersey City as part of NJADN and the area of the LHRE (3.8 x 10^8 m^2). Atmospheric deposition fluxes to the Hudson River watershed were estimated using measured total fluxes at Jersey City as representative of the local inputs to urban-industrial areas and the lowest fluxes measured at rural east coast sites, including NJADN sites (Ag, Cd, Cu-dry deposition, Pb-dry deposition), Chesapeake Bay Atmospheric Deposition Study sites (*3*, Cu-wet deposition, Pb-wet deposition), and the NADP Essex County site (*48*, Hg), to represent the regional background fluxes. Local and regional fluxes were distributed over the Hudson River Basin in an effort to simulate the relative impacts of urban and industrial emissions (1/3 of the watershed) and background deposition to rural areas (2/3 of the watershed). This somewhat arbitrary distribution of local and regional fluxes is perhaps a bit conservative in that the local urban-industrial signal likely impacts less than 1/3 of the watershed area. Its impact on the average watershed flux is most

pronounced for Cd, Cu, and Pb whose local and regional atmospheric fluxes differ by more than a factor of 4.

Table 32. Total (wet plus dry particle) annual atmospheric deposition fluxes representative of the local urban-industrial signal (Jersey City) and the regional background in the northeast U.S.

	Total annual atmospheric deposition fluxes ($\mu g\ m^{-2}\ y^{-1}$)	
Metal	Urban-industrial	Regional
Ag	151 ± 30	26 ± 5
Cd	176 ± 35	39 ± 7.8
Cu	4960 ± 992	474 ± 95
Hg	15 ± 2.9	8.8 ± 1.8
Pb	6760 ± 1350	985 ± 197

Metal Inputs to the LHRE from River Flow, Atmospheric Deposition, and Sewage Treatment Plant Effluents

Metal inputs to the LHRE (Table 33) are dominated by river inputs (Cd, Cu, Pb), sewage treatment plant effluent (Ag), or a combination of the two (Hg). Direct atmospheric deposition accounts for only 2% to 6% of the total inputs. Thus direct deposition of these metals to the surface of the LHRE is not a major source of *total* metal. It is important to recognize, however, that the direct deposition of some metals, particularly Cu, may contribute substantially to the bioavailable, inorganic metal pool. For example, a 2 cm rainfall event, could increase the concentration of inorganic Cu in the upper 2 m of the water column by a factor of eight. The impacts of such episodic inputs of bioavailable metals have not been examined.

Atmospheric deposition in the Hudson River watershed is also a source of metals to the LHRE. Watershed runoff carries metals deposited in the watershed as well as those from point and natural sources. The indirect input of atmospheric metals to surface waters by runoff depends on atmospheric deposition in the watershed and the "watershed yield" which is the fraction of metal deposited on land that is not bound by soils. For coastal wetlands and estuaries

which have watershed to water body surface area ratios of 10 to 100, the indirect contribution of atmospheric metals via watershed runoff could be very large.

Table 33. Trace metal inputs (kg y^{-1}; % of total inputs) to the Lower Hudson River Estuary (LHRE). Riverine inputs are based on streamflow for the greater Hudson River Estuary watershed and dissolved and particulate trace metal concentrations for the fresh water Hudson River. Direct atmospheric deposition inputs were estimated from the wet and dry particle fluxes of metals measured at Jersey City and the area of the LHRE. Waste treatment plant inputs were estimated from effluent concentrations in Connecticut and the annual wastewater discharge rate to the LHRE.

Metal	Riverine Inputs	%	Direct Atmo.	%	WTP	%
Ag	150 ± 34	12	57 ± 11	4	1100 ± 300	84
Cd	990 ± 430	77	67 ± 13	5	225 ± 150	18
Cu	92000 ± 22000	88	1900 ± 380	2	11000 ± 4500	10
Hg	118 ± 47	70	5.5 ± 1.1	3	46 ± 16	27
Pb	37000 ± 28000	87	2600 ± 510	6	3000 ± 1500	7

A comparison of the atmospheric and riverine watershed fluxes and watershed runoff efficiencies of metals for the greater Hudson River Estuary is shown in Table 34. For all of the metals examined except Cu, the atmospheric deposition flux was greater than the riverine flux indicating significant retention (70% - 95%) of these metals in the aquatic or terrestrial ecosystems of the watershed. The watershed runoff efficiency estimated for Hg (25%) is somewhat higher than those estimated for other watersheds (*70*, *71*). Watershed yields for Hg are typically less than 20% (*70*, *71*), but efficiencies as high as 25-30% have been measured in small catchments (*72*). Few attempts have been made to estimate watershed yields for other metals (*3*). The very high apparent runoff of atmospheric Cu indicates either very poor retention of Cu or significant additional sources of Cu in the greater Hudson River watershed. A more detailed analysis of Cu discharges in the watershed is needed to address this issue.

Table 34. Atmospheric and riverine fluxes of trace metals ($\mu g\ m^{-2}\ y^{-1}$) and potential metal runoff efficiencies in the greater Hudson River Estuary watershed. Atmospheric fluxes are based on weighted (1/3 urban, 2/3 rural) total (wet plus dry particle) deposition measured at Jersey City and rural east coast sites. Riverine fluxes are estimated riverine inputs divided by the area of the greater Hudson River Estuary watershed. Metal runoff efficiencies are the ratios of riverine to atmospheric fluxes.

Metal	Atmospheric flux	Riverine flux	Runoff efficiency (%)
Ag	68 ± 14	3.7 ± 0.81	5
Cd	85 ± 17	24 ± 10	28
Cu	2000 ± 400	2200 ± 540	110
Hg	11 ± 2.1	2.8 ± 1.1	25
Pb	2900 ± 580	880 ± 680	30

II.B6. Section II.B. References

1. Offenberg, J.H.; Baker, J.E. *Environ. Sci. Technol.* **1997,** *31***,** 1534-1538.
2. Polissar, A.V.; Hopke, P.K.; Poirot, R.L. *Environ. Sci. Technol.* **2001**, *35*, 4604-4621.
3. Scudlark, J.R., Conko, K.M., Church, T.M. *Atmos. Environ.* **1994**, *28*, 1487-1498.
4. Landing, W.M., Perry, J.J., Guentzel, J.L., Gill, G.A., Pollman, C.D. *Water Air Soil Pollut.* **1995**, *80*, 343-352.
5. Wu, Z.Y., Han, M., Lin, Z.C. and Ondov, J.M. *Atmos. Environ.* **1994**, *28*, 1471-1486.
6. Meili, M. *Water Air Soil Pollut.* **1991**, *55*, 131-157.
7. Watras, C.J.; Bloom, N.S. Limnol. Oceanogr. **1992**, *37*, 1313-1318.
8. Watras, C.J.; Back, R.C.; Halvorsen, S.; Hudson, R.J.M.; Morrison, K.A.; Wente, S.P. *Sci. Total Environ.* **1998**, *219*, 183-208.
9. Burger, J.; Gochfeld, M. *Environ. Res.* **1997**, *75*, 160-172.
10. Gnamus, A.; Byrne, A.R.; Horvat, M. *Environ. Sci. Technol.* **2000**, *34*, 3337-3345.
11. Stern, A.H.; Korn, L.R.; Ruppel, B.E. *J. Exp. Anal. Environ. Epidemiol.* **1996**, *6*, 503-527.
12. Rolfhus, K.R.; Fitzgerald, W.F. *Water Air Soil Pollut.* **1995**, *80*, 291-297.
13. Downs, S.G.; Macleod, C.L.; Lester, J.N. *Water Air Soil Pollut.* **1998**, *108*, 149-187.
14. Mason, R.P.; Fitzgerald, W.F.; Morel, F.M.M. *Geochim. Cosmochim. Acta* **1994**, *58*, 3191-3198.
15. Sorenson, J.A.; Glass, G.E.; Schmidt, K.W. *Environ. Sci. Technol.* **1994**, *28*, 2025-2032.
16. Pirrone, N.; Allegrini, I.; Keeler, G.J.; Nriagu, J.O.; Rossman, R.; Robbins, J.A. *Atmos. Env.* **1998**, *32*, 929-940.
17. Lindqvist, O.; Johansson, K.; Astrup, M.; Anderson, A.; Bringmark, L.; Hovsenius, G.; Hakanson, L.; Iverfeldt, A.; Meili, M.; Timm, B. *Water Air Soil Pollut.* **1991**, *55*, 73-100.
18. Engstrom, D.R.; Swain, E.B. *Environ. Sci. Technol.* **1997**, *31*, 960-967.
19. Hermanson, M.H. *Water Air Soil Pollut.* **1998**, 101, 309-321.
20. Landers, D.H.; Gubala, C.; Verta, M.; Lucotte, M.; Johansson, K.; Vlosova, T.; Lockhart, W.L. *Atmos. Env.* **1998**, *32*, 919-928.
21. Lorey, P.; Driscoll, C.T. *Environ. Sci. Technol.* **1999**, *33*, 718-722.
22. Fitzgerald, W.F.; Mason R.P.; Vandal, G.M. *Water Air Soil Pollut.* **1991**, *56*, 745-767.
23. Mason, R.P.; Lawson, N.M.; Sullivan, K.A. *Atmos. Environ.* **1997a**, *31*, 3531-3540.
24. Guentzel, J.L.; Landing, W.M.; Gill, G.A.; *Environ. Sci. Technol.* **2001**, *35*, 863-873.
25. Keeler, G.; Glinsorn, G.; Pirrone, N. *Water Air Soil Pollut.* **1995**, *80*, 159-168.
26. Fitzgerald, W.F. *Water Air Soil Pollut.* **1995**, *80*, 245-254.
27. Lamborg, C.H.; Fitzgerald, W.F.; Vandal, G.M.; Rolfhus K.R. *Water Air Soil Pollut.* **1995**, *80*, 189-198.
28. Hoyer, M.J.; Burke, J.; Keeler, J.*Water Air Soil Pollut.* **1995**, *80*, 199-208.
29. Mason, R.P., Lawson, N.M., Sheu, G.-R. *Atmos. Environ.* **2000**, *34*, 1691-1701.
30. Fitzgerald, W.F.; Mason R.P.; Vandal, G.M.; Dulac, F. In *Mercury Pollution: Integration and Synthesis*; Watras, C.J. Huckabee, J.W., Eds.; Lewis : Boca Raton, **1994**; pp. 203-220.
31. Stevenson, E.R.; R. England; B. Ruppel. A pilot study to assess trace levels of Hg in New Jersey Lakes and precipitation. Research Project Report, NJ DEP, **1995**, Trenton, NJ.
32. Olmez, I.; Ames, M.R.; Gullu, G. *Environ. Sci. Technol.* **1998**, *32*, 3048-3054.
33. Rea, A.W.; Keeler, G.J.; Scherbatskoy, T. *Atmos. Environ.* **1996**, *30*, 3257-3263.

34. Burke, J.; Hoyer, M.; Keeler, G.; Scherbatskoy, T. *Water Air Soil Pollut.* **1995**, *80*, 353-362.
35. Mason, R.P.; Lawson, N.M.; Sullivan, K.A. *Atmos. Environ.* **1997**b, *31*, 3541-3550.
36. Lindberg, S.E., Stratton, W.J. *Environ. Sci. Technol.* **1998**, *32*, 49-57.
37. Stratton, W.J., Lindberg, S.E., Perry, C.J. *Environ. Sci. Technol.* **2001**, *35*, 170-177.
38. Sheu, G.R., Mason, R.P. *Environ. Sci. Technol.* **2001**, *35*, 1209-1216.
39. Brosset, C.; Lord, E., *Water Air Soil Pollut.* **1991**, *56*, 493-506.
40. Horwitz, R.J., Ruppel, B., Wisniewski, S., Kiry, P., Hermanson, M. and Gilmour, C. Water Air Soil Pollut. **1995**, *80*, 885-888.
41. Eisenreich, S.J., Emmling, P.J., Beeton, A.M. *Internat. Assoc. Great Lakes Res.* **1977**, *3*, 291-304.
42. Morales, J.A., Albornoz, A., Socorro, E., Morillo, A. *Water Air Soil Pollut.* **2001**, *128*, 207-221.
43. Manny, B.A. and Owens, R.W. J. Great Lakes Res. **1983**, *9*, 403-420.
44. Delumyea, R.G. and Petel, R.L. U.S. Environ. Protection Agency, Ecological Research Series, **1977**, EPA 600/3-77-038.
45. Ahn, H. *J. Amer. Water Resources Assoc.* **1999**, *35*, 301-310.
46. Kramer, P.R.G., Jonkers, D.A., van Liere, L. Interactions of Nutrients and Toxicants in the Food Chain of Aquatic Ecosystems. RIVM report no. 703715001: The Hague, The Netherlands, **1996**, 3-8.
47. Migon, C., Sandroni, V., 1999. *Limol. Oceanogr.* **1999**, *44*, 1160-1165.
48. National Atmospheric Deposition Program (NRSP-3)/National Trends Network. NADP Program Office, Illinois State Water Survey, 2204 Griffith Drive, Champaign, IL 61820, **2004**.
49. Pollman, C.D.; Landing, W.M.; Perry, J.J. Jr; Fitzpatrick, T. *Atmos. Env.* **2002**, *36*, 2309-2318.
50. Callaway, R. M.; Nadkarni, N. M. Plant and Soil, **1991**, *137*, 209-222.
51. Herut, B., Krom, M.D., Pan, G., Mortimer, R. *Limnol. Oceanogr.* **1999**, *44*, 1683-1692.
52. Ahn, H. and James, R.T. *Water Air Soil Pollut.* **2001**, *126*, 37-51.
53. Miller, S. M.; Sweet, C. W.; DePinto, J. V., Hornbuckle, K.C. *Environ. Sci. Technol.* **2000**, *34*, 55-61.
54. Yang, X.; Miller, D. R.; Xu, X.; Yang, L.H.; Chen, H-M.; Nikolaidis, N.P. *Atmos. Env.* **1996**, *30*, 3801-3810.
55. Gibson, C.E.; Wu, Y.; Pinderton, D. *Freshwater Biol.* **1995**, *33*, 385-392.
56. Boynton, W. R.; Garber, J.H.; Summers, R.; Kemp, W. M. *Estuaries* **1995**, *18*, 285-314.
57. Fu, J-M.; Winchester, J.W. *Geochim. Cosmo. Acta* **1994**, *58*, 1581-1590.
58. Thursby, G.B., Stern, E.A., Scott, K.J., Heltshe, J. *Environ. Toxicol. Chem.* **2000**, *19*, 2678-2682.
59. Fitzgerald, W.F., O'Connor, J.S. Mercury cycling in the Hudson/Raritan River Basin. Report to the NYAS Industrial Ecology, Pollution Prevention and the NY/NJ Harbor project, **2001**, New York Academy of Sciences.
60. Rozan, T.F. and Benoit, G. *Limnol. Oceanogr.* **2001**, *46*, 2032-2049.
61. Blumberg, A.F. and D.W. Pritchard. *J. Geophys. Res.-Oceans* **1997**, *102*, 5685-5703.
62. Sañudo-Wilhelmy, S.A. and Gill, G.A. *Environ. Sci. Technol.* **1999**, *33*, 3477-3481.
63. Roditi, H.A., Fisher, N.S., Sanudo-Wilhelmy, S.A. *Environ. Sci. Technol.* **2000**, *34*, 2817-2825.

64. Windom, H.L. In: Sherman, K. Jaworski, N.A., and Smayda, T.J. eds., The Northeast Shelf Ecosystem, **1996,** Blackwell, Malden, MA, pp 313-325.
65. Findlay, S., M. Pace, D. Fischer. *Estuaries* **1996**, *19*, 866-873.
66. Mason, R.P. and Sullivan, K.A. *Environ. Sci. Technol.* **1997**, *31*, 942-947.
67. Mason, R.P. and Sullivan, K.A. *Water Res.* **1998**, *32*, 321-330.
68. Interstate Sanitation Commission. Annual Report **1997**, (NY:ISC).
69. Fitzgerald, W.F., G.M. Vandal, K.R. Rolfhus, C.H. Lamborg and C.S. Langer. *J. Environ. Sci*. **2000**, *12*, 92-101.
70. Hurley, J.P., Benoit, J.M., Babiarz, C.L., Shafer, M.M., Andren, A.W., Sullivan, J.R., Hammond, R., Webb, D.A. *Environ. Sci Technol.* **1995**, *29*, 1867-1875.
71. Mason, R.P., Lawson, N.M., Lawrence, A.L., Leaner, J.J., Lee, J.G., Sheu, G.R. Mar. Chem. **1999**, *65*, 77-96.
72. Engstrom, D.R., Swain, E.B., Henning, T.A., Brigham, M.E. and Brezonik, P.L. In: Baker, L.A., ed., Environmental Chemistry of Lakes and Reservoirs, **1994**, ACS, Washington, pp.33-66.